Understanding the mechanisms of phosphatidylserine exposure in sickle cells

Rasiqh Wadud

under the supervision of

Prof. John S. Gibson

This dissertation is submitted for the degree of Doctor of Philosophy

Clare College   **October 2021**

University of Cambridge

Declaration

I, hereby declare that my dissertation entitled *"Understanding the mechanisms of phosphatidylserine exposure in sickle cells"* is the result of my own original work and includes nothing which is the outcome of work done in collaboration except where specifically indicated in the text. Any parts of the dissertation have not been submitted for any other qualification. This dissertation does not exceed the word limit of 60,000 in agreement with the Degree Committee for the Faculties of Clinical Medicine and Veterinary Medicine.

Rasiqh Wadud

Cambridge, October 2021

Dedication

I dedicate this thesis to my amazing parents and wife, as their continuous support, encouragement and patience made this work possible.

"Allah does not burden a soul beyond it can bear…"

- Qur'an (02:286)

Abstract

Understanding the mechanisms of phosphatidylserine exposure in sickle cells

Rasiqh Wadud

Sickle cell disease (SCD) is the most common severe inherited disorder affecting millions of people worldwide. HbS polymerisation leads to a change in red blood cells' (RBCs) membrane permeability, high phosphatidylserine (PS) exposure, altered RBC rheology and fragility. The high PS exposure is considered to cause some of the hallmark complications of the disease such as vascular occlusion, anaemia and inflammation. This study investigates the possible physiological and cellular signalling pathways involved in PS exposure in RBCs from SCD patients. In the first part, conditions specific to the renal medulla were examined as the majority of SCD patients suffer from nephropathy early in life. It is hypothesised that the ambient conditions of the renal medulla promote polymerisation of RBCs and PS exposure, and so contribute to the detrimental effects of SCD. Thus, the impact of the medullary environment, which is hypoxic, acidotic, hyperosmotic and hypertonic, on RBCs of SCD patients was investigated. In the second part of the thesis, intracellular signalling pathways which could cause high PS exposure were investigated. The study aimed to establish the molecular identity of P_{sickle} and strengthen the link between P_{sickle} and PS exposure. It was hypothesized that PIEZO1, a mechanosensitive ion channel, is a potential candidate for P_{sickle} and a major channel for Ca^{2+} entry in RBCs. Thus, drugs acting on PIEZO1 such as Yoda1, Dooku1 and GsMTx4 were used to examine their effects on Ca^{2+} entry and PS exposure. The results from the first part of the thesis suggest that while the hypoxic, hyperosmotic and hypertonic environment have a substantial effect on sickling and PS exposure, the effect of pH is minimal. Furthermore, the experiments have also shown that urea inhibits both sickling and PS exposure (highly significantly in all the above conditions). Results from the second part of the thesis strongly suggest that PIEZO1 can be a major channel for Ca^{2+} entry leading to PS exposure, together with a Ca^{2+}-independent pathway leading to PS exposure, which is reliant on protein kinase C (PKC). Furthermore, the sphingomyelinase (SMase) signalling pathway was also explored to identify its role in PS exposure. Results with a SMase inhibitor and ceramide on RBCs of SCD patients showed a strong correlation between SMase activity and PS exposure. Moreover, experiments revealed that urea inhibited SMase strongly and might be potentially working through this pathway to reduce PS exposure. These findings further increase our understanding of the conditions and mechanisms, which promote PS exposure and suggest potential future therapeutic targets.

Acknowledgements

ABBREVIATION LIST

5-HMF- 5-hydroxymethylfurfural

A23187- Divalent cation ionophore

ADMA- Assymetric dimethylarginine

ATP- Adenosine tri-phosphate

BEL-A cell lines- Bristol erythroid line adult

Ca^{2+}- Calcium ion

Cl^- - Chloride ion

cf- Confer

DAG- Diacylglycerol

DMSO- Dimethyl sulphoxide

DNA- Deoxyribonucleic acid

EDTA- Ethylene diamine tetraacetic acid

EGTA- Ethylene glycol tetraacetic acid

FDA- Food and Drug Administration

FITC- Fluorescein isothiocyanate

GsMTx4- *Grammastola spatulata* mechanotoxin-4

GD6P- Glucose-6-phosphate dehydrogenase

Hb- Haemoglobin

HbA- Normal adult haemoglobin

HbF- Fetal haemoglobin

HbS- Sickle haemoglobin

HbSS- Homozygous for HbS

HbSS RBCs- Red blood cells from homozygous HbS patients

Hct- Haematocrit

HDL- High density lipoprotein

HEPES- 4-(2-hydroxyethyl)-1-piperazineethanesulfonic acid

HSCT- Haematopoietic stem cell transplantation

HU- Hydroxyurea (hydroxycarbamide)

HUDEP- Human umbilical cord-derived erythroid progenitor cell line

HX- Hereditary xerocytosis

ISCs- Irreversibly sickled cells

K^+- Potassium ion

KCC- Potassium chloride cotransporter

LA- Lactadherin

LPS- Lipopolysaccharide

Mg^{2+}- Magnesium ion

Mn^{2+}- Manganese ion

MCHC- Mean corpuscular hemoglobin concentration

Na^+- Sodium ion

N_2- Nitrogen

NKCC- Sodium-potassium-two chloride cotransporter

NMDA- N-methyl-d-aspartate

NO- Nitric oxide

NOS- Nitric oxide synthase

NSAIDs- Non-steroidal anti-inflammatory drugs

O_2- Oxygen

PC- Phosphatidylcholine

PE- Phosphatidylethanolamine

PIP2- Phosphatidylinositol 4,5-biphosphate

PLC- Phospholipase C

PLD- Phospholipase D

PS- Phosphatidylserine

PMCA- Plasma membrane calcium pump

P_{sickle}- Deoxygenation-induced cation conductance

RBCs- Red blood cells

RT- Room temperature

S.E.M.- Standard error of mean

SCA- Sickle cell anaemia

SCD- Sickle cell disease

SM- Sphingomyelin

SMase: Sphingomyelinase

TLR4- Toll-like receptor 4

TRPC- Transient receptor potential channels of canonical type

VOC- Vaso-occlusive crisis

WHO- World Health Organization

Zn^{2+}- Zinc ion

List of publications resulting from this work

(i) Articles published in journals

1. **R Wadud**, CY Lu, A Hannemann, D Rees, JN Brewin & JS Gibson. Pathophysiological relevance of renal medullary conditions on the behaviour of sickle cells. *Frontiers in Physiology 12:653545; (2021)*.

2. **R Wadud**, A Hannemann, D Rees, JN Brewin & JS Gibson. Yoda1 and phosphatidylserine exposure in red cells from patients with sickle cell anaemia. *Nature Scientific Reports 10, 20110 (2020)*.

3. JS Gibson, **R Wadud**, CY Lu, JN Brewin & D Rees. Oxidative stress and haemolytic anaemia in dogs and cats: a comparative approach. *International Journal of Veterinary Bioscience, 3 (3) 1-5 (2020)*.

4. CY Lu, A Hannemann, **R Wadud**, D Rees, JN Brewin, PS Low & JS Gibson. The role of WNK in modulation of KCL cotransport activity in red cells from normal individuals and patients with sickle cell anaemia. *Pflügers Archiv-European Journal of Physiology, 471, 1539-1549 (2019)*.

5. CY Lu, **R Wadud**, A Hannemann, D Rees & JS Gibson. 2021. Effect of media composition on KCl cotranport activity in low potassium-containing sheep red cells. *(in progress)*.

(ii) Posters

1. **R Wadud**, A Hannemann, CY Lu, D Rees, JN Brewin & JS Gibson, PIEZO1-mediated phosphatidylserine exposure in red cells from sickle cell patients. **ERCS (European Red Cell Society) September 2020.**

2. JS Gibson, CY Lu, **R Wadud** & PS Low. Regulation of red cell KCl and NaKCl cotransporters and its importance. **American Red Cell Club October 2020.**

3. CY Lu, **R Wadud**, A Hannemann, D Rees & JS Gibson. Effect of media composition on KCl cotransport activity in low potassium-containing sheep red cells. **ERCS (European Red Cell Society) September 2020.**

Table of Contents

1 INTRODUCTION

1.1 Sickle cell disease

Sickle cell disease (SCD) was identified as a molecular disease in 1949 when Pauling et al. using gel electrophoresis showed a significant difference in mobility of haemoglobin of normal individuals (HbAA) compared to those with SCD (HbSS), which evidently proved that there must be a structural difference in the haemoglobin of the two groups. It is known that in SCD a simple genetic mutation causes aberrant cellular behaviour making it a multifaceted disease with complex pathophysiologic mechanisms. Vermont Ingram identified that the defect of the disease lay in the sixth position of the β chain of haemoglobin, a protein only expressed in red blood cells (RBCs), where a single base pair change from A (adenosine) to T (Thymine) results in alteration of single amino acid (glutamic acid to valine) (Ingram, 1957; Marotta et al., 1977). Individuals known to have the sickle cell trait have one copy of the normal β gene and one of the HbS (HbAS). They usually lack symptoms, although their cells can be induced to sickle *ex vivo* and they are protected from malaria. However, under conditions of high stress (e.g. athletes) or low oxygen tensions (e.g. high altitude) symptoms of SCD have been reported (Key and Derebail, 2010; Lew and Bookchin, 2005). While the homozygous individuals (HbSS) are the most common amongst SCD patients and develop the most severe form of SCD, other notable genotypes also exist which are described below (Stuart and Nagel, 2004):

● HbS/β thalassaemia	Severe double heterozygote for HbS and β° thalassaemia and almost indistinguishable from SCD phenotypically.
● HbSC	Double heterozygote for HbS and HbC with intermediate clinical severity.
● HbS/ β+ thalassaemia	Mild to moderate severity, but variable in different ethnic groups.
●HbS/hereditary persistence of fetal HbS/HPHP	Very mild phenotype or symptom free

● HbS/HbE syndrome   Very rare and generally very mild clinical course.

● HbS/GD6P (Glucose-6-   Heterozygote for HbS and GD6P (metabolic enzyme
phosphate dehydrogenase)   involved in the pentose-phosphate pathway in RBC
                                    metabolism) *deficiency.*

● Rare combinations   HbS with HbD Los Angeles, HbO Arab, G-
                                    Philadelphia, among others.

The name "sickle" derives from the "peculiar elongated and sickle-shaped red corpuscles" which were first observed by Dr James Herrick and Dr Ernest Irons in 1910 in a dental student from Grenada as shown in Figure 1.1. James Herrick subsequently published the findings in a medical journal in which he used the term sickle-shaped cells.
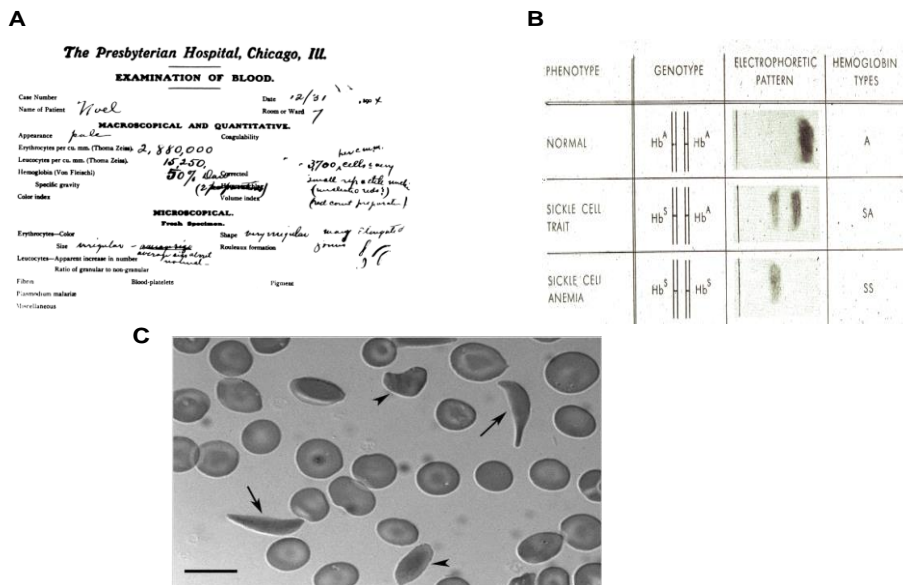
Figure 1.1: Initial examinations of SCD. (A) Describes the peculiar appearance of sickle RBCs (Herrick, 1910). (B) Electrophoresis of different blood genotypes. (C) Peripheral blood smear from a patient with SCD obtained during a routine clinic visit (Frenette and Atweh, 2007).

Later in 1927, Hahn and Gillespie showed that RBCs of these patients in low oxygen conditions resulted in the sickle shape. This sickling of RBCs takes place due to the loss of negative charge and insolubility of HbS when it becomes deoxygenated leading to formation of polymers that aggregate into tubular fibres. The mutated valine in the β^6 position of the

HbS molecule is able to bind to the adjacent phenylalanine β^{85} and leucine β^{88} of the neighbouring HbS molecule resulting in polymerisation (Figure 1.2). As they enlarge, they distort the RBCs causing the characteristic sickle shape as well as creating other bizarre morphologies. This polymerisation of HbS occurs with a lag time following deoxygenation during which no polymer is detected, followed by an exponential increase in polymer formation. This lag time is inversely proportional to a very high power of the HbS concentration ($[HbS]^{-30}$ is often quoted), showing that a small increase in HbS concentration substantially promotes sickling of red cells (Eaton and Hofrichter, 1987). If the transition time of RBCs through hypoxic regions of the circulation is shorter than the lag time then RBCs can escape HbS polymerisation. However, if the transition time is prolonged through the hypoxic regions (due to blocked vessels) then RBC polymerisation is initiated and, with repeated episodes, sickling eventually becomes irreversible (Ferrone, 2004; Scheinman, 2009). Another reason for RBCs to sickle is due to dehydration which occurs because of abnormal activity of multiple channels and transporters in the plasma membrane, resulting in loss of cations with water following osmotically, eventually causing haemolysis, removal by phagocytes and other deleterious sequelae (Apovo et al., 1994; Borgese et al., 1991).
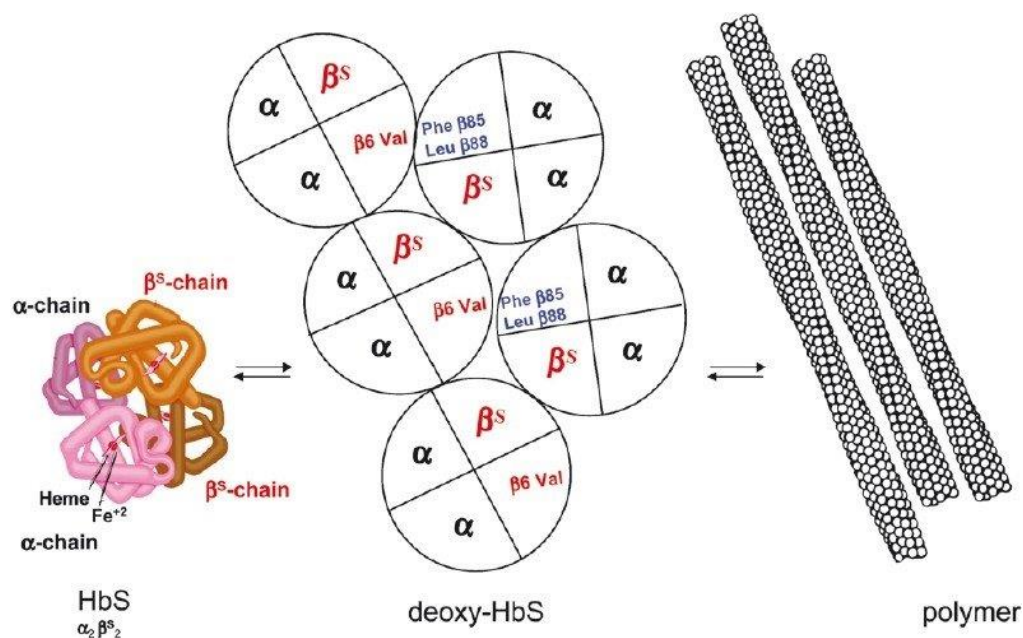
Figure 1.2: Formation of linear aggregates between molecules of sickle haemoglobin (Odièvre et al., 2011). Removal of oxygen from the haemoglobin opens a complementary site (phenylalanine and leucine) in the β^{85} and β^{88} position to which valine binds to and results in the formation of polymer. The polymer is a rope like helical fibre, made up of 7 double stranded HbS chains.

Thus, the drugs developed until now have been designed to target one or more of these pathophysiological factors, in order to improve the overall prognosis of the disease, as well as to treat or minimize the cardinal manifestations. However, none of them has made a serious impact in curing the disease. Moreover, the ones that did appear beneficial had major side effects limiting their use. Therefore, it is of utmost importance to unravel the pathogenesis of the disease in order to design novel therapeutic agents.

1.2 Epidemiology

SCD is one of the commonest severe inherited disorders in the world, affecting 71 % of 229 countries and these affected countries include 89 % of all births worldwide. Approximately 5.2 % of the world's population carries trait genes for haemoglobin disorders, with 1.1 % of couples worldwide at risk of giving birth to children with a haemoglobin disorder (2.7 per 1000 conceptions are affected) (Modell and Darlison, 2008). In the UK around 250,000 people are carriers of the sickle gene and approximately 12-15,000 people are affected by the disease (Piel et al., 2013). In a more recent survey by Dormandy et al. 2017 using the information from the national database it was calculated that 14,000 people in the UK are living with SCD, equivalent to 1 in 4,600 people (Table 1.1). It is also estimated in the UK that one baby out of 2,400 is born with the condition and that the frequency is significantly higher in certain urban areas at 1 in 300 (Modell and Darlison, 2008). In USA approximately 100,000 are affected by SCD. About 1 in 13 African-American babies are born with sickle cell trait and SCD occurs in 1 out of 365 African-American births (WHO, 2006).

Table 1.1 Estimates of people living with SCD in UK (Dormandy et al., 2017)

Data source	Numbers	Notes
NHS Sickle Cell and Thalassaemia Screening Programme	1670	Screen positive babies for 5 years 2009/10–2013/14
		Screen positive includes HbSS, HbS/ beta thalassaemia, HbS/HPFH, HbSC, HbS/D-Punjab, HbS/E, HbS/O Arab
National Haemoglobinopathy register	9677	This includes people with HbSS, HbSC, HbS/DPunjab, HbS/O Arab, HbS/ HPFH, HbS/Lepore, HbSE, HbS β0thal, HbSβ+thal
		There are 750 children under 5 years old
Newborn outcomes project	1154 Children under 5	(793 SS babies and 361 SC babies)
Cardiff Sickle Cell and Thalassaemia centre	79	This includes HbSS, HbSC, HbS/beta thalassaemia
National Specialist and Screening Services Directorate (NSD), NHS National Services Scotland	168	This includes HbS/beta thalassaemia, HbSC, HbSD and HbSS
Newborn Screening Northern Ireland	<5	Screen positive babies (SCD suspected) for the 2 years 2012/13–2013/14
Royal Belfast Hospital for Sick Children	7	Number of children known to the service with sickle cell disease living in Northern Ireland
Republic of Ireland	358 paediatric	Paediatric haematology lead Ireland
	305 SS	Adult haematology lead Ireland
	45 SC	
	<5S D Punjab	
	<5S β 0 thal	
	4<5SSβ + thal	
	68 adult	

Although countries in Africa are most affected, the highest frequency being in sub-Saharan Africa, the disease in these regions is poorly studied due to lack of diagnostic facilities, absence of routine screening tests, causes of death not properly documented, etc (Rees et al., 2010). Estimates suggest that approximately 230,000 affected children are born in this region every year and up to 70 % of these occur in sub-Saharan Africa and approximately 50-80 % of affected children die annually (Makani et al., 2010; Modell and Darlison, 2008). However, the WHO and United Nations have established early life screening in several parts of the countries in Africa and have also formed Global Sickle Cell Disease Network which promotes research in the field in an attempt to reduce prevalence of the disorder.

High HbS gene frequency can also be found in some parts of the Middle East and India. Saudi Arabia and Iraq are as high as 12-22 %, and others including Qatar (7 %), Kuwait (6 %) and Oman (6 %) (El-Hazmi et al., 2011). The frequency in endemic areas such as Gujarat, Maharastra, Madhya Pradesh, Chhattisgarh, western Odisha, Tamil Nadu and Kerala in India can be as high as 35-40 % (Desai and Dhanani, 2003; Serjeant, 2013). SCD in India mainly exists in tribal populations who are very isolated from the mainstream society (Desai and Dhanani, 2003). However, studies have shown that both Saudi Arabia and India have a milder form of SCD or delayed onset of SCD complications than patients of African ancestry, due to a higher concentration of fetal haemoglobin which also continues to be produced into adulthood (Alsultan et al., 2014; Jastaniah, 2011; Kar et al., 1987; Perrine et al., 1972; Serjeant, 2013).
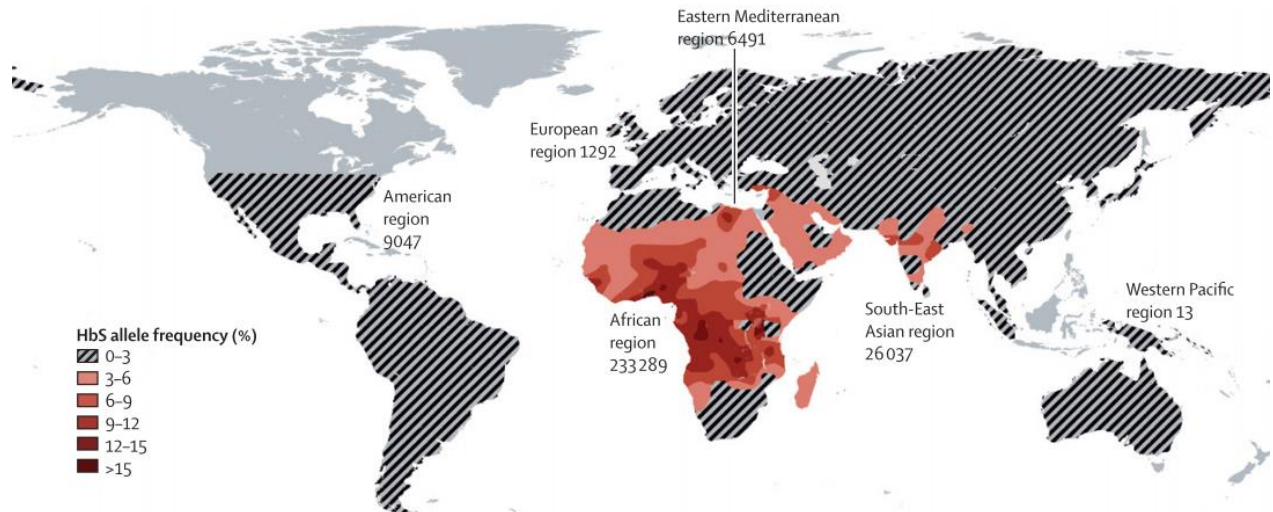
Figure 1.3: Global Distribution of HbS (Rees et al., 2010).

Since the mutation affords protection from malaria caused by *Plasmodium falciparum*, it is thought to originate from places where the parasite is endemic (Livingstone, 1958; Nagel and Steinberg, 2001). This is supported by a five year study conducted in Tanzania which showed that the frequency of malaria in sickle cell anaemia patients was lower compared to that in individuals with normal haemoglobin (Makani et al., 2010). Although in the western world the disease was first observed in 1910, the symptoms of sickle cell disease, which are now recognized, were in fact recorded thousands of years ago. The first recorded cases of sickle cell disease were observed in Egypt (3,200 BC), in the Persian Gulf (2,130 years before present), and in Ghana (1,670 AD). Moreover, malaria specifically that caused by *Plasmodium falciparum* in Egypt occurred approximately 4,000 years ago, but the presence of *Plasmodium falciparum* in Africa could have been several thousand years earlier (Konotey-Ahulu, 1974; Marin et al., 1999).

Previously, the β globin gene has been classified into five haplotypes according to geographic regions: Arabian/Indian, Benin, Cameroon, Central African Republic (CAR), and Senegal. These designations do not necessarily mean the place in which they originated, although earlier epidemiological studies were thought to have shown that the HbS mutation had separate origins in equatorial Africa, Middle East and India. Later, slave trading, wars, voluntary migration, etc. allowed HbS to spread throughout the world (Antonarakis et al., 1984; Bhagat et al., 2013; Hanchard et al., 2007; Kulozik et al., 1986; Lapoumeroulie et al., 1992; Pagnier et al., 1984). One good example of such increased incidence is France, which is one of the countries in

Europe with the highest prevalence of SCD, in which the overall birth prevalence was 1 in 2065 in 2007, ahead of other genetic disorders such as phenylketonuria (1/10,862), congenital hypothyroidism (1/3,132), congenital adrenal hyperplasia (1/19,008) and cystic fibrosis (1/5014). This is due to massive immigration from North and sub-Saharan Africa, and now SCD is a major health problem and the most common genetic disorder in France (Bardakdjian-Michau et al., 2009).

Recently a paper published by Shriner and Rotimi (2018) identified a single origin for SCD. Their data suggest that the sickle mutation might have originated in the middle of the Holocene Wet Phase, or Neolithic Subpluvial, which lasted from 7,500–7,000 BC to 3,500–3,000 BC. At this time, the Sahara experienced wet and rainy conditions, encouraging mosquito breeding and thus suggesting "Green Sahara" as the most likely place where the sickle cell mutation originated, approximately 7,300 years ago. After that, a population split occurred from this original location, which is in present day Cameroon, which was later followed by the Bantu expansion around 5,000 years ago to yield the five different haplotypes of β globin gene (Shriner and Rotimi, 2018).

1.3 SCD as a red cell membrane transport disorder: ions and membrane lipids

(i) Ions

In RBCs, intracellular cation homeostasis is maintained mainly by movements of Na^+ and K^+ through various transport pathways in the membrane. A major difference between the RBCs of SCD patients and those from normal individual is their increase in cation permeability, which eventually leads to dehydration (Figure 1.4). This dehydration causes extensive polymerization due to the increase in HbS concentration as aforementioned, leading to formation of the densest sickle cells and irreversibly sickle cells with marked membrane abnormalities. Moreover, the changes in membrane integrity lead to vaso-occlusion due to increased adhesiveness of the RBCs, which is discussed later in the Chapter. Tosteson and Hoffman were the pioneers in describing and defining the abnormalities of cation homeostasis, mainly of Na^+ and K^+, in deoxygenated HbSS RBCs. The table (Table 1.2) below gives an historical account of our understanding of the altered permeability of HbSS RBCs, highlighting some of the more significant finding. Later thorough research in the field revealed these movements of cations are regulated by three important membrane transport systems present in the membrane of RBCs: (a) the Ca^{2+}-activated K^+ channel (or *Gárdos channel)* (b) the KCl cotransporter (KCC) and (c) P_{sickle}.

Table 1.2 Historical account of the transport systems present in RBCs and their actions

Authors	Findings
Tosteson, 1955; Tosteson et al., 1952	Tosteson and associates were the first to describe an abnormal monovalent cation (K^+ and Na^+) homeostasis in deoxygenated HbSS RBCs
Tosteson and Hoffman, 1960	Formulated the "pump-leak" concept using sheep RBCs. Showed swelling and bursting of RBCs was prevented by maintaining cation homeostasis inside RBCs with the help of pump.
Gardos, 1958, 1956	Showed that in human RBC membrane an electrogenic calcium-dependent potassium pathway is present. Gárdos found the channel through metabolic depletion of RBCs.
Schatzmann, 1966	Described for the first time the presence of a ATP-dependent Ca^{2+} pump using human RBCs.
Hamill et al., 1981	The patch-clamp technique was used for the first time in RBCs and provided direct electrophysiological evidence for the presence of ionic channels. First ever recording of Ca^{2+}-activated K^+ channel.
Lew et al., 1982; Schatzmann, 1983	More work on Ca^{2+} pump in RBCs and showed its effectiveness in maintaining intracellular Ca^{2+} concentration.
Ellory and Stewart, 1982	Provided evidence of at least two distinct Cl^--dependent transport pathways for K^+. Later found to be NKCC and KCC.
Mohandas et al., 1986	Provided evidence that deoxygenation induced morphological changes and formation of polymers which caused an increase in cation permeability in HbSS RBCs.
Haas, 1989	Provided evidence for the existence of potassium/sodium/two chloride cotransporter (NKCC)

Semplicini et al., 1989	Provided evidence for the existence of sodium/proton (Na^+/H^+) exchanger.
Rhoda et al., 1990	Provided evidence that deoxygenation in HbSS RBCs increased Ca^{2+} permeability which can activate channels sensitive to Ca^{2+} like the Gárdos channel.
Borgese et al., 1991	Showed the sensitivity of KCC to oxygenation in trout red cells.
Joiner et al., 1995, 1993, 1988	Showed P_{sickle} is activated in deoxygenated condition in HbSS and is permeable to inorganic mono- and divalent cations and partially inhibited by stilbenes and dipyridamole.
Gibson et al., 1998, 1994	Showed sensitivity of KCC to different oxygen tensions in equine, and in human HbA and HbSS RBCs.
Xu et al., 1994	Identified the gene encoding for NKCC.
Pellegrino et al., 1998	Identified the molecular identity of KCC in RBCs.
Hoffman et al., 2003	Provided evidence that hSK4 is the gene that codes for the Gárdos channel in human RBCs.
Browning et al., 2007a; Ellory et al., 2008, 2007	Showed P_{sickle} might also be permeable to non-electrolytes.
Vandorpe et al., 2010	Provided evidence that deoxygenation induced Ca^{2+} permeability is inhibited by *Grammastola spatulata* mechanotoxin-4 (GsMTx4).
Ma et al., 2012	Showed deoxygenation induced non-specific cation conductance was inhibited by tarantula spider toxin GsMTx4 and aromatic aldehyde in HbSS RBCs.

(a) Gárdos channel

George Gárdos provided the first evidence of the existence of a Ca^{2+}- activated K^+ channel and indeed this was the first channel to be found in the RBC's membrane. In mature human

RBCs the channel normally remains functional, unlike in many other mammals where their functional state is lost when the RBC is matured (Brown et al., 1978). However, due to very low levels of intracellular Ca^{2+} ions in HbAA RBCs the channels are mostly inactive. The activation of the channel is dependent on an increase in free intracellular Ca^{2+} concentration. Usually the free intracellular concentration of Ca^{2+} is approx 20-50nM, whilst in order to activate this channel a free intracellular concentration of about 100-150nM is required (Simons, 1976; Tiffert et al., 1988). The presence of a high capacity plasma membrane calcium pump (PMCA) in the membrane of RBCs which actively removes intracellular Ca^{2+} using energy from ATP hydrolysis, together with their relative impermeability to Ca^{2+}, is the main reason for the Gárdos channel remaining inactive (Tiffert et al., 2007; Tiffert and Lew, 2001).

The channel has also proved to have a peculiar temperature dependence in relation to saturating Ca^{2+}. The single channel conductance showed a continuous decrease in Gárdos activity with decrease in temperature. However, increased activity of the channel was observed at a saturated concentration of intracellular Ca^{2+} (10 µM) when the temperature was decreased from 35 °C-30 °C. Moreover, upon decreasing the temperature to 0 °C and reducing the intracellular Ca^{2+} in RBCs to half the EC_{50} for the Ca^{2+}, there is a marked increase in activity of the channel. This indicates that even at very low temperatures with a minimal concentration of Ca^{2+}, the Gárdos channel may be activated (Grygorczyk, 1987). Numerous times blood is kept refrigerated for storage purposes, later to be used for transfusion or analyses, and it is important to be aware that the Gárdos channel may be active and may have a harmful effect on the cell volume under these conditions.

The physiological function of the Gárdos channel in normal RBCs is still uncertain. Some studies have shown a protective role against haemolysis induced by mechanical stress and others also suggested that it is involved in reduction of cell volume in early erythroid development (Halperin et al., 1989; Johnson and Tang, 1992). Conversely, it is also described as a "suicide mechanism", triggered by increase in intracellular Ca^{2+} during clot formation in thrombotic events as well as during RBC clearance. Moreover, prolonged activation of the channel affects the rheological, rigidity and stiffness properties of the RBCs which is essential for proper circulation (Fermo et al., 2017; Glogowska et al., 2015; Rapetti-Mauss et al., 2015). In HbSS cells, the channel becomes hyperactive, as there is an elevation of intracellular Ca^{2+} due to entry via P_{sickle}. The ensuing efflux of K^+ with Cl^- following

electrically through separate anion channels, leads to dehydration and contributes to shrinking of the red cell.

(b) KCl cotransporter (KCC)

KCC is found in variety of cell types including RBCs and is a solute-linked carrier causing a coupled efflux of both K^+ and Cl^-. It is a member of the *SLC12* family with four homologous polypeptides, *SLC12A4*/KCC1, *SLC12A5*/KCC2, *SLC12A6*/KCC3, and *SLC12A7*/KCC4. KCC1, KCC3 and KCC4 are present in RBCs, whilst KCC2 is confined to neural tissues (Arroyo et al., 2013; Crable et al., 2005; Gamba, 2005; Markadieu and Delpire, 2014).

In RBCs, the activity of KCC is majorly regulated by the level of oxygen tension, although there are other factors that might contribute such as intracellular acidification, cell swelling, cell aging, concentration of Mg^{2+}, oxidation of sulfuhydryl groups and urea. KCC is activated through dephosphorylation of serine-threonine residues for which its functional state is regulated by conjugate protein kinase and phosphatase enzymes (Bize et al., 2003, 1999). Levels of Mg^{2+}-ATP are therefore important. Activity of KCC in HbAA RBCs increases with an increase in oxygen tension but is reduced substantially as the RBC matures and the transporter becomes quiescent. Its high activity in reticulocytes results in volume reduction of larger reticulocytes in the blood stream during their maturation, which is considered to be one of the crucial physiological functions of KCC. However, the opposite is observed in HbSS, where the KCC remains very active although the RBCs have matured. This occurs possibly to compensate for the ongoing anaemia, for which there is an increased number of reticulocytes in the circulation, and thus the KCC activity is high in HbSS RBCs.

Additionally, there is an altered relationship between activity of KCC and oxygen tension. The activity of KCC remains high in high oxygen tension and does show a reduction in activity as the oxygen tension decreases, but as the oxygen tension falls below 40 mmHg it becomes active again reaching a maximum at 0 mmHg (Gibson et al., 2004, 2001; Hannemann et al., 2011). This abnormal activity in HbSS RBCs causes about a 50-fold more rapid loss of K^+ and Cl^- compared to that observed in HbAA RBCs, leading to substantial loss of water osmotically and dehydration, which eventually results in sickling of RBCs.

(c) P$_{sickle}$

In 1973, Eaton et al. and Palek et al. reported independently an increased intracellular concentration of Ca^{2+} in HbSS cells during deoxygenation especially in irreversible sickle

cells (ISCs), which suggested a permeable pathway for Ca^{2+} in HbSS RBCs. Later this pathway was named as "P_{sickle}". P_{sickle} is referred to as a deoxygenation-induced non-specific cation channel and is thought to be activated by HbS polymerisation and the sickling shape change (Mohandas et al., 1986). However, deoxygenation-induced activation of P_{sickle} appears to be stochastic, occurring in only a proportion of the cells during each episode of deoxygenation (Lew et al., 1997). Radioisotope flux and electrophysiological studies of the channel have shown it is able to transport various mono- and di-valent cations such as Na^+, K^+, Ca^{2+} and Mg^{2+}, while it is inhibited by Zn^{2+} and Mn^{2+} (Browning et al., 2007b; Joiner et al., 1993; Lew and Bookchin, 2005; Ma et al., 2012). Investigations have also revealed that it is poorly permeable to other small inorganic monovalent and divalent cations (Joiner et al., 1993). Moreover, experiments with anion fluxes showed no significant effect upon deoxygenation of HbSS RBCs, which shows that anion movement through this channel is either absent or so low that it has no physiological impact (Clark and Rossi, 1990; Joiner et al., 1990). In recent times, P_{sickle} is thought to have a major influence in the overall prognosis of the disease.

As aforementioned, deoxygenation causes this channel to become abnormally active, which allows K^+ efflux and Na^+ entry into the cell (Gibson et al., 2001; Hannemann et al., 2011; Joiner et al., 1993). The greater loss of K^+ causes net solute loss and water to follow osmotically which culminates in dehydration of RBCs (Ellory et al., 2008, 2007; Joiner et al., 1993). Moreover, opening of this channel allows Ca^{2+} to enter into the cell, which then is responsible for activation of the Gárdos channel. Up-regulation of P_{sickle} also causes efflux of Mg^{2+} which then leads to activation of KCC via altered activity of the phosphorylation cascade, all of these contributing to loss of cations and water (Rhoda et al., 1990). Additionally, entry of Ca^{2+} may also lead to abnormal intracellular signalling which can be detrimental to RBCs, such as through increasing phosphatidylserine (PS) exposure (Barber et al., 2009; Cytlak et al., 2013; Henseleit et al., 1990). Since the activity of P_{sickle} is dependent on sickling of RBCs, the factors that causes polymerisation of RBCs such as low pH and temperature also increase P_{sickle} permeability even in oxygenated conditions (Joiner et al., 1993; Ma et al., 2012). Activity of P_{sickle} is also increased when oxygen tension falls below 40 mmHg, similarly to KCC (Gibson et al., 2001; Hannemann et al., 2011). It has been suggested that HbS polymerisation causes polymers to randomly come into contact with regulatory sites in the cell membrane of RBCs which causes this increase in permeability (Lew et al., 1997). However, P_{sickle} is still enigmatic as its molecular identity

and regulatory pathways are yet to be uncovered unlike the case for the Gárdos channel and KCC. The table below (Table 1.3) provides evidence of the work done on all the potential candidates until now.
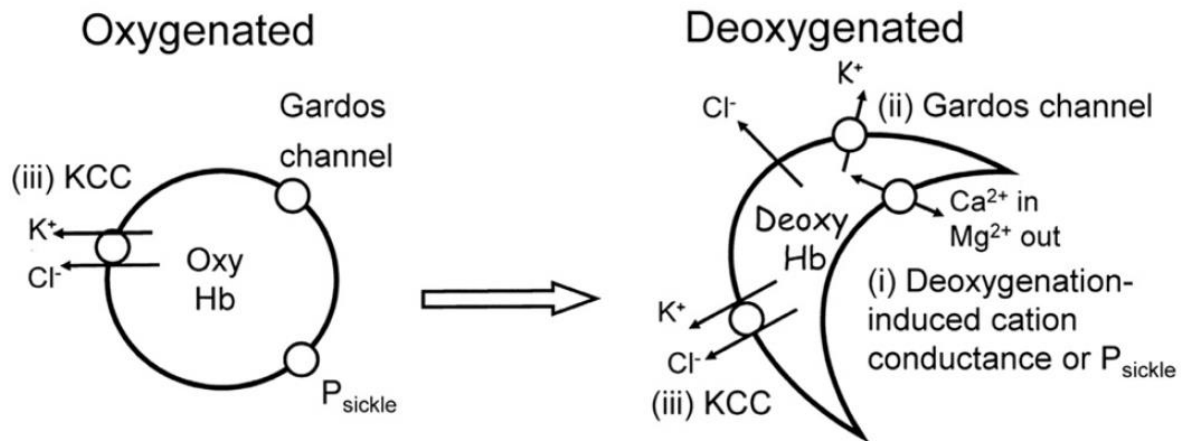
Figure 1.4: Summary of the pathways involved in solute loss causing dehydration of HbSS RBCs (Hannemann et al., 2015). HbSS RBCs in oxygenated conditions (left) shows that only KCC is active and others are inactive. However, HbSS RBCs in deoxygenated conditions (right) activates other transport systems which lead to loss of cations and water leading to dehydration, HbS polymerisation and sickling.

Table 1.3 Potential candidates for P_{sickle}

Authors	Findings
PIEZO1	
van der Harst et al., 2012	Showed a genome-wide association screen that PIEZO1 locus is responsible for affecting the RBC mean corpuscular hemoglobin concentration (MCHC) in humans.
Zarychanski et al., 2012	Showed that PIEZO1 mutation is associated with anemic disease hereditary xerocytosis.
Albuisson et al., 2013	Showed that gain-of-function of PIEZO1 phenotype increased permeability of cations in red blood cells of dehydrated hereditary stomatocytosis patients.

Andolfo et al., 2013; Archer et al., 2014	Showed that R2456H and R2488Q mutations in PIEZO1 alter mechanosensitive channel regulation, leading to increased cation transport in erythroid cells.
Ma et al., 2012	Showed that deoxygenation-induced non-specific cation conductance was inhibited by tarantula spider toxin GsMTx4 in HbSS RBCs.
Bae et al., 2013	Showed that mutation of PIEZO1 in xerocytosis patients alter the kinetics of the mechanosensitive channel.
Faucherre et al., 2014	Showed that PIEZO1 is involved in erythrocyte volume homeostasis, disruption of which results in swelling/lysis of red blood cells and consequent anemia in zebrafish.
Cahalan et al., 2015	Showed Yoda1, which is a chemical activator of PIEZO1, causes influx of Ca^{2+} and subsequent dehydration of RBCs in mice.
Cinar et al., 2015	Showed that PIEZO1 is involved in release of ATP from human RBCs by controlling the shear-induced Ca^{2+}. Moreover, showed human RBCs treated with PIEZO1 inhibitors or having mutant PIEZO1 channels, the amounts of shear-induced ATP release and Ca^{2+} influx decreased significantly.
Glogowska et al., 2017	Showed evidence of channel inactivation, alterations in mutant PIEZO1 channel kinetics, differences in response to osmotic stress, and altered membrane protein trafficking in individuals with hereditary xerocytosis (HX) and/or undiagnosed congenital hemolytic anemia with PIEZO1 mutation.
Ma et al., 2018	Provided evidence that one third of African population carry a PIEZO1 gain-of-function allele. Mice with PIEZO1 gain-of-function showed symptoms of hereditary xerocytosis and were protected from malaria.
Wadud et al., 2020	Showed that PIEZO1 is major channel for the passage of Ca^{2+} into the RBCs of sickle cell patients, utilizing Yoda1, Dooku1 and GsMTx4.

N-methyl-d-aspartate (NMDA)	
Genever et al., 1999	Showed the presence of NMDAR1 and NMDAR2D receptors in rat marrow cell and human megakaryocytes.
Makhro et al., 2010	Showed the presence of NMDA receptors in rat reticulocytes and erythrocytes.
Makhro et al., 2013	Showed the subunit composition of the NMDA receptor present during human erythropoiesis and in circulating RBCs and its function. Showed decrease in NMDA receptors in circulating RBCs compared to erythroid precursor cells.
Peripheral-type benzodiazepine receptor	
Glogowska et al., 2010	Showed the presence of maxi-anion channel with multiple conductance level in human erythrocytes.
Bouyer et al., 2011	Showed that the maxi-anion channel is a peripheral type benzodiazepine receptor. Ligands blocking this receptor in *Plasmodium falciparum* infected erythrocytes showed reduction membrane transport and conductance.
Transient receptor potential channels of canonical type (TRPC channels)	
Foller et al., 2008	Showed the presence of TRPC6 channel in human and mouse erythrocytes. Moreover, showed TRPC6 channel causes Ca^{2+} leak in erythrocytes leading to apoptosis.
Tong et al., 2008	Showed that activation of TRPC3 by erythropoietin allows entry of Ca^{2+} in human erythroid cells.

(d) PIEZO1 as a candidate for P_{sickle}

PIEZO1, which is a mechanosensitive ion channel, has been considered as a potential candidate for P_{sickle}. PIEZO1 is a multi-pass transmembrane protein with a propeller-like structure and contains a central cation selective pore, allowing Na^+, K^+ and Ca^{2+} ions to pass through (Figure 1.5). However, PIEZO1 has shown to exhibit preference for Ca^{2+} influx in

endothelial cells in response to fluid shear stress (Saotome et al., 2018; Zhao et al., 2018). Both PIEZO1 and PIEZO2 are found to be expressed in hollow organs such as the stomach, intestines, bladder and endothelial cells lining the lumen of blood vessels. PIEZO1 is involved in many important physiological functions such as blood flow, vascular maturation, blood pressure regulation, urinary osmoregulation and axonal growth. Its pathological significance has also been identified by both gain-of-function and loss-of-function, which includes haemolytic anaemia, hereditary xerocytosis, lymphoedema and arthrogryposis (Coste et al., 2013; Fotiou et al., 2015; Gudipaty et al., 2017; Li et al., 2014; Ranade et al., 2014a; Retailleau et al., 2015). PIEZO1 is also assumed to have a central role in erythrocyte volume regulation, causing efflux of ions and water osmotically. Knock-outs of PIEZO1 in mice have shown to cause vascular architecture deformity and embryonic lethality as well (Li et al., 2014; Ranade et al., 2014b).

Extracellular view   Side view   Intracellular view
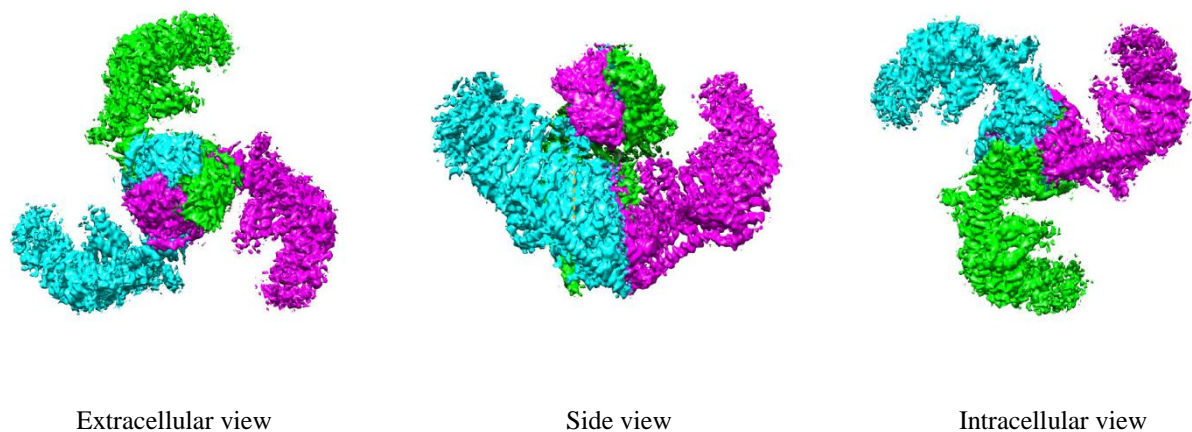
Figure 1.5: Overall structure of PIEZO1 (Zhao et al., 2018).

Consecutive deoxygenation episodes in sickle cells triggers increases in Ca^{2+} permeability and thus the deoxy-induced increase in Ca^{2+} channel/pathway was named P_{sickle}. Patch clamp studies on sickle RBCs treated with *Grammastola spatulata* mechanotoxin-4 (GsMTx4) have shown inhibitory effects on P_{sickle} activity, suggesting that it is some kind of stretch-activated channel (Andolfo et al., 2013; Archer et al., 2014; Bae Chilman et al .,2011; Vandorpe et al., 2010; Zarychanski et al., 2012). Shear stress under physiological conditions release ATP in normal RBCs which was shown to depend on external Ca^{2+} and this was inhibited by GsMTx4 suggesting the role of PIEZO1 in stimulating Ca^{2+} influx under normal physiological stress (Cinar et al., 2015). A recent paper published by Ma et al. 2018 showed that RBCs in mice expressing a mutated gain-of-function form of PIEZO1 showed RBC

dehydration and protection from cerebral malaria. Additionally, Ma et al. 2018 showed that almost one third of the African population were heterozygotes for this mutation. Based on these considerations PIEZO1 appears to be a prime candidate for P_{sickle}, however more conclusive results are required in order to be absolutely certain.

Currently there are no known endogenous agonists or antagonists of PIEZO1. However, it is known to be activated by mechanical stimuli and a recently discovered synthetic small molecule called Yoda1. Yoda1 was discovered in 2015 through high throughput screening. It is an invaluable tool to study PIEZO1 as it modulates the channel without the need for mechanical stimulation (Syeda et al., 2015). Yoda1 acts as a gate modifier by stabilizing the open conformation of the channel as a result of a wedge-like mechanism which partially activates it (Botello-Smith et al., 2019; Lacroix et al., 2018). Moreover, Cahalan et al. 2015 showed that Yoda1 in RBCs causes influx of Ca^{2+} leading to dehydration of RBCs. In this report, Yoda1 was used to study its effect on HbSS RBCs.

(ii) Membrane lipids: Phosphatidylserine (PS) in SCD

(a) Cell membrane components of RBCs

The plasma membrane of mature RBCs is made up of a lipid bilayer that interacts with integral membrane proteins. The lipid bilayer is composed of phospholipids, cholesterol and glycolipids. Cholesterol is spread out uniformly throughout the membrane and there are 4 major phospholipids that are asymmetrically arranged. The aminophospholipids, which are PS and phosphatidylethanolamine (PE), are on the inner side of the membrane whereas the choline-containing phospholipids, phosphatidylcholine (PC) and sphingomyelin, are on the outside (Figure 1.6) (Kuypers, 2007). Disruption of this asymmetry of the phospholipids can cause premature destruction of RBCs.
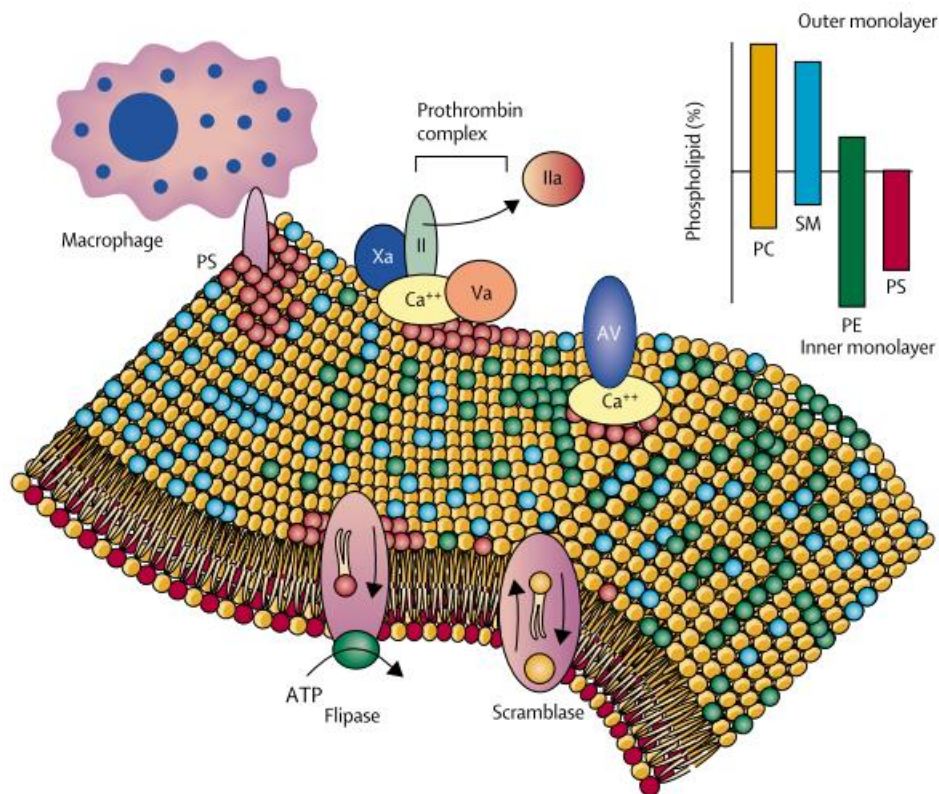
Figure 1.6: Distribution and perturbations in RBC membrane lipids in SCD (Stuart and Nagel, 2004). SM = Sphingomyelin. PC = Phosphatidylcholine. PE = Phosphatidylethanolamine. PS = Phosphatidylserine. Phosphatidylserine exposed on the cell surface forms a docking site for prothrombinase complex (factor Xa, Va, and II). Additionally, phosphatidylserine is recognised by macrophages and interacts with proteins such as annexin V, allowing its measurement by flow cytometry. Cell-surface phosphatidylserine also aids erythrocyte adhesion to the vascular endothelium.

(b) Mechanism of PS exposure

The exact mechanism of the externalization of PS on to the outer surface of RBCs is still not known, however, it is assumed that membrane proteins might facilitate the transmembrane passage. Three integral membrane proteins are involved, the floppase, the flippase and the scramblase. The floppase works against the concentration gradient by transferring PC from the inner leaflet of RBC membrane to the outside. Secondly, the flippase, which is an ATP-dependent transport system, actively pumps aminophospholipids (PS and PE) from the outside leaflet to the inner leaflet of RBCs. Thirdly, the scramblase, which is a Ca^{2+}-dependent protein, initiates transport of phospholipids in a non-specific bidirectional way, down concentration gradients.

Externalisation of PS depends on both inhibition of the flippase and activation of the scramblase. The activity of the ATP-dependent transporter protein flippase helps to maintain

the proper distribution of phospholipids in the bilayer, which causes PS to remain in the inner leaflet. It is the activity of scramblase that causes rapid disruption of the asymmetry (Middelkoop et al., 1988; Seigneuret and Devaux, 1984). In order for PS to be exposed to the surface of RBCs the activity of the flippase needs to be inhibited and *vice versa* for the scramblase. It is proposed that an increase in intracellular Ca^{2+} concentration can cause both inhibition and activation of the flippase and scramblase, respectively (Barber et al., 2009; Henseleit et al., 1990; Kamp et al., 2001). A small rise of intracellular Ca^{2+} to 0.2-1 µM has been reported to cause inhibition of flippase (Bitbol et al., 1987; Zachowski et al., 1986), whereas more recently PS scrambling has also been shown to occur at a intracellular Ca^{2+} of < 1 µM in RBCs from SCD patients (Weiss et al., 2012, 2011). This increase in Ca^{2+} concentration can be observed in sickle RBCs due to the hyperactivity of the P_{sickle} channel. In the presence of Ca^{2+}, the scramblase acts like a channel for phospholipids, causing them to move from one monolayer to the other down their concentration gradients.

From this, we can understand that Ca^{2+} has a substantial role to play in changing the asymmetry of the phospholipid, however, it is still not known exactly how elevation of Ca^{2+} brings about this change. A number of hypotheses have been proposed, including an increase in oxidative stress and depletion of ATP in RBCs from SCD patients, which subsequently leads to activation of the sphingomyelinase via platelet-activating factor (PAF). This enzyme helps in the synthesis of ceramide which is thought to increase the affinity of the scramblase to Ca^{2+} (Lang et al., 2010). Moreover, an increase in Ca^{2+} concentration can in turn activate the Gárdos channel, which causes efflux of K^+ and consequently causes water to follow out of cells, which finally results in cell shrinkage. This shrinking of cells can also be a cause for externalisation of PS.

Furthermore, it has recently been found that an increase in cytosolic Ca^{2+} in HeLa cells causes the flippase to be endocytosed. Interestingly, stimulation of the Gq receptor through histamine and serotonin in HeLa cells also cause flippase endocytosis. It is known that the Gq receptor causes an increase in Ca^{2+} concentration which causes activation of protein kinase C (PKC) (Takatsu et al., 2017). Thus, it can also be postulated that PKC may also have a significant role in inhibiting the activity of flippase and subsequently increasing the activity of scramblase. Presence of four types of PKCs which are α, ζ, ι and µ has already been shown to exist in RBCs. There is also evidence of over expression of PKC α in both cytosol and membrane of RBCs in SCD patients than in HbAA.

1.4 Pathophysiology: to highlight areas of particular interest for the thesis work or of special significance in the biology of the disease

Notwithstanding its simple aetiology, the pathophysiology of SCD is complex involving multiple organ systems and with multiple mechanisms potentially participating in producing the clinical manifestations. The following summarises some of these highlighting those of particular interest to the work of this thesis.

HbS polymerization

HbS polymerization is the underlying pathophysiological occurrence in SCD and this results in sickling of RBCs in hypoxic condition, which makes the RBCs more fragile and causes extreme dehydration of RBCs (polymerisation mechanism is explained in Section 1.1). Thus, HbS polymerisation changes the shape and physical properties of RBCs, which leads to haemolytic anaemia and vascular occlusion. Furthermore, it has also been found using Wide-field digital interferometry (WDMI), that compared to normal HbAA RBCs biconcave HbSS RBCs are 2- to 3-times stiffer, and sickled RBCs are 2-times stiffer again (Shaked et al., 2011).

HbS polymerisation is also known to alter the lipid bilayer and proteins in the membrane of the RBCs. This affects the three major membrane transport systems in RBCs, which are KCC, the Gárdos channel and P_{sickle}. Moreover, HbS polymerisation also affects the band 3 anion transport protein, which is responsible for providing structural functions as well as anion exchange. This causes membrane microvesiculation and, as a result, leads to shedding of microparticles from the plasma membrane due to the constant cellular stress to the membrane and cytoskeleton (Piccin et al., 2007; Westerman et al., 2008). These microparticles or microvesicles contains micro RNAs, cell surface markers and cytoplasmic proteins, which can cause inflammation, adhesion and coagulation (Alayash, 2018; Hebbel and Key, 2016).

Compared to HbA the oxygen affinity of HbS is lower, which further exacerbates polymerisation of HbS during deoxygenation. It is thought to occur due to the presence of high amounts of 2,3-diphosphoglycerate (2,3-DPG) in sickle RBCs. 2,3-DPG is a glycolytic intermediate which by interacting with β-globin sub-units during deoxygenation reduces the oxygen affinity of Hb including HbS (Rogers et al., 2013). Moreover, there have been reports of increased sphingosine kinase activity in sickle RBCs, which results in formation of sphingosine-1-phosphate, which also decreases oxygen affinity (Zhang et al., 2014). Further complications associated with the disease include pain, acute chest syndrome, stroke,

nephropathy, osteonecrosis, leg ulcers, and reduced lifespan (Steinberg, 1998; Vekilov, 2007). However, the frequency and severity of the problems vary amongst patients.

Phosphatidylserine exposure

RBCs are extremely sensitive cells and have a life span of about 120 days. However, for sickle RBCs the life span decreases significantly to only 10-20 days (McCurdy and Sherman, 1978; Rees et al., 2010). Although RBCs lack a nucleus and mitochondria, they still undergo programmed cell death that is similar to apoptosis in nucleated cells and which in the case of the RBC is called eryptosis. Part of the process is helped by macrophages phagocytically scavenging RBCs from the circulation (Dasgupta et al., 2009; Kuypers et al., 1996; Lang et al., 2006). These macrophages secrete lactadherin (LA) which is able to bind to the PS expressed on the surface of RBCs and induce phagocytosis. This process is stimulated at least in part by externalized PS. Externalization of PS in sickle RBCs occurs in about 2-10 % of RBCs which accounts for about 0.5-2.5 trillion RBCs in humans and is further encouraged by deoxygenation. Normally PS exposure in healthy individuals will be less than 1 % (Kuypers et al., 1998, 1996; Lubin et al., 1981).

The altered phospholipid asymmetry in membrane of RBCs in SCD plays a critical role in the complications of the disease. Increased PS exposure not only leads to reduced life span of RBCs, but it also causes increased interaction with endothelial cells and eventually resulting in vascular occlusion, one of the landmark complications of the disease. The activated endothelial cells along with leukocytes and platelets contain adhesion receptors that are able to recognize the exposed PS on the surface of RBCs resulting in increase in cell-to-cell interactions. This in turn causes increase in production of proinflammatory cytokines which leads to a chronic inflammatory state and also increases expression of procoagulant proteins which ultimately increases procoagulant activity of HbSS RBCs (Kuypers, 2007; Kuypers and de Jong, 2004). Furthermore, exposure of PS forms a docking site for prothrombinase complex, where prothrombin is cleaved to thrombin leading to blood coagulation (Zwaal and Schroit, 1997). PS exposing cells are also targets for enzymatic breakdown by phospholipases. Secretory phospholipase A$_2$ (sPLA$_2$), which is an important lipid mediator in inflammation, will hydrolyse lipids in PS exposing RBCs. This in turn will produce free fatty acids and lysophospholipids, which will have a deleterious effect on the vascular integrity and also will be used by the body to generate thromboxanes and leukotrienes (Kuypers et al., 2007; Neidlinger et al., 2006). Thus, high exposure of PS in

HbSS RBCs can promote some of the cardinal signs of SCD such as chronic anaemia, thrombosis and damage of vascular integrity (Weiss et al., 2011; Yasin et al., 2003).

Renal damage

In SCD, renal damage is one of the most common occurrences and about one third of the SCD patients develop chronic kidney disease (Falk et al., 1992). It has been reported that about 16-18 % of mortality in SCD is linked to kidney disease (Hamideh and Alvarez, 2013; Platt et al., 1994). Some of the consequences are described as early as in infancy such as hyperfiltration, hypertrophy and urinary concentrating ability (Ware et al., 2010). This steady development of renal complications over time shortens the average lifespan of SCD patients.

The conditions in the renal medulla like low partial pressure of oxygen, low pH and high osmolality are favourable for HbS polymerisation. This leads to vascular occlusion causing renal infarction with necrosis and medullary fibrosis. Moreover, changes in renal haemodynamics in SCD results in increased renal blood flow rate, plasma flow rate, glomerular filtration rate and decreased medullary perfusion. These alterations in renal haemodynamics also leads to renal enlargement. The alterations in renal haemodynamics results in increased supply of salt and water to the proximal tubule, and thus in turn cause increased tubular reabsorption of sodium and water. To maintain this high sodium reabsorption in proximal tubule the renal oxygen demand and consumption increases. The increased metabolic work stimulates mitochondrial processes and adaptive cellular responses, which eventually leads to proximal tubular and overall renal enlargement.

Most of the patients suffering from SCD develop nephrotic protein loss, losing more than 3.5 g protein in 24 h (Scheinman, 2009). Proteinuria is age dependent in SCD. It usually occurs in about a third of SCD patients in the first three decades and occurs in up to two thirds of older SCD patients. It is assessed either as microalbuminuria (30 – 300 mg.g^{-1} creatinine) or as macroalbuminuria (> 300 mg.g^{-1} creatinine). The cause of the progression from microalbuminuria to macroalbuminuria and macroalbuminuria to nephrotic-range proteinuria is poorly understood, however, the following factors are thought to play a major role: increased blood pressure (Aygun et al., 2011; Gordeuk et al., 2008; Thompson et al., 2007), low haemoglobin levels (Faulkner et al., 1995; Lebensburger et al., 2011), haemolysis (Day et al., 2012; Hamideh et al., 2014), stroke (Wigfall et al., 2000) and acute chest syndrome (Laurin et al., 2014). Other complications associated with renal damage

include tubular dysfunction leading to increased secretion of uric acid and high reabsorption of phosphates (hyperphosphataemia).

Oxidative Stress

There is also increased oxidative stress in SCD, which results in reduced lifespan of RBCs by ≥ 75 % due to haemolysis and other events. In SCD, haemloysis takes place in two ways, principally through phagocytosis by macrophages but a fraction also takes place due to intravascular haemolysis (roughly one third) (Crosby, 1955). Extracellular Hb and haem in plasma induces oxidative stress in blood vessels and blood cells. Auto-oxidation of Hb produces superoxide which is converted to hydrogen peroxide, a potent oxidative species which causes membrane damage, erythrocyte aging and more haemolysis (Alayash, 2018; Hebbel and Key, 2016). The oxidative species includes ferryl ion which promotes vasoconstriction, and extracellular Hb also scavenges nitric oxide (NO) resulting in decreased bioavailability of NO leading to vascular dysfunction (Reiter et al., 2002). Additionally, various oxidants studied previously such as nitrite and peroxynitrite have had stimulatory effects on K^+ transport systems in RBCs from HbAA individuals causing further RBC solute loss and dehydration (Kucherenko et al., 2005). Intravascular haemolysis results in release of two factors: arginase 1 and assymetric dimethylarginine (ADMA). Arginase 1 competes with L-arginine for nitric oxide synthase (NOS), and ADMA is a NOS inhibitor both resulting in reduced production of NO and hence promotes vascular remodelling with production of reactive oxygen species (Antoniades et al., 2009; Landburg et al., 2010; Luo et al., 2014).

Innate immune system activation

Due to various reasons, the innate immune system is also highly active in patients suffering from SCD (Kato et al., 2017). Toll-like receptor 4 (TLR4) is highly expressed in immune cells in SCD and has the ability to bind to lipopolysaccharide (LPS) from gram negative bacteria and causes vaso-occlusive crises. This partly explains why SCD patients suffering from infection have a high incidence of vascular occlusion. TLR4 also activates monocytes and macrophages to release inflammatory cytokines (Gladwin and Ofori-Acquah, 2014; van Beers et al., 2015). Platelet activation and thrombosis in SCD causes activation of placenta growth factor (PGF). The activated PGF binds with vascular endothelial growth factor 1 receptor on macrophages and endothelial cells, promoting release of a vasoconstrictor endothelin 1 which contributes to pulmonary hypertension (Wang et al., 2014). Finally, there

is increased expression of proinflammatory mediators from peripheral blood mononuclear cells, which are components of inflammation pathway. This occurs due to excess of intracellular iron in SCD due haemolysis and transfusion of RBCs (van Beers et al., 2015).

Altered plasma lipid levels

SCD patients are also known to suffer from dyslipidaemia, with high levels of tri-glyceride but low total cholesterol levels (Zorca et al., 2010). Individuals with SCD also have low levels of apolipoprotein A-I, which is involved in the catabolism of lipids and one of the main components of "good cholesterol", high density lipoprotein (HDL) (Tumblin et al., 2010). All of this contributes to vascular occlusion, endothelial cell dysfunction and pulmonary hypertension.

Acute chest syndrome

Acute chest syndrome is the second most common reason for hospitalization and a leading cause of death in SCD patient (Novelli and Gladwin, 2016; Platt et al., 1994). In adults, more than 10 % of cases are fatal or the syndrome can lead to serious neurological complications and multi-organ failure. The syndrome occurs due to the development of a new pulmonary infiltrate of at least one lung segment accompanied by fever and respiratory symptoms. It is multifactorial, but occurs mainly due to infection, fat embolism and vaso-occlusion. A study conducted in 30 participating centres revealed that about a third of cases of acute chest syndrome were due to infections and a tenth due to fat embolism (Vichinsky et al., 2000). Various microorganisms such as bacteria, virus, mycoplasma and chlamydial were responsible for the infection, hence macrolide antibiotics are thought to be the preferred treatment (Lowenthal et al., 1996). Moreover, the syndrome is hypoxia-driven, for which the vasculature constricts in the lungs leading to more polymerisation of HbS and eventually slowing capillary transit time (Stuart and Setty, 2001, 1999).
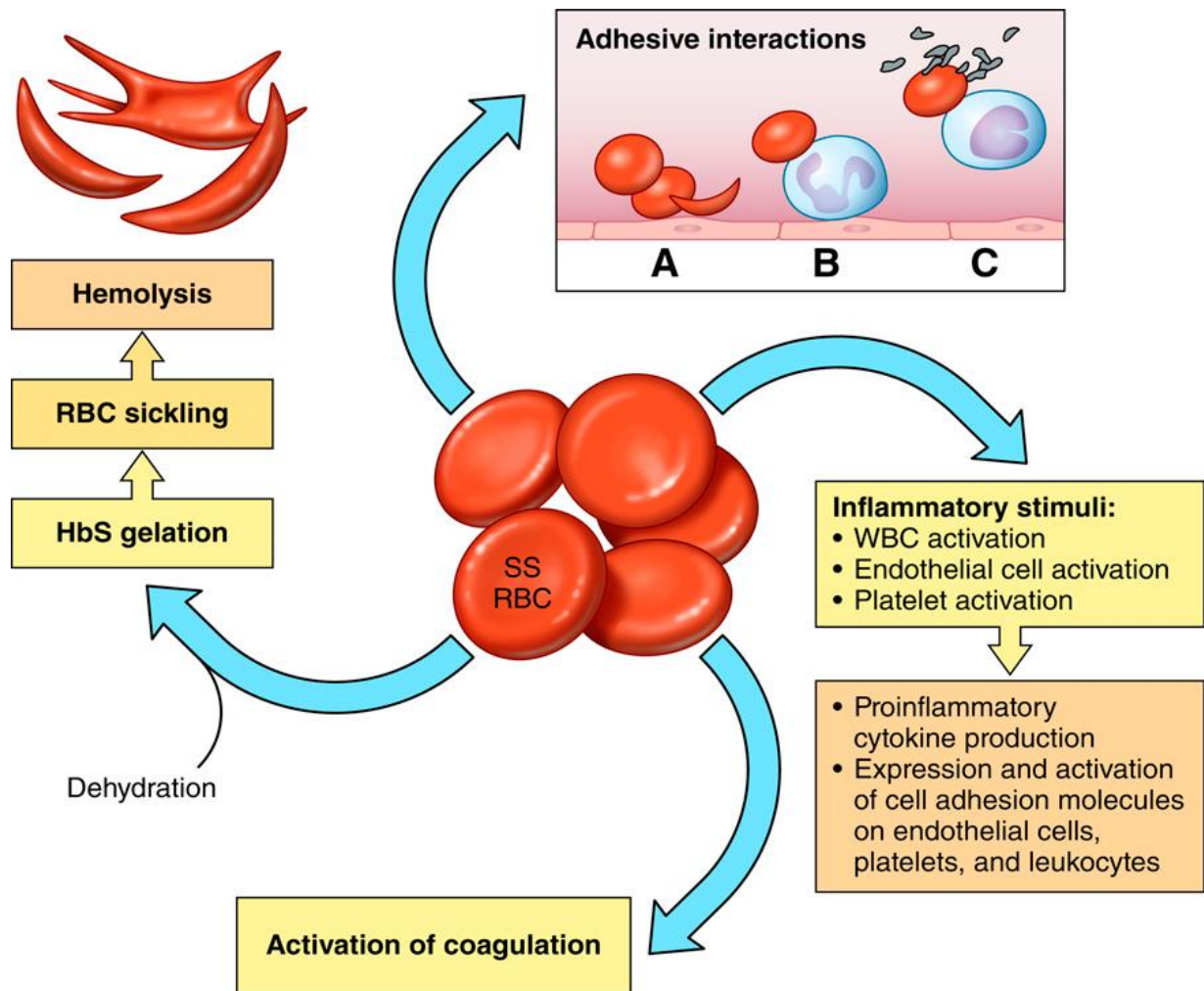
Figure 1.7: Multiple pathophysiological pathways in SCD (Telen, 2015). This Figure shows the various pathophysiological pathways that become active in SCD which leads to serious complications such as RBC polymerisation, inflammation and vascular occlusion. It also helps to identify the therapeutic targets to treat these complications. (A) HbSS adhesion to endothelial cells and neutrophils. (B) HbSS form aggregates with monocytes and platelets. (C)This stimulates abnormal signalling leading to release of more adhesion proteins from HbSS RBCs leading to increased adhesion interaction, cell-to-cell interaction and release inflammatory mediators.

1.5 Treatment strategies for SCD

After obtaining Food and Drug Administration (FDA) approval in 1998, hydroxyurea (HU; also known as hydroxycarbamide), a chemotherapeutic agent previously used for chronic myeloid leukaemia and polycythaemia has been the primary drug used to treat SCD. Although the mechanism by which HU works is still uncertain, evidence has shown that HU is a ribonucleotide inhibitor that increases HbF levels by stimulating expression of the gamma chain of haemoglobin. In adult SCD patients an increase in concentration of HbF is seen from

5 % at baseline to 15 % while in children it can reach even higher levels (Charache et al., 1992; Hankins et al., 2014). This reduces the concentration of HbS polymer formation causing only some of the milder forms of SCD (see section 1.2), and thus helps decrease vascular occlusion (Brawley et al., 2008). Nevertheless, the concentration of HbF achieved is still lower than the optional required therapeutic level, which is 30 % to prevent fully the complications of SCD. However, the exact mechanism by which HU works is not completely understood. In addition, the associated toxic effects such as its potentially teratogenic effects, leg ulcers, renal failure, etc. are detrimental for patients and up to 50 % of patients will not benefit from long term treatment of HU (Rees, 2011). It is therefore usually restricted to more severely affected individuals. An alternative therapy that is also used regularly is blood transfusion, which helps to reduce stroke and vascular occlusion, by replacing HbSS RBCs and improving blood flow. A study conducted to measure the efficacy of blood transfusion compared to treatment with HU in children with SCD, was stopped prematurely due to high number of strokes in HU group (Ware et al., 2011). However, its potential benefits have been limited by its adverse effects like iron overload and alloimmunization (Hyacinth et al., 2015, 2014).

In SCD, non-steroidal anti-inflammatory drugs (NSAIDs) and opioids are also used to treat the episodes of pain, and, as patients are prone to infections, antibiotics such as penicillin are also prescribed routinely (Ballas et al., 2012; Gaston et al., 1986), whilst vaccination against the commoner pathogens such as pneumococcus are also very valuable in protecting children. Although, in more advanced countries, the life expectancy of people suffering from SCD has improved remarkably in the last 10 years due to advances in medical practice (Figure 1.8), however, quality of life of patients has still remained very poor (Hamideh and Alvarez, 2013) and morbidity and mortality remains high in poorer areas of the world where SCD is most prevalent. Patients suffer from pain, fatigue and poor physical functioning from early childhood onwards. Thus, more research is required into understanding the pathogenesis of the disease in order design a better therapeutic target or provide optimum multi-drug therapy, which seems to be healthier approach.
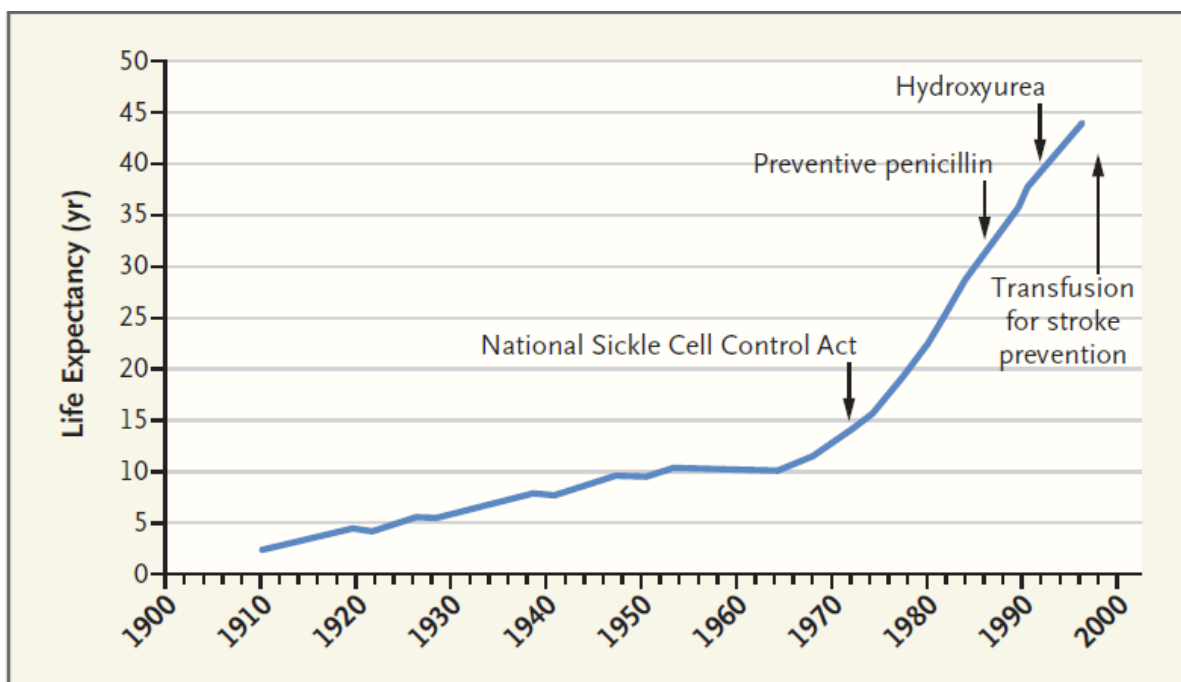
Figure 1.8: Increase in life expectancy of patients with sickle cell disease (Wailoo, 2017).

Membrane transporters and channel inhibitors

Membrane transporters and channels in RBC have also been targeted in order to reduce solute loss and dehydration. Mg^{2+} supplementation showed promising results in mice as it inhibited KCC and reduced dehydration (De Franceschi et al., 1996). Initial treatments with Mg^{2+} pidolate in 10 patients showed decreased KCC activity with increased concentration of Mg^{2+} and K^+ in RBCs. More studies on treating 20 patients with Mg^{2+} pidolate for six months resulted in decreased dehydration and painful episodes (De Franceschi et al., 2000). However, further studies of Mg^{2+} supplements in clinical trials did not bring any significant change to RBCs (De Franceschi et al., 1997; Hankins et al., 2008).

In 1992, Alvarez and colleagues were the first to show the inhibitory effects of clotrimazole on the Gárdos channel and later this was confirmed by experiments which showed it displaced bound 125I-charrybdotoxin, a specific ligand of the channel (Brugnara et al., 1993). Clotrimazole is also used to treat systemic mycotic infection and tropical treatment for vaginal mycotic infections. However, due to the presence of an imidazole ring, it induced irreversible liver damage when administered for prolonged periods (Brugnara et al., 1996; De Franceschi et al., 1994). Later, a clotrimazole analogue named Senicapoc was developed without the ring imidazole, which proved to be a powerful inhibitor of Gárdos channel. It successfully went through clinical trial phases 1 and 2, but, using episodes of pain and hospitalisation as the end

point, failed to show any clinical benefit for patients suffering from SCD in phase 3 trials (Ataga et al., 2011, 2008, 2006). NS1652 is another candidate, which blocks Cl^- conductance with high affinity for that in RBCs. This leads to inhibition of K^+ movement through the Gárdos channel, as Cl^- efflux is required to accompany that of K^+, otherwise K^+ loss is reduced by the marked hyperpolarisation of the RBC membrane, without directly affecting the Gárdos channel. *In vitro* application of this compound causes reduced loss of KCl from deoxygenated sickle cells (Bennekou et al., 2000). Similar results are seen in sickle mice treated with NS3623 which has the same mechanism as NS1652, leading to an increase in intracellular concentration of K^+ and Na^+ in RBCs and fewer numbers of dense RBCs (Bennekou et al., 2001). Finally, deoxygenation-induced cation fluxes across the RBCs membrane is inhibited by dipyridamole a derivative of the pyrimidine, which probably acts through inhibiting the anion exchanger (or band 3) which is also implicated in conductive Cl^- efflux. Dipyridamole at 10 µM inhibited 65 % of net fluxes of Na^+ and K^+ in deoxygenated HbSS RBCs (Joiner et al., 2001).

Targeting cell adhesion

Another popular therapeutic target for SCD is inhibition of cell adhesion, which will help to reduce vascular occlusion and release of inflammatory mediators. Selectins have emerged as a potential target, as selectins allow adhesion of cells and also activate leukocytes (Zennadi et al., 2008). Human and animal studies have provided evidence that inhibition of both P-selectin and E-selectin lead to inhibition of vaso-occlusion.

Recently, NICE (National Institute of Health & Care Excellence) has recommended crizanlizumab to be used in the treatment of SCD on its own or alongside HU. Crizanlizumab is a humanized monoclonal antibody that can bind to P-selectin and therefore can block cell-to-cell interaction that leads to vaso-occlusive crises in SCD. Many selectin inhibitors are in various stages of trial, but Rivipansel has been the most successful one to date. In clinical trial phases 1 and 2, it has been shown to reduce vascular occlusion, reduced pain and achieved shorter stays in hospital. Currently it is now in clinical trial phase 3 (Chang et al., 2010; Telen et al., 2015; Wun et al., 2014). There are others that are in the pipeline such as heparin analogues which act as a P-selectin blocker and are currently in phase 2 of clinical trials (Matsui et al., 2002). Sevuparin has been one such analogue that retains the P-selectin binding ability while lacking the anti-coagulant property of heparin. Sevuparin, initially being trialled as an adjunct therapy for malaria, did not show encouraging signs in phase 2 trials conducted for SCD (Batchvarova et al., 2013; Leitgeb et al., 2011).

Non-specific inhibitors of adhesion receptors, like poloxamer 188 that acts like a surfactant and alters the interaction of cells, have also been under investigation. Poloxamer 188 moderately reduced duration of painful episodes in a phase 3 trial. It is now being investigated in second stage of phase 3 trial (Cheung et al., 2004; Orringer et al., 2001). It has also been suggested that β2 adrenergic signalling pathway activate red cells adhesion receptors. Thus drugs like propranolol which blocks the β2 adrenergic pathway is also being investigated for its effect on SCD (De Castro et al., 2012). However, it has failed to show any significant difference in lowering the activation of adhesion receptors in red cells in SCD.

Antisickling agents

There have also been positive reports on the use of anti-sickling agents in SCD directly targeting Hb. Usually in SCD, as for normal Hb, HbS in RBCs is in one of two states: (i) the tense state (T) in which the rigid polymers are formed and which occurs following deoxygenation, and (ii) the relaxed state (R) under oxygenated conditions in which polymer formation has not taken place and the affinity of Hb for oxygen is high, (MacDonald, 1977; Safo et al., 2011). Anti-sickling agents such as the aromatic aldehyde 5-HMF (5-hydroxymethylfurfural) and GBT440 have ensured prolonged duration of Hb in the R state, by increasing the oxygen affinity of HbS, resulting in less polymer formation, vascular occlusion and cell adhesion (Dufu et al., 2018; Hannemann et al., 2014; Hutchaleelaha et al., 2019; Oksenberg et al., 2016; Patel et al., 2014). Sanguinate, which is a polyethylene glycol-modified form of bovine Hb, provides oxygen to oxygen deprived cells and tissues, and reduces sickling by producing carbon monoxide which is delivered locally to Hb. Attached carbon monoxide prevents HbS polymerisation and is also known to produce anti-inflammatory effects. Sanguinate has been given the orphan drug status by FDA and is now in phase 2 clinical trial after a successful phase 1. However, further clinical investigation is required for these to be used as a permanent therapy for SCD.

Antioxidant therapy

Antioxidant therapy has proven beneficial in many cases, as the disease causes increase in oxidative stress markers, and it also decreases antioxidant levels which provide protection from oxidative stress. Early and life-long treatment with antioxidants for SCD patients could be promising, as the free radical starts accumulating at an early stage and the intensity of its effect increases radically with time. Table 1.4 below gives the summary of antioxidants under investigation.

Table 1.4 Summary of antioxidants under investigation

Therapy	Findings	Reference
Iron Chelators (Deferiprone and Deferasirox)	• Deferiprone removes iron from the membrane of sickle cell RBCs, which results in decreased lipid peroxidation and hemichrome formation. • Deferasirox decreases lipid peroxidation and also showed increased overall antioxidant capacity levels.	• Shalev et al., 1995 • Belini et al., 2012
Glutamine	• Glutamine showed significant increase in NAD redox potential and NADH level as well.	• Niihara et al., 1998 • Niihara et al., 2018
α-lipoic acid	• Protects RBCs from peroxyl radical induced hemolysis and also increase GSH (glutathione) levels in cells. • Increase antioxidant gene expression such as NF-κB .	• Marangon et al., 1999 • Vichinsky, 2012
Acetyl-L-carnitine	• Protects sickle RBCs from peroxidative damages also allows RBCs to hold its shape at lower oxygen tensions.	• Ronca et al., 1994
Statins	• Provided protective effect from oxidative injury by increasing NO metabolites and C-reactive protein.	• Hoppe et al., 2011
N-acetylcysteine	• Increased levels of GSH and also decreased hemolysis.	• Pace et al., 2003 • Nur et al., 2012

Vitamin C	• Vitamin C supplementation decreased production of ROS and also resulted in increased levels of GSH. This resulted in prevention of hemolysis.	• Amer et al., 2006
Melatonin	• Increased levels of antioxidant and decreased rate of hemolysis.	• da Silva et al., 2015
Flavonoids (quercetin, rutin and morin)	• Showed inhibitory effect on hemolysis due to reduce thiol (-SH) group oxidation in membrane of RBCs.	• Asgary et al., 2005

Stem cell and gene therapy

Haematopoietic stem cell transplantation (HSCT) and gene therapy are other approaches that offer potential cure for the disease. Over the years, HSCT has been performed on over 1000 patients and over 90 % were cured (Gluckman et al., 2017). Thus, it is now a widely accepted therapeutic option. However, the severe lack of available donors, technical difficulty and expense only allow a few patients to have access to this option, making it unavailable for the majority (Gragert et al., 2014; Justus et al., 2015; Walters et al., 1996). Haploidentical transplantation using blood-forming cells from half-matched donors was thought to have the potential to overcome the problem. However, there is higher risk of graft rejection in SCD patients due to an already hyperactive immune system because of anaemia and chronic inflammation. Nonetheless, there are ongoing trials to optimize the haploidentical model using pre-transplant immunosuppressive therapy, non-myeloablative regimens, etc.

Gene therapy mainly includes two approaches: (i) β^S globin gene correction in order to make normal adult haemoglobin (HbA) or (ii) induction of HbF expression. Studies in mice have revealed successful gene correction leading to production of HbA. There are currently eight clinical trials investigating genetic manipulation methodologies to treat SCD. BCL11A is reported to be a potent repressor of HbF production. Several studies have shown that loss of BCL11A led to a significant increase in HbF production (Basak et al., 2015; Sankaran et al., 2009, 2008; Xu et al., 2011). However, the drawback of targeting BCL11A is that its normal

physiological functions include neuron development and B-cell lymphopoiesis, which might be affected with the potential of significant side effects (John et al., 2012; Liu et al., 2003; Wiegreffe et al., 2015; Yu et al., 2012). There are currently two studies (NCT02186418 and NCT03282656) which are investigating the virally mediated γ-globin modification in SCD patients. Preliminary data from NCT03282656, which reduced expression of BCL11A by 90 %, showed increased expression of HbF from about 30 % to 60 % with expression of γ globin mRNA in erythroid cells of over 80 % (Brendel et al., 2016; Esrick et al., 2018; Leonard et al., 2020).

1.6 Hypothesis and aims

As aforementioned, it has been well established that PS exposure is higher in HbSS RBCs, compared to HbAA ones, in certain circumstances. This thesis investigates the conditions, which stimulate PS exposure and attempts to identify the mechanism and signalling processes by which PS exposure takes place in HbSS RBCs. Initially conditions in the renal medulla were examined as kidney is often the most affected organ in SCD and the pathogenesis might be due, in part or to a larger extent, to high PS exposure. Additionally, this thesis will try to identify the role of P_{sickle} in PS exposure of HbSS RBCs and will investigate the possible role of PIEZO1, a mechanosensitive sensitive ion channel, as a molecular candidate for P_{sickle}. Whilst elevated Ca^{2+} concentration is considered essential for PS exposure, however, it is still not certain exactly how Ca^{2+} enters RBCs nor the intracellular signalling process by which it leads to externalisation of PS. Better understanding of the mechanism of PS exposure stimulation or activation will help to identify potential pharmacological targets to mitigate the deleterious effects of the condition.

1.6.1 Aims

1. To determine the role of unique environment encountered by HbSS RBCs in the renal medulla in stimulating PS exposure.

2. To determine the involvement of PIEZO1, Ca^{2+} and other second messenger pathways in inducing PS exposure in HbSS RBCs.

1.6.2 Specific aims

Chapter 4: Investigation of different pHs and oxygen tension in sickling and PS exposure of HbSS RBCs.

Chapter 5: Investigation of hyperosmotic shock, hypertonicity and urea in sickling and PS exposure of HbSS RBCs.

Chapter 6: Investigation of PIEZO1-induced Ca^{2+} entry and the role of Ca^{2+} and protein kinase C (PKC) in PS exposure in HbSS RBCs by utilizing pharmacological activators and inhibitors.

Chapter 7: Investigation of sphingomyelinase (SMase) signalling pathway in PS exposure in HbSS RBCs.

2 Materials

2.1 Blood samples

Anonymised, discarded, routine blood samples were collected in EDTA anticoagulant from normal HbAA or individuals homozygous for HbSS, with consent and ethical permission (16 / LO / 1309) from King's College Hospital, kindly provided by Prof. David C. Rees. Samples were stored at 4 °C and used within 72 h of collection.

2.2 Chemicals and solutions

2.2.1 Chemicals

Name	Supplier	Application
Fluorochromes		
Alexa Fluor647 anti-Hb α chain	Abcam, Cambridge, UK	Anti-Hb α chain can recognize and bind to alpha chain of haemoglobin, excitation 652 nm, emission 668 nm (red)
Anti-glycophorin A phycoerythrin	BD Biosciences, San Jose, CA, USA	Anti-human glycophorin A receptor antibody, for recognition of RBCs, excitation 488 nm, emission 575 nm (yellow)
Bovine lactadherin fluorescein isothiocyanate (LA-FITC)	Innovative Research, Inc. Peary Court, USA	Bovine LA conjugated with fluorescein isothiocyanate (FITC) binds to phosphatidylserine (PS), excitation 413 nm, emission 519 nm (green)
Fluo-4AM (acetoxymethyl ester)	Invitrogen, Thermo Fisher Scientific, UK	Intracellular calcium dye, excitation 494 nm, emission 506 nm (green)

Phalloidin-iFluor 647	Abcam, Cambridge, UK	Phalloidin-iFluor 647 is a phalloidin conjugate that binds to actin filaments known as F-actin, excitation 650 nm, emission 668 nm (red)

Agonist, antagonists and inhibitors

Calphostin C	Abcam, Cambridge, UK	Potent cell permeable inhibitor of protein kinase C. Less specific for atypical PKC
Chelerythrine chloride	Abcam, Cambridge, UK	Cell permeable inhibitor of protein kinase C, broad spectrum
C_6-Ceramide	Abcam, Cambridge, UK	A breakdown product of sphingomyelin by sphingomyelinase (SMase)
3,4-Dichloroisocoumarin	Sigma-Aldrich, UK	Inhibitor of SMase
Dooku1	Tocris, Abingdon, UK	Competitive antagonist of Yoda1
Grammastola spatulata mechanotoxin-4 (GsMTx4)	Tocris, Abingdon, UK	Inhibitor of stretch-activated cation channels

Yoda1	Tocris, Abingdon, UK	Chemical activator of PIEZO1 channel
Other reagents		
Bromo-A23187	Calbiochem	Divalent cations (Ca^{2+} & Mg^{2+}) ionophore, non-fluorescent derivative of A23187
tert-butyl hydroperoxide (*t*BHP)	Sigma-Aldrich, UK	A lipid soluble radical forming oxidant, which causes rapid and intensive lipid peroxidation of cell membrane
Ethylene glycol tetraacetic acid (EGTA)	Sigma-Aldrich, UK	Calcium chelator
Glutaraldehyde	Sigma-Aldrich, UK	Cellular fixing agent
Potassium ferricyanide	BDH, Poole, UK	Used in oxygen saturation measurements to displace O_2 form haem
Sodium *ortho*-vanadate	Sigma-Aldrich, UK	Inhibitor of P-type ATPases, including the plasma membrane Ca^{2+} ATPase (PMCA), Na^+/K^+ pump and flippase

2.2.2 Buffers

All the solutions used had an osmolality of 290 mOsm.kg^{-1} ± 5 unless otherwise stated. Various pHs (6.0, 6.4, 6.8, 7.0, 7.4) were used at either room temperature (RT) or 37 °C and were adjusted by addition of NaOH or HCl.

1. Wash buffers:
    A. **High potassium 4-(2-hydroxyethyl)-1-piperazineethanesulfonic acid (HEPES)-buffered saline (HK-HBS):**
        90 mM KCl
        50 mM NaCl
        10 mM HEPES
        10 mM Inosine
        0.15 mM MgCl$_2$
    B. **Low potassium HEPES-buffered saline (LK-HBS):**
        4 mM KCl
        140 mM NaCl
        10 mM HEPES
        10 mM Inosine
        0.15 mM MgCl$_2$
2. **Ca^{2+} LK-HBS**
    1.1 mM CaCl$_2$ in LK-HBS
3. **Ca^{2+}-vanadate LK-HBS**
    1.1 mM CaCl$_2$ and 1 mM *ortho*-vanadate in LK-HBS
4. **Vanadate LK-HBS**
    1 mM *ortho*-vanadate in LK-HBS
5. **Urea LK-HBS (490 -1200 mOsm.kg^{-1})**
    200 mM, 600 mM & 900 mM urea in LK-HBS
6. **Sucrose LK-HBS (940 mOsm.kg^{-1})**
    650 mM sucrose in LK-HBS
7. **Sucrose-urea LK-HBS (940-1840 mOsm.kg^{-1})**
    650 mM sucrose 200 mM / 600 mM / 900 mM urea in LK-HBS
8. **NaCl LK-HBS (1200 mOsm.kg^{-1})**
    600 mM NaCl in LK-HBS

9. **NaCl-urea LK-HBS (1200-1500 mOsm.kg^{-1})**

   300 mM NaCl 600 mM / 900 mM urea in LK-HBS

10. **Lactadherin (LA-FITC) labelling buffer, pH 7.4 at RT**

    16 nM LA-FITC and 1 mM vanadate in incubation buffer

11. **Phalloidin-iFluor 647 labelling buffer, pH 7.4 at RT**

    1:400 dilution in incubation buffer (stock concentration is 1 mg.ml^{-1})

12. **Alexa Fluor647 anti-Hb α chain labelling buffer, pH 7.4 at RT**

    1:100 dilution in incubation buffer (stock concentration is 0.5 mg.ml^{-1})

13. **Measurement of sickling**

    0.3 % glutaraldehyde in LK-HBS

2.3 Major equipment

- Advanced Micro-Osmometer 3MO plus, Advanced Instruments Inc., Norwood, MA

- Balances: Sartorius, Basic BA61 and Sartorius MC210P, Bradford, MA

- BD Vacutainer® test tubes, Becton Dickinson, Plymouth, UK.

- Centrifuge 5415D, Eppendorf Ltd, UK.

- Gas mixing pump: H. Wösthoff Messtechnik GmbH, Bochum, Germany.

- Kutofix C tonometers, Eschweiler, Kiel, Germany.

- Bright field microscope: Nikon eclipse E400, 20x0.40, ∞/0.17 WD1.3, Surrey, UK.

- pH meter: SevenEasy and combination liquid filled electrodes, InLabRMicro, Mettler Toledo AG, Schwerzenbach, Switzerland

- Water bath: Grant, Grant Instruments (Cambridge) Ltd, Shepreth, Cambridgeshire, UK and VWR Techne, Bibby Scientific Ltd., Stone, Staffordshire. UK.

- Flow Cyotometer BD Accuri^{TM} C6 Plus BD Biosciences, San Jose, CA, USA.

- Clark –type electrode coupled to an oxygen meter CB1-D3, Hansatech, King's Lynn, UK.

- iMark Mircoplate Absorbance Reader BIO-RAD Laboratories Ltd. Station Road, Watford, Hertfordshire. UK.

2.4 List of Software

- BD Accuri C6
- GraphPad prism version 9
- Microsoft Office 2016

3. Methods

3.1 Preparation of RBCs

Samples were washed three times in HK-HBS by centrifuging for 3 min at 600 g, followed by careful withdrawal of the supernatant to remove plasma and buffy coat. A final wash was carried out in the incubation buffer.

3.2 Testing the linearity of gas mixer

The gas mixer was used extensively in this study, hence, testing the accuracy of the H. Wösthoff Messtechnik was necessary (Figure 2.1). This was done by connecting the gas mixer to the Clark-type electrode coupled to an oxygen meter CB1-D3 and the oxygen tension was measured. The Clark-type electrode was assembled. The gas mixer was set to 100 % air and a very thin layer of HK-HBS was added to the electrode chamber and the output results were recorded. This was repeated with a range of O_2 tensions from 100 % - 0 % air (replaced with N_2). A linear regression was plotted and the equation for the line is $y = 1.027*x + 3.279$.
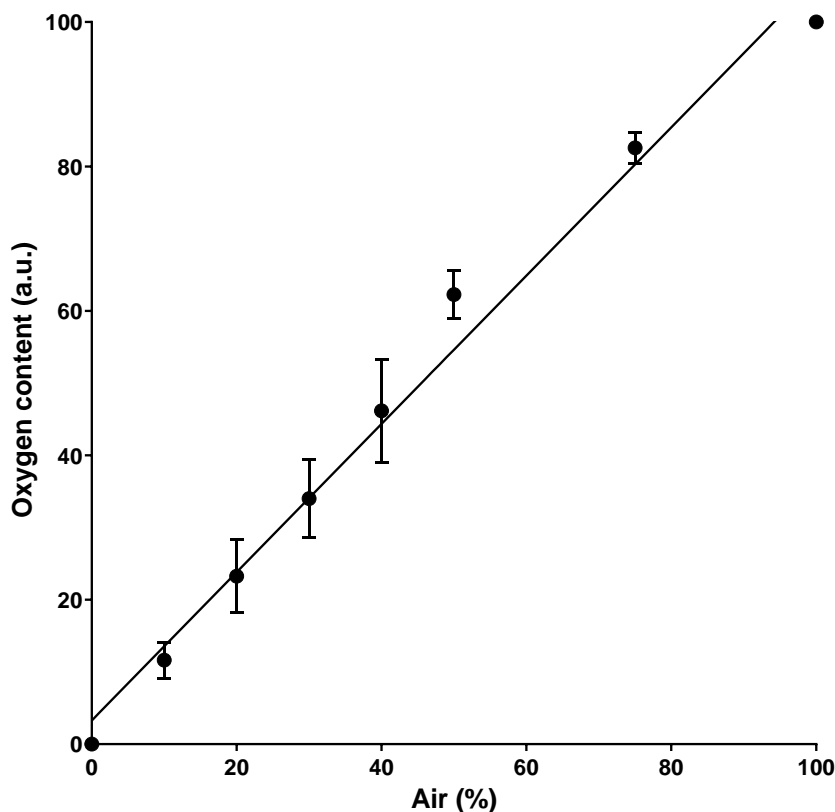
Figure 2.1: Linearity test of the H. Wösthoff Messtechnik gas mixer. The gas mixer was connected to the Clark-type electrode coupled to an oxygen meter CB1-D3 and oxygen readings as air was replaced with N_2. Oxygen readings are given in arbitrary units (a.u.). Symbols represent means ± S.E.M, n = 3.

3.3 Oxygen saturation curve

To measure oxygen saturation, aliquots of RBC suspensions (10 % Hct, 1 ml) were removed from tonometers and transferred to a Clark-type electrode coupled to an oxygen meter (CB1-D3). In this case, the measuring chamber contained saponin (0.3 % w/v) to lyse RBCs and potassium ferricyanide (0.6 % w/v) to oxidise haem Fe^{2+} to Fe^{3+}, which then displaces Hb-bound O_2. The O_2 content of fully oxygenated blood was measured in RBC suspensions equilibrated with air. The percentage oxygen saturation at other oxygen tensions was calculated in relation to that of fully oxygenated RBCs.

In this control experiment (Figure 2.2), the Hb oxygen saturation change over time in RBCs from HbSS patients was investigated. Initially the sample was equilibrated at fully oxygenated conditions (100 % air), later the sample was exposed to fully deoxygenated conditions (0 % air) and Hb oxygen saturation change over time was measured. It took only 15 min for RBCs from HbSS patients at 10 % Hct to fully deoxygenate (0 % oxygen saturation) and remained same for the duration of the experiment (30 min). It can also be observed 50 % change in oxygen saturation was achieved between 3-4 min.
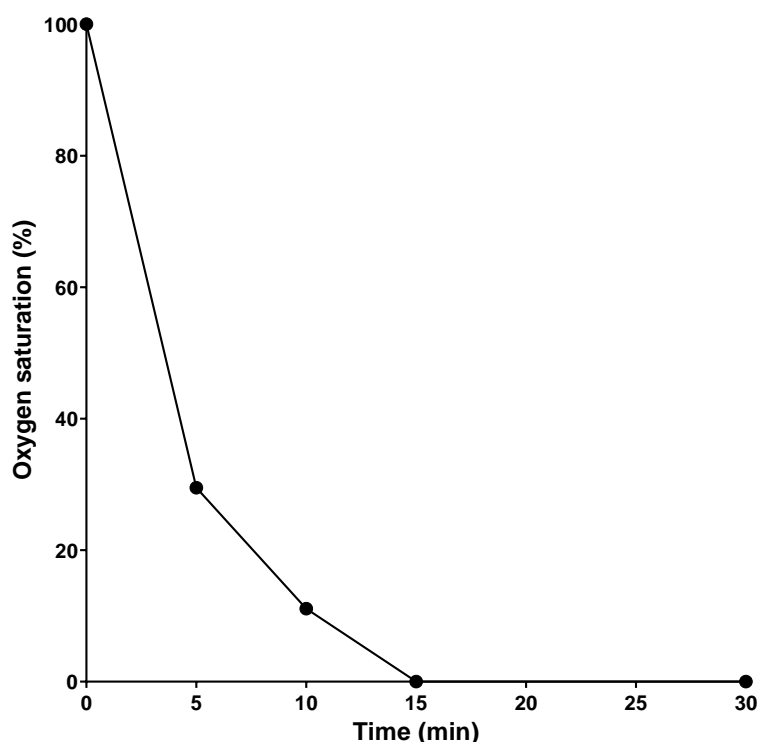
Figure 2.2: Time course of the change in Hb oxygen saturation of RBCs from HbSS patients. RBCs (10 % Hct, 1 ml) were equilibrated in Eschweiler tonometer initially at 100 % air and later deoxygenated to 0 % air. At 0, 5, 10, 15 and 30 min in 0 mmHg aliquots of RBCs were removed to measure oxygen saturation using a Clark-type electrode. Symbols represent a single determination representative of two others.

3.4 Determining measurement gates for RBCs in flow cytometry

The mouse monoclonal IgG antibody against human glycophorin A receptor (known as CD235a) conjugated to a yellow fluorochrome was used. Suspensions of RBCs at 0.5 % Hct, were diluted to 0.01 % Hct into a solution containing HK-HBS and anti-glycophorin A-phycoerythrin (stock concentration is 0.2 mg.ml^{-1}; GlyA- phycoerythrin). Similarly, a control tube was setup without the GlyA- phycoerythrin. Both were incubated for 15 min at RT in the dark. Then RBCs were pelleted for 7 s at 11,000 g and resuspended into HK-HBS. Samples were kept on ice until analysis by flow cytometry. Phycoerythrin label was visible in the FL-2 channel. Mature, non-nucleated RBCs are characteristically GlyA positive.

### 3.5 PS exposure

Different conditions were tested on HbSS RBCs to study their effects on PS exposure. Both the plasma membrane calcium ATPase or pump (PMCA) and the flippase were inhibited to study the phospholipid scrambling process (Barber et al., 2009; de Jong et al., 2001). Thus, sodium *ortho*-vanadate (vanadate), was used in most experiments (Lew et al., 2002). Additionally, the presence of vanadate prevents any ATP-depletion by either or both enzymes (Tiffert and Lew, 2001). Previous control experiments showed that vanadate does not interfere with lactadherin binding (Weiss et al., 2012).

3.5.1 Hypoxia-induced PS exposure

For this experiment, suspensions of RBCs were diluted to 0.5 % Hct in Ca^{2+}-vanadate LK-HBS (specified pH at 37 °C). The mixtures were then transferred into the Eschweiler tonometers and incubated for 80 min at 37 °C at the specified oxygen tension. Every 20 min aliquots of RBC suspension were diluted to 0.05 % Hct in Ca^{2+}-vanadate LK-HBS (pH 7.4 at RT) and later processed to measure PS exposure.

Deoxygenation of RBCs was carried out either by using rotating Eschweiler tonometers or test tubes. Different oxygen tensions were achieved by using the H. Wösthoff Messtechnik gas mixing pump. For experiments investigating the effect of deoxygenation on PS exposure, suspensions of RBCs (specified Hct) were deoxygenated with warmed (37 °C) humidified N$_2$ (flow rate 2-4 bubbles in the outlet tubing submerged in water) for up to 80 min, in the presence of specified buffer, in test tubes or rotating (160-180 revolutions.min^{-1}) Eschweiler tonometers. Humidified gas is necessary to prevent dehydration of the samples. Additionally, all glassware and tubing were submerged and kept at the same temperature (37 °C) to prevent condensation. Samples were later collected at various time points for determination of PS exposure by flow cytometry.

3.5.2 pH-induced PS exposure

Suspensions of RBCs were diluted to 10 % Hct in Ca^{2+}-vanadate LK-HBS buffer at either pH 7.4 or 6.8 at 37 °C and equilibrated in tonometers at the required oxygen tension for 20 min. At time 0 min and 20 min, aliquots of RBCs were removed and diluted to 0.05 % Hct in Ca^{2+}-vanadate LK-HBS and later processed to measure PS.

After 20 min, RBC suspension from Eschweiler tonometers were transferred to four test tubes each containing Ca^{2+}-vanadate LK-HBS buffer (diluting to 0.5 % Hct) at four different pHs (7.4, 7.0, 6.8 and 6.0) at 37 °C and the incubation continued for a further 60 min at the same oxygen tension. Every 20 min aliquots of RBCs were diluted to 0.05 % Hct in Ca^{2+}-vanadate LK-HBS (pH 7.4 at RT) and later processed to measure PS.

For experiments, where suspensions of RBCs in specified buffer (5-10 % Hct) were deoxygenated initially in Eschweiler tonometers before diluting them into test tubes (final 0.5 % Hct), the test tubes were pre-equilibrated with N_2. The test tubes were closed with a rubber stopper allowing access for thin plastic catheter tubes used to flush the test tubes with warmed humidified N_2. After the addition of RBCs, bubbling of the suspension was avoided to prevent RBC lysis. Instead, gas flow was maintained just above the solution.

3.5.3 Yoda1-induced PS exposure

Washed RBCs at 0.5 % Hct were incubated in air with specified concentrations of Yoda1 in various buffers, as indicated. After 20 min incubation, the samples were centrifuged for 7 s at 11,000 g followed by careful aspiration of the supernatant. Then the same volume of buffer was added again and gently vortexed to resuspend the pellet and processed to measure PS. In cases where inhibitors were used such as Dooku1, GsMTx4, chelerythrine chloride and calphostin C, the washed RBCs were initially pre-incubated in air with the specified inhibitors for 10 min and then the RBCs were exposed to Yoda1.

Calcium loading with the ionophore Br-A23187 in the presence or absence of Yoda1

In certain experiments, PS exposure was stimulated using the divalent cation ionophore Br-A23187 and later the effect on the action of Yoda1 was investigated. RBCs were washed into either HK- or LK-HBS (0 Ca^{2+}, 2 mM EGTA) to remove contaminant Ca^{2+}. To alter the intracellular calcium concentration, RBCs at 0.5 % Hct were exposed to Br-A23187 dissolved in DMSO (with a final concentration of Br-A23187 of 6 μM and DMSO of 0.5 %) in the presence of different extracellular calcium concentrations, clamped with 2 mM

EGTA, in HK- or LK-HBS (containing 1mM vanadate). Then specified Yoda1 doses were added and incubated for 30 min at 37 °C in air. All solutions were well vortexed while adding Br-A23187 (before the addition of RBCs) to avoid precipitation of the ionophore (Tsien, 1981). After incubation, Co^{2+} at a final concentration 0.4 mM was added to block the ionophore, to prevent change in intracellular Ca^{2+} should the calcium concentration outside be altered. Then the samples were centrifuged for 7 s at 11,000 g, the supernatant carefully removed and the same volume of LK- or HK-HBS, 0 Ca^{2+}, 1 mM vanadate, pH 7.4 at RT was added. Finally, aliquots of RBCs were diluted to Hct 0.01-0.02 % into LA-FITC (16 nM) labelling buffer and PS exposure was determined by flow cytometry. In experiments where chelerythrine chloride was used in combination with Yoda1, the washed RBCs were initially pre-incubated with chelerythrine chloride (10 µM) for 10 min, and then Br-A23187 and Yoda1 were added.

3.5.4 Hyperosmotic- and hypertonicity-induced PS exposure

Washed RBCs at 0.5 % Hct were incubated in solutions of different osmolalities ranging from 290-1500 mOsm.kg^{-1} to simulate the conditions found in the renal medulla using sucrose, NaCl and urea, alone or in combination, and at various oxygen tensions. At specified time intervals, aliquots were removed and processed to measure the PS.

3.5.5 Effect of 3,4-dichloroisocoumarin and ceramide on PS exposure

3,4-Dichloroisocoumarin is a serine protease inhibitor that can inhibit activation of the enzyme sphingomyelinase (SMase), which is responsible for the metabolism of sphingomyelin to ceramide and phosphorylcholine. Ceramides are important bioactive lipids belonging to the sphingolipid family and have been shown to affect cell signalling pathways that mediate growth, proliferation, motility, adhesion, differentiation, senescence, growth arrest and apoptosis (Galadari et al., 2013; Ruvolo, 2003). Effect of both 3,4-dichloroisocoumarin and ceramide on PS exposure was observed in HbSS RBCs under both oxygenated and deoxygenated conditions.

Washed RBCs at 0.5 % Hct were initially pre-incubated in Ca^{2+}-vanadate LK-HBS (pH 7 at 37 °C) with 3,4-dichloroisocoumarin (200 µM) or ceramide (50 µM) for 30 min. After pre-incubation, samples were removed and added to the respective pre-equilibrated oxygenated or deoxygenated test tubes, and further incubated for 60 min. Every 20 min, samples were collected and diluted to 0.05 % Hct, and later on processed for determination of PS exposure by flow cytometry.

3.5.6 Measurement of PS with LA-FITC

The negatively charged PS, when exposed on the cell surface, attracts other cell types such as macrophages and endothelial cells. Macrophages secrete lactadherin (LA), a glycoprotein that has the ability to bind to PS and facilitates engulfment of PS-expressing cells. It has been shown that bovine LA conjugated with fluorescein isothiocyanate (FITC) binds to exposed PS and can detect very low levels of PS (Albanyan et al., 2009). Annexin V is an alternative PS-binding protein that has been widely used to detect PS exposure in sickle RBCs (Albanyan et al., 2009; Dasgupta et al., 2006; Weiss et al., 2011). However, it requires a higher threshold of PS exposure in RBCs (2-8 %) for binding to occur and is Ca^{2+}-dependent, which is not ideal in experiments designed to test the Ca^{2+} dependence of PS exposure (Albanyan et al., 2009; Hou et al., 2011). Whereas, LA can detect PS exposing cells at levels as low as 0.5 % and is Ca^{2+} independent (Albanyan et al., 2009; Shi et al., 2006; Waehrens et al., 2009).

RBCs at a final Hct of 0.01-0.02 % were placed in LA-FITC (16 nm) labelling buffer (pH 7.4 at RT), and incubated at RT for 10 min in the dark. Then RBCs were pelleted for 7 s at 11,000 g and resuspended into the same buffer without LA-FITC. Samples were kept on ice until analysis by flow cytometry.

3.5.6 Flow cytometer measurement

A BD Accuri C6 flow cytometer was utilized in all the experiments, which is equipped with a diode red laser and a solid state blue laser allowing excitation at 640 nm and 488 nm. It is also composed of four colour optical standard filters: FL1 533 / 30 nm, FL2 585 / 40 nm, FL3 > 670 nm and FL4 675 / 25 nm.

Percentages of RBCs with PS exposed on their external membrane were measured in the FL-1 channel of the flow cytometry, with an emission wavelength for FITC of 519 nm. PS positive cells from 10,000 events were collected and analysed in the quadrant (x > 10^3 and y < 10^4). As shown in the figure below (Figure 2.3), treating HbSS RBCs (0.5 % Hct) with Yoda1 (1 µM) caused the HbSS RBCs to expose PS, allowing LA-FITC to bind to PS positive cells and shift to the lower right quadrant (Figure 2.3B). Whereas, treating HbSS RBCs with DMSO caused no such effect, and majority of the cells remained in the lower left quadrant in the unlabelled region (Figure 2.3A). The percentage of positive cells were measured in this case and found to be more informative than the median fluorescence. The position of the positive gate was set according to Cytlak (2014).
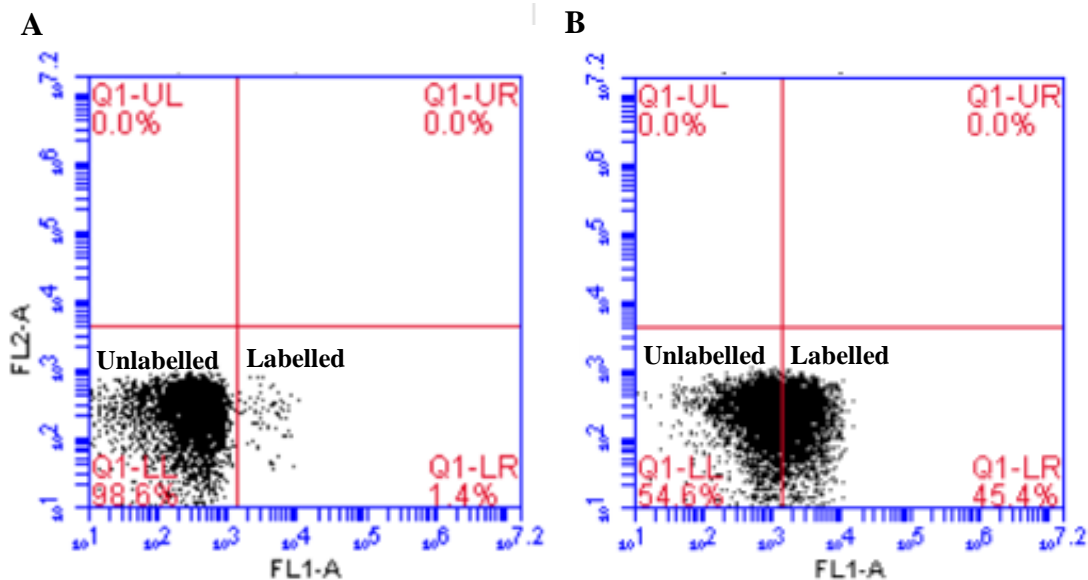
Figure 2.3 Unlabelled (PS negative) and labelled (PS positive) PS in HbSS RBCs using LA-FITC. A: HbSS RBCs (0.5 % Hct) treated with DMSO. B: HbSS RBCs treated with Yoda1 (1 μM).The negative gate is taken as x < 10^3 that typically gives 1-2 % positive cells in labelled RBCs. PS positive cells are taken as those with a higher fluorescence x > 10^3, in this case about 45 %.

3.6 Measuring membrane integrity using phalloidin-iFluor 647 and Alexa Fluor647 anti-Hb α chain

Membrane integrity of HbSS RBCs was measured at different doses of Yoda1 using phalloidin-iFluor 647 and Alexa Fluor647 anti-Hb α chain. Phalloidin-iFluor 647 is a phalloidin conjugate that binds to actin filaments known as F-actin with high affinity. Size of phalloidin conjugates are small with diameter of 1.2-1.5 nm and a molecular weight of < 2000 Daltons (Da). However, phalloidin is not cell permeable. Alexa Fluor647 anti-Hb α chain is a recombinant monoclonal antibody, which can recognize and bind to the alpha chain of haemoglobin. It is an IgG isotype with molecular weight of 150 kDa. Ordinarily these labels (Phalloidin-iFluor 647 and Alexa Fluor647 anti-Hb α chain) would not gain access to their targets, which are inside the RBCs, unless membrane integrity had been compromised.

3.6.1 Measurement of membrane integrity using phalloidin-iFluor 647

An aliquot of treated RBCs (final 0.5 % Hct) was placed into incubation buffer containing phalloidin-iFluor 647 (1:400; stock concentration is 1 mg.ml^{-1}) and vanadate LK-HBS (pH 7.4 at RT). This was then further incubated at room temperature for 20 min in the dark. RBCs were then pelleted by centrifugation for 7 s at 11,000 g and resuspended into vanadate

LK-HBS (pH 7.4 at RT) in same volume. Samples were kept on ice until analysis by flow cytometry.

3.6.2 Measurement of membrane integrity using Alexa Fluor647 anti-Hb α chain

An aliquot of RBCs (final 0.5 % Hct) was placed into incubation buffer containing Alexa Fluor647 anti-Hb α chain (1:100; stock concentration is 0.5 mg.ml^{-1}) and vanadate LK-HBS (pH 7.4 at RT), incubated at room temperature for 20 min the dark. Then RBCs were pelleted for 7 s at 11,000 g and resuspended into vanadate LK-HBS (pH 7.4 at RT) in same volume. Samples were kept on ice until analysis by flow cytometry.

3.6.3 Flow cytometer measurement

Both phalloidin-iFluor 647 and Alexa Fluor647 anti-Hb α chain positive cells were measured in the FL-4 channel of BD Accuri C6 flow cytometer and 10,000 events were collected. The median fluorescence intensity was measured in this case as it was found to be more informative than the percentage of positive cells.

3.7 Measurement of RBC haemolysis

Isosmotic haemolysis solution (buffered isosmotic sucrose solution) was transferred to an Eschweiler tonometer at 37 °C. The tonometer was flushed with humidified N_2 or air, and allowed to equilibrate for 30 min. Washed packed HbAA or HbSS RBCs (2 ml at about 2 % Hct) were initially treated with Yoda1 or DMSO for 20 min and then added to the tonometer. The contents of the tonometer were gently mixed (speed of rotation usually about 180 rpm) and continuously flushed with the appropriate gas. At pre-determined intervals, serial aliquots were removed and diluted 1:4 into ice-cold isosmotic sucrose solution in an eppendorf tube and immediately centrifuged (15 s, 14,000 g). The supernatant was transferred to a cuvette and the extent of haemolysis was determined by measuring the optical density (OD) at 540 nm. Maximal (100 %) haemolysis was measured with the same dilution of RBCs transferred to a solution of 0.1 % Triton X-100, followed by determination of the OD (540 nm).

3.8 Calcium measurement

The intracellular Ca^{2+} concentration in HbSS RBCs was measured using Fluo-4AM, a membrane permeable acetoxymethyl ester, which is hydrolysed to its active form in the cytosol. In RBCs, formaldehyde accumulates as a by-product when acetomethyl esters are used, which can be toxic to cells if accumulated and may lead to irreversible ATP depletion

by inhibition of glycolysis. To prevent this consequence of formaldehyde accumulation, pyruvate and inosine is used (Garda-sancho, 1985; Tiffert et al., 1984).

HbSS RBCs (final 1.5 % Hct) were added to LK-HBS (pH 7.4 at 37 °C) containing pyruvate (5 mM final) and Fluo-4AM (5 µM final). They were then incubated in a water bath at 37 °C for 45 min. After 45 min, RBCs were washed twice in LK-HBS (pH 7.4 at RT) for 3 min at 600 g to remove extracellular fluorophore finally resuspended into LK-HBS (pH 7.4 at RT).

Aliquots of Fluo-4-loaded HbSS RBCs were diluted to 0.07 % Hct in specified buffer. Specified drug / inhibitor doses were added and samples were then incubated in the water bath at 37 °C for 20 min. In cases where cells were also exposed to Yoda1, the HbSS RBCs were pre-incubated with inhibitor for 10 min and then treated with Yoda1 at 37 °C for 20 min. After incubation, RBCs were then pelleted by centrifugation for 7 s at 11,000 g and resuspended into the same volume of vanadate LK-HBS (pH 7.4 at RT). From these mixtures an aliquot of HbSS RBCs were diluted to 0.002 % Hct in vanadate LK-HBS (pH 7.4 at RT). Samples were kept on ice until analysis by flow cytometry.

3.8.1 Flow cytometer measurement

Fluo-4 has an excitation wavelength of 488 nm and emission wavelength of 516 nm. Fluo-4 positive cells were measured in the FL-1 channel of BD Accuri C6 flow cytometer and 10,000 events were collected. The median fluorescence was measured in this case as it was found to be more informative rather than the percentage of positive cells.

3.9 Sphingomyelinase (SMase) Assay

SMase activity was measured using the Abcam sphingomyelinase assay kit (colorimetric). Initially a standard linear dose response curve was carried out using a range of SMase concentrations (10 mU.ml^{-1}, 5 mU.ml^{-1}, 2.5 mU.ml^{-1}, 1.25 mU.ml^{-1} 0.625 mU.ml^{-1}, 0.313 mU.ml^{-1}, 0.156 mU.ml^{-1} and 0.078 mU.ml^{-1}). Specified concentrations of SMase were incubated at a 1:1 dilution in standard working solution containing sphingomyelin (50 mM) for 2 h at 37 °C in 96-well plates. During this incubation period, SMase will be able to break down sphingomyelin to phosphocholine and ceramide. After 2 h, Ab blue indicator was added at a 1:3 dilution and further incubated for 2 h at 37 °C. The Ab blue indicator can bind to the phosphocholine, which was produced by the breakdown of sphingomyelin by SMase. Then the absorbance of the solutions in the 96-well plates were measured in microplate reader. The absorbance was monitored at a wavelength of 655 nm.

3.9.1 Effect of urea on SMase

Further experiments were done to measure the inhibitory effect of different concentrations of urea (50 mM, 200 mM, 600 mM and 900 mM final) on SMase activity. Specified concentrations of urea were added to the SMase solution at a 1:1 dilution and then the mixture (urea + SMase standard solution, at a final SMase concentration of 1.25 mU.ml^{-1}) was incubated in standard working solution containing sphingomyelin at 1:1 dilution for 2 h at 37 °C in 96-well plate. After 2 h, Ab blue indicator was added at a 1:3 dilution and further incubated for 2 h at 37 °C. Then the absorbance of the solutions in the 96-well plates was measured in microplate reader.

3.9.2 Effect of HbAA RBCs on the SMase absorbance assay

Any quenching or other interference by intact HbAA or lysed RBCs (0.5 %, 5 %, 10 % Hct) on the absorbance assay (Ab blue indicator plus phosphocholine) was investigated in control experiments. SMase (1.25 mU.ml^{-1}) was incubated in the standard working solution containing sphingomyelin at 1:1 dilution for 2 h at 37 °C in 96-well plate. After 2 h, Ab blue indicator was added at 1:3 dilution and further incubated for 2 h at 37 °C. Finally after the 2 h incubation with the indicator, intact or lysed HbAA RBCs were added, and the absorbance of the solutions in the 96-well plates was measured in microplate reader immediately.

In another circumstance (Figure 7.12), HbAA RBCs of final 0.5 % Hct were added concomitantly with SMase (1.25 mU.ml^{-1}) and sphingomyelin at the start, and incubated for longer hours (2 h) to see if the enzymatic effect of the SMase is altered. The SMase standard solution (1.25 mU.ml^{-1}) with HbAA RBCs of 0.5 % Hct was incubated in standard working solution at 1:1 dilution for 2 h at 37 °C in 96-well plate. After 2 h, Ab blue indicator was added at 1:3 dilution and further incubated for 2 h at 37 °C. Finally, after the 2 h incubation with the indicator, the absorbance of the solutions in the 96-well plates were measured in microplate reader.

3.10 Measurement of sickling

RBCs were fixed in 0.3 % glutaraldehyde in LK-HBS at a final Hct of 0.2 %. This maintains RBC shape for several weeks (Hanneman et al, 2014; Milligan et al 2013). Cell morphology was later viewed using a Nikon Eclipse E400, 20x0.40, ∞/0.17 WD1.3. A minimum of 300 cells were counted and the results were given as a percentage of sickled RBCs. The RBCs that attained the morphology of sickles, holly leaves and other elongated, distorted shapes were counted as sickled RBCs, not the RBCs with normal biconcave discs.

3.11 Statistics

Unless otherwise indicated, data are presented as means ± S.E.M. for RBC samples taken from n different individuals. In most cases statistical comparisons of paired variables were made using two-tailed Student's t-test or one-way ANOVA with Tukey (to compare paired values) or Dunnett's (to compare to a control value). A Two-way repeated measures ANOVA was used where appropriate (e.g. Figure 5.1, 5.2, 5.4, 5.7 and 5.8). $p < 0.05$ was accepted as significant. All graphs were made using GraphPad Prism. Calculations were done using Microsoft Office Excel 2016 software or GraphPad Prism version 9.

4 Renal conditions important in PS exposure 1: Effect of different pH conditions and oxygen tension on sickling and PS exposure in RBCs from HbSS patients

4.1 Introduction

As aforementioned the mutation in the Hb of sickle cell patients results in polymerisation (mentioned in Section 1.1), however it polymerises when the concentration of the deoxygenated form of Hb exceeds a critical threshold. Therefore, polymerisation is also determined by conditions surrounding the HbSS RBCs notably oxygen tension, pH, osmolality and levels of urea. The hypoxic, acidotic and hyperosmotic conditions in the renal medulla provide the ambient conditions to stimulate polymerisation causing HbSS RBCs to sickle. Additionally, sickle RBCs are known to exhibit abnormally high adhesion to the endothelium, perhaps through PS exposure slowing their transit through the hypoxic renal medulla and causing further deleterious effects.

Expression of PS on the surface of the HbSS RBCs is significantly higher than in HbAA RBCs, which contributes to a decreased life span of RBCs, increased vaso-occlusion and cell-to-cell interactions (explained in Section 1.4). Exposed PS on the surface of RBCs increases the surface negative charge, which allows complexes to be formed with tenase and prothrombinase resulting in activation of coagulation pathway, triggering blood clotting and thrombosis (Whelihan et al., 2012). One of the reasons for PS exposure is the loss of ion and water homeostasis in HbSS RBCs, which depends on abnormal transport regulation across the membrane. Apart from the Na^+/K^+ pump and anion exchanger, the other three major transport systems (KCC, Gárdos channel and P_{sickle}) in RBCs are either directly or indirectly affected by oxygen tension. A part of the thesis aims to investigate the most important systems that work towards exposing PS in HbSS RBCs.

It is already known that activity of some of the membrane transport systems in HbAA RBCs are regulated by oxygen tension. KCC is a primary example, at high oxygen tension the transporter is highly active, as the oxygen tension decreases so too does its activity, and at very low oxygen levels, it is inactivated (Gibson et al., 1998). The Na^+-K^+-Cl^- cotransporter (NKCC) is another example, which acts opposite to KCC. NKCC is inhibited by high oxygen tension and stimulated by low oxygen tension (Gibson et al., 2000; Muzyamba et al., 1999). As aforementioned, these membrane transporters are dependent on oxygen tension, but changes in oxygen tension does not usually create any cation imbalance in

normal HbAA RBCs. However, in HbSS RBCs there is significantly altered membrane transport activity and only under deoxygenated conditions is there massive loss of cations leading to dehydration and eventually sickling (explained in Section 1.3). Usually in normal HbAA RBCs, as they mature over their life span of 120 days, they slowly lose water and intracellular solutes over time and are later removed from the body (Hoffman, 1958). However, the rapid irreversible loss of cations and water through osmosis in HbSS RBCs during deoxygenation contributes to a reduced life span, such that they survive for only 10-20 days and the shrunken RBCs are either removed from the body or end up blocking the capillaries. Moreover, Joiner and colleagues showed that at lower oxygen tension P_{sickle} is activated in HbSS RBCs, which allows net loss of monovalent cations through it, but importantly also allows Ca^{2+} to enter and Mg^{2+} to exit. This activity of P_{sickle} is not observed in HbAA RBCs. Thus, initially the effect of different oxygen tension on sickling and PS exposure was investigated.

Hypoxic capillary beds with low pH are the most vulnerable regions. Maintenance of a proton gradient is an energy dependent process, which is likely to be impaired due to the medullary ischaemia. Moreover, there are multiple reports of incomplete tubular acidosis in several individuals with SCD (DeFronzo et al., 1979; Goossens et al., 1972; Kong and Alleyne, 1971; Oster et al., 1976). A study conducted on more than 400 homozygous patients with SCD in 2014, showed that over 40 % of SCD patients encountered metabolic acidosis which might be related to impaired availability of ammonia (Stojanovic et al., 2014). Joiner et al. 1993 provided evidence that deoxygenation-induced Rb^+ fluxes changed with pH, with high fluxes being achieved between pH 6.8-7. This meant that at pH 6.8-7 rapid and high amount of RBC cations were lost. Furthermore, Joiner et al., also showed that deoxygenation-induced sickling caused HbSS RBCs to attain different morphologies at different pHs. Hence, an extensive study on HbSS RBCs was carried out to study the behaviour of PS exposure to various oxygen tension and pHs.

4.2 Results

4.2.1 Effect of deoxygenation on sickling and PS exposure in RBCs

In this experiment, sickling of HbSS RBCs was tested at six different oxygen tensions (150, 100, 70, 40, 20, 0 mmHg), in order to analyse the pattern of sickling in decreasing oxygen tensions. Figure 4.1 shows that the initial sickling percentage increased from 9.7 ± 1.3 % at 150 mmHg oxygen tension to 18.7 ± 6.8 % ($p < 0.05$) at 100 mmHg oxygen tension. Compared to 150 mmHg oxygen tension, a significant rise of sickled RBCs to about 57.2 ± 5.4 % ($p < 0.001$) was observed as the oxygen tension was reduced to 20 mmHg. Finally, under fully deoxygenated condition, sickling increased to 85.1 ± 1.6 % ($p < 0.001$).
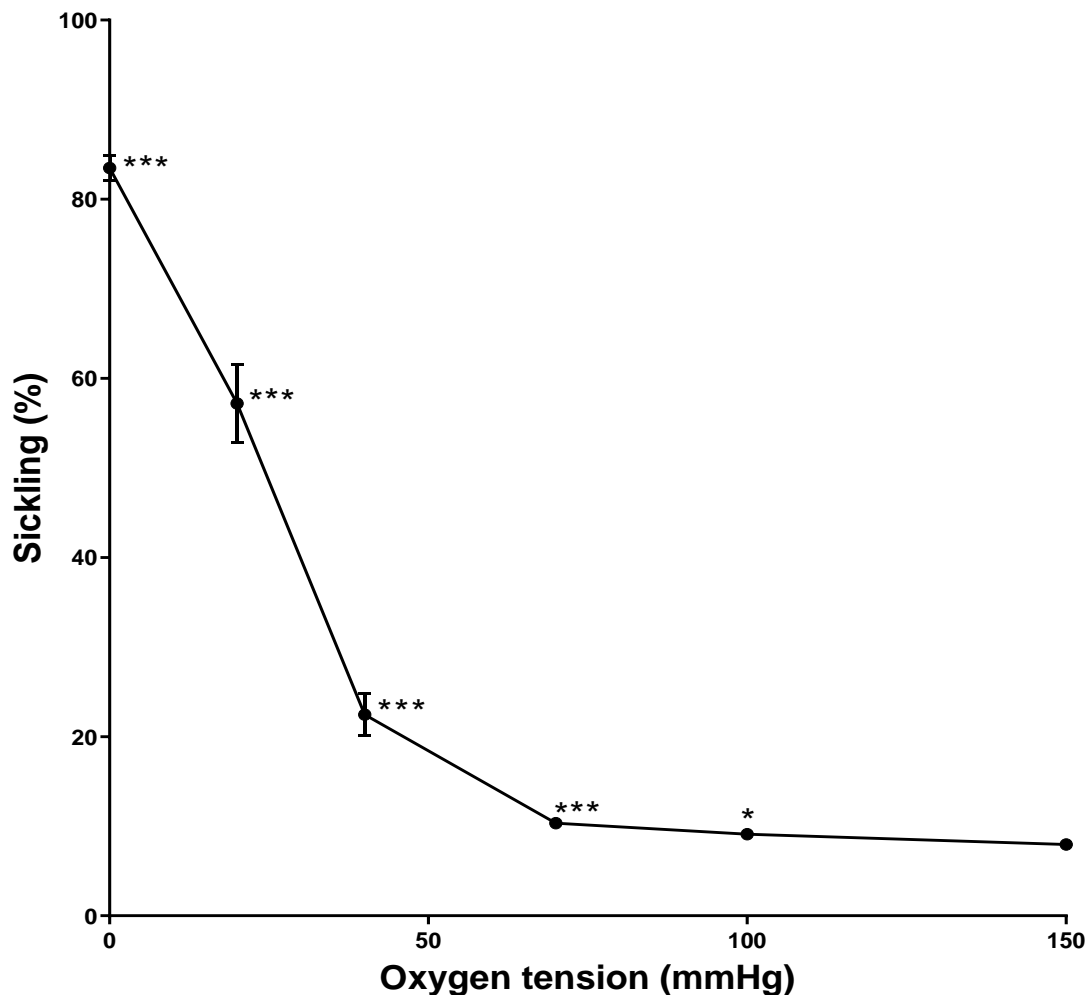
Figure 4.1: **Effect of different oxygen tensions on sickling of RBCs from HbSS patients.** RBCs (5 % Hct, 1 ml) were equilibrated in Eschweiler tonometers for 15 min at the desired oxygen tension in LK-HBS at pH 7.4, 37 °C, after which aliquots were fixed in 0.3 % glutaraldehyde. RBC shape change was assessed by light microscopy counting a minimum of 300 RBCs. Data points represent means ± S.E.M, n = 6. * $p < 0.05$ and *** $p < 0.001$ compared to oxygen tension at 150 mmHg.

The effect of oxygenation (150 mmHg) and deoxygenation (0 mmHg) on the percentage of RBCs exposing PS over 80 min was investigated in the second set of experiments, using RBCs from HbSS patients (Figure 4.2). This experiment examined the effect of deoxygenation on PS exposure in HbSS RBCs presumably through activation of P_{sickle}. At full oxygenation (150 mmHg), there was only a slight overall increase of PS over 80 min from 0.9 ± 0.5 % to 3.1 ± 1.2 % (not significant). However, under full deoxygenation (0 mmHg), there was a continual increase in PS exposure over time. In contrast to 150 mmHg oxygen tension, the PS exposure at 0 mmHg oxygen tension increased significantly from 2 ± 0.6 % at 0 min to 5 ± 1.5 %, 10.3 ± 3.3 % ($p < 0.05$), 12.4 ± 2.9 % ($p < 0.01$) and 16.2 ± 3.9 % ($p < 0.001$) at 20, 40, 60 and 80 min, respectively.
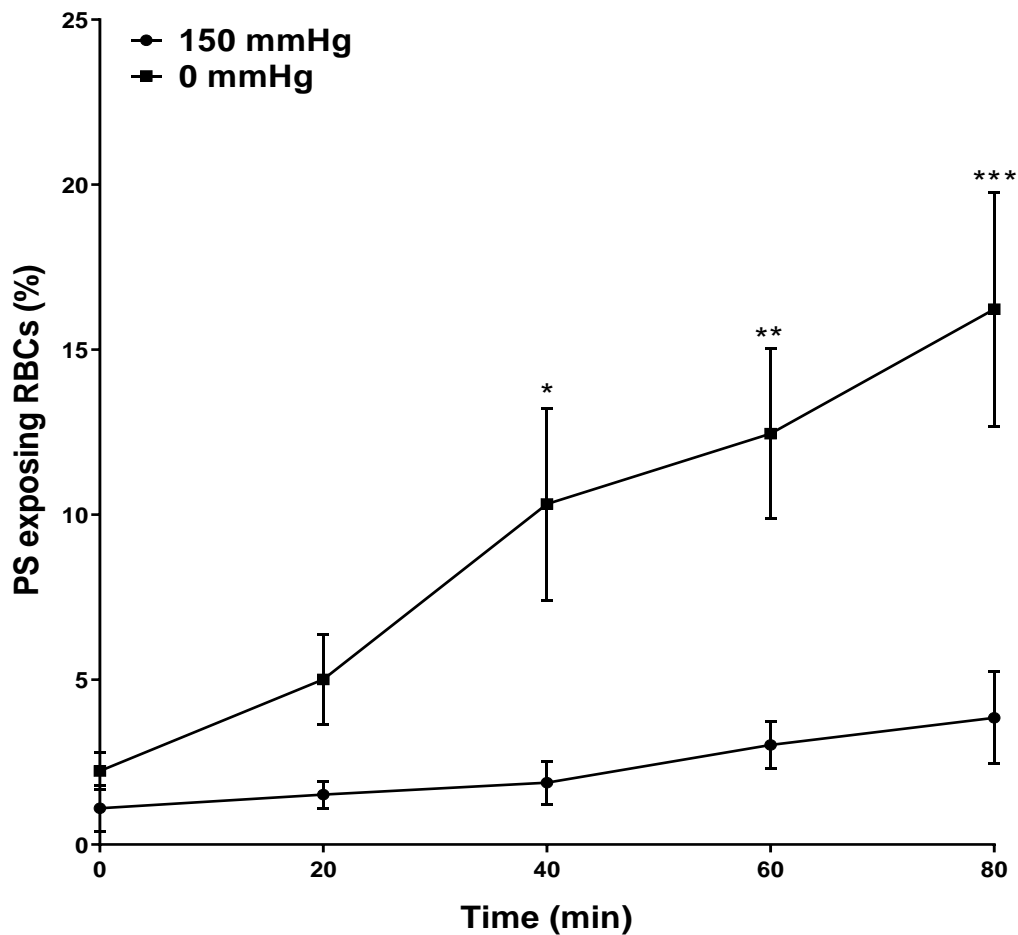
Figure 4.2: Time course of the change in PS exposure of RBCs from HbSS patients in 150 mmHg and 0 mmHg oxygen tension. RBCs (0.5 % Hct, 1 ml) were incubated in Ca^{2+}- vanadate LK-HBS pH 7.4 at 37 °C in Eschweiler tonometers for 80 min. Every 20 min RBC aliquots were removed and exposed PS labelled with LA-FITC. Staining was detected using flow cytometry. Data points represent means $\pm$ S.E.M, n = 5. * $p < 0.05$, ** $p < 0.01$ and *** $p < 0.001$ compared to oxygen tension at 150 mmHg.

4.2.2 Effect of different oxygen tensions and pHs on sickling

The effect on sickling in RBCs from SCD patients at three different oxygen tensions (100 mmHg, 30 mmHg and 10 mmHg) and at three different pHs (7.4, 6.8 and 6.0) was investigated next (Figure 4.3). This experiment was done in order to examine if the rate of sickling of RBCs differed greatly between pHs, as this might have an effect on P_{sickle} activity. Sickling was lowest at 100 mmHg oxygen tension (Figure 4.3A) for all the three pHs reaching 17.3 % ± 2.1 %, 27.1 % ± 4.1 % and 32.2 % ± 11.4 % at pH 7.4, pH 6.8 and pH 6.0 respectively. At an intermediate oxygen tension of 30 mmHg (Figure 4.3B), the sickling percentage remained low at pH 7.4 but increased from 5 % ± 0.5 % at 0 min to 24.1 % ± 1.2 % after 80 min. In contrast, at both pH 6.8 and 6.0 there was a sharp rise in sickling within 20 min increasing from 5.7 % ± 1 % and 5.1 % ± 0.9 % to 81.2 % ± 3.1 % ($p < 0.01$) and 61.7 ± 13.1 % ($p < 0.05$), at pH 6.8 and 6.0, respectively, reaching a plateau after 40 min, and remaining high at 80 min for both pH 6.8 and 6.0 at 91.3 % ± 1.8 % ($p < 0.001$) and 84.1 ± 3.4 % ($p < 0.001$), respectively. Finally, at 10 mmHg oxygen tension (Figure 4.3C), all three pHs showed a similar pattern with a significant increase in sickling from 0 min to 20 min, reaching a plateau thereafter. However, sickling over the time was highest for pH 6.8 with sickling of 93.8 % ± 1.2 % at 80 min and at pH 7.4 and 6.0, 86.8 ± 2.2 % and 86.9 ± 1.9 % respectively, but the difference was not significant.

In fully oxygenated RBCs, there was little change in sickling with time regardless of pH whilst in fully deoxygenated RBCs, sickling was almost complete regardless of pH. However, at 30 mmHg, sickling was minimal at pH 7.4 but increased markedly at pH 6.8 and 6.0. As shown in figure 4.3D, a significant difference in sickling ($p < 0.001$) was seen between pH 7.4 after 80 min (24.1 % ± 1.2 %) compared to pH 6.8 (91.3 % ± 1.8 %) and pH 6.0 (84.1 ± 3.4 %).
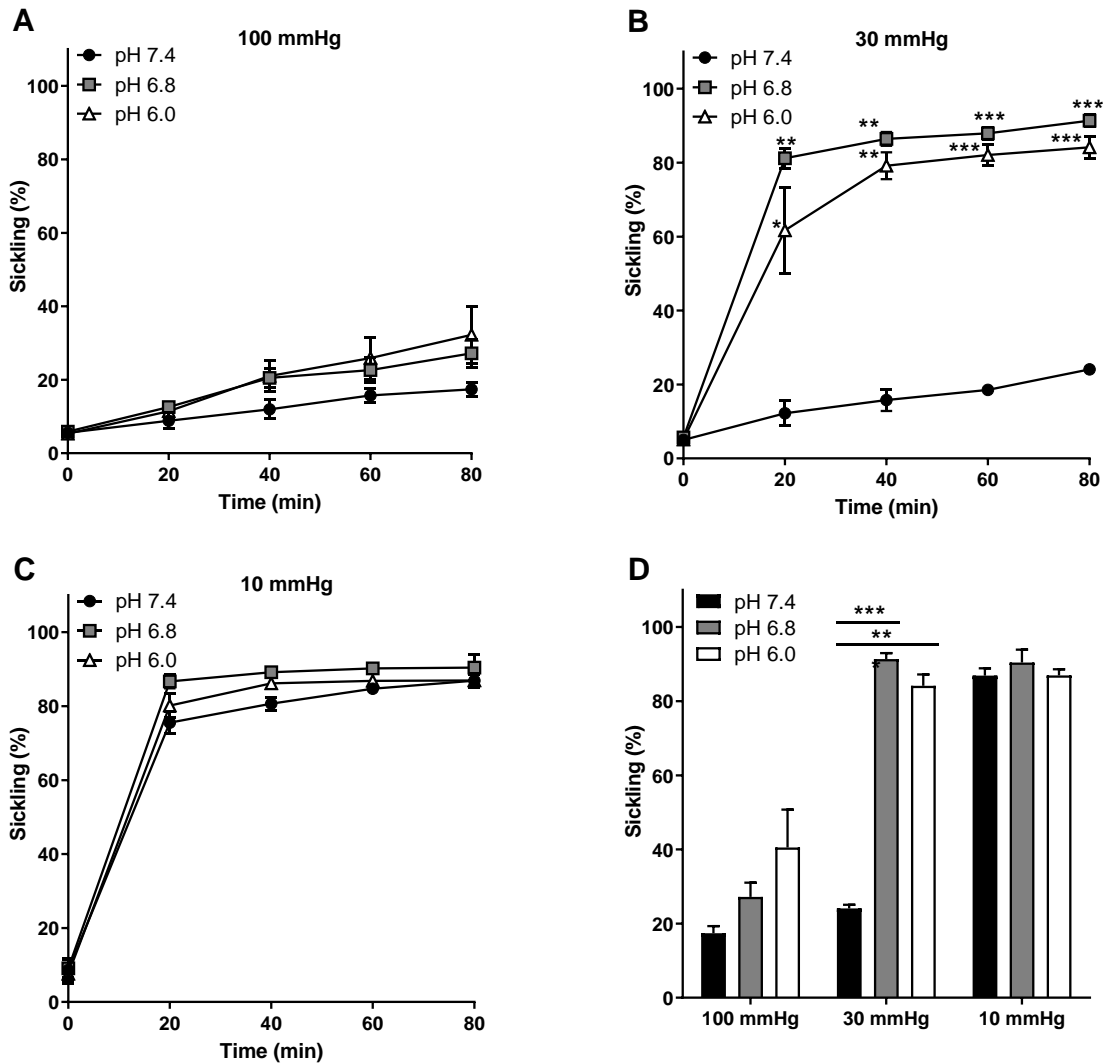
Figure 4.3: Effect of different oxygen tensions and pHs on sickling of RBCs from HbSS patients. RBCs (5 % Hct, 1 ml) were equilibrated in Eschweiler tonometers in Ca^{2+}- vanadate LK-HBS over 80 min at the desired oxygen tension and pH. Every 20 min, RBC aliquots were removed fixed in 0.3 % glutaraldehyde and RBC shape change was assessed by light microscopy. **A:** Sickling at 100 mmHg. **B:** Sickling at 30 mmHg. **C:** Sickling at 10 mmHg. **D:** Percentage sickling after 80 min in 100 mmHg, 30 mmHg and 10 mmHg oxygen tension at pH 7.4, 6.8 and 6.0. Data points represent means $\pm$ S.E.M, n = 5. * p < 0.05, ** p < 0.01 *** p < 0.001 compared to sickling effect in HbSS RBCs at pH 7.4 in 30 mmHg with pH 6.8 and 6.0.

4.2.3 Effect of different oxygen tensions and pHs on PS exposure

Next, the PS exposure of RBCs from SCD patients was investigated under the same condition as sickling (Figure 4.4). Assuming different pHs might have an effect on both HbS polymerisation and on activation of P_{sickle} or its permeability to ions once activated, this experiment examined the effect of various pHs on PS exposure at three respective oxygen tensions.

At 100 mmHg oxygen tension (Figure 4.4A), the PS level at pH 7.4 remained minimal, changing from 0.9 ± 0.4 % to 1.6 ± 1.1 % after 80 min. In contrast, PS exposure at pH 6.8 and pH 6.0 started increasing after 20 min and 40 min, respectively. After 80 min, PS exposure reached 6 ± 2.4 % at pH 6.8, and 3.2 ± 0.7 % at pH 6.0, although significance was not reached. Similar to 100 mmHg oxygen tension, PS exposure at pH 7.4 at 30 mmHg oxygen tension (Figure 4.4B) remained stable and low at 2-3 % over the entire 80 min period incubation. At 30 mmHg oxygen tension, PS exposure of RBCs at pH 6.8 and 6.0 increased to 3.3 ± 2.3 % and 3.1 ± 0.6 % at 60 min, respectively, but not significantly. An increase in PS exposure was seen at 80 min at pH 6.8 reaching 9 ± 4.5 %, whereas at pH 6.0 it increased to 5 ± 6.5 %, both not significant. At 10 mmHg oxygen tension (Figure 4.4C), an increase in PS exposure over time was seen at all the three pHs tested, although not significant. In this case, pH 7.4 and 6.0 showed a similar pattern, where initially PS exposure remained low, and only increased after 60 min. After 80 min, PS exposure remained at comparable levels at 8.3 ± 2.1 % and 7.9 ± 1.7 % at pH 7.4 and pH 6.0, respectively. For pH 6.8, an increase in PS exposure to 9 ± 4.2 % was observed at 40 min, eventually reaching 11.25 ± 6 % at 80 min, however not significant.

Overall, PS exposure increased after 80 min when oxygen tension was reduced, regardless at the pH of incubation (Figure 4.4D). However, PS exposure in pH 6.8 was always highest (although not significant), independent of the oxygen tension. With the exception of 100 mmHg oxygen tension, this pattern was similar to that seen for sickling (Figure 4.4D). Notwithstanding, the changes in PS exposure were generally more pronounced, suggestive that whilst altered pH alters HbS polymerisation and sickling there is a greater effect on PS exposure, which would be consistent with an additional effect of pH on P_{sickle} permeability, as observed by Joiner et al, 1993. Furthermore, it is interesting to speculate that Joiner et al's findings – greater sickling at higher pHs but greater P_{sickle} activity at lower ones – would result overall in higher permeation and hence PS exposure at intermediate pHs. This was explored further in the next series of experiments.
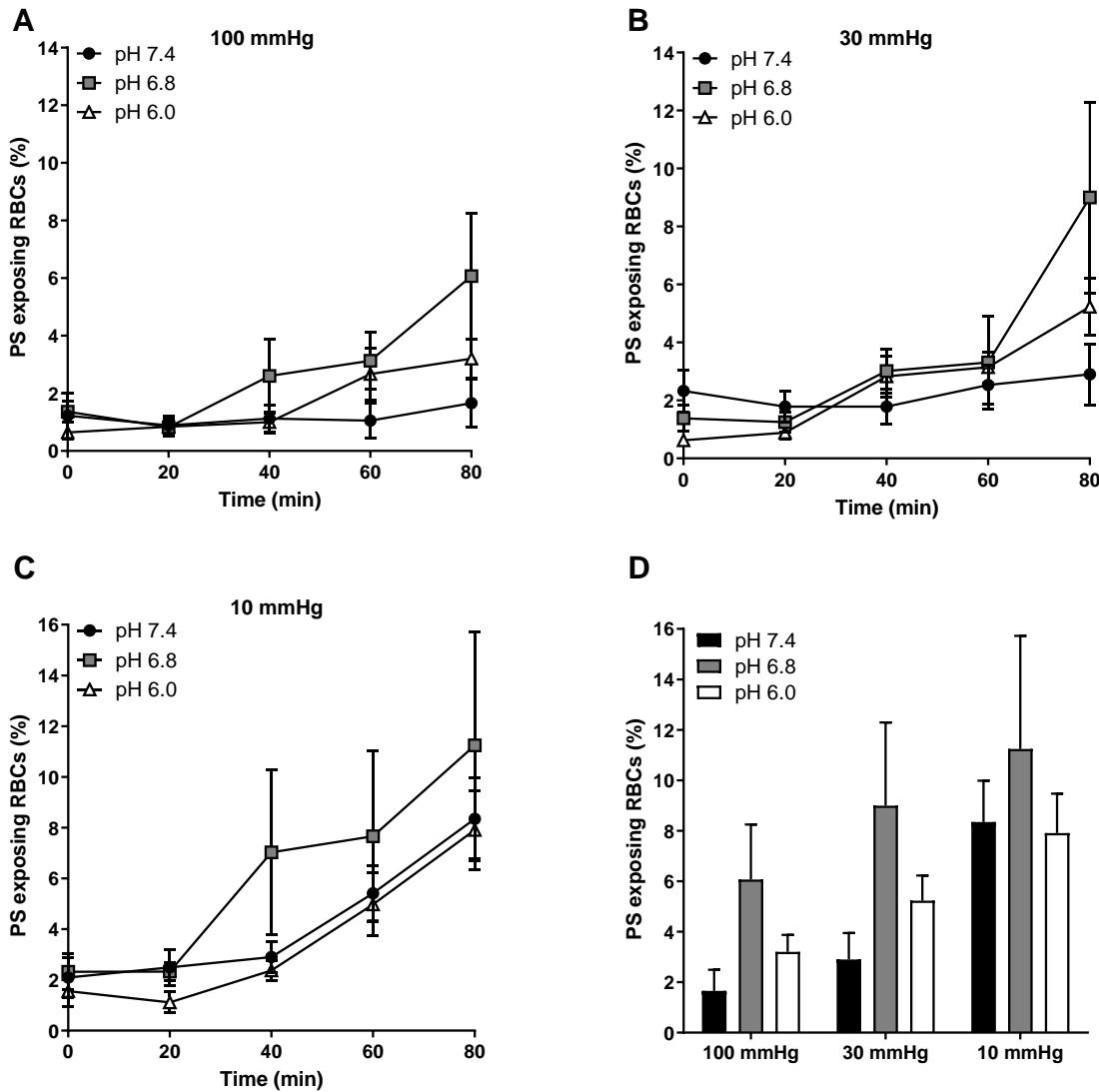
Figure 4.4: Effect of different oxygen tensions and pHs on PS exposure of RBCs from HbSS patients. At the desired oxygen tension and pH, RBCs (0.5 % Hct, 1 ml) were incubated in Ca^{2+}- vanadate LK-HBS at 37 °C in tonometers for 80 min. Every 20 min, RBC aliquots were removed and labelled with LA-FITC prior to flow cytometry analysis. **A:** PS exposure of HbSS RBCs at 100 mmHg at pH 7.4, 6.8 and 6.0. **B:** PS exposure of HbSS RBCs at 30 mmHg at pH 7.4, 6.8 and 6.0. **C:** PS exposure of HbSS RBCs at 10 mmHg at pH 7.4, 6.8 and 6.0. **D:** The level of PS exposure after 80 min at 100 mmHg, 30 mmHg and 10 mmHg at pH 7.4, 6.8 and 6.0. Data points represent means ± S.E.M, n = 5. No significant changes were observed when PS exposure was compared between pHs at respective oxygen tensions.

4.2.4 Effect of pH on sickling and PS at 10 mmHg oxygen tension

It was shown previously (Joiner et al., 1993) that higher P_{sickle} activities were achieved when RBCs were sickled at more alkaline pHs (i.e. pH 7.5 > 7.3 > 7.0). Conversely, during the actual measurement of P_{sickle} activity, fluxes were highest at lower pHs (pH 7.0 > 7.5 > 7.3 > 7.5). The next series of experiments were therefore carried out under deoxygenated conditions to investigate whether initial sickling of HbSS RBCs at pHs 7.4 or 6.8 for 20

min, and then subsequently transferring RBC aliquots to a range of different pHs and further incubating for 60 min, had any effect on sickling and PS exposure.

Both Figures 4.5A and B show sickling of HbSS RBCs after 80 min after an initial incubation at pH 7.4 and 6.8, respectively. There is no significant difference in sickling amongst different pHs in either condition - sickling at both pHs were similar to each other.

In Figure 4.5C, RBCs from HbSS patients were first equilibrated at 10 mmHg oxygen tension at pH 7.4 for 20 min. After 20 min, aliquots of RBCs were removed and transferred to three additional pHs (pH 7.0, 6.8 and 6.4), as well as the pH of sickling (pH 7.4), and further incubated for 60 min. Overall, it can be observed in Figure 4.5C, that there was no substantial difference in PS exposure between pH 7.4 and the other pHs. PS at 40 min was similar for all the pHs 6.2 ± 1.8 %, 5.5 ± 1.3 %, 6.1 ± 1.4 % and 4.9 ± 1.1 % for pH 7.4, 7.0, 6.8 and 6.4, respectively. However, at 60 min PS exposure for pH 6.8 was 12.8 ± 4.4 % which was higher compared to 8.6 ± 2.4 in pH 7.4, 9.3 ± 2.2 % in pH 7.0 and 8.1 ± 1.9 % in pH 6.4, but not significantly. After 80 min PS was very similar for pHs 7.4, 7.0 and 6.4, but remained high for pH 6.8, however the change was not significant.

In Figure 4.5D, RBCs from HbSS patients were equilibrated at 10 mmHg oxygen tension at pH 6.8 for 20 min. After 20 min, aliquots of RBCs were removed and transferred to three different pHs 7.4, 7.0 and 6.4 as well as pH 6.8 and further incubated for 60 min. After 40 min, PS exposure was highest for pH 6.8 (7.1 ± 2.2 %) compared to pH 7.4 (4.9 ± 1 %), pH 7.0 (5 ± 0.9 %) and pH 6.4 (4.4 ± 1 %), but not significantly. From 60-80 min, PS exposure increased for all pHs and were similar at pH 7.4, 7.0 and 6.4, but at pH 6.8 PS exposure was higher compared to the other three pHs, however the change was not significant.

Figure 4.5E shows PS exposure after 80 min at four different pHs, after initial incubation in pH 7.4 for 20 min. Overall, it can be observed that PS at 80 min for pH 6.8 was highest (18.1 ± 5.4 %), compared to pH 7.4 (14.3 ± 4.2 %), 7.0 (11.2 ± 2.7 %) and pH 6.4 (13.5 ± 3.9), but not significantly. In Figure 4.5F, PS exposure after 80 min at four different pHs was measured after initial incubation in pH 6.8 for 20 min. It can be observed that PS exposure was similar for all pHs: 12.1 ± 3.2 %, 10.3 ± 2.7 %, 12.3 ± 3.7 % and 9.7 ± 2.7 % for pH 7.4, 7.0, 6.8 and 6.4, respectively.

In conclusion, overall, the pattern of sickling and PS exposure at different pHs in Figures 4.4 and 4.5 were similar to the pattern of P_{sickle} activity shown in Joiner et al., 1993. It would

be useful to confirm this supposition measuring P_{sickle} activity under the same conditions used for these experiments on PS exposure which, as explained previously, differ from those of Joiner et al (ie Eshweiler tonometers, gas flushing, shorter incubation times).
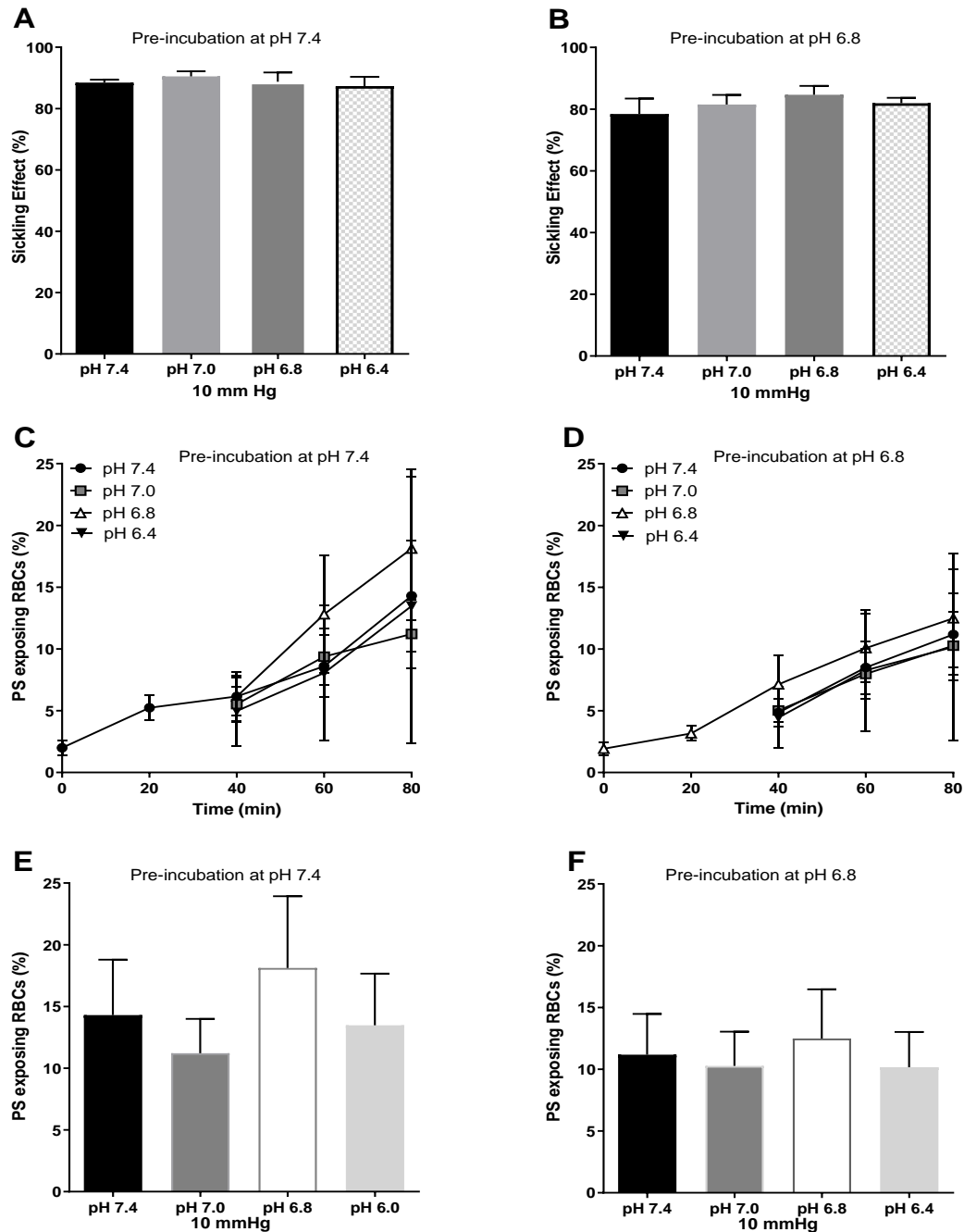
Figure 4.5: Effect of pH on sickling and PS at 10 mmHg oxygen tension in RBCs from HbSS patients. Initially, HbSS RBCs (10 % Hct, 1 ml) were equilibrated in Ca^{2+}- vanadate LK-HBS at either pH 7.4 or 6.8 for 20 min. After 20 min, aliquots of RBCs were removed and equilibrated for a further 60 min at all four pHs (pH 7.4, 7.0, 6.8 and 6.0) after which both PS and sickling were measured. **A:** Sickling at 80 min after initial incubation at pH 7.4. **B:** Sickling at 80 min after initial incubation at pH 6.8. **C:** PS exposure after initial incubation at pH 7.4 for 20 min. **D:** PS exposure after initial incubation at pH 6.8 for 20 min.. **E:** PS at 80 min after initial incubation at pH 7.4. **F:** PS at 80 min after initial incubation at pH 6.8. Data points represent means ± S.E.M, n = 5. No significant changes were observed when PS exposure was compared between any of the conditions. No significant changes were observed when sickling was compared between any of the conditions.

4.3 Discussion

The present findings were an attempt to correlate deoxygenation-induced sickling and P_{sickle} activity with PS exposure. The underlying hypothesis was that the manoeuvres or conditions that were previously studied, which stimulated the activity of P_{sickle} in HbSS RBCs should correlate with PS exposure. All of these conditions are physiologically relevant, as RBCs in SCD patients are exposed to such conditions in the renal medulla and active muscle beds. Joiner et al 1993 showed that under deoxygenated conditions, HbSS RBCs behaved differently at different pHs. They reported that the deoxygenation-induced cation movement and the sickling morphology changed at different pHs. Rb^+ influx in nitrate buffer was maximal at pH 7.0, declining as pH became more acidic or alkaline. Moreover, sickling morphology was altered at different pHs, with more irregular, granular shapes of sickled present at low pH, whilst, at higher pHs more elaborate sickling shapes were seen. Notwithstanding clear effects of pH on sickling and PS exposure in the present work, however, findings were not sufficiently unambiguous to conclude that a strong correlation exists between PS exposure and pH-induced P_{sickle} activity or between the effect of change in morphology with PS exposure

From the first series of experiments in Figure 4.4D it was observed that the overall PS exposure was higher at pH 6.8 compared to pH 7.4 and 6.0, although not significantly. Variation of PS exposure with pH in Figure 4.4D also showed a similar trend to the effect on deoxygenation-induced Rb^+ influx in Joiner et al 1993, where pH 7.0 showed maximal Rb^+ influx. Since the experiments in Joiner et al 1993 were carried out in nitrate buffer with ouabain, it is assumed that the flux measured was due to the activity of P_{sickle}, which would be consistent with the highest PS exposure at pH 6.8 (not significant), observed here. P_{sickle} is believed to be a deoxygenation-induced non-specific cation channel and is thought to allow entry of Ca^{2+}. As PS exposure increases during deoxygenation due to increased intracellular Ca^{2+}, PS exposure would be expected to follow effects on P_{sickle} activity, albeit indirectly, as Ca^{2+}-induced PS scrambling is a further step away from sickling-induced membrane permeability to cations. The present findings are therefore consistent with a role for P_{sickle} activation in deoxygenation-induced PS exposure. This is in agreement with previous work from this laboratory in which deoxygenation-induced PS exposure required extracellular Ca^{2+} and was inhibited if RBCs were loaded with a Ca^{2+} chelator (Cytlak et al., 2013; Weiss et al., 2012). Moreover, in Fig 4.3D, it can be seen that there was a significant difference in sickling at pH 7.4 compared with pH 6.8 and 6.0 at an intermediate oxygen

tension of 30 mmHg. An alternative explanation might be the greater activation of the Gárdos channel at lower pHs in intermediate oxygen tension, which causes efflux of K^+ and results in hyperpolarisation and eventually greater sickling of RBCs as cells become shrunken, whilst that is not the case at pH 7.4 (Halperin et al., 1989), although over the time course of the present experiments the change in cell volume would be minimal.

Furthermore, Joiner et al. 1993 also showed that HbSS RBCs sickled at pH 7.5 under deoxygenated conditions showed the highest Rb^+ influx at pH 7.0. Thus, it was interesting to examine if HbSS RBCs sickled at higher pHs in deoxygenated conditions had any difference in PS exposure when measured at different pHs. It is possible that the elaborate sickling morphology of HbSS RBCs achieved at alkaline pHs, might enable HbS polymers to randomly make contact with regulatory sites at the RBC membrane controlling ion permeability, thus activating P_{sickle}, which is presumed to be a mechanosensitive ion channel (PIEZO1). In addition, PIEZO1 ion permeability *per se* shows some pH dependence, being lower at more acidic pHs (Bae et al., 2015) which also needs to be taken into account. Bae et al. 2015 showed that at lower pHs inactivated state of PIEZO1 was more stabilized, and suggested it may serve as a protective mechanism to inhibit excessive fluxes through this channel.

Therefore, an experiment was designed (Figure 4.5) where HbSS RBCs were sickled at either pH 7.4 or 6.8 for 20 min under deoxygenated conditions, allowing RBCs to attain their respective morphology. Later, these sickled RBCs were transferred to different pHs (pH 7.4, 7.0, 6.8 and 6.4) and a time course of PS exposure determined. As shown in Figure 4.5, the results showed no significant differences in PS exposure at altered pH. However, the results of PS exposure do follow the trend shown in Joiner et al. 1993, with respect to P_{sickle} activity and HbSS RBCs sickled at a higher pH. Joiner et al. 1993 also showed HbSS RBCs sickled at higher pH will have higher P_{sickle} activity when later measured at any pH compared to HbSS RBCs sickled at lower pH. In Figure 4.5C and D, it can be observed that PS exposure in HbSS RBCs when sickled (pre-incubated) at pH 7.4 was high for all the pHs compared to PS exposure when sickled (pre-incubated) at pH 6.8, however the difference was not significant.

The lack of significance in the extent of PS exposure measured at various pHs could be due to the different conditions used to deoxygenate HbSS RBCs. Joiner et al. 1993 used sealed flasks and a relatively long duration of deoxygenation (60 min) whereas tonometers were

used in the present work, which deoxygenate relatively rapidly (within 10 min – see Materials and Methods, Figure 2.2). Speed of deoxygenation would also affect sickling morphology and hence deoxygenation-induced cation movements. Thus, these experimental differences could have resulted in changes in P_{sickle} activity in the two studies, therefore affecting PS exposure. It would be interesting to measure P_{sickle} activity as a K^+ flux or electrophysiologically under the identical conditions used here, and to correlate these with PS exposure.

5 Renal conditions important in PS exposure 2: Effect of Urea on PS exposure

5.1 Introduction

SCD patients have a markedly increased incidence of nephropathy with about a third progressing to a dependence on renal dialysis or transplantation. Inability to concentrate urine occurs at an early age with necrosis and fibrosis of the renal medulla commonly observed. The detailed pathogenesis underlying these manifestations remains unclear, however, the unique environment found in the renal medulla is implicated. This tissue has a particularly low blood flow, less than 1 % of the total renal blood flow. It is, in addition, markedly hypoxic with an O_2 partial pressure of about 15 mmHg. Accumulation of lactic acid from anaerobic metabolism presents an acid load. Furthermore, during maximal antidiuresis, the medulla is also hypertonic with accumulation of salt (up to 300 mM NaCl) and urea (up to 600 mM). Hypoxia, low pH and hypertonicity all stimulate HbS polymerisation. It is therefore likely that they will encourage sickling and PS exposure and these factors coupled with the sluggish rate of blood flow may serve to promote adhesion of sickle cells and increase ischaemia and damage to the renal medulla.

The effect of low pH was examined in Chapter 4. Therefore, in this Chapter, in a series of experiments, deoxygenation, hyperosmotic shock and hypertonicity were investigated as manoeuvres likely to increase PS exposure in HbSS RBCs. Exposing normal RBCs to hyperosmotic shock has already been shown to cause apoptosis with the externalisation of PS (Lang et al., 2003). In nucleated cells, hyperosmotic shock leading to apoptosis has been extensively studied, the mechanisms include upregulation of tumor necrosis factor, triggering of death receptor membrane trafficking, activation of Akt pathway, induction of transcriptionally active p53 and activation of heat-shock transcription factor 1 (Lang et al., 2002; Lu et al., 2000; Reinehr et al., 2002; Rosette and Karin, 1996; Terada et al., 2001). Moreover, a significant role for mitochondria has also been identified, where an osmotic stress-sensing module on the outer membrane of mitochondria allows the cell to integrate a variety of stress signals and cause loss of mitochondrial function (Desai et al., 2002). However, it is known that RBCs lack all the major organelles that are involved in inducing apoptosis through hyperosmotic shock in nucleated cells. Nevertheless, osmotic shock in RBCs activates a Ca^{2+} permeable channel, which causes an increase in cytosolic Ca^{2+} (Lang et al., 2003). This leads to activation of the scramblase that translocates PS to the outer membrane (Dekkers et al., 2002; Woon et al., 1999). Moreover, osmotic shock stimulates

the sphingomyelinase that leads to the formation of ceramide, which increases sensitivity of Ca^{2+} to membrane scramblase eventually increasing translocation of PS (Lang et al., 2010; Lang et al., 2004). Furthermore, osmotic shock has also been shown to increase oxidative stress and stimulate membrane scramblase in other cell types (Amer et al., 2008; Chong et al., 2004; Fabisiak et al., 2000; Kagan et al., 2002; Lang et al., 2008; Reinehr and Haussinger, 2006). Thus, sucrose (650 mM) was utilized as well as NaCl and urea to expose RBCs from SCD patients to hyperosmotic shock in order to examine its effects on PS exposure.

Urea has been shown to have a moderate inhibitory effect on PS exposure in normal HbAA RBCs. However, this has only been shown in normal HbAA RBCs exposed to hyperosmotic shock (Lang et al., 2003). Urea has previously been shown to alter the activity of several RBC transport systems such as the Na^+-K^+-ATPase, KCC and Na^+-K^+-$2Cl^-$ cotransport (Kaji et al., 1998; Kaji and Gasson, 1995; Lim et al., 1995; Speake and Gibson, 1997). Intravenous and oral urea have also been administered to investigate whether they reduce painful SCD crises. Oral therapy was unsuccessful although this was carried out only in 5 patients and the required urea blood level was never achieved (Nalbandian, 1972). Nevertheless, intravenous treatment did prove to have beneficial effects on the painful crisis of sickle cell disease. However, the researchers advise cautious interpretation of these data as the trial was uncontrolled and the treatment period was very short (McCurdy & Mahmood, 1971).

Hence, the effects of urea in HbSS RBCs was investigated where PS and sickling was induced by deoxygenation, hyperosmotic shock and hypertonicity. Table 5.1 further demonstrates the affect that each condition has on RBCs. These conditions may result from both renal functional disturbances and anatomical alterations observed in SCD patients.

Table 5.1 Different physiological conditions and their effect on RBCs

Conditions	Effect of Conditions on RBCs	Results section
Urea + standard buffer (SB; Ca^{2+}-vanadate LK-HBS, 290 mOsm.kg^{-1})	Hyperosmotic	5.2.2
SB + sucrose	Hyperosmotic and hypertonic	5.2.3
SB + urea + sucrose	Hyperosmotic and hypertonic	5.2.3
SB + NaCl	Hyperosmotic and hypertonic	5.2.4
SB + urea + NaCl	Hyperosmotic and hypertonic	5.2.4

5.2 Results

5.2.1 Inhibitory effect of urea on deoxygenation-induced sickling in HbSS RBCs

In the following experiment, the ability of urea to inhibit deoxygenation (0 mmHg)-induced sickling was investigated (Figure 5.1A and B). HbSS RBCs (0.5 % Hct) were treated with respective urea concentrations (200 mM, 600 mM & 900 mM) at 0 mmHg for 80 min. Every 20 min, aliquots of RBCs were removed and sickling was measured. Initially at 20 min (Figure 5.1A), sickling was significantly low for 600 mM ($p < 0.001$) and 900 mM ($p < 0.0001$) concentrations of urea compared to without urea. However, urea 900 mM was able to keep the sickling significantly low until 40 min ($p < 0.05$). Finally, at 80 min although sickling was lower in the presence of 600 mM and 900 mM urea, this reduction was not significant in comparison with RBCs incubated in the absence of urea. For 200 mM urea, at 20 min to 40 min the sickling percentage was lower compared to without urea, but not significantly. Later for 200 mM of urea, the sickling percentage was almost similar to that observed without urea from 60 min to 80 min.

In Figure 5.1B, HbSS RBCs (10 % Hct) were equilibrated at 0 mmHg for 20 min. After 20 min, aliquots of RBCs were removed and equilibrated for a further 60 min in respective urea concentrations (600 mM & 900 mM) after which sickling was measured. Unlike experiment in Figure 5.1A, in Figure 5.1B the HbSS RBCs are not initially exposed to urea. The HbSS RBCs are only exposed to urea after majority of them have sickled in the initial 20 min to determine whether urea addition could affect the morphology of previously sickled RBCs. The sickling was modestly reduced but significantly different for both concentrations of urea compared to without urea. The final sickling percentage was 84 % ± 3 % ($p < 0.001$) and 80 % ± 3 % ($p < 0.01$) for 600 mM and 900 mM concentrations of urea, while without urea was 89 % ± 3 %.
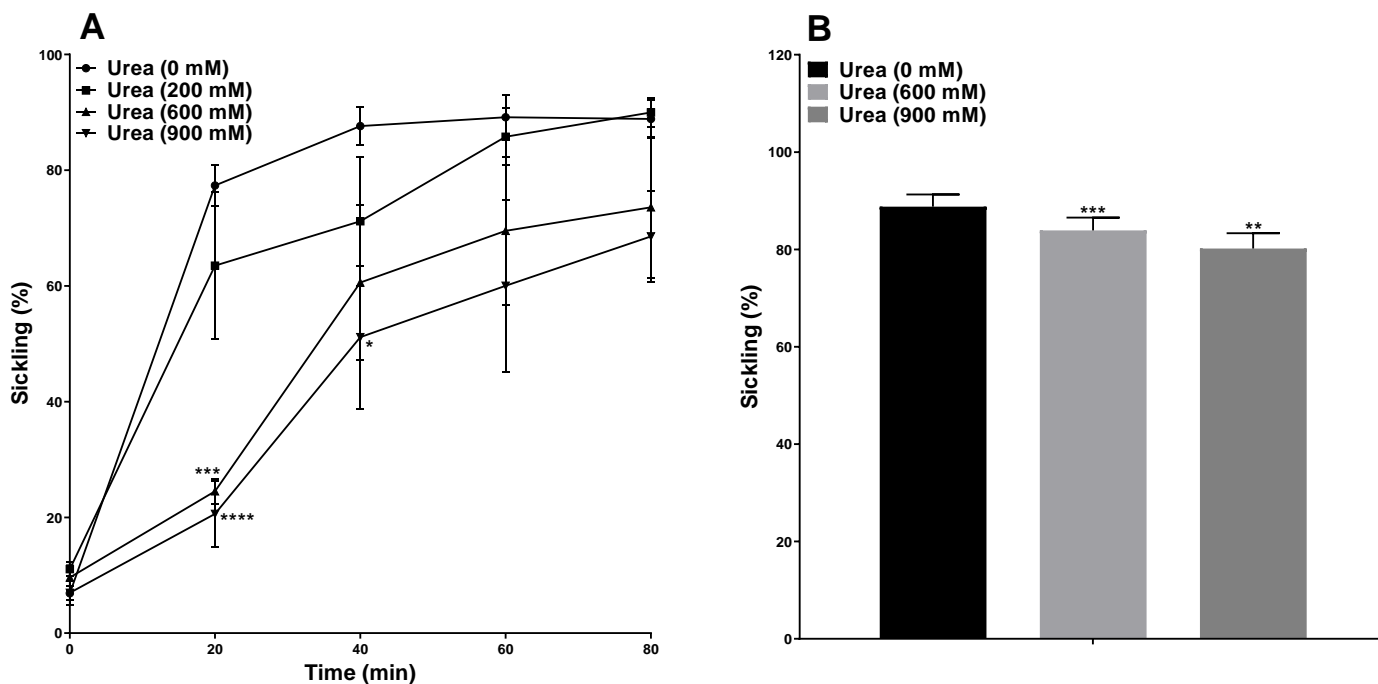
Figure 5.1: A: Effect of urea (200 mM, 600 mM & 900 mM) on sickling at 0 mmHg in RBCs from HbSS patients. B: Effect of urea (600 mM & 900 mM) on sickling in pre-incubated HbSS RBCs at 0 mmHg for 20 min. A: HbSS RBCs (0.5 % Hct, 1 ml) were treated with respective urea concentrations (200 mM, 600 mM & 900 mM) and in 0 mM urea (Ca^{2+}-vanadate LK-HBS, 290 $mOsm.kg^{-1}$) at 0 mmHg at 37 ° C, pH 7.0 in Eschweiler tonometers for 80 min. After every 20 min, aliquots of RBCs were removed and fixed using 0.3 % glutaraldehyde. * $p < 0.05$, *** $p < 0.001$ and **** $p < 0.0001$ comparing HbSS RBCs in the absence and presence of urea (600 mM and 900 mM). Data points represent means ± S.E.M, n = 4. B: Initially HbSS RBCs (10 % Hct, 1 ml) were equilibrated in 0 mM urea (Ca^{2+}-vanadate LK-HBS, 290 $mOsm.kg^{-1}$) at 0 mmHg at 37 ° C, pH 7.0 in Eschweiler tonometers for 20 min. After 20 min, aliquots of RBCs were removed and equilibrated in test tubes (pre-equilibrated at 0 mmHg) for a further 60 min in respective urea concentrations (600 mM & 900 mM), and fixed using 0.3 % glutaraldehyde. ** $p < 0.01$ and *** $p < 0.001$, comparing HbSS RBCs in the absence and presence of urea (600 mM and 900 mM). Histograms represent means ± S.E.M, n = 3.

5.2.2 Inhibitory effects of urea on deoxygenation-induced PS exposure

In this experiment, the effect of different concentrations of urea (200 mM, 600 mM & 900 mM) on PS exposure in HbSS RBCs was investigated in oxygenated (100 mmHg) and deoxygenated (0 mmHg) conditions (Figure 5.2). At 100 mmHg (Figure 5.2A), a significant difference from 40 min can be observed in 600 mM and 900 mM concentrations of urea compared to without urea. Finally, at 80 min a substantial decrease in PS is observed in all three concentrations compared to without urea (100 % normalised, actual mean value is 10.5 %), with 35.7 % ± 3 % ($p < 0.001$), 31.3 % ± 14.9 % ($p < 0.01$) and 29.6 % ± 12.9 % ($p < 0.0001$) at 200 mM, 600 mM and 900 mM concentrations of urea, respectively.

However, at 0 mmHg (Figure 5.2B), a significant difference from 60 min can be observed in 600 mM ($p < 0.0001$) and 900 mM ($p < 0.0001$) concentrations of urea compared to without urea. At 80 min a substantial decrease in PS to 16.7 % ± 2 % ($p < 0.0001$) and 14.3 % ± 4.9 % ($p < 0.0001$) is observed in both 600 mM and 900 mM concentrations of urea respectively, compared to without urea (100 %, actual mean value is 17.1 %). Although, the PS was low throughout the 80 min time course in 200 mM urea compared to without urea, the decrease was not significant.
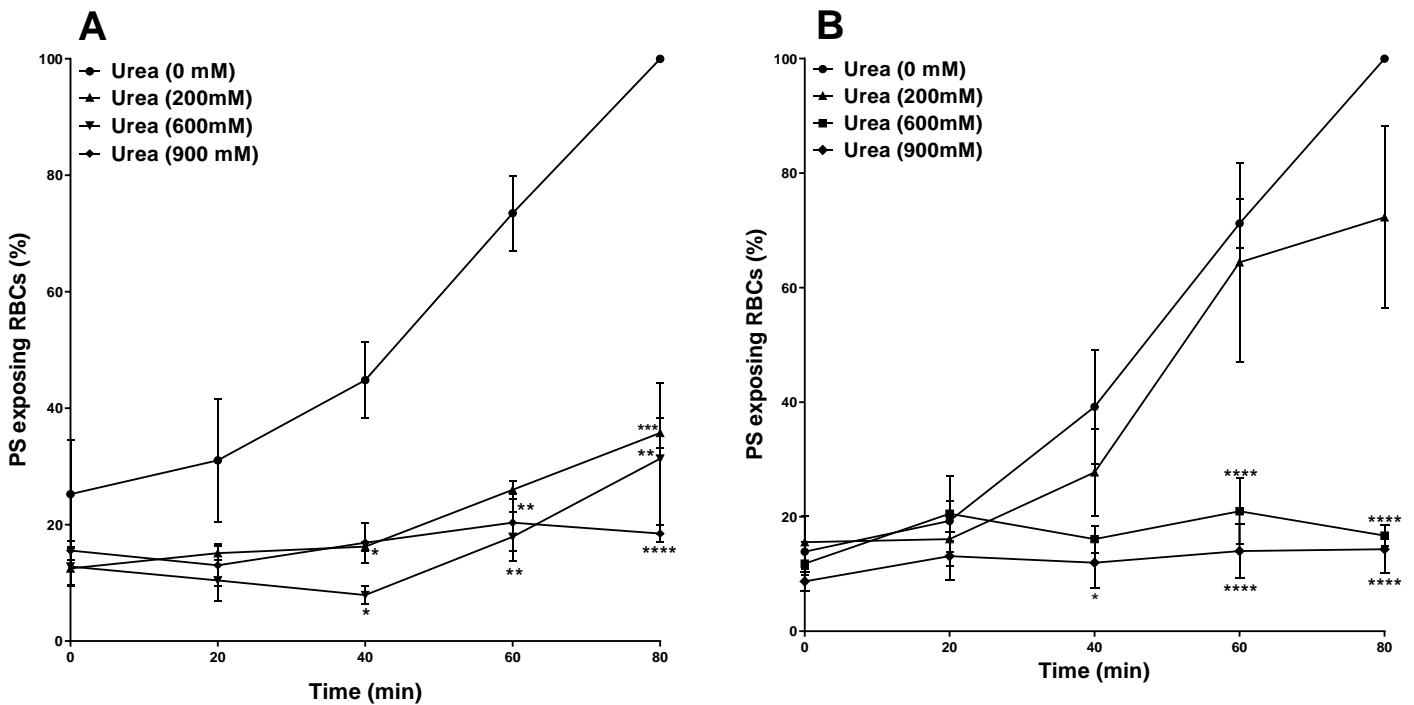

Figure 5.2: A: Effect of urea (200 mM, 600 mM & 900 mM) on PS exposure at 100 mmHg in RBCs from HbSS patients. B: Effect of urea (200 mM, 600 mM & 900 mM) on PS exposure at 0 mmHg in RBCs from HbSS patients. A: HbSS RBCs (0.5 % Hct, 1 ml) were treated with respective urea concentrations (200 mM, 600 mM & 900 mM) and 0 mM urea (Ca^{2+}-vanadate LK-HBS) in pH 7.0 at 37° C, at 100 mmHg in Eschweiler tonometers for 80 min. After every 20 min, aliquots of RBCs were removed and exposed PS labelled with LA-FITC. * $p < 0.05$, ** $p < 0.01$, *** $p < 0.001$ and **** $p < 0.0001$ comparing HbSS RBCs in the absence and presence of urea (200 mM, 600 mM and 900 mM) at 100 mmHg. The data points have been normalized, the actual mean PS exposure values at 80 min are urea 0 mM = 10.5 %, urea 200 mM = 3.8 %, urea 600 mM = 3.4 and urea 900 mM = 1.5 %. Data points represent means ± S.E.M, n = 4. B: HbSS RBCs (0.5 % Hct, 1 ml) were treated with respective urea concentrations (200 mM, 600 mM & 900 mM) and 0 mM urea (Ca^{2+}-vanadate LK-HBS) in pH 7.0 at 37° C, at 0 mmHg in Eschweiler tonometers for 80 min. After every 20 min, aliquots of RBCs were removed and exposed PS labelled with LA-FITC. * $p < 0.05$ and **** $p < 0.0001$, comparing HbSS RBCs in the absence and presence of urea (600 mM and 900 mM) at 0 mmHg. The data points have been normalized, the actual mean PS exposure values at 80 min are urea 0 mM = 17.1 %, urea 200 mM = 10.3 %, urea 600 mM = 2.6 % and urea 900 mM = 1.9 %. Data points represent means ± S.E.M, n = 4.

In the next series of experiments, HbSS RBCs are initially treated at 0 mmHg in the absence of urea for 20 min (Figure 5.3A) or 80 min (Figure 5.3B) to stimulate PS exposure, and later exposed to respective concentrations of urea, to measure if it can inhibit exposed PS. Firstly, HbSS RBCs were equilibrated at 0 mmHg for 20 min. After 20 min, aliquots of RBCs were removed and equilibrated for a further 60 min in respective urea concentrations (600 mM & 900 mM) after which PS was measured (Figure 5.3A). From Figure 5.3A it can be observed that there is a significant decrease in PS exposure between both concentrations of urea and without urea at 40 min and 80 min. Finally, at 80 min a substantial decrease in PS to 24.9 % ± 3.3 % ($p < 0.001$) and 12.7 % ± 3.6 % ($p < 0.001$) is observed in both 600 mM and 900 mM concentrations of urea respectively, compared to without urea (100 % normalised, actual mean value is 17.5 %).

Secondly, HbSS RBCs (10 % Hct) initially were equilibrated at 0 mmHg for 80 min. After 80 min, aliquots of RBCs were removed and equilibrated for a further 20 min in respective urea concentrations (600 mM & 900 mM) after which PS was measured (Figure 5.3B). A significant reduction in PS exposure was observed with both concentrations of urea compared to without urea. The final PS exposure at 100 min was 43.8 % ± 4.4 % ($p < 0.01$) and 32.7 % ± 7.5 % ($p < 0.01$) for both 600 mM and 900 mM concentrations of urea respectively, which was much lower than without urea (100 % normalised, actual mean value is 26.1 %).
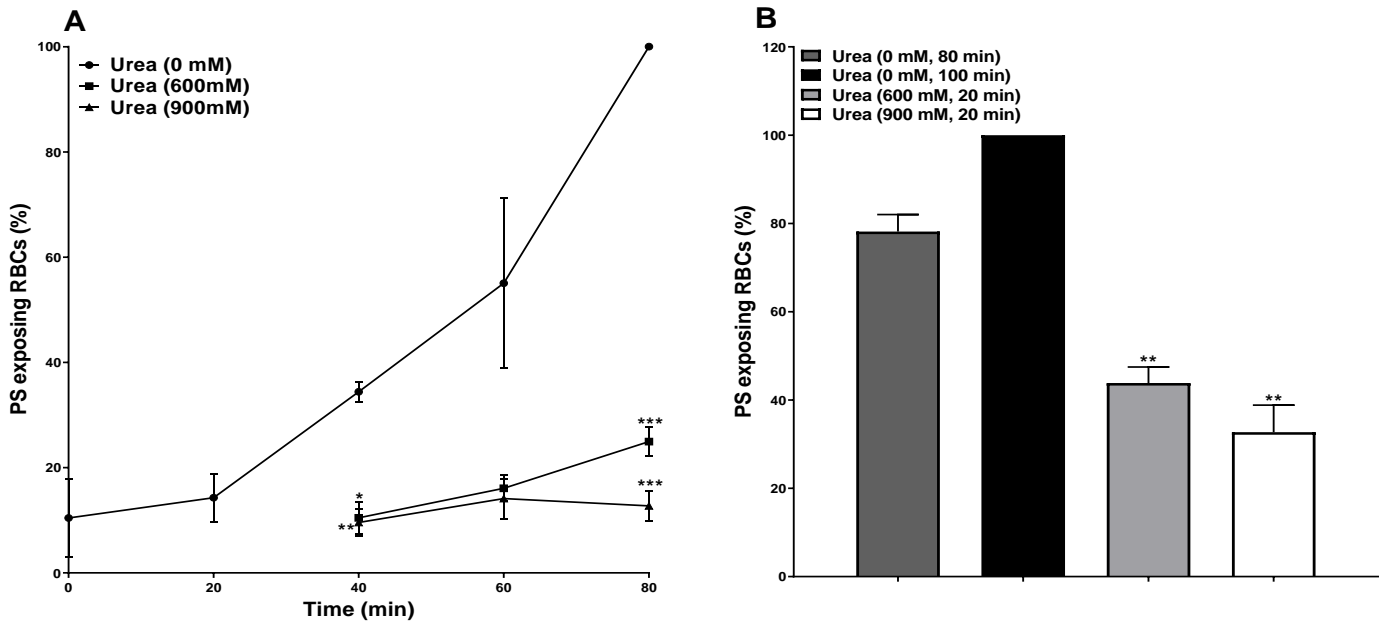
Figure 5.3: A: Effect of urea (600 mM & 900 mM) on PS exposure in HbSS RBCs pre-incubated at 0 mmHg for 20 min. B: Effect of urea (600 mM & 900 mM) on PS exposure in HbSS RBCs pre-incubated at 0 mmHg for 80 min. A: Initially HbSS RBCs (10 % Hct, 1ml) were equilibrated at 0 mmHg in urea 0 mM in pH 7.0 at 37° C in Eschweiler tonometers for 20 min. After 20 min, aliquots of RBCs were removed and equilibrated in test tubes (pre-equilibrated at 0 mmHg) for a further 60 min in respective urea concentrations (600 mM & 900 mM) after which PS was measured. * $p < 0.05$, ** $p < 0.01$ and *** $p < 0.001$, comparing HbSS RBCs in the absence and presence of urea (600 mM and 900 mM). The data points have been normalized, the actual mean PS exposure values at 80 min are urea 0 mM = 17.5 %, urea 600 mM = 4.22 % and urea 900 mM = 2.07 %. Data points represent means ± S.E.M, n = 3. B: Initially HbSS RBCs (10 % Hct, 1 ml) were equilibrated at 0 mmHg in urea 0 mM in pH 7.0 at 37° C in Eschweiler tonometers for 80 min. After 80 min, aliquots of RBCs were removed and equilibrated in test tubes (pre-equilibrated at 0 mmHg) for a further 20 min in respective urea concentrations (600 mM & 900 mM) in test tubes after which PS was measured. ** $p < 0.01$, comparing HbSS RBCs in the absence and presence of urea (600 mM and 900 mM). The data points have been normalized, the actual mean PS exposure values are urea (0 mM 80 min) = 20.3 %, urea (0 mM, 100 min) = 26.1 %, urea (600 mM, 20 min) = 12 % and urea (900 mM, 20 min) = 7.8 %. Histograms represent means ± S.E.M, n = 3

5.2.3 The effect of urea on hypertonicity (sucrose 650 mM)-induced PS exposure

In the following experiment, the effect of different concentrations of urea on PS exposure was compared in RBCs incubated in sucrose (650 mM) solutions under oxygenated (100 mmHg) and deoxygenated (0 mmHg) conditions (Figure 5.4). At 100 mmHg (Figure 5.4A), a highly significant decrease in PS exposure from 0 min to 80 min can be observed in all three concentrations of urea compared to sucrose (650 mM) without urea. At 80 min, PS exposure is 3.8 % ± 0.7 % ($p < 0.001$), 3.4 % ± 1.7 % ($p < 0.001$) and 1.8 % ± 1.7 % ($p < 0.001$) at 200 mM, 600 mM and 900 mM concentrations of urea, respectively, compared to 70.5 % ± 2.6 % in sucrose (650 mM) only.

Similarly, at 0 mmHg (Figure 5.4B), a significant difference in PS exposure from 0 min to 80 min can be observed in all the three concentrations of urea compared to sucrose (650 mM) only. At 80 min, PS exposure is 10.3 % ± 2.3 % (p < 0.0001), 2.6 % ± 0.6 % (p < 0.0001) and 1.8 % ± 0.02 % (p < 0.0001) at 200 mM, 600 mM and 900 mM concentrations of urea respectively, compared to 80.4 % ± 2.8 % in sucrose (650 mM).
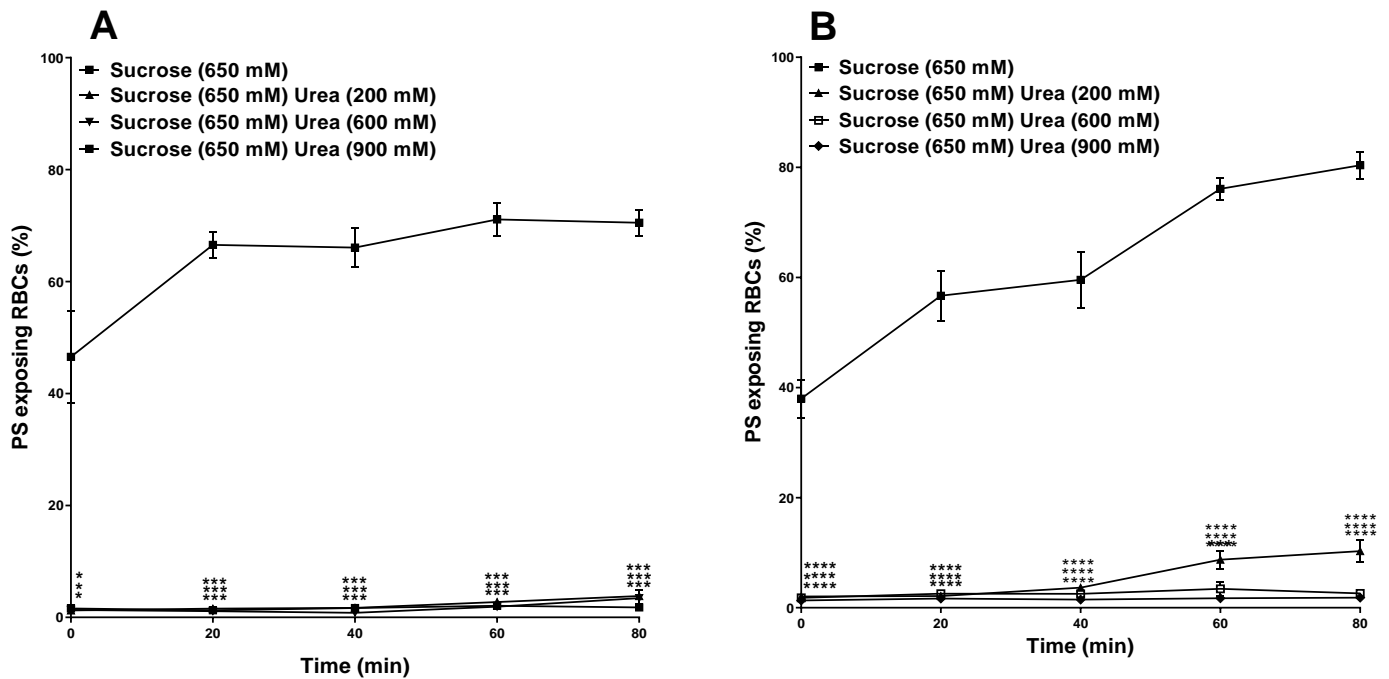

Figure 5.4: A: Effect of urea (200 mM, 600 mM & 900 mM) on sucrose (650 mM) induced PS exposure at 100 mmHg in RBCs from HbSS patients. B: Effect of urea (200 mM, 600 mM & 900 mM) on sucrose (650 mM) induced PS exposure at 0 mmHg in RBCs from HbSS patients. A: HbSS RBCs (0.5 % Hct, 1 ml) were treated with respective urea concentrations (200 mM, 600 mM & 900 mM) and sucrose (650 mM) in pH 7.0 at 37° C, at 100 mmHg in Eschweiler tonometers for 80 min. After every 20 min, aliquots of RBCs were removed and exposed PS labelled with LA-FITC. * p < 0.05 and *** p < 0.001, comparing HbSS RBCs in the absence and presence of urea (200 mM, 600 mM and 900 mM) at 100 mmHg. Data points represent means ± S.E.M, n = 4. B: HbSS RBCs (0.5 % Hct, 1 ml) were treated with respective urea concentrations (200 mM, 600 mM & 900 mM) and sucrose (650 mM) in pH 7.0 at 37° C, at 0 mmHg in Eschweiler tonometers for 80 min. After every 20 min, aliquots of RBCs were removed and exposed PS labelled with LA-FITC. **** p < 0.0001, comparing HbSS RBCs in the absence and presence of urea (200 mM, 600 mM and 900 mM) at 0 mmHg. Data points represent means ± S.E.M, n = 4.

In the next series of experiments, the HbSS RBCs were initially treated in sucrose (650 mM) at 100 or 0 mmHg in the absence of urea for 20 min or 80 min to stimulate PS exposure, and later exposed to respective concentrations of urea, to measure if it can reverse exposed PS (Figures 5.5 and 5.6). In the first part of the experiment (Figure 5.5A), HbSS RBCs (10 % Hct) were equilibrated at 100 mmHg in sucrose (650 mM) for 20 min. After 20 min, aliquots

of RBCs were removed and equilibrated for a further 60 min in respective urea concentrations (600 mM & 900 mM, as well as without urea) after which PS was measured. Throughout the time course both concentrations of urea were highly effective in reducing the sucrose (650 mM)-induced PS exposure. The final PS at 80 min was 1.6 % ± 1.3 % (p < 0.001) and 0.9 % ± 0.3 % (p < 0.001) for 600 mM and 900 mM concentrations of urea respectively, while PS exposure without urea was 69.2 % ± 1.2 %. In the second part of the experiment (Figure 5.5B), HbSS RBCs (10 % Hct) were equilibrated at 100 mmHg in sucrose solutions for 80 min. After 80 min, aliquots of RBCs were removed and equilibrated for a further 20 min in respective urea concentrations (600 mM & 900 mM) after which PS was measured. Both concentrations of urea were highly effective in reducing the sucrose (650 mM)-induced PS exposure. The final PS was 24.4 % ± 1.4 % (p < 0.01) and 19.4 % ± 1.5 % (p < 0.01) for 600 mM and 900 mM concentrations of urea respectively, while PS exposure without urea was 60.7 % ± 4.1 %.

Figure 5.5: A: Effect of urea (600 mM & 900 mM) on PS exposure in HbSS RBCs pre-incubated at 100 mmHg in sucrose (650 mM) for 20 min. B: Effect of urea (600 mM & 900 mM) on PS exposure in HbSS RBCs pre-incubated at 100 mmHg in sucrose (650 mM) for 80 min. A: Initially HbSS RBCs (10 % Hct, 1 ml) were equilibrated in sucrose (650 mM) at 37° C, pH 7.0 in Eschweiler tonometers for 20 min. After 20 min, aliquots of RBCs were removed and equilibrated in test tubes (pre-equilibrated at 100 mmHg) for a further 60 min in respective urea concentrations (600 mM & 900 mM) after which exposed PS was labelled with LA-FITC. ** p < 0.01 and *** p < 0.001, comparing HbSS RBCs in the absence and presence of urea (600 mM and 900 mM). Data points represent means ± S.E.M, n = 3. B: Initially HbSS RBCs (10 % Hct, 1 ml) were equilibrated in sucrose (650 mM) at 37° C, pH 7.0 in Eschweiler tonometers for 80 min. After 80 min, aliquots of RBCs were removed and equilibrated in test tubes (pre-equilibrated at 100 mmHg) for a further 20 min in

respective urea concentrations (600 mM & 900 mM) after which exposed PS was labelled with LA-FITC. ** p < 0.01, comparing HbSS RBCs in presence of sucrose (650 mM) alone and urea (600 mM and 900 mM) at 100 mmHg at 100 min. Histograms represent means ± S.E.M, n = 3.

HbSS RBCs (10 % Hct) were equilibrated at 0 mmHg in sucrose (650 mM) for 20 min. After 20 min, aliquots of RBCs were removed and equilibrated for a further 60 min in respective urea concentrations (600 mM & 900 mM) after which PS was measured (Figure 5.6A). Throughout the time course both concentrations of urea successfully reduced the sucrose (650 mM)-induced PS exposure. The final PS at 80 min was 15.2 % ± 2.1 % (p < 0.001) and 5.7 % ± 2.5 % (p < 0.001) for both 600 mM and 900 mM concentrations of urea, respectively, while PS exposure without urea was 83.2 % ± 1.6 %. In the second part of the experiment (Figure 5.6B), HbSS RBCs (10 % Hct) were equilibrated at 0 mmHg sucrose for 80 min. After 80 min, aliquots of RBCs were removed and equilibrated for a further 20 min in respective urea concentrations (600 mM & 900 mM) after which PS was measured. Both concentrations of urea were highly successful in reducing the sucrose (650 mM) induced PS exposure. The final PS was 56.9 % ± 2.8 % (p < 0.05) and 46.5 % ± 3.2 % (p <0.01) for both 600 mM and 900 mM concentrations of urea, respectively, while PS exposure without urea was 77.5 % ± 1.3 %.
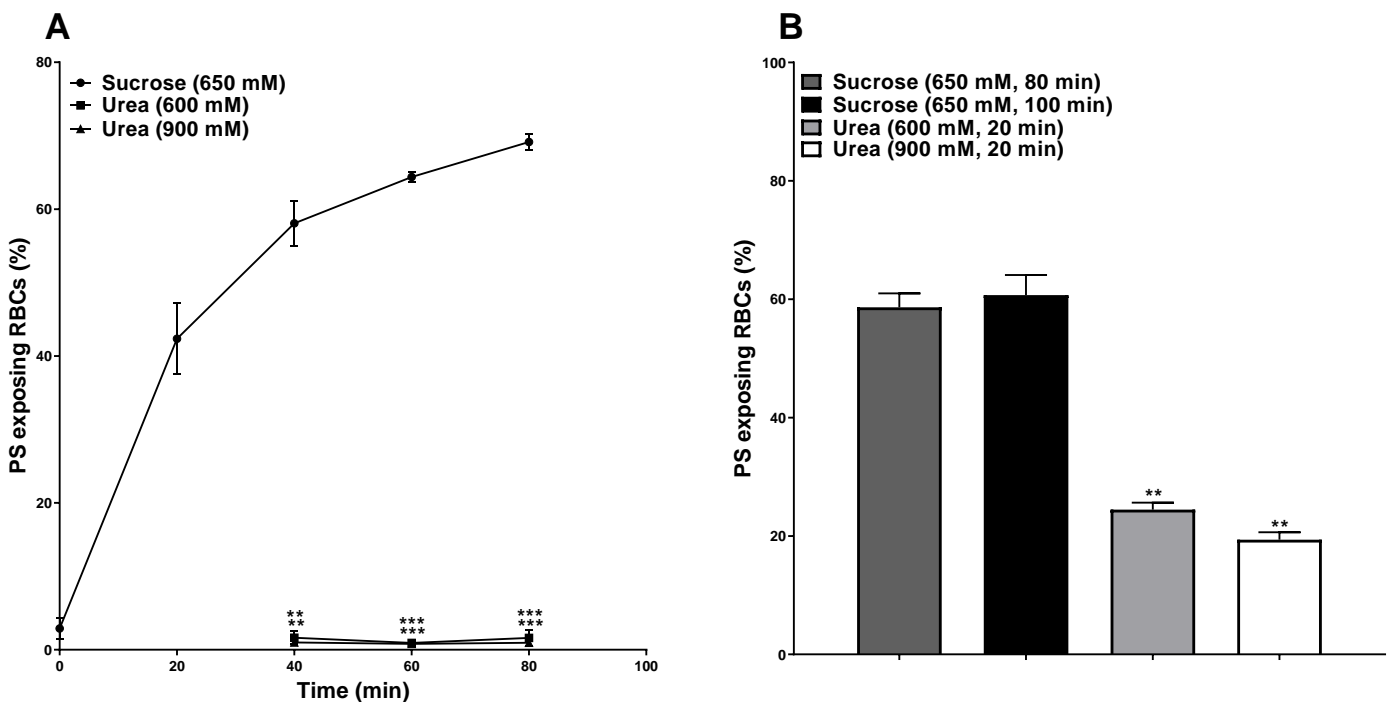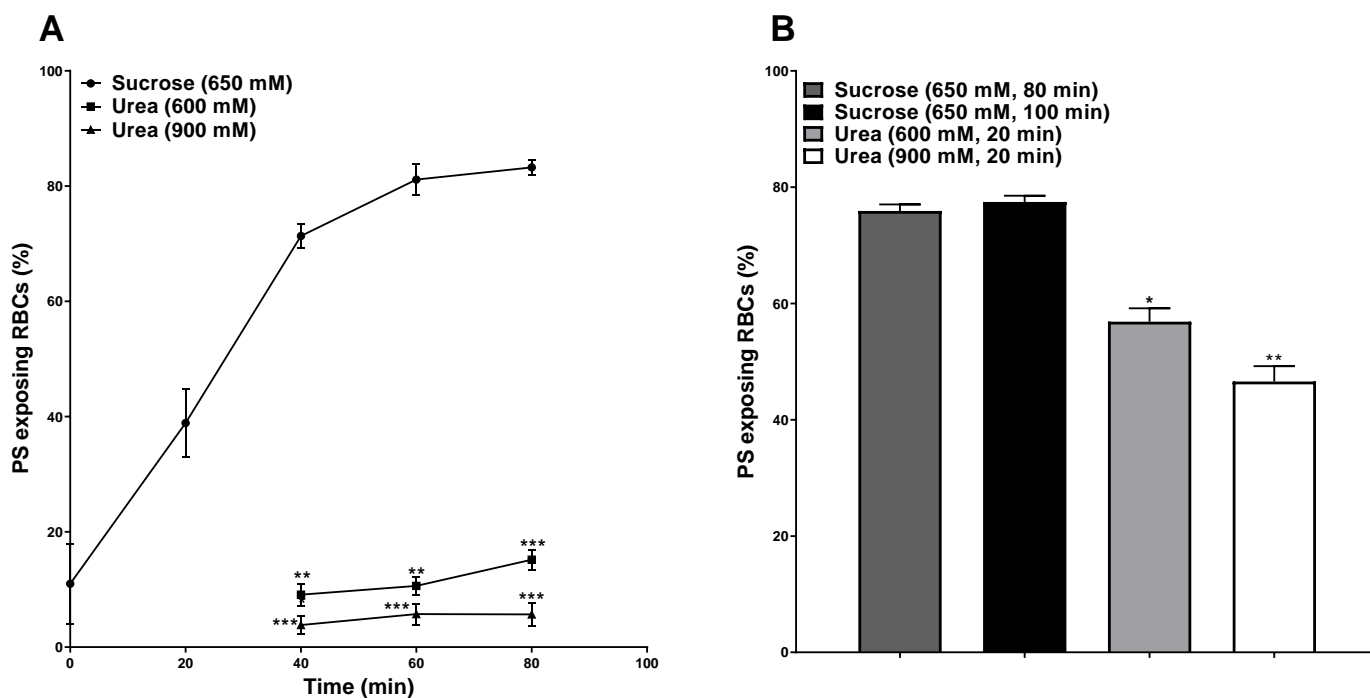
Figure 5.6: A: Effect of urea (600 mM & 900 mM) on PS exposure in HbSS RBCs pre-incubated at 0 mmHg in sucrose (650 mM) for 20 min. B: Effect of urea (600 mM & 900 mM) on PS exposure in HbSS RBCs pre-incubated at 0 mmHg in sucrose (650 mM) for 80 min. A: Initially HbSS RBCs (10 % Hct, 1 ml) were equilibrated at 0 mmHg in sucrose (650 mM) at 37° C, pH 7.0 in Eschweiler tonometers for 20 min. After 20 min, aliquots of RBCs were removed and equilibrated in test tubes (pre-equilibrated at 0 mmHg) for a further 60 min in respective urea concentrations (600 mM & 900 mM) after which exposed PS was labelled with LA-FITC. ** $p < 0.01$ and *** $p < 0.001$, comparing HbSS RBCs in the absence and presence of urea (600 mM and 900 mM). Data points represent means ± S.E.M, n = 3. B: Initially HbSS RBCs (10 % Hct, 1ml) were equilibrated at 0 mmHg in sucrose (650 mM) at 37° C, pH 7.0 in Eschweiler tonometers for 80 min. After 80 min, aliquots of RBCs were removed and equilibrated in test tubes (pre-equilibrated at 0 mmHg) for a further 20 min in respective urea concentrations (600 mM & 900 mM) after which exposed PS was labelled with LA-FITC. * $p < 0.05$ and ** $p < 0.01$, comparing HbSS RBCs in the presence of sucrose (650 mM) alone and urea (600 mM and 900 mM) at 0 mmHg at 100 min. Histograms represent means ± S.E.M, n = 3.

5.2.4 The effect of urea on hypertonicity (NaCl)-induced sickling and PS exposure

Hypertonicity in deoxygenated RBCs was achieved through addition of NaCl (to a total osmolality of 1200 mOsm.kg⁻¹). In both control (Ca²⁺-vanadate LK-HBS, 290 mOsm.kg⁻¹) and NaCl (600 mM) more than 80 % of HbSS RBCs have already sickled by 20 min and showed that over a period of 80 min deoxygenation-induced sickling was very similar in both conditions (Figure 5.7). However, in presence of urea 600 mM the deoxygenation-induced sickling in NaCl (300 mM) was significantly lower at both 20 ($p < 0.001$) and 40 min ($p < 0.01$) compared to control. Although after 40 min the sickling was also lower in

presence of urea 600 mM, this effect was not significant. Nevertheless, in the presence of 900 mM urea deoxygenation-induced sickling in NaCl (300 mM) was significantly lower compared to control throughout the 80 min incubation. Urea 900 mM was able to strongly inhibit sickling until 40 min ($p < 0.0001$) and a sharp rise was observed, although still significantly lower than control.
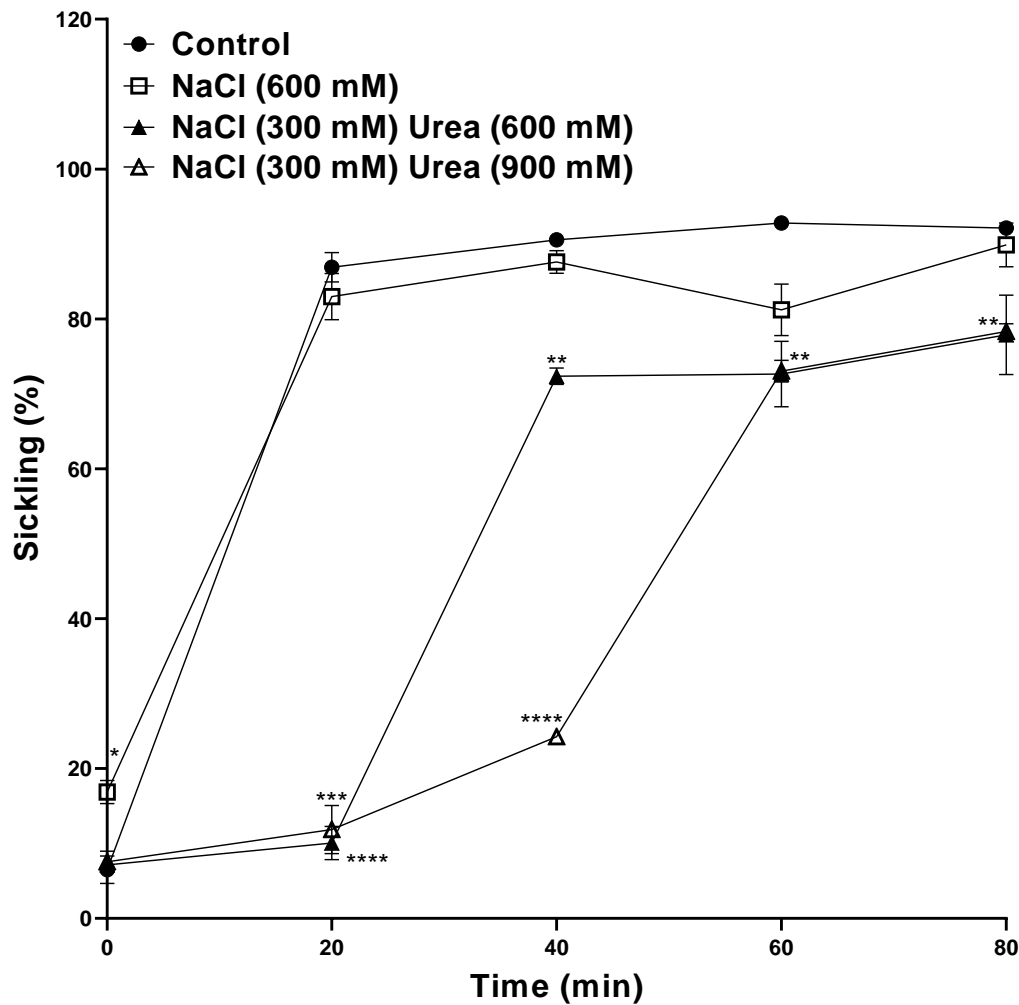
Figure 5.7: Effect of urea (600 mM & 900 mM) on NaCl-induced sickling at 0 mmHg. HbSS RBCs (0.5 % Hct, 1 ml) were incubated in Eschweiler tonometers at 37 °C, pH 7.0, and an osmolality of 290-1200 mOsm.kg^{-1} (through addition of hypertonic NaCl) for up to 80 min under fully deoxygenated (0 mmHg oxygen) conditions in the absence of urea or at two different urea concentrations (600 and 900 mM). Every 20 min, aliquots of RBCs were removed and fixed using 0.3 % glutaraldehyde. * $p < 0.05$ comparing HbSS RBCs in NaCl (600 mM) and control (Ca^{2+}-vanadate LK-HBS, 290 mOsm.kg^{-1}). ** $p < 0.01$, *** $p < 0.001$ and **** $p < 0.0001$ comparing HbSS RBCs treated in control and urea (600 mM and 900 mM). Data points represent means ± S.E.M, n = 3.

In this experiment, hypertonicity had minimal effect on the progressive increase in PS exposure observed during deoxygenation. As it can be seen from Figure 5.8, PS exposure

after 80 min in deoxygenated conditions in both control (Ca^{2+}-vanadate LK-HBS, 290 mOsm.kg^{-1}) and NaCl (600 mM) is very similar and there was no significant difference. However, the presence of urea (600 or 900 mM) prevented any increase in PS exposure over the time course of the experiment. The final PS percentage at 80 min for both the urea concentrations was approximately 10 % ± 0.5 % ($p < 0.0001$) compared to 100 % (actual mean value is 21 %) in control and 80 % ± 10% in NaCl (600 mM; N.S. cf control).
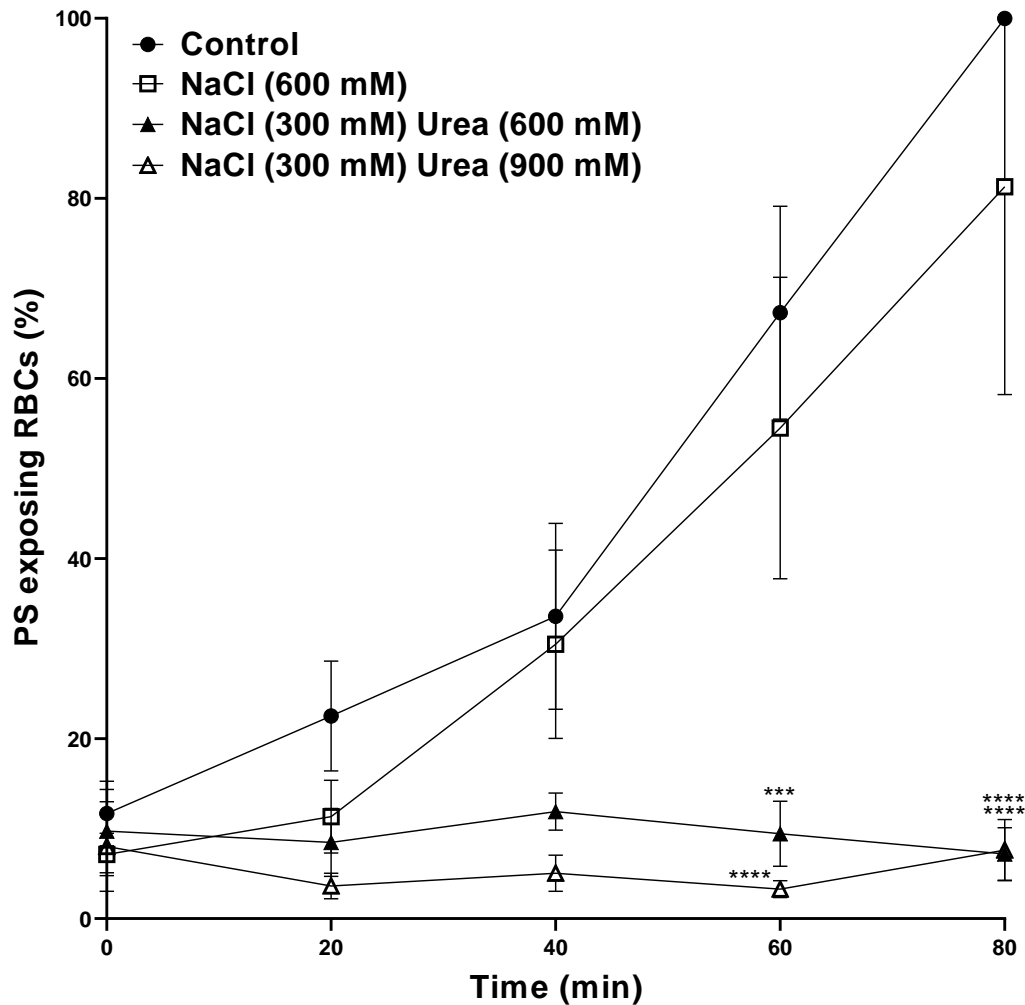
Figure 5.8: The effect urea and hypertonic NaCl on PS exposure in deoxygenated HbSS RBCs. HbSS RBCs (0.5 % Hct, 1 ml) were incubated in Eschweiler tonometers at 37 °C, pH 7.0 and an osmolality of 290 - 1200 mOsm.kg^{-1} (through addition of hypertonic NaCl) for up to 80 min under fully deoxygenated (0 mmHg oxygen) conditions in the absence of urea or at two different urea concentrations (600 and 900 mM). After every 20 min, RBC aliquots were removed and exposed PS labelled with LA-FITC. *** $p < 0.001$ and **** $p < 0.0001$ comparing HbSS RBCs treated in control (Ca^{2+}-vanadate LK-HBS, 290 mOsm.kg^{-1}) and urea (600 mM and 900 mM). The data points have been normalized, with maximal PS after 80 min reaching 21 % in control RBCs. Data points represent means ± S.E.M, n = 4.

5.3 Discussion

The present findings show that the main conditions - namely hypoxia, hyperosmotic and hypertonicity - found in a healthy renal medulla during antidiuresis, increased PS exposure, and where studied sickling, in RBCs from patients with SCD. High concentrations of urea markedly reduced these effects.

Hyperosmotic and hypertonicity induced by sucrose (Figure 5.4-5.6), however, was much more effective than that elicited by high levels of NaCl (Figure 5.8). It might be because extracellular Cl$^-$ limits activation of a nonselective cation conductance significantly compared to sucrose (Lang et al., 2004). This would: (i) limit Ca^{2+} entering into RBCs compared to RBCs exposed to sucrose and (ii) limiting cation conductance would also reduce dehydration and hence shrinking of RBCs. Moreover, sucrose could possibly through oxidative stress stimulate PS exposure (Duranton et al., 2002; Hannemann et al., 2018). These three possibilities might explain the relatively low PS exposure induced by NaCl compared to those with sucrose. Urea at high concentrations was protective, particularly against PS exposure (Figure 5.2-5.6, and 5.8). It could be that progressive loss of the ability to accumulate urea, which would occur – hyposthenuria - as the renal medulla became progressively damaged, would contribute to pathogenesis.

The effects of osmotic shock on RBCs have been studied extensively by the group of Lang et al., (2003 and 2004), although mainly on normal (HbAA) red cells. In normal red cells, PS exposure induced by hypertonicity involves several pathways: it causes the opening of cation channels permeable to Ca^{2+} (Lang et al., 2004) and also stimulates sphingomyelinase with resulting increase in levels of ceramide, a compound associated with PS externalisation (Lang et al., 2004) . Furthermore, hypertonicity also stimulates cyclooxygenase with production of PGE2, which acts *via* phospholipase A2 to activate sphingomyelinase (Lang et al., 2005). It will be interesting to investigate the involvement of these mechanisms in sickle cells. Thus, in Chapter 7, experiments are carried out to explore the role of SMase signalling process, in an attempt to identify its effect in PS exposure in RBCs.

Lang's group also examined the protective effect of urea. In normal RBCs and platelets, urea was also seen to reduce PS exposure induced by hyperosmotic shock (Gatidis et al., 2010; Lang et al., 2004). Urea appeared to act by inhibiting sphingomyelinase, reducing the synthesis of ceramide, and was thus ineffective in preventing PS exposure in response to added ceramide (K S Lang et al., 2004). Furthermore, urea did not block, but rather activated, the RBC cation

conductance, indicating that this channel is not the main mechanism by which hyperosmotic shock results in PS exposure pointing to a pre-eminent contribution by ceramide (Lang et al., 2010; Lang et al., 2004).

Urea also probably affects the hydrophobic bonds within the HbS molecules that result in polymerisation (May and Huehns, 1975; Nalbandian, 1972). Thus, having a significant effect on sickling of HbSS RBCs (Figure 5.1 and 5.7). As such, it has been proposed as a possible treatment for SCD patients (McCurdy & Mahmood, 1971). In reality, however, it is likely that the concentrations required would be excessively high, near molar levels. Because of this, other potential reagents, such as cyanate, which prevent polymerisation at much lower (low mM) concentrations have been suggested (Cerami and Manning, 1971) although it has been shown to be ineffective as a clinical therapy for SCD.

Finally, a number of manoeuvres considered here, will also alter the permeability of the RBC membrane acting *via* transport systems, which include stimulation of the KCl cotransporter (KCC) and effects on P_{sickle} (Gibson and Ellory, 2002). Urea also stimulates KCC in RBCs from other species (including dog, sheep, and horse) – see Gibson and Ellory (2003). Such changes in membrane permeability may therefore also contribute to effects on sickling and PS exposure.

In conclusion, the hypoxic, hyperosmotic shock and hypertonic conditions in the renal medulla act to increase sickling and PS exposure in RBCs from SCD patients, an effect markedly reduced by high concentrations of urea.

6 Pharmacological elucidations of mechanisms 1: Role of PIEZO1 and PKC in sickling and PS exposure in RBCs from HbSS patients

6.1 Introduction

Free Ca^{2+} is an important and universal second messenger in all cells, including RBCs. Compared to other cell types, RBCs do not have intracellular organelles such as endoplasmic reticulum or mitochondria in which Ca^{2+} are stored (Moras et al., 2017). Therefore, they do not have the ability to regulate free cytosolic Ca^{2+} concentration and thereby Ca^{2+} signalling using these mechanisms. Thus, their only way to control the free intracellular Ca^{2+} is by the regulation of membrane transport. The intracellular Ca^{2+} in RBCs is tightly maintained and regulated primarily by the Ca^{2+} pumps PMCA1 and PMCA4 (Lew et al., 1982; Schatzmann, 1983). Increase in intracellular Ca^{2+} is not only a signalling mechanism for cell death, it also has other effects such as clot formation, modulation of the RBCs O_2 binding properties and also causes brief transient cellular volume adaptation allowing RBCs to pass through small capillaries or slits in the spleen (Andrews and Low, 1999; Danielczok et al., 2017; Kaestner et al., 2004; Makhro et al., 2013). The exact mechanism of PS exposure in HbSS RBCs is still uncertain, however, although it has been suggested that elevated intracellular Ca^{2+} during deoxygenation plays a crucial role (Bitbol et al., 1987; Lubin et al., 1981; Williamson et al., 1992). This increased permeability to Ca^{2+} is, at least in part, due to the activation of a deoxygenation-induced cation conductance called P_{sickle}.

The P_{sickle} pathway is activated by HbS deoxygenation, polymerisation and the sickling shape change (Mohandas et al., 1986), and as well as making the cell leaky to univalent cations, it also mediates entry of Ca^{2+} (Joiner et al., 1993), together with loss of Mg^{2+} (Section 1.3). As mentioned in Section 1.3 (ii)(b) PS exposure requires both inhibition of the flippase together with activation of the scramblase (Kuypers, 1998; Zwaal and Schroit, 1997). Both of these may be precipitated by increases in intracellular Ca^{2+} concentration which under normal circumstances is kept at very low levels, around 30 nM, in comparison with a free plasma Ca^{2+} concentration some five orders of magnitude higher (at about 1.1–1.2 mM). If intracellular Ca^{2+} approaches a few hundred nanomolar, the co-ordinated inhibition of the flippase and activation of the scramblase is initiated. It is not surprising therefore that deoxygenation of sickle cells has been associated with increase in PS exposure, which are both dependent on the presence of extracellular Ca^{2+} and which may be inhibited by intracellular Ca^{2+} chelation (Cytlak et al., 2013; Weiss et al., 2012). With its

proposed central role in SCD pathogenesis, it is understandable that considerable attention has been focused on regulation of P_{sickle} and identification of potential therapeutic inhibitors. Notwithstanding its significance, however, the molecular identity of P_{sickle} still remains uncertain. Various pathways for mediation of P_{sickle} activity have been proposed, ranging from a simple disintegration of the plasma membrane, to specific protein-mediated pathways including VDAC, NMDA receptors, TRPV channels - as well as others (Table 1.3). Latterly attention has focused on PIEZO1 (Cahalan et al., 2015).

PIEZO1 is a non-selective cation channel that shows a significant preference to Ca^{2+} and also to some monovalent cations (Saotome et al., 2018; Zhao et al., 2018). Activation of the channel has been shown to cause significant changes to the RBCs physiology and plays an active role in erythropoiesis (Caulier et al., 2020). Under physiological conditions, PIEZO1 is responsible for RBC volume and hydration homeostasis by maintaining ion balance (Cahalan et al., 2015; Lew and Tiffert, 2017; Svetina et al., 2019). There are compelling pieces of evidence, which make a strong case supporting PIEZO1 as the molecular identity of P_{sickle} (Section 1.3), such as gain-of-function mutations in PIEZO1 found in patients with hereditary xerocytosis (Bae et al., 2013; Picard et al., 2019; Zarychanski et al., 2012) and stomatocytosis (Albuisson et al., 2013; Andolfo et al., 2013) with a proposed mechanism of increased Ca^{2+} entry via PIEZO1 causing aberrant Gárdos channel activation and therefore K^+ loss and dehydration. P_{sickle} has long thought to be unique to RBCs from SCD patients, which is odd given that the underlying mutation resides in the β globin gene, and not in any membrane transport protein. Findings with PIEZO1 suggest that the protein responsible for the P_{sickle} entity may therefore be present and perhaps even functional in RBCs of all people.

Recently, several pharmacological agonists / antagonists of PIEZO1 have been described, including Yoda1, Dooku1 and Jedi1 (Syeda et al., 2015; Evans et al., 2018; Wang et al., 2018; Botello-Smith et al., 2019). Here the effect of Yoda1, an agonist for PIEZO1, was investigated on RBCs of SCD patients to examine its role in Ca^{2+} entry and PS exposure. Moreover, a competitive antagonist of Yoda1 called Dooku1 and the PIEZO1 channel blocker GsMTx4 were also tested to investigate their effect on PIEZO1 activation and changes in intracellular Ca^{2+}.

6.2 Results

6.2.1 Yoda1-induced Ca^{2+} entry

The effect of Yoda1 on intracellular Ca^{2+} concentration was investigated using Fluo-4 in HbSS RBCs, incubated in two different conditions: the presence (1.1 mM) and absence (EGTA 1 mM & 0 Ca^{2+}) of extracellular Ca^{2+} (Figure 6.1). All the experiments in this chapter were carried out in eppendorf tubes and incubated in air at 37 ° C. This experiment was done to establish that in HbSS RBCs Yoda1 causes entry of Ca^{2+} from extracellular fluid and to examine whether Yoda1 stimulated release of Ca^{2+} from any intracellular stores, if present, albeit unlikely as discussed in the Introduction (Section 6.1). HbSS RBCs incubated in the presence of extracellular Ca^{2+} showed significant increases in intracellular Ca^{2+} with increasing Yoda1 concentrations. The effect became significant at a very low concentration of Yoda1 i.e. 100 nm ($p < 0.01$). The median Fluo-4 fluorescence (in arbitrary units) increased from 4,016 without Yoda1 to 33,963 at 5 µM Yoda1 in the presence of extracellular Ca^{2+}. However, in HbSS RBCs incubated in the absence of extracellular Ca^{2+}, the median Fluo-4 remained low. In this case, the median Fluo-4 fluorescence changed from 1,630 without Yoda1 to only 1,665 at 5 µM Yoda1. These results are consistent with Yoda1-induced Ca^{2+} entry, presumably through activation of PIEZO1.
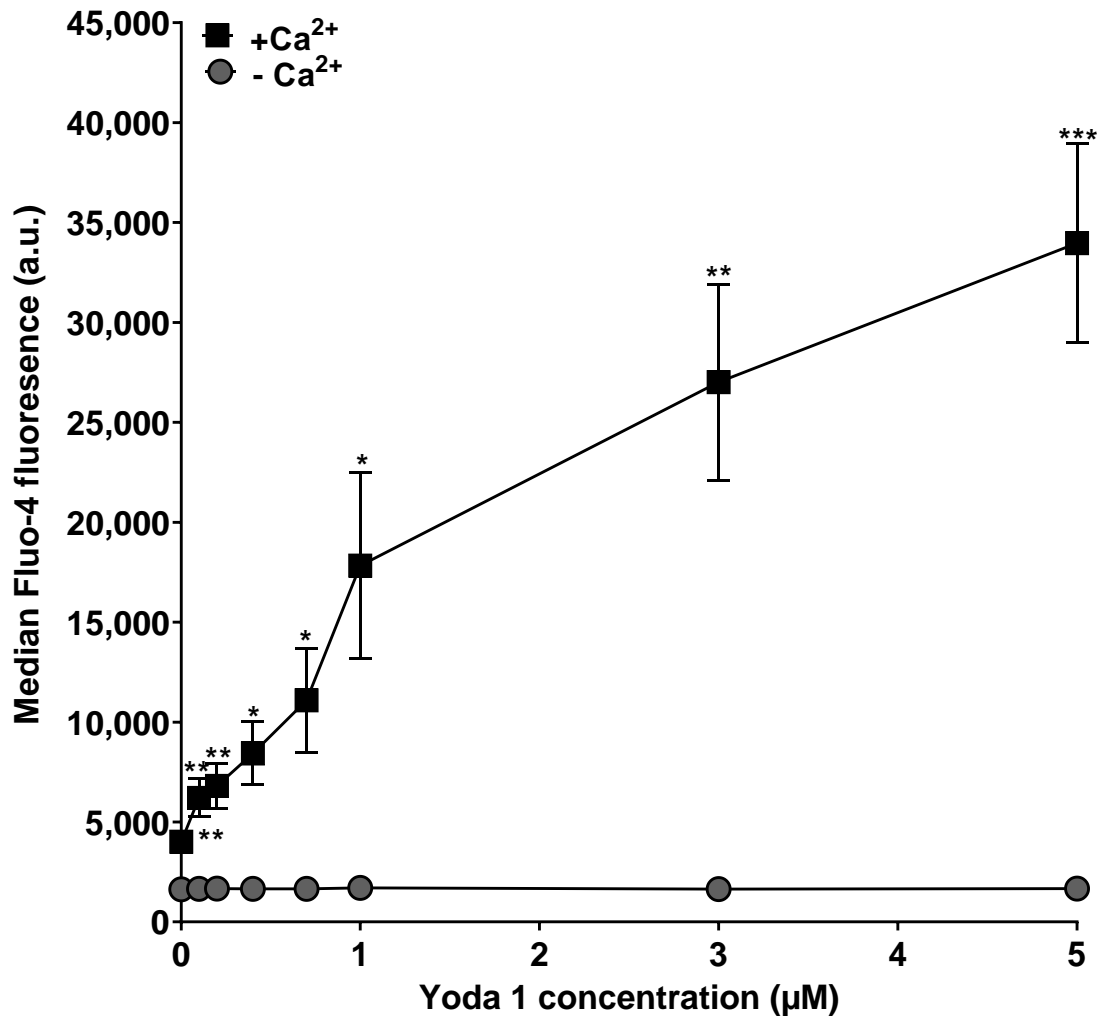
Figure 6.1: Effect of Yoda1 on intracellular Ca^{2+} concentration in RBCs from HbSS patients. HbSS RBCs (0.5 % Hct), pre-loaded with Fluo-4AM (5 µM), were equilibrated in air and treated with Yoda1 (0.1 µM to 5 µM) for 20 min at 37 °C in the presence (1.1 mM) and absence (EGTA 1mM & 0 Ca^{2+}) of extracellular Ca^{2+}. Intracellular Ca^{2+} was measured using Fluo-4. All the experiments in this chapter were carried out in eppendorf tubes and incubated in air at 37 °C. * $p < 0.05$, ** $p < 0.01$ and *** $p < 0.001$ comparing HbSS RBCs treated with Yoda1 in the presence and absence of extracellular Ca^{2+}. Data points represent means ± S.E.M, n = 4.

6.2.2 Inhibition of Yoda1-induced Ca^{2+} entry

In the next set of experiments, a known antagonist of Yoda1 called Dooku1 (Figure 6.2) and a known PIEZO1 channel blocker GsMTx4 (a tarantula spider venom) (Figure 6.3) were utilized to determine any inhibitory effect on Yoda1-induced Ca^{2+} entry.

In the presence of extracellular Ca^{2+}, the median Fluo-4 fluorescence increased significantly (Figure 6.2, $p < 0.01$) from 3,986 in the absence of Yoda1 to 7,921 in its presence (1 µM). However, increasing concentrations of Dooku1 (1 µM & 10µM) in the presence of Yoda1 (1 µM) decreased the median Fluo-4 fluorescence significantly ($p < 0.01$) from 7,921 to 6,496 and 4,282, respectively. As expected, in the absence of extracellular Ca^{2+} there was

no change in the median Fluo-4 fluorescence in the presence of either Yoda1 or Dooku1 alone, or when Yoda1 was combined with Dooku1.

Figure 6.2: Effect of various Dooku1 concentrations (0.1 µM, 1 µM and 10 µM) on intracellular Ca^{2+} concentration in the presence of Yoda1 (1 µM) in RBCs from HbSS patients. HbSS RBCs (0.5 % Hct), pre-loaded with Fluo-4AM (5 µM), were pre-incubated with Dooku1 (0.1 µM, 1 µM and 10 µM) for 10 min at 37 °C, following which they were treated with Yoda1 (1 µM) for a further 20 min at 37 °C. Intracellular Ca^{2+} was measured using Fluo-4 in the presence (1.1 mM) and absence (EGTA 1mM & 0 Ca^{2+}) of extracellular Ca^{2+}. ** $p < 0.01$, comparing HbSS RBCs in presence of Yoda1 (1 µM) alone and in combination with pre-incubated Dooku1 (1 µM & 10 µM) in presence of extracellular Ca^{2+}. Histograms represent means ± S.E.M, n = 5.

In the presence of extracellular Ca^{2+}, the median Fluo-4 fluorescence increased significantly (Figure 6.3, $p < 0.01$) from 4,320 in the absence of Yoda1 to 8,514 in its presence (1 µM). However, increasing concentrations of GsMTx4 (5 µM & 10µM) in the presence of Yoda1 (1 µM) decreased the median Fluo-4 fluorescence significantly ($p < 0.05$) from 8,514 to

6,156 and 6,172 respectively, although its effect was smaller compared to that of Dooku1. GsMTx4 (10 µM) also slightly, but significantly ($p < 0.05$), reduced the resting intracellular Ca^{2+} concentration in the absence of Yoda1, which would indicate a constitutively active pathway sensitive to this inhibitor. As expected, in the absence of extracellular Ca^{2+} there was no change in the median Fluo-4 fluorescence in the presence of either Yoda1 or GsMTx4. Both these results provide compelling evidence that Yoda1 induces Ca^{2+} entry through the PIEZO1 channel.
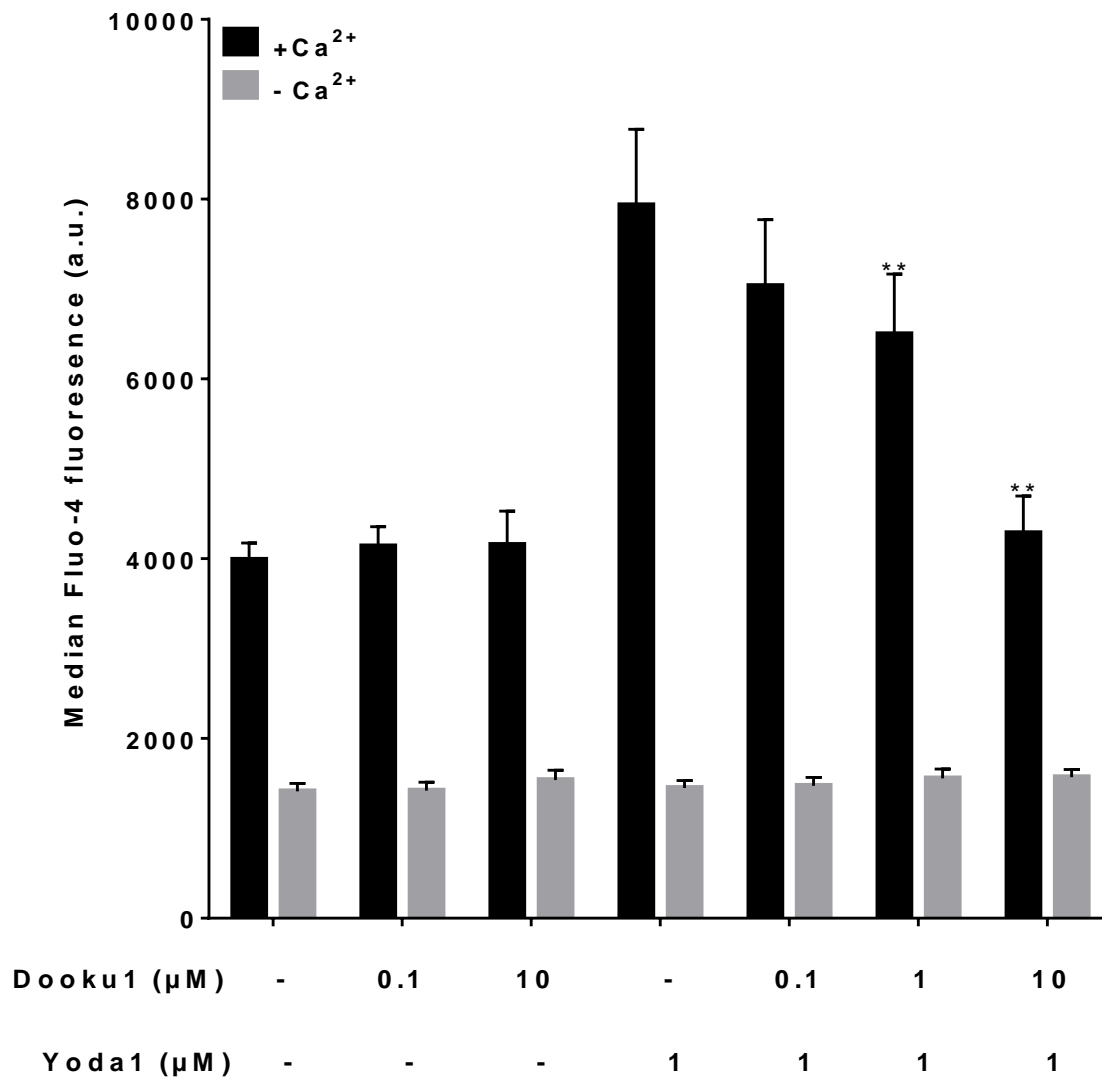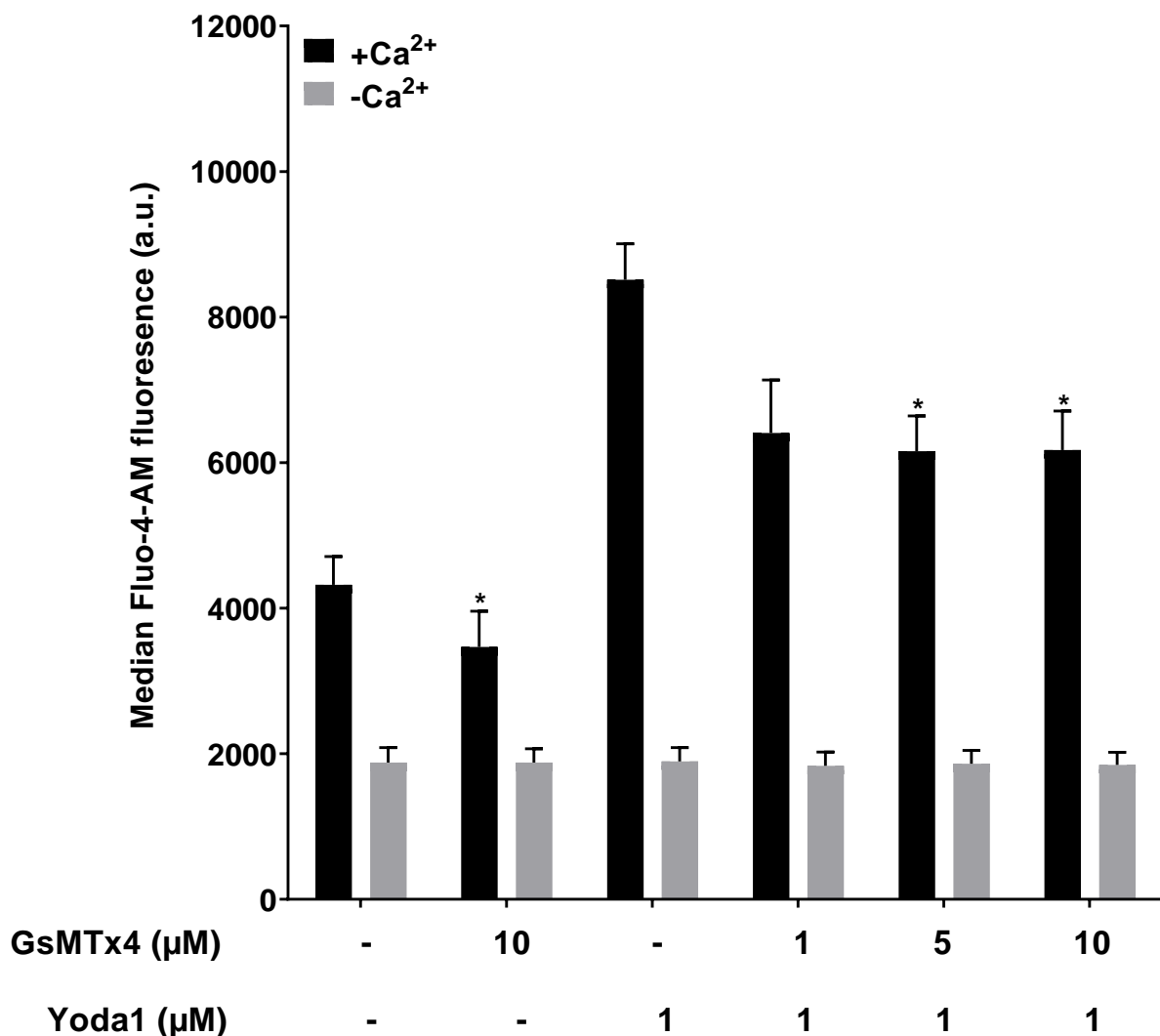

Figure 6.3: Effect of various GsMTx4 concentrations (1 µM, 5 µM and 10 µM) on intracellular Ca^{2+} concentration the in presence of Yoda1 (1 µM) in RBCs from HbSS patients. HbSS RBCs (0.5 % Hct), pre-loaded with Fluo-4AM (5 µM), were pre-incubated with GsMTx4 (0.1 µM, 1 µM and 10 µM) for 10 min at 37 °C, following which they were treated with Yoda1 (1 µM) for a further 20 min at 37 °C. Intracellular Ca^{2+} was measured using Fluo-4 in the presence (1.1 mM) and absence (EGTA 1mM & 0 Ca^{2+}) of extracellular Ca^{2+} * $p < 0.05$ comparing HbSS RBCs in presence of Yoda1 (1 µM) alone and in combination with pre-incubated GsMTx4 (5 µM and 10 µM) in presence of extracellular Ca^{2+}. *$p < 0.05$ comparing HbSS RBCs in DMSO and in presence of GsMTx4 (10 µM) in presence of extracellular Ca^{2+}. Histograms represent means ± S.E.M, n = 5.

6.2.3 Yoda1 and PS exposure

In the next series of experiments, the effect of Yoda1 on PS exposure in HbSS RBCs was investigated. Initially PS exposure in HbSS RBCs was examined in two conditions (Figure 6.4): in the presence (1.1 mM) and absence (EGTA 1 mM & 0 Ca^{2+}) of extracellular Ca^{2+} at seven different Yoda1 concentrations (0.1 µM, 0.2 µM, 0.4 µM, 0.7 µM, 1 µM, 3 µM and 5 µM).

As expected from its effects on intracellular Ca^{2+}, Yoda1 treatment resulted in increased PS exposure in the majority (about 80 %) of the RBC population, at similar concentrations to those required to mediate elevation of intracellular Ca^{2+}, with a significant increase in PS exposure occurring at a Yoda1 concentration of ≥ 100 nM ($p < 0.05$). Whilst these findings suggest that Ca^{2+} entry was directly responsible for the lipid scrambling, there was, however, little, or no, inhibitory effect on Yoda1-induced PS exposure when RBCs were incubated in a Ca^{2+}-free buffer. PS exposures at the highest dose of Yoda1 (5 µM) were similarly high in both conditions, 72.9 ± 7.5 % and 74.6 ± 14 % in the presence and absence of Ca^{2+}, respectively. At a Yoda1 concentration of 0.7 µM, a sharp increase in PS exposure was observed in the presence of extracellular Ca^{2+} to 29.9 ± 16 % in contrast to 16.1 ± 8 % in the absence of extracellular Ca^{2+}, although this effect was not significant. Otherwise, PS exposure in both the buffers increased in a similar pattern with increase in Yoda1 concentration. At concentrations of Yoda1 ≥ 0.5 µM, PS exposure was identical in the presence or absence of extracellular Ca^{2+}.

The overall pattern suggested that Yoda1 increased PS in a dose dependent manner, but that the effect was not dependent on the presence of extracellular Ca^{2+} nor a rise in intracellular Ca^{2+}.
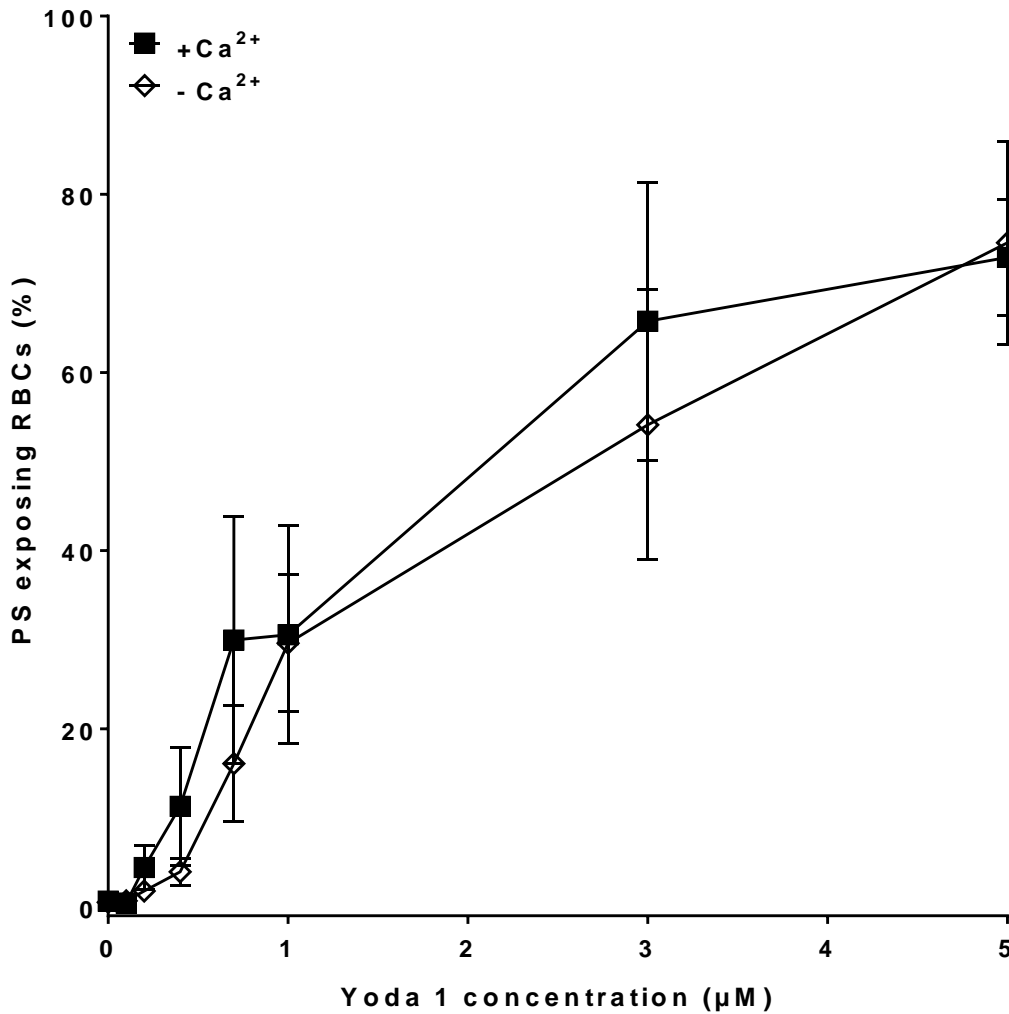
Figure 6.4: Effect of increasing concentration of Yoda1 on PS exposure in RBCs from HbSS patients. HbSS RBCs (0.5 % Hct) were equilibrated in air with the respective Yoda1 concentrations for 20 min at 37 °C in the presence (1.1 mM) and absence (EGTA 1mM & 0 Ca^{2+}) of extracellular Ca^{2+}. After 20 min aliquots of RBCs were removed and exposed PS labelled with LA-FITC, which was detected using flow cytometry. Data points represent means ± S.E.M, n = 4. No significant change in PS exposure was observed between the two conditions, at different concentrations of Yoda1.

In the next experiment, the effect of Ca^{2+} was investigated in HbSS RBCs treated with the ionophore bromo-A23187 (6 µM) to clamp intracellular Ca^{2+} over a range of concentrations from 0 to 1 µM. HbSS RBCs were incubated in two concentrations (0.2 µM and 1 µM) of Yoda1 and compared with those incubated in its absence (Figure 6.5). In the absence of Yoda1, PS exposure increased as extracellular Ca^{2+} concentrations increased with an EC_{50} of 0.37 µM and with a plateau reached at about 0.45 µM at which about 40 % cells were positive for externalised PS. Although PS exposure at 0.2 µM Yoda1, was also Ca^{2+} dependent, the concentration dependence was altered to significantly lower values with an EC_{50} of about 0.18 µM. Even in the absence of Ca^{2+}, with 0.2 µM Yoda1 PS exposure reached about 18 % ± 0.4 %, compared to 2.6 % ± 1.2 % without Yoda1 (p < 0.05).

Moreover, almost all cells were positive for external PS with Ca^{2+} concentrations of ≥ 0.5 µM at 0.2 µM Yoda1 and about 35 % in the absence of Yoda1 at the highest Ca^{2+} concentration tested. However, at 1 µM Yoda1, PS exposure became Ca^{2+}-independent and all cells were positive for PS over the whole Ca^{2+} titration, including cells incubated in the absence of Ca^{2+}.
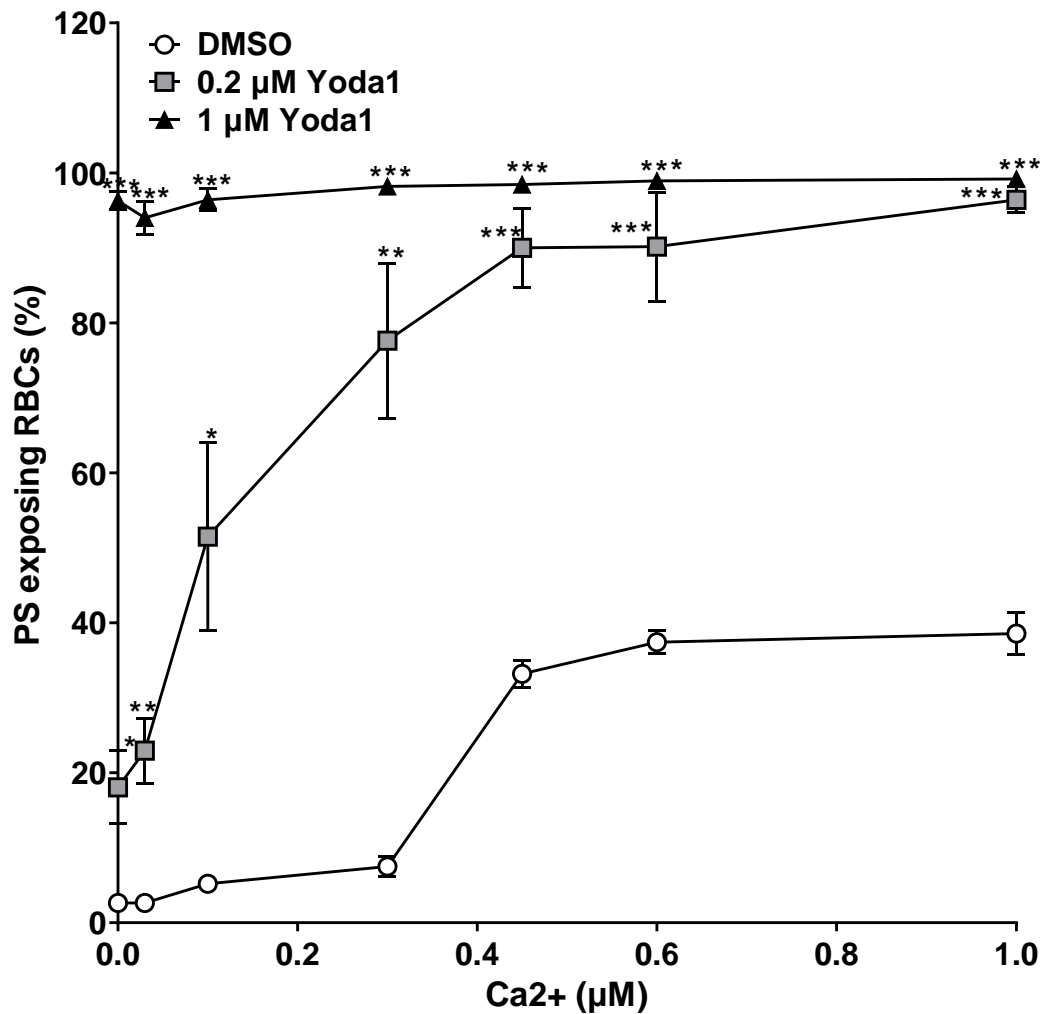
Figure 6.5: Effect of Yoda1 on PS exposure at different concentrations of Ca^{2+} in RBCs from HbSS patients. HbSS RBCs (0.5 % Hct) were equilibrated in air with 0.2 µM and 1 µM Yoda1 at various extracellular Ca^{2+} concentrations (0, 0.03 µM, 0.1 µM, 0.3 µM, 0.45 µM, 0.6 µM, 1 µM) for 30 min at 37 °C. Following which RBC aliquots were removed and exposed PS was labelled with LA-FITC.* $p < 0.05$, ** $p < 0.01$ and *** $p < 0.001$ comparing HbSS RBCs in the absence and presence of Yoda1 (0.2 µM and 1 µM) at respective free extracellular Ca^{2+} concentrations. EC_{50}s for extracellular Ca^{2+} were 0.37 µM and 0.18 µM for DMSO and 0.2 µM Yoda1, respectively. Data points represent means ± S.E.M, n = 5.

6.2.4 Effect of Yoda1 antagonist and PIEZO1 channel blocker on PS exposure

The effects of Dooku1 and GsMTx4 on PS exposure were also tested in combination with Yoda1. Dooku1 (up to 10 µM) reduced Yoda1-induced PS exposure, in both the presence (1.1 mM) and absence (EGTA 1 mM & 0 Ca^{2+}) of extracellular Ca^{2+} (Figure 6.6), consistent

with its action as a Yoda1 antagonist. In contrast, GsMTx4 (up to 5 µM) had variable effects on PS exposure (Figure 6.7).

Effect of Dooku1 (10 µM) on reduction of Yoda1-induced PS exposure was highly significant (Figure 6.6, $p < 0.001$) from 65.8 % ± 3.2 % to 24.6 % ± 4.6 % in presence (1.1 mM) of extracellular Ca^{2+}. A similar significant reduction ($p < 0.05$) of Yoda1-induced PS when exposed to Dooku1 (10 µM) was observed in the absence (EGTA 1 mM 0 Ca^{2+}) of extracellular Ca^{2+}, from 68 % ± 9.7 % to 41.8 % ± 6.3 %.
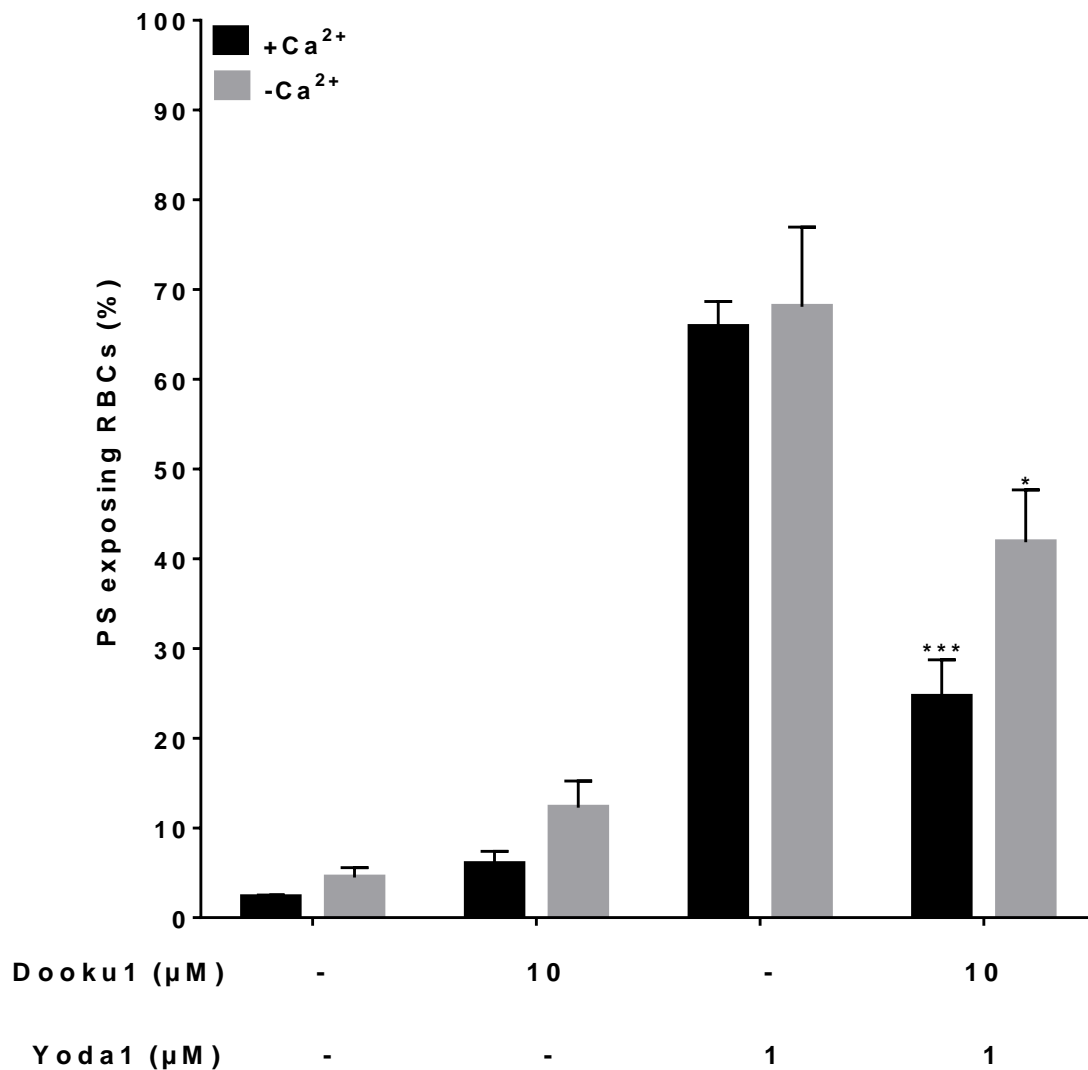
Figure 6.6: Effect of Dooku1 (10 µM) on Yoda1 (1 µM)-induced PS exposure in RBCs from HbSS patients. HbSS RBCs (0.5 % Hct) were incubated in air in the presence (1.1 mM) and absence (EGTA 1mM & 0 Ca^{2+}) of extracellular Ca^{2+}. HbSS RBCs were initially incubated for 10 min with Dooku1 (10 µM) and then treated with Yoda1 (1 µM) for a further 30 min, all at 37 °C. * $p < 0.05$ and *** $p < 0.001$ comparing HbSS RBCs in presence of Yoda1 (1 µM) alone and those pre-incubated with Dooku1 (10 µM) in the presence (1.1 mM) and absence (EGTA 1mM & 0 Ca^{2+}) of extracellular Ca^{2+}. Histograms represent means ± S.E.M, n = 6.

Addition of GsMTx4 (1 µM & 5 µM) on Yoda1 (1 µM)-induced PS exposure caused PS to increase in both the presence (1.1 mM) and absence (EGTA & 0 Ca^{2+}) of extracellular Ca^{2+} (Figure 6.7). The increase was significant in the absence of Ca^{2+} in both the concentrations of GsMTx4, 1 µM and 5 µM, from 46.8 % ± 10.1 % to 57.6 % ± 15.4 % (p < 0.05) and 61.7 % ± 10.5 % (p < 0.01), respectively. Moreover, incubation with both the concentrations of GsMTx4 1 µM and 5 µM alone, without Yoda1, in the absence of extracellular Ca^{2+} caused significant increases (p < 0.05) in PS compared to DMSO. The PS increased in DMSO from 3.2 % ± 0.4 % to 6.6 % ± 1.6 % and 28.8 % ± 1.9 % at 1 µM and 5 µM GsMTx4, respectively.
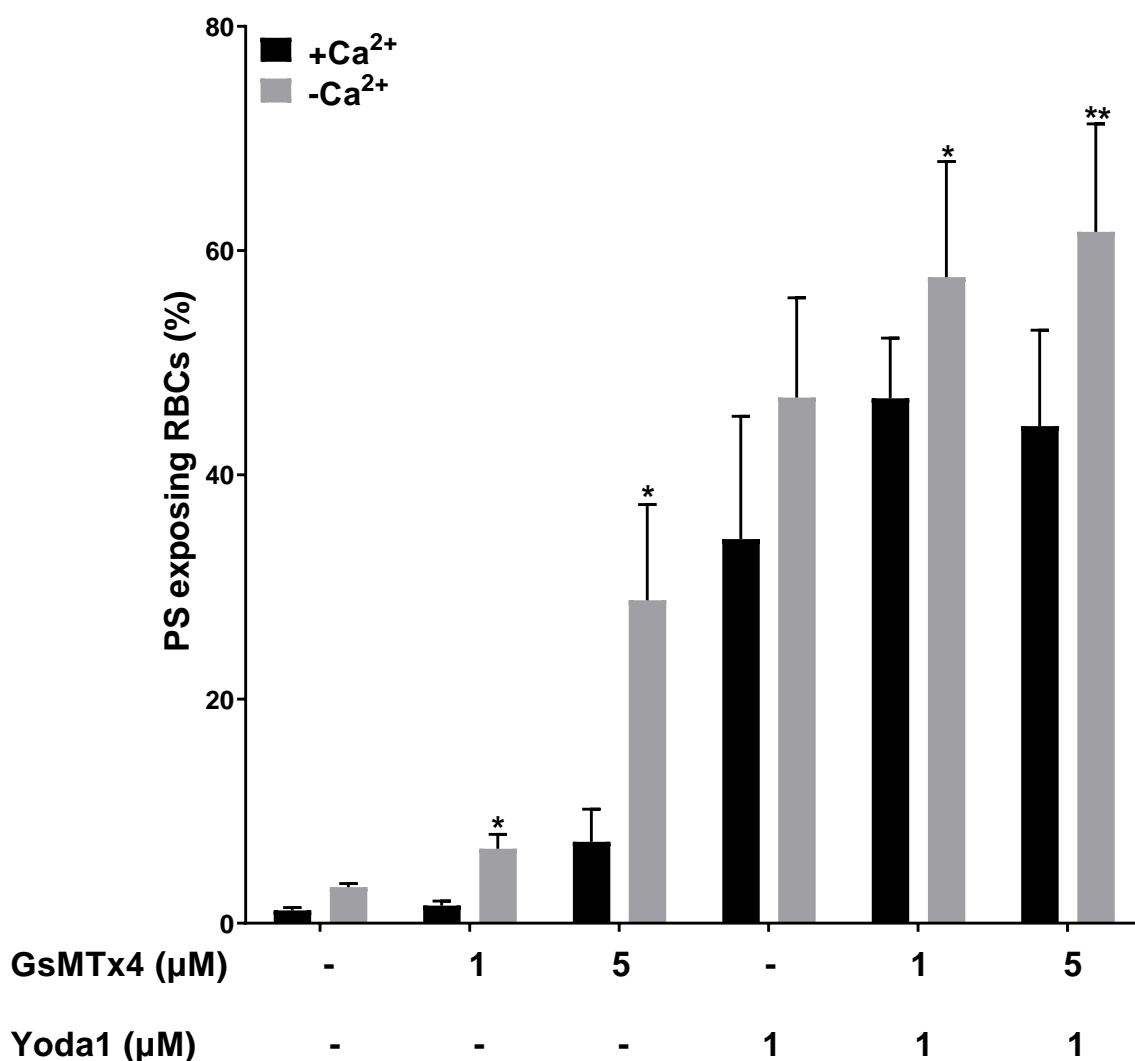
Figure 6.7: Effect of GsMTx4 (1 µM and 5 µM) on Yoda1 (1 µM)-induced PS exposure in the presence (1.1 mM) and absence (EGTA) of extracellular Ca^{2+}on HbSS RBCs. HbSS RBCs (0.5 % Hct) were incubated in air in the presence (1.1 mM) and absence (EGTA 1mM & 0 Ca^{2+}) of extracellular Ca^{2+}. HbSS RBCs were initially incubated for 10 min with GsMTx4 (1 µM & 5 µM) and then treated with Yoda1 (1 µM) for a further 30 min, all at 37 °C. * p < 0.05 and ** p < 0.01 comparing HbSS RBCs in the presence of Yoda1

(1 µM) and those pre-incubated with GsMTx4 (1 µM and 5 µM) in the absence (EGTA 1mM & 0 Ca^{2+}) of extracellular Ca^{2+}. * p < 0.05 comparing HbSS RBCs in presence of DMSO and those in presence of GsMTx4 (1 µM & 5 µM) in the absence (EGTA 1mM & 0 Ca^{2+}) of extracellular Ca^{2+}. Data points represent means ± S.E.M, n = 6.

6.2.5 Yoda1 and membrane integrity

The above findings showed that Yoda1-induced PS labelling was Ca^{2+}- dependent at lower concentrations but, unexpectedly became Ca^{2+}- independent at higher concentrations. One possibility to account for these observations was a breakdown in the lipid bilayer caused by higher Yoda1 concentrations, such that the fluorescent PS label (LA-FITC) had access to phospholipids at both the inner, as well as the outer, leaflet. Results consistent with this hypothesis have been previously obtained using the oxidant *tert*-butyl hydroperoxide (*t*BHP) (Hannemann et al., 2018). If LA-FITC had been able to access the inside of the lipid bilayer, positively labelled cells would be present in the absence of PS externalisation. To ascertain whether this possibility had occurred, red cells were exposed to fluorescently-labelled phalloidin (phalloidin-iFluor 647) which binds to intracellular actin filaments, but can only gain access to its target if the membrane integrity is disrupted.

HbSS RBCs were exposed to phalloidin-iFluor 647 (PF). For the first three conditions in Figure 6.8 where the HbSS RBCs were incubated for 20 min in air in DMSO (-*t*BHP-PF), PF (1:400; stock concentration is 1 mg.ml^{-1}) and *t*BHP (0.78 mM) at 37 °C no significant change in fluorescence was observed. Following exposure to the oxidant *t*BHP at concentrations that disrupt the lipid bilayer, HbSS RBCs stained positively with PF due to the membrane damage. In the last condition (*t*BHP+PF) HbSS RBCs were initially treated with *t*BHP, incubated for 20 min at 37 °C and later labelled with PF, the fluorescence was high and reached 20,754. The results showed phalloidin was effective in measuring membrane integrity in HbSS RBCs.
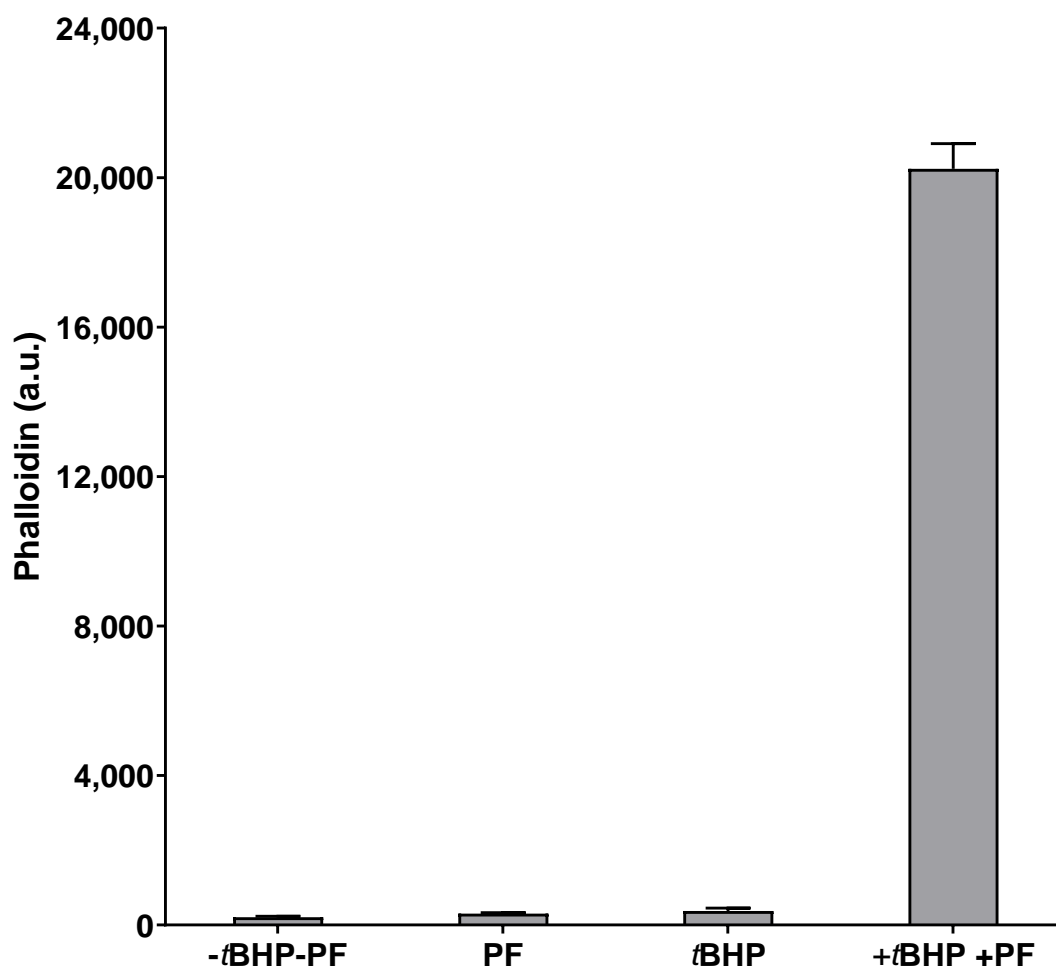
Figure 6.8 Measuring membrane integrity in RBCs from HbSS patients using phalloidin-iFluor647 (PF). Effect of *ter*t-butyl hydroperoxide (*t*BHP) (0.78 mM): HbSS RBCs were incubated for 20 min without – *t*BHP or with + *t*BHP (0.78 mM) and then exposed to phalloidin-iFluor 647 (1:400; stock concentration is 1 mg.ml⁻¹; +PF) or left unlabelled (-PF). Controls without *t*BHP or PF, or with PF alone, are also shown. Phalloidin-iFluor 647 fluorescence is given in arbitrary units (a.u.). Histograms represent means ± S.E.M, n = 5.

HbSS RBCs membrane integrity was then examined using phalloidin-iFluor647 (PF) in the presence (1.1 mM) or absence (EGTA & 0 Ca^{2+}) of extracellular Ca^{2+} in increasing concentrations of Yoda1 (Figure 6.9). The PF (1:400; stock concentration is 1 mg.ml⁻¹) fluorescence in both conditions without Yoda1 was 338.7 and 298.5, which changed to 201.5 and 325 at 5 µM Yoda1, respectively. In both the conditions, therefore phalloidin fluorescence remained stable without any significant increase as the concentration of Yoda1 increased to 5 µM. These results showed that Yoda1 in either the presence or absence of extracellular Ca^{2+} did not disrupt the membrane integrity of HbSS RBC.
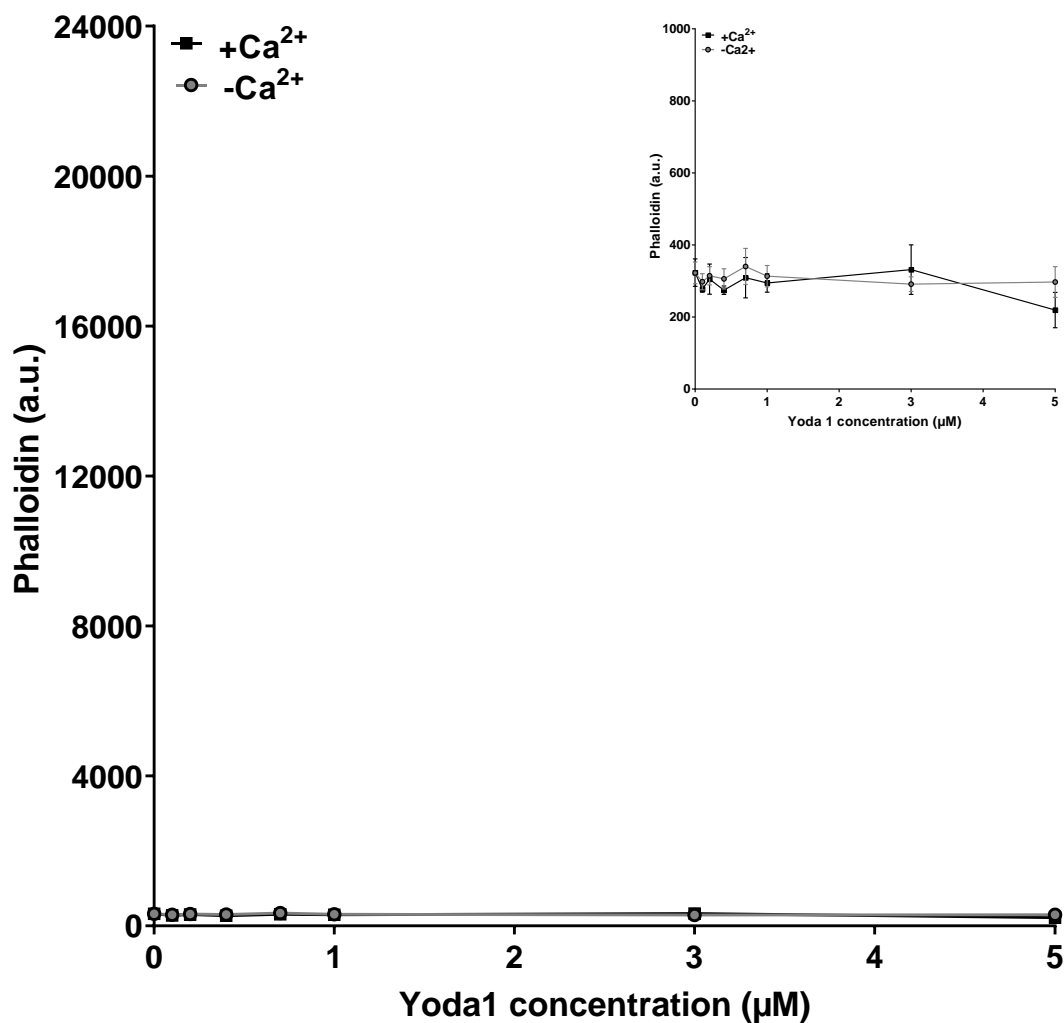
Figure 6.9: Measurement of membrane integrity using phalloidin in RBCs from HbSS patients with increasing concentration of Yoda1. HbSS RBCs (0.5 % Hct) were incubated in air for 20 min at 37 °C with various Yoda1 concentrations in the presence (1.1 mM) or absence (EGTA 1mM & 0 Ca^{2+}) of extracellular Ca^{2+}. After 20 min aliquots of RBCs were removed and labelled with phalloidin-iFluor 647 (1:400; stock concentration is 1 mg.ml^{-1}; PF). Phalloidin fluorescence was detected using flow cytometry. Data points represent means ± S.E.M, n = 4.

To further confirm that Yoda1 did not affect membrane integrity, HbSS RBC membrane integrity was tested at increasing concentrations of Yoda1 using fluorescently-labelled phalloidin (phalloidin-iFluor 647) and anti-Hb α chain (Alexa Fluor647 anti-Hb α chain) (Figure 6.10). This experiment was done to conclusively prove that at any concentrations of Yoda1 the membrane of HbSS RBCs does not get disrupted. For both labels the fluorescence remained low even with high concentration of Yoda1. Without Yoda1, intensity was 232 and 307, and at final concentration of 3 μM Yoda1 intensity measured 254 and 532 for alexa fluor647 anti-Hb α chain (1:100; stock concentration is 0.5 mg.ml^{-1}; anti-HbA) and phalloidin-iFluor 647 (1:400; stock concentration is 1 mg.ml^{-1}; PF), respectively. No change in fluorescence suggests that Yoda1 did not disrupt the membrane integrity.

Intensity (a.u.)

PF
Anti-HbA

20,000
15,000
10,000
5,000
0

0   1   2   3

Yoda 1 concentration (µM)
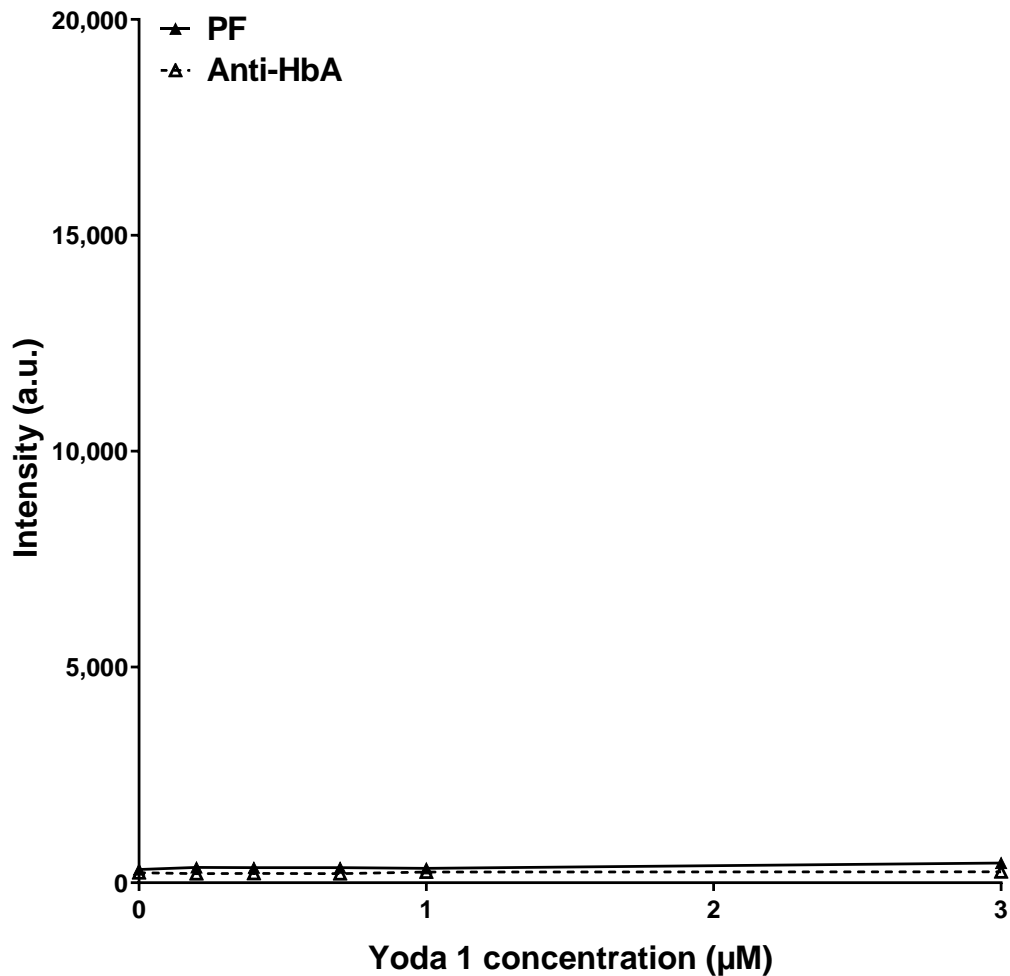
Figure 6.10: Comparing membrane integrity using phalloidin-iFluor 647 (PF) and Alexa Fluor647 anti-Hb α chain (Anti- HbA) upon treating in RBCs from HbSS patients with increasing concentrations of Yoda1. HbSS RBCs were incubated in air with respective Yoda1 concentration for 20 min at 37 °C. After 20 min aliquots of RBCs were removed and labelled with PF (1:400; stock concentration is 1 mg.ml^{-1}) and anti-HbA (1:100, stock concentration is 0.5 mg.ml^{-1}) respectively. Fluorescence for actin filaments and haemoglobin were detected using flow cytometry. Data points represent a single determination.

6.2.6 Yoda1 and PKC inhibitors

From the above, it would therefore appear that Yoda1 did indeed induce PS exposure, but that neither the presence of extracellular Ca^{2+}, nor a rise in intracellular Ca^{2+} concentration, were required. Activation of PIEZO1 by Yoda1 with ensuing Ca^{2+} influx across the red cell membrane was therefore not a prerequisite for lipid scrambling. Rather there must be some alternative mechanism of action of Yoda1. Previously, Yoda1 has been shown to activate protein kinases in other tissues (Dela Paz and Frangos, 2018), and there is also strong evidence of a role for protein kinase C (PKC) in PS exposure (Koshkaryev et al., 2020; Nguyen et al., 2011; Wesseling et al., 2016) either via Ca^{2+} entry through cation channels or via a Ca^{2+}- independent action. The effect of Yoda1 in HbSS RBCs was therefore examined

in combination with two different inhibitors of PKC: chelerythrine chloride that inhibits the active phosphorylation site of PKC, and calphostin C, which is an irreversible inhibitor of the diacylglyceraldehye-binding site (Figure 6.11-6.14).

The effect of chelerythrine chloride on Yoda1-induced increase in intracellular Ca^{2+} is shown in Figure 6.11. As before, in the absence of extracellular Ca^{2+}, Yoda1 (3 μM) had no effect on intracellular Ca^{2+} levels whilst in the presence of extracellular Ca^{2+}, an increase in intracellular Ca^{2+} was observed. The rise in intracellular Ca^{2+} was abolished by chelerythrine chloride (10 μM), such that values were unchanged compared to cells incubated in the absence Yoda1 ($p < 0.01$).

| Yoda1 (μM) | - | 3 | - | 3 |
| Chelerythrine Chloride (μM) | - | - | 10 | 10 |
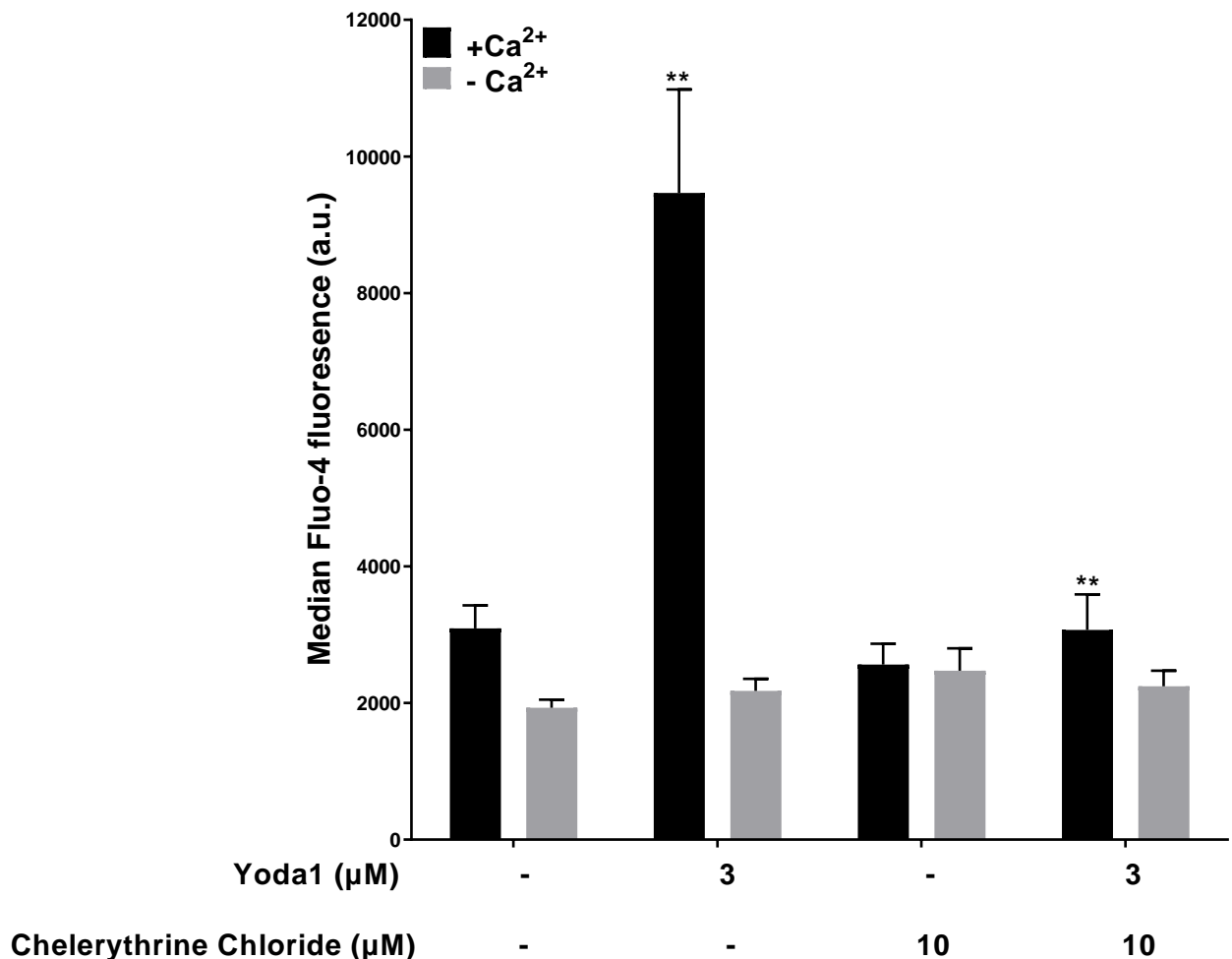
Figure 6.11: Effect of chelerythrine chloride (10μM) on Yoda1 (3μM)-induced rise in intracellular Ca^{2+} concentration in the presence (1.1 mM) and absence (EGTA 1mM & 0 Ca^{2+}) of extracellular Ca^{2+} in RBCs from SCD patients. HbSS RBCs (0.5 % Hct), pre-loaded with Fluo-4AM (5 μM), were incubated in air and pre-incubated with chelerythrine chloride (10 μM) for 10 min following which they were treated with Yoda1 (3 μM) for a further 20 min, all at 37 °C, in the presence (1.1 mM) or absence (EGTA 1mM & 0 Ca^{2+}) of extracellular Ca^{2+}. ** $p < 0.01$ comparing HbSS RBCs in presence of Yoda1 (3 μM) alone and in

combination with pre-incubated chelerythrine chloride (10 µM) or DMSO in the presence (1.1 mM) of extracellular Ca^{2+}. Histograms represent means ± S.E.M, n = 6.

In the next series of experiments, the effect of the two PKC inhibitors, chelerythrine chloride (Figure 6.12) and calphostin C (Figure 6.13) was investigated on Yoda1-induced PS exposure. Both the PKC inhibitor showed a significant reduction in Yoda1-induced PS exposure in the presence (1.1 mM) or absence (EGTA & 0 Ca^{2+}) of extracellular Ca^{2+}.

When investigating chelerythrine chloride (10 µM) on PS exposure on its own, this PKC inhibitor had no effect. (Figure 6.12). Chelerythrine chloride (10 µM) in combination with Yoda1 (1 µM) reduced PS exposure significantly from 21.6 % ± 5.8 % to 1.9 % ± 1 % (p < 0.01) and from 23.7 % ± 3.4 % to 8.9 % ± 1.9 % (p < 0.01) in the presence and absence of extracellular Ca^{2+}, respectively. Similar results were observed with chelerythrine chloride (10 µM) in combination with Yoda1 (3 µM) which resulted in significant reduction in PS exposure from 54.8 % ± 14 % to 11.2 % ± 8.9 % (p < 0.01) and from 64.6 % ± 8.6 % to 19.3 % ± 7 % (p < 0.01) in the presence and absence of extracellular Ca^{2+}, respectively. This Figure also again shows that the stimulatory effect of Yoda1 on PS exposure did not require Ca^{2+}.
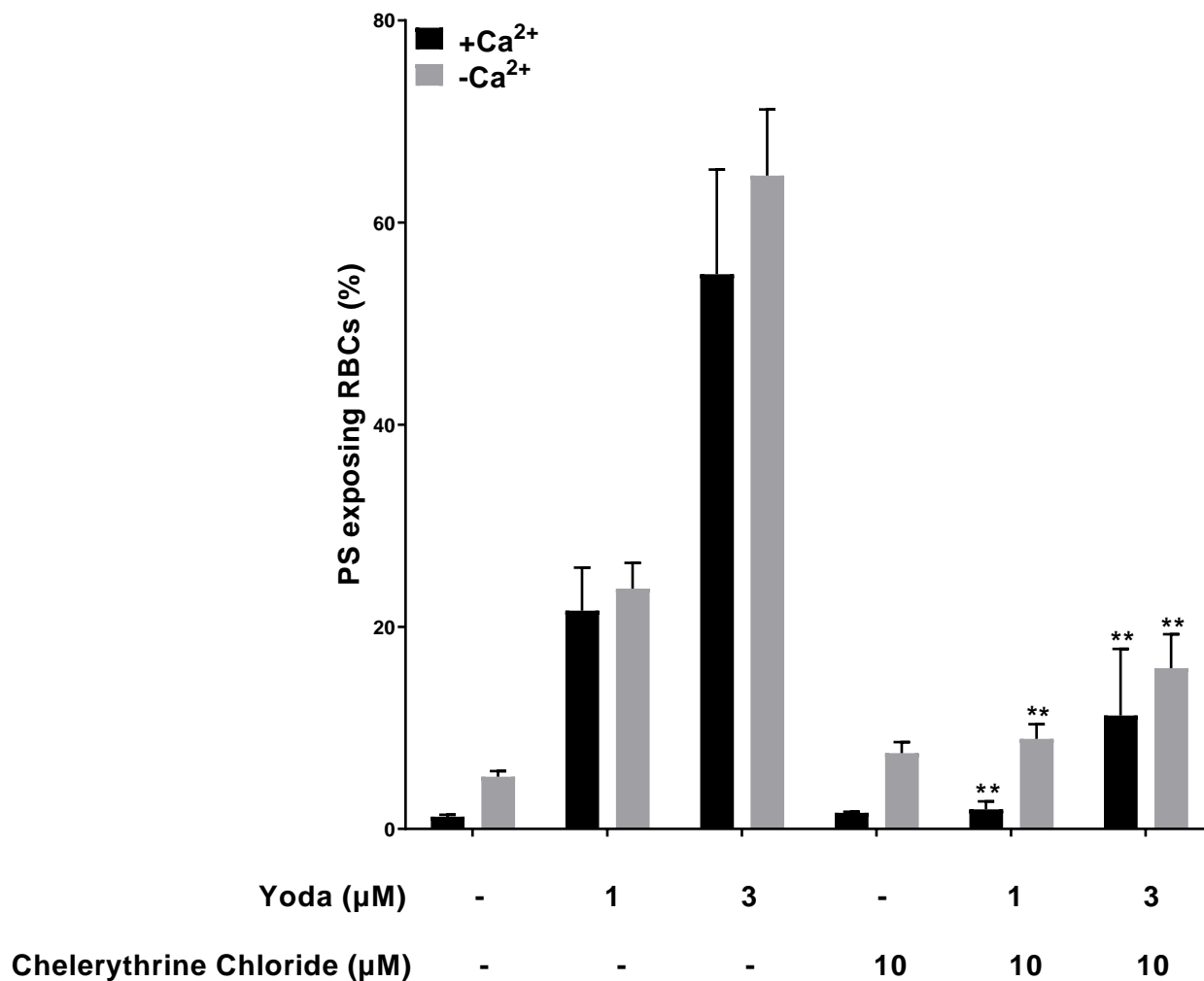
Figure 6.12: Effect of chelerythrine chloride (10 µM) on Yoda1 (1 µM & 3 µM)-induced PS exposure in RBCs from SCD patients. HbSS RBCs (0.5 % Hct) were equilibrated in air and pre-incubated with chelerythrine chloride (10 µM) for 10 min following which they were treated with Yoda1 (1 µM & 3 µM) for a further 20 min, all at 37 °C in the presence (1.1 mM) or absence (EGTA 1mM & 0 Ca^{2+}) of extracellular Ca^{2+}. RBC aliquots were then removed and exposed PS labelled with LA-FITC. ** $p < 0.01$ comparing HbSS RBCs in presence of Yoda1 (1 µM and 3 µM) alone and in combination with pre-incubated chelerythrine chloride (10 µM) in the presence (1.1 mM) or absence (EGTA 1mM & 0 Ca^{2+}) of extracellular Ca^{2+}. Histograms represent means ± S.E.M, n = 6.

In the next experiment (Figure 6.13), the effect of the second PKC inhibitor, calphostin C, was investigated. Calphostin C (10 µM) in combination with Yoda1 (1 µM) reduced PS exposure significantly from 31.7 % ± 4.8 % to 6.5 % ± 2.6 % ($p < 0.001$) in the presence of extracellular Ca^{2+}. However, in the absence of extracellular Ca^{2+}, calphostin C (10 µM) in combination with Yoda1 (1 µM) reduced PS exposure but not significantly from 41.4 % ± 7.2 % to 25.2 % ± 5.9 %. Calphostin C (10 µM) in combination with Yoda1 (3 µM) resulted in a significant reduction in PS exposure from 64.4 % ± 10.9 % to 26.1 % ± 4.9 % ($p < 0.05$) and from 78.5 % ± 5.4 % to 55 % ± 9.4 % ($p < 0.05$) in the presence and absence of

extracellular Ca^{2+}, respectively. Calphostin C (10 µM) on PS exposure, on its own, had no effect.
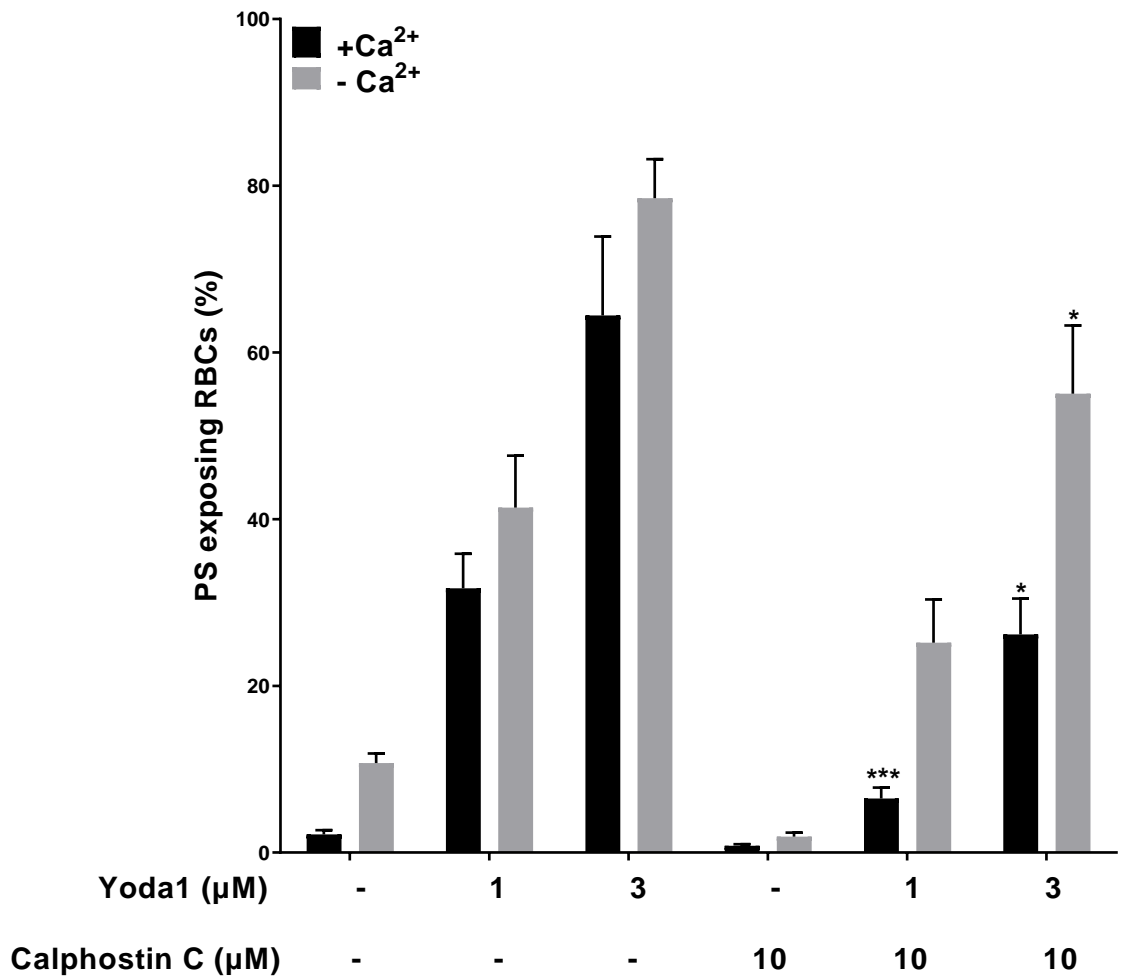
Figure 6.13: Effect of calphostin C (10 µM) on Yoda1 (1 µM & 3 µM)-induced PS exposure. HbSS RBCs (0.5 % Hct) were equilibrated in air and pre-incubated with calphostin C (10 µM) for 10 min following which they were treated with Yoda1 (1 µM & 3 µM) for 20 min, all at 37 °C in the presence (1.1 mM) or absence (EGTA 1mM & 0 Ca^{2+}) of extracellular Ca^{2+}. RBC aliquots were then removed and exposed PS labelled with LA-FITC. * p < 0.05 and *** p < 0.001 comparing HbSS RBCs in presence of Yoda1 (1 µM and 3 µM) alone and in combination with pre-incubated calphostic C (10 µM) in the presence (1.1 mM) or absence (EGTA 1mM & 0 Ca^{2+}) of extracellular Ca^{2+}. Histograms represent means ± S.E.M, n = 4.

The effect of chelerythrine chloride on PS exposure on Ca^{2+}-clamped HbSS RBCs was then investigated (Figure 6.14). At low intracellular Ca^{2+} concentrations (0.1 µM to 0.45 µM), chelerythrine chloride substantially inhibited the Yoda1-induced PS exposure, by about 50 %. This inhibition was reduced, however, as the concentration of Ca^{2+} was increased such that at a intracellular Ca^{2+} concentration of 10 µM inhibition was very small, although significant (about 10 % reduction, p < 0.01). These findings suggest that at low Ca^{2+} levels,

Yoda1-induced PS exposure is PKC dependent but at higher values it becomes PKC independent.
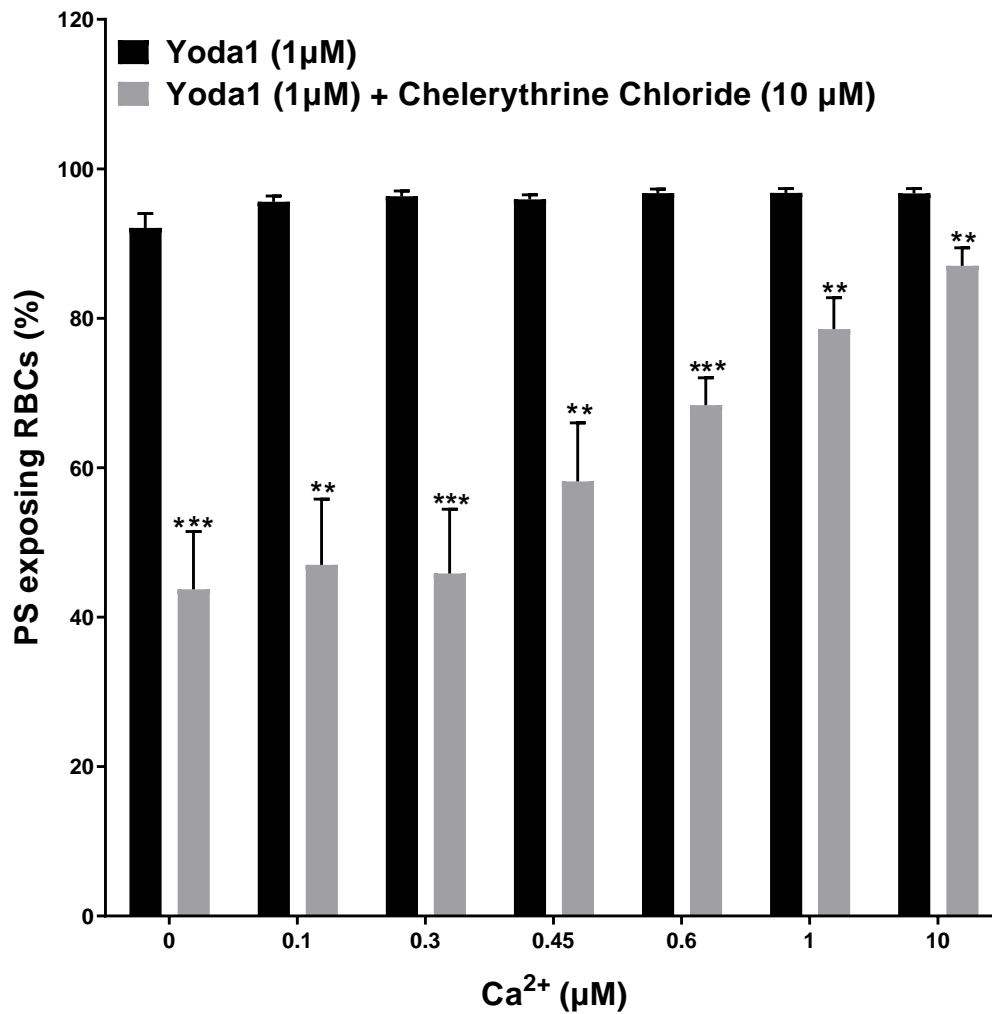
Figure 6.14: Effect of chelerythrine chloride (10 μM) and Yoda1 in Ca^{2+}-clamped RBCs from SCD patients. HbSS RBCs (0.5 % Hct) were equilibrated in air and treated with Yoda1 (1 μM) at different extracellular Ca^{2+}s for 30 min at 37 °C. HbSS RBCs (0.5 % Hct) were equilibrated in air and pre-incubated with chelerythrine chloride (10 μM) at different extracellular Ca^{2+}s for 10 min, following which they were treated with Yoda1 (1 μM) for 20 min, all at 37 °C. RBC aliquots were then removed and exposed PS labelled with LA-FITC. ** $p < 0.01$ and *** $p < 0.001$ comparing HbSS RBCs in presence of Yoda1 (1 μM) alone and in combination with pre-incubated chelerythrine chloride (10 μM) at respective Ca^{2+} concentrations. Histograms represent means ± S.E.M, n = 6.

6.2.7 Effect of Yoda1 on haemolysis of HbSS RBCs and HbAA RBCs in oxygenated and deoxygenated conditions

The effect of Yoda1 (1 µM) on haemolysis of HbSS RBCs (Figure 6.15 A &B) and HbAA RBCs (Figure 6.15 C & D) under both oxygenated (150 mmHg) and deoxygenated (0 mmHg) conditions were investigated in RBCs incubated in isosmotic sucrose solutions. Increased haemolysis of HbSS RBCs at 150 mmHg can be observed in the presence of Yoda1 (1 µM) compared to its absence, from 30 min to 60 min. A significant change was observed between in haemolysis in the presence of Yoda1 (1 µM) and its absence at 30 min ($p < 0.05$) and 60 min ($p < 0.05$) in Figure 6.15A. Moreover, increased haemolysis of HbSS RBCs at 0 mmHg can be observed in the presence of Yoda1 (1 µM) compared to its absence, from 10 min to 60 min. A significant change was observed in haemolysis comparing HbSS RBCs in the presence of Yoda1 (1 µM) and its absence from 10 to 50 min ($p < 0.05$) with a further substantial increase at 60 min ($p < 0.01$) in Figure 6.15B. However, no such significant changes in haemolysis of HbAA RBCs was observed without or with Yoda1 (1 µM) at either 150 mmHg and 0 mmHg.

Figure 6.15: Effect of Yoda1 (1 µM) on haemolysis of HbSS (A and B) and HbAA (C and D) at 150 mmHg and 0 mmHg oxygen tension in iso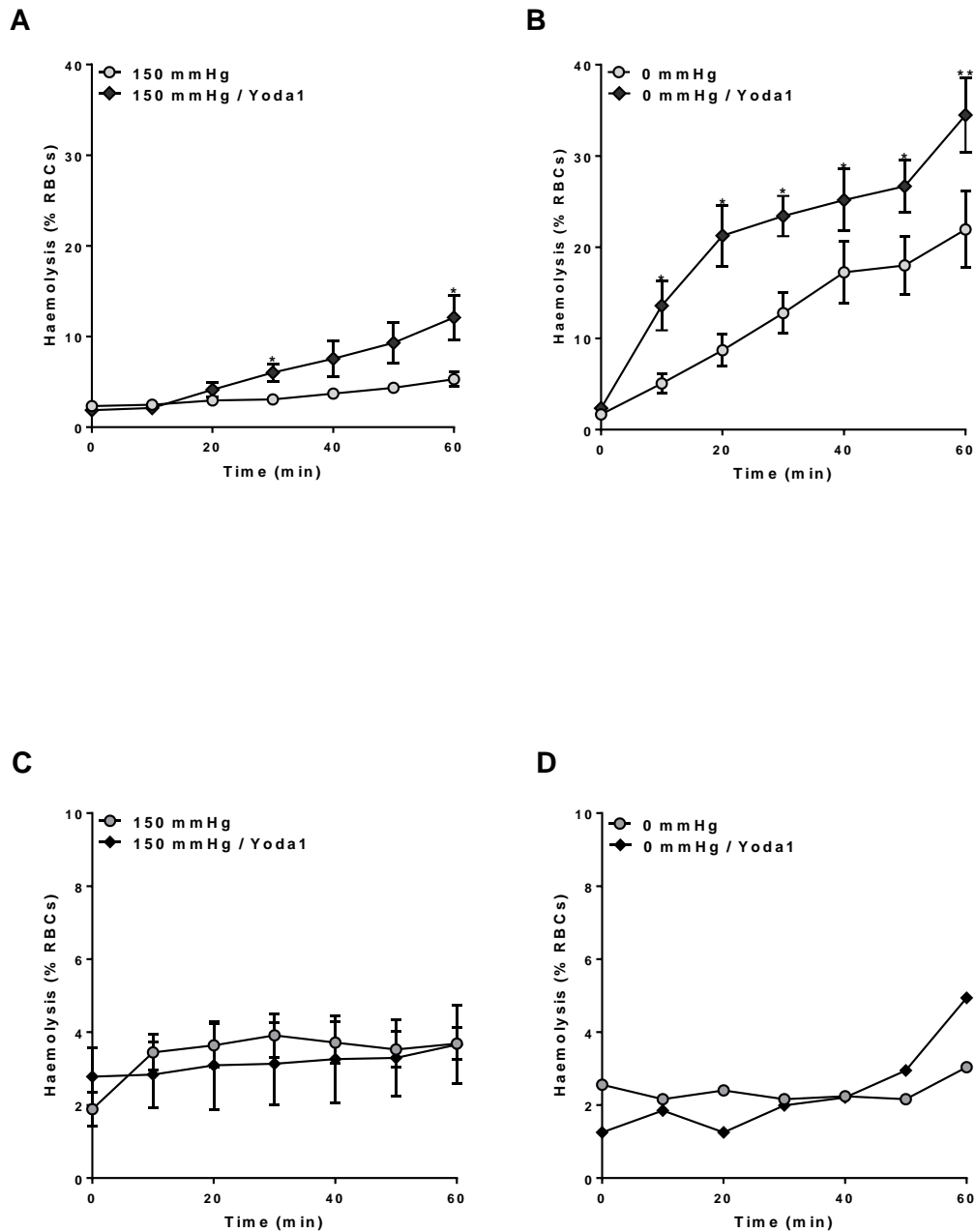smotic sucrose solutions. * $p < 0.05$ comparing HbSS RBCs in the presence and absence of Yoda1 (1 µM) in 150 mmHg. * $p < 0.05$ and ** $p < 0.01$ comparing HbSS RBCs in the presence and absence of Yoda1 (1 µM) in 0 mmHg. Data points represent means ± S.E.M, n = 5.

6.3 Discussion

The molecular identity of P_{sickle} is still unknown and over the years various candidates have been identified for P_{sickle} (Table 1.3). Findings strongly favour P_{sickle} to be the mechanosensitive ion channel PIEZO1. In this report the role of P_{sickle} in PS exposure was investigated further assuming its molecular identity to be PIEZO1. Yoda1 was used as a known activator of the PIEZO1 channel. The effect of Yoda1 on intracellular Ca^{2+} and PS exposure in HbSS RBCs was evaluated under different conditions in an attempt to establish a more direct link between P_{sickle} and PS exposure. The present findings are in agreement with previous reports (Table 1.3) implicating PIEZO1 as a major Ca^{2+} channel through which Ca^{2+} can enter RBCs. However, findings also revealed that Yoda1 can cause PS exposure in both a Ca^{2+} dependent and a Ca^{2+}-independent mechanism, with the latter involving, at least in part, PKC.

The initial experiment in Figure 6.1 showed Yoda1 caused a rise in intracellular Ca^{2+}, dependent on the presence of extracellular Ca^{2+}, consistent with its increased entry across the plasma membrane. As expected, HbSS RBCs incubated in conditions without extracellular Ca^{2+} showed no such increase in intracellular Ca^{2+} concentration even at the highest Yoda1 concentration used (5 µM). It is known that RBCs lack major intracellular organelles such as mitochondria, endoplasmic reticulum, etc., although intracellular vesicles of Ca^{2+} are present. Notwithstanding, however, this experiment conclusively excludes the possibility that Yoda1 stimulates any Ca^{2+} stores to cause release of Ca^{2+} intracellularly, to levels detectable by Fluo-4. The majority of HbSS RBCs and HbAA RBCs (data not presented in thesis, but available) responded to Yoda1 implying that most sickle and normal RBCs express a functional PIEZO1 in their membranes, notwithstanding the stochastic increase in cation permeability in response to deoxygenation and the sickling shape change observed in sickle cells (Lew et al., 1997) and the apparent absence of a P_{sickle}-like conductance in normal RBCs, at least under most conditions. Findings that the PIEZO1 inhibitors, Dooku1 and GsMTx4, inhibited the elevation in intracellular Ca^{2+} were consistent with this mechanosensitive channel being the likely target of Yoda1 for the Ca^{2+} rise (Figures 6.2 & 6.3).

In the case of PS exposure (Figure 6.4), Yoda1-induced externalisation occurred in the presence, but also in the complete absence, of extracellular Ca^{2+}, indicating that Yoda1 was able to stimulate PS exposure independent of a rise in intracellular Ca^{2+}, although low basal Ca^{2+} levels would remain present. In addition, it was also noticeable that the extent of PS

exposure in response to Yoda1, whilst always present, differed between RBC samples, indicative of the marked heterogeneous behaviour of sickle cells observed across SCD patients with respect to several features. Moreover, using Ca^{2+} clamped with ionophore, it was also shown that Ca^{2+} and Yoda1 interact such that Yoda1 shifts the EC_{50} for Ca^{2+}-induced PS exposure to lower values (Figure 6.5). However, such interaction with intracellular Ca^{2+} is only seen at lower concentration of Yoda1 (0.2 µM), whilst at higher Yoda1 (1 µM) concentrations the effect on PS exposure was completely Ca^{2+}-independent. Moreover, any doubts of Yoda1 disrupting the membrane of HbSS RBCs and not giving the true label of outer membrane PS, is eliminated with the series of experiments carried out in Figure 6.8-6.10 utilizing phalloidin-iFluor 647 and Alexa Fluor647 anti-Hb α chain.

The effects of Dooku1 and GsMTx4 on PS exposure were also tested in combination with Yoda1. Dooku1 (up to 10 µM) reduced Yoda1-induced PS exposure, in both the presence and absence of Ca^{2+} (Figure 6.6), consistent with its action as a Yoda1 antagonist. In contrast, GsMTx4 (up to 5 µM) had variable effects on PS exposure (Figure 6.7). This occurs perhaps due to the indirect action of GsMTx4 on PIEZO1. It has been shown that GsMTx4 inhibits the mechanosensitive ion channel by changing the membrane property upon interacting with the membrane rather than directly acting on the channel itself (Gupta et al., 2015; Suchyna et al., 2004). This might cause the PS to be exposed for which our results have shown variable effects on PS exposure with GsMTx4. Alternatively, these findings may result from the difficulty in obtaining reproducibly pure chemical with consistent $IC_{50}s$ and it is often found to have variable effects.

Taken together, the results suggest that Yoda1 must be able to increase PS exposure through a Ca^{2+}-independent mechanism. Frangos (2018) showed that in addition to activation of PIEZO1, Yoda1 also activates Akt and ERK1/2 in endothelial cells. Moreover, they also showed that despite blocking activity of the PIEZO1 cation channel with different drugs Yoda1 still activated these phosphorylation pathways. Thus, Yoda1 can activate Akt and ERK1/2 in endothelial cells independent of its effect on PIEZO1. It is therefore possible that Yoda1 activates a signalling pathway or directly acts on an endogenous protein like the scramblase to cause PS exposure on the outside of HbSS RBCs. In this context, it is interesting to note that a member of protein kinases has been associated with PS exposure in RBCs. Identifying this / these pathway / pathways will inform the search for drugs that could specifically block alternative signalling mechanisms involved in PS exposure in HbSS RBCs, and which may therefore be therapeutically valuable.

With respect to the two inhibitors of protein kinase C (PKC) tested, chelerythrine chloride reduced the Yoda1-induced increase in intracellular Ca^{2+}, consistent with Yoda1 acting also via a PKC-activated cation channel (Figure 6.11). Both chelerythrine chloride and calphostin C also reduced Yoda1-induced PS exposure (Figures 6.12 and 6.13), but did not abolish it, also indicating an action partially via PKC. Notwithstanding, inhibition of PS exposure by chelerythrine chloride was attenuated as intracellular Ca^{2+} was increased using a Ca^{2+}ionophore (Figure 6.14), indicating an additional effect of intracellular Ca^{2+} independent of PKC. This shows that high Ca^{2+} can overcome PKC inhibition, presumably through direct effects on the scramblase, but probably only at concentrations, which would damage the cell in other ways.

Previous work using phorbol myristate acetate (PMA), lysophosphatidic acid (LPA) and the Ca^{2+} ionophore A23187 together with chelerythrine chloride and calphostin C has also produced evidence for PKC-mediated PS exposure in normal and sickle cells, through both Ca^{2+}- dependent and Ca^{2+}- independent mechanisms (Koshkaryev et al., 2020; Nguyen et al., 2011; Wagner-Britz et al., 2013; Wesseling et al., 2016). The Ca^{2+}- dependent effect of PKC could be mediated via Ca^{2+} entry, with the participation of ω-agatoxin-TKsensitive, Cav2.1-like, Ca^{2+} channels or possibly the non-selection cation channel (Andrews and Low, 1999; Kaestner et al., 2020). Ca^{2+} could also act via activation of the scramblase (Wesseling et al., 2016).

The present findings using the novel compound, Yoda1, are largely in agreement with these models. They are therefore consistent with Yoda1 acting as a PKC activator, as well as via PIEZO1 channels. These previous reports using PMA and LPA (Koshkaryev et al., 2020; Nguyen et al., 2011) failed to show a clear correlation between RBCs with elevations in Ca^{2+} levels and those showing PS exposure. They also suggested that PMA- and LPA-induced PS exposure could not occur in the absence of extracellular Ca^{2+} (Koshkaryev et al., 2020), however, contrary to the present findings with Yoda1.

Finally, it is already known that in contrast to HbAA RBCs, a fraction of HbSS RBCs undergo haemolysis when deoxygenated in isosmotic non-electrolyte solution (Browning et al., 2007a; Milligan et al., 2013). Haemolysis often correlates with P_{sickle} activity and is taken as a measure of RBC fragility. As shown in Figure 6.15B, Yoda1 treatment caused a significant increase in the rate of haemolysis at all time points at 0 mmHg compared to that in the absence of Yoda1 in HbSS RBCs. Moreover, similar significant increases in the rate

of haemolysis could also be observed in HbSS RBCs at 150 mmHg in the presence of Yoda1 compared to its absence (Figure 6.15A). This clearly suggests that Yoda1 in both oxygenated and deoxygenated conditions causes solute loss or gain in HbSS RBCs perhaps by activating PIEZO1 and in turn making RBCs more fragile.

Therefore, the results show that the novel compound, Yoda1 can cause PS exposure by acting as a PKC activator and as well as via PIEZO1 channels. Thus, PS exposure in HbSS RBCs can be initiated in two pathways, either independent of Ca^{2+} acting directly through PKC or through PIEZO1 channel by increasing intracellular Ca^{2+}.

7 Pharmacological elucidations of mechanisms 2: Role of sphingomyelinase (SMase) and its signalling pathway in PS exposure

7.1 Introduction

Sphingomyelin is the most abundant of the mammalian sphingolipids and a major lipid component comprising 10 % of the mammalian cell membrane (Ohanian and Ohanian, 2001). Sphingomyelinases (SMase) are enzymes which catalyse the hydrolysis of sphingomyelin to ceramide and phosphocholine (Goñi and Alonso, 2002). There are three types of SMase in mammalian cells that stimulate degradation of sphingomyelin: (i) acid SMase (ii) neutral SMase and (iii) alkaline SMase. The acid SMase is active at a pH of around 4.8 and has two isoforms, an endosomal/lysosomal acid isoform and a Zn^{2+}-dependent SMase (Schissel et al., 1996; Spence, 1993). Neutral SMase is highly active at a pH of around 7.5, and it is a membrane-bound Mg^{2+}-dependent enzyme (Martín et al., 2001). The alkaline SMase is active at an alkaline pH, has a molecular mass of 58 kDa and is Mg^{2+}-independent (Abe et al., 2013).

However, it is known that RBCs do not possess any SMase activity of their own and it has also been reported that SMase is not part of the RBCs proteome (Alessandro et al., 2010; Hanada et al., 2000). Nonetheless, RBCs can still be exposed to SMases that are secreted from the endothelial cells, leukocytes and platelets (Jenkins et al., 2009). Thus, these can cause an increase in production of ceramide through the breakdown of sphingomyelin in the RBC membrane. Increase in ceramide levels can lead to a wide range of cellular signalling effect, which might have a consequence in the normal functioning of cells. Ceramides are lipids made up of fatty acids varying in length from C14 to C16, together with sphingosine (Kumari, 2018). They are involved in multiple functions such as regulation of inflammation by altering the production of inflammatory metabolites, obesity-associated insulin resistance, impaired fatty acid oxidation, etc. (Aburasayn et al., 2016; Coen et al., 2013; Fucho et al., 2017; Hannun, 1996). Diseases with excess ceramides include Alzheimer's, type-2 diabetes and insulin resistance (Mielke and Lyketsos, 2010; Sokolowska and Blachnio-Zabielska, 2019). Ceramides are also involved in differentiation, proliferation and apoptosis of cells (Geilen et al., 1997). Thus, in this Chapter, the role of the SMase signalling pathway on PS exposure in HbSS RBCs was explored and the aim of the work was to measure SMase activity in HbAA RBCs.

Due to the problem with obtaining samples towards the end of my laboratory work, the full programme of experiments envisaged were not possible to complete.

7.2 Results

7.2.1 Effect of isocoumarin on PS exposure

In order to ascertain the involvement of SMase (sphingmyelinase), in this experiment the effect of 3,4-dichloroisocoumarin, an inhibitor of SMase, on PS exposure of HbSS RBCs was investigated in deoxygenated (0 mmHg) conditions (Figure 7.1) and later compared to HbSS RBCs in oxygenated (100 mmHg) conditions (Figure 7.2). HbSS RBCs were pre-incubated for 30 min in air with 3,4-dichloroisocoumarin (200 µM) or DMSO (-Isocoumarin). After pre-incubation, the cells were deoxygenated (0 mmHg) for a further 60 min (Figure 7.1). Throughout the 60 min period, at every time point 3,4-dichloroiscoumarin significantly inhibited the deoxygenation-induced PS exposure compared to without isocoumarin. Finally, at 60 min the PS was 30 % ± 7.8 (p < 0.001) for 200 µM 3,4-dichloroisocoumarin, significantly lower compared to RBCs incubated without isocoumarin (100 %, actual mean value is 14.5 %).
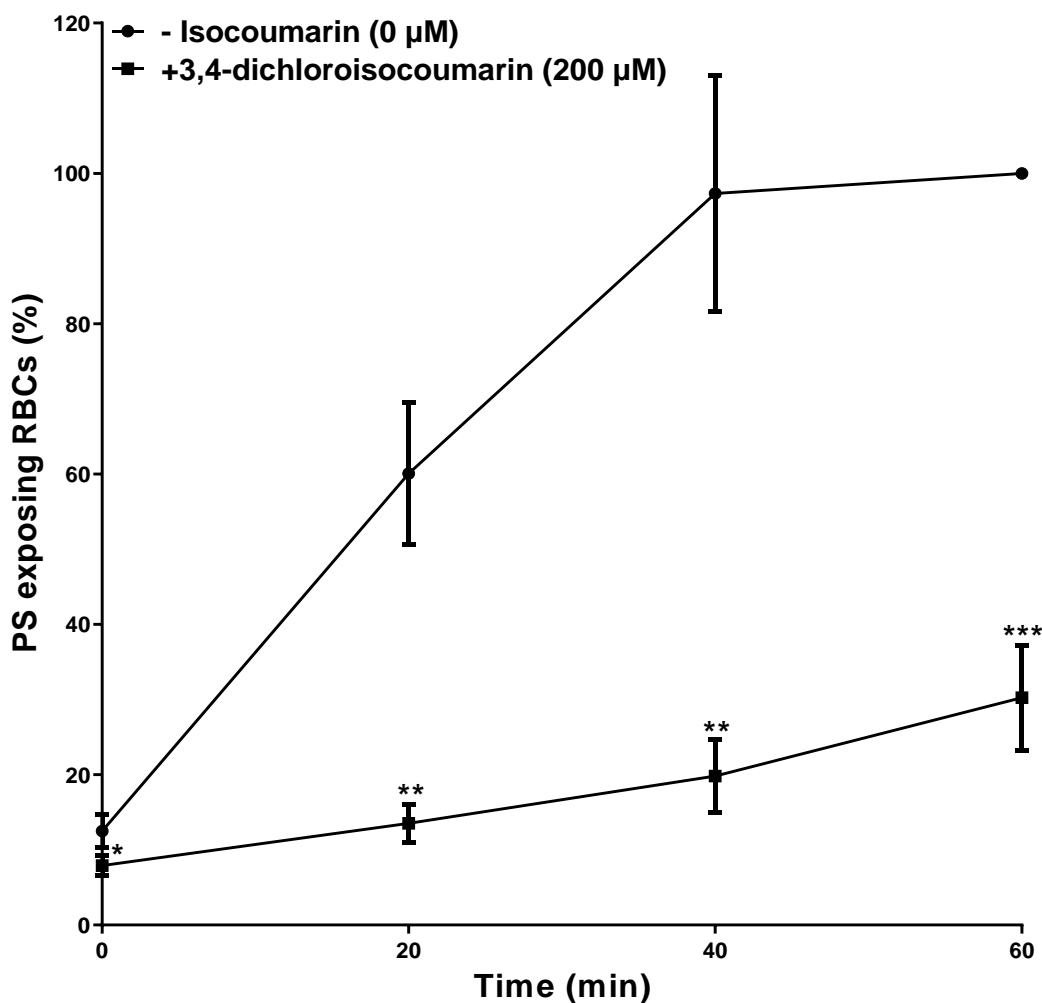

Figure 7.1: Effect of 3,4-dichloroisocoumarin (200 µM) on PS exposure at 0 mmHg in RBCs from SCD patients. HbSS RBCs (0.5 % Hct) were pre-incubated in Ca^{2+}-vanadate LK-HBS at 37 ° C, pH 7.0 in

eppendorf tubes for 30 min with 3,4-dichloroisocoumarin (200 µM) or DMSO (- Isocoumarin). After pre-incubation the HbSS RBCs (0.5 % Hct, 1 ml) were deoxygenated (0 mmHg) in Eschweiler tonometers for a further 60 min. After every 20 min, aliquots of RBCs were removed and exposed PS labelled with LA-FITC. * $p < 0.05$, ** $p < 0.01$, ** $p < 0.01$ and *** $p < 0.001$ comparing HbSS RBCs in the presence and absence of 3,4-dichloroisocoumarin (200 µM). Data points have been normalized, the actual mean PS exposure values at 80 min were 3,4-dichloroisocoumarin (200 µM) = 4.1 % and DMSO = 14.5 %. Data points represent means ± S.E.M, n = 5.

The following experiment was performed to compare the PS exposure in presence of 3,4-dichloroisocoumarin (200 µM) at 0 mmHg with PS exposure in the absence of isocoumarin at 100 mmHg (Figure 7.2). The PS exposure in the presence of 3,4-dichloroisocoumarin (200 µM) at 0 mmHg was lower throughout the time period compared to PS exposure in absence of isocoumarin at 100 mmHg, however the difference was only significant at 60 min. The PS exposure at 60 min in presence of 3,4-dichloroisocoumarin (200 µM) at 0 mmHg was 4.2 % ± 1 % ($p < 0.05$) while the PS exposure in absence of isocoumarin at 100 mmHg was 7.3 % ± 1.9 %. This comparison was done to show the magnitude of effect that 3,4-dichloroiscoumarin has on PS exposure in HbSS RBCs. It shows that HbSS RBCs treated with 3,4-dichloroisocoumarin in fully deoxygenated condition (hypoxic) was successful in keeping it lower than HbSS RBCs in fully oxygenated condition (where RBCs are usually healthy, not sickled and have low PS exposure).
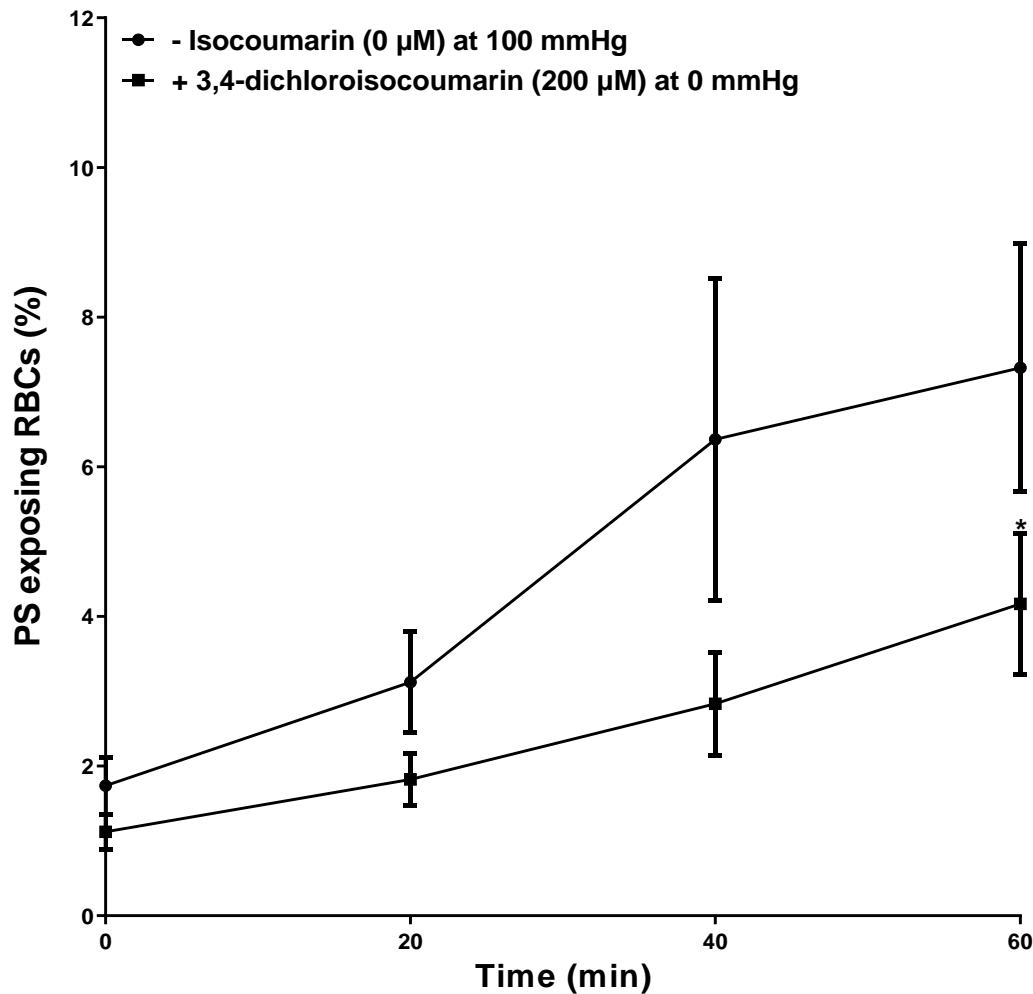
Figure 7.2: Effect of 3,4-dichloroisocoumarin (200 µM) on PS exposure at 0 mmHg compared to DMSO (- Isocoumarin) at 100mmHg in RBCs from SCD patients. HbSS RBCs (0.5 % Hct) were pre-incubated in Ca^{2+}-vanadate LK-HBS at 37 ° C, pH 7.0 in eppendorf tubes for 30 min with 3,4-dichloroisocoumarin (200 µM) or DMSO (- Isocoumarin). After pre-incubation the HbSS RBCs (0.5 % Hct, 1 ml) treated with 3,4-dichloroisocoumarin (200 µM) were deoxygenated (0 mmHg) in Eschweiler tonometers for a further 60 min and the HbSS RBCs (0.5 % Hct, 1 ml) treated with DMSO were oxygenated (100 mmHg) in Eschweiler tonometers for a further 60 min. After every 20 min, aliquots of RBCs were removed and exposed PS labelled with LA-FITC * $p < 0.05$, comparing HbSS RBCs in the presence and absence of 3,4-dichloroisocoumarin (200 µM) at 0mmHg and 100mmHg, respectively. Data points represent means ± S.E.M, n = 5.

In the final experiment of this section (Figure 7.3), the inhibitory effect of 3,4-dichloroisocoumarin on sucrose (650 mM)-induced PS exposure was examined to assess, if it had a similar inhibitory effect under hypertonic conditions compared to the hypoxic conditions previously tested. HbSS RBCs were pre-incubated at 100 mmHg in sucrose (650 mM) for 30 min with 3,4-dichloroisocoumarin (200 µM) or DMSO (- Isocoumarin). After pre-incubation, the cells were oxygenated (100 mmHg) for a further 60 min. The PS exposure was lower for the first 20 min in RBCs treated with 3,4-dichloroisocoumarin (200

µM) (52.6 % ± 3.2%) than in ones without isocoumarin (62.6 % ± 5.4 %), but not significantly. However, from 40 min to 60 min the PS exposure was similar for both the conditions, indicating that this SMase inhibitor was less effective on reducing PS exposure under hypertonicity.
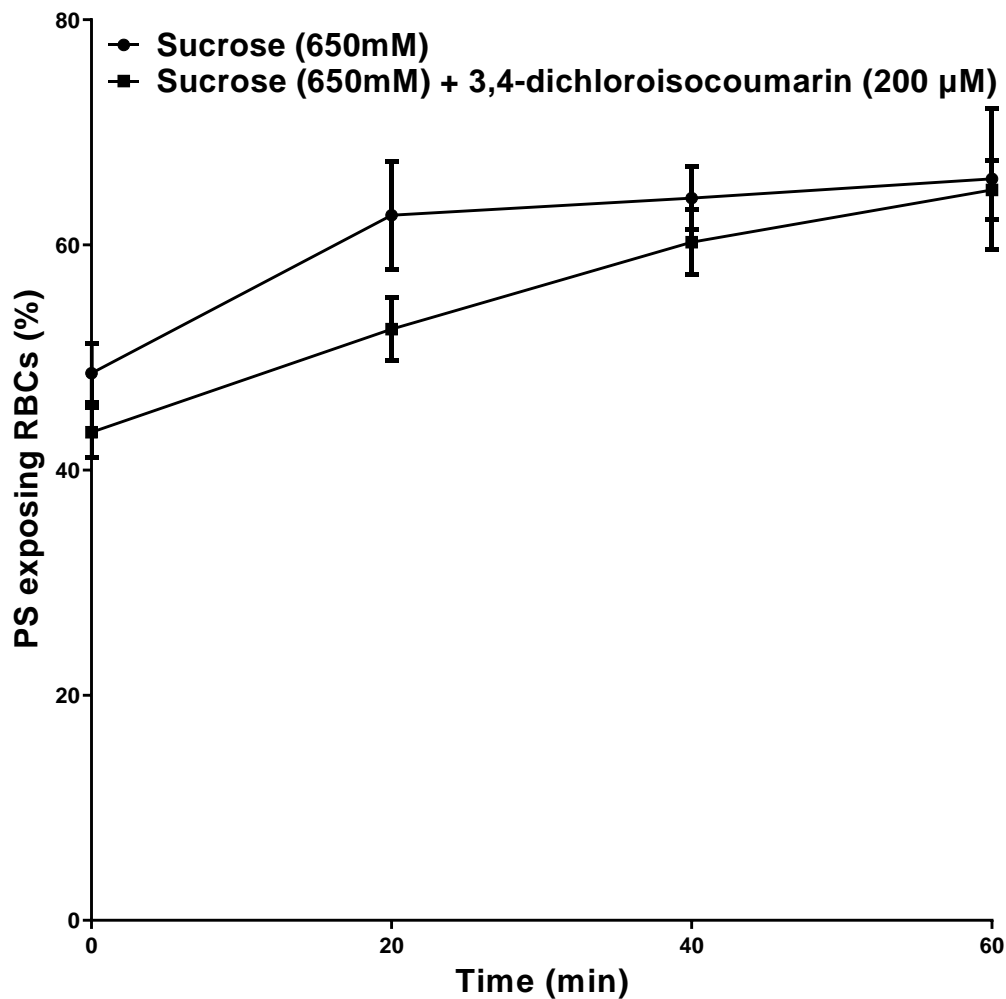
Figure 7.3: Effect of 3,4-dichloroisocoumarin (200 µM) on PS exposure in sucrose (650 mM) at 100 mmHg in RBCs from SCD patients. HbSS RBCs (0.5 % Hct) were pre-incubated in sucrose (650 mM) at 37 ° C, pH 7.0 in eppendorf tubes for 30 min with 3,4-dichloroisocoumarin (200 µM) or DMSO (-Isocoumarin). After pre-incubation the HbSS RBCs (0.5 % Hct, 1 ml) were oxygenated at 100 mmHg in Eschweiler tonometers for a further 60 min. After every 20 min, aliquots of RBCs were removed and exposed PS labelled with LA-FITC. Data points represent means ± S.E.M, n = 5.

7.2.2 Effect of ceramide on PS exposure

These series of experiments (Figure 7.4-7.6) were done to establish the effect of ceramide, which is a breakdown product of sphingolmyelin catalysed by SMase, on PS exposure in RBCs from SCD patients in different conditions. In the first set of experiments (Figure 7.4

and 7.5), the effect of ceramide on PS exposure of HbSS RBCs was investigated at two different oxygen tensions (0 mmHg and 100 mmHg). HbSS RBCs were pre-incubated for 30 min with ceramide (50 µM) or DMSO (- Ceramide). After pre-incubation, the cells were oxygenated 100 mmHg for a further 60 min (Figure 7.4). Although at all time points HbSS RBCs treated with ceramide (50 µM) had a PS exposure which was always 2-fold higher than in control HbSS RBCs treated with DMSO (- Ceramide), the increase was only significant at 60 min (5.6-fold, $p < 0.05$).
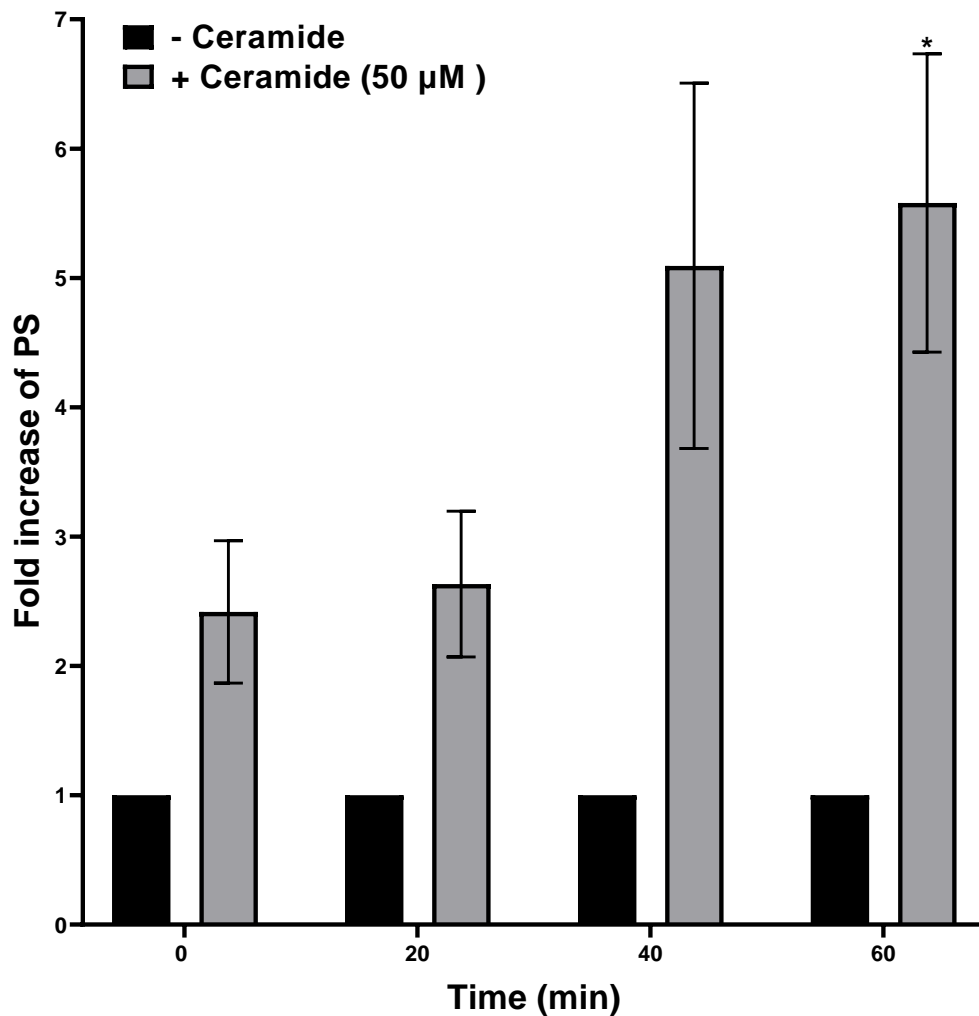
Figure 7.4: Effect of ceramide (50 µM) on PS exposure at 100 mmHg in RBCs from SCD patients. HbSS RBCs (0.5 % Hct) were pre-incubated in Ca^{2+}-vanadate LK-HBS at 37 ° C, pH 7.0 in eppendorf tubes for 30 min with ceramide (50 µM) or DMSO (- Ceramide). After pre-incubation the HbSS RBCs (0.5 % Hct, 1 ml) were oxygenated (100 mmHg) in Eschweiler tonometers for a further 60 min. After every 20 min, aliquots of RBCs were removed and exposed PS labelled with LA-FITC. * $p < 0.05$ comparing HbSS RBCs in the presence and absence of ceramide (50 µM). The actual mean PS exposure values at 60 min are DMSO (- Ceramide) = 7.7 %, + Ceramide (50 µM) = 41.9 %. Histograms show the fold increase in PS exposure and represent means ± S.E.M, n = 4.

In the next experiment, HbSS RBCs were pre-incubated for 30 min with ceramide (50 µM) or DMSO (- Ceramide). After pre-incubation, the cells were deoxygenated at 0 mmHg for a further 60 min (Figure 7.5). Apart from 40 min, at every time point ceramide significantly increased (p < 0.05) the PS exposure of HbSS RBCs. At 60 min, the increase for HbSS RBCs treated with ceramide (50 µM) was 2.4-fold higher (p < 0.05) than HbSS RBCs without ceramide.
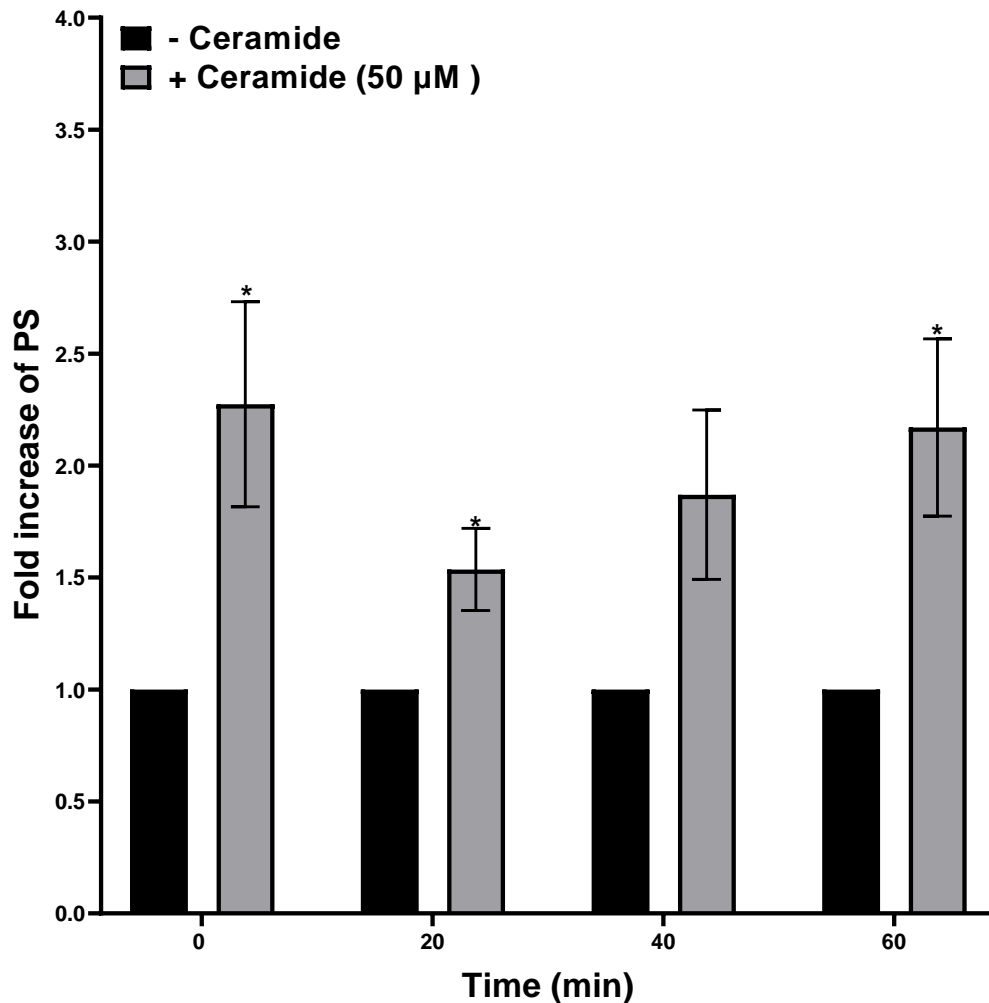
Figure 7.5: Effect of ceramide (50 µM) on PS exposure at 0 mmHg in RBCs from SCD patients. HbSS RBCs (0.5 % Hct) were pre-incubated in Ca^{2+}-vanadate LK-HBS at 37 ° C, pH 7.0 in eppendorf tubes for 30 min with ceramide (50 µM) or DMSO (- Ceramide). After pre-incubation the HbSS RBCs (0.5 % Hct, 1 ml) were oxygenated (0 mmHg) in Eschweiler tonometers for a further 60 min. After every 20 min, aliquots of RBCs were removed and exposed PS labelled with LA-FITC. * p < 0.05 comparing HbSS RBCs in the presence and absence of ceramide (50 µM). The actual mean PS exposure values at 60 min are DMSO (- Ceramide) = 9.6 %, + Ceramide (50 µM) = 22.7 %. Histograms show the fold increase in PS and represent means ± S.E.M, n = 5.

The final experiment of this section (Figure 7.6) was performed to explore the effect of ceramide on PS exposure in HbSS RBCs under hypertonic conditions induced by adding sucrose (650 mM), which in Chapter 5 was observed to be much more effective in exposing PS. HbSS RBCs were pre-incubated at 100 mmHg in sucrose (650 mM) for 30 min with ceramide (50 µM) or DMSO (- Ceramide). After pre-incubation, the cells were oxygenated (100 mmHg) for a further 60 min. The PS exposure was significantly higher throughout 60 min at every time points in HbSS RBCs treated with ceramide (50 µM) than in ones without ceramide showing that ceramide still had a stimulatory effect on PS externalisation even under hypertonic conditions.
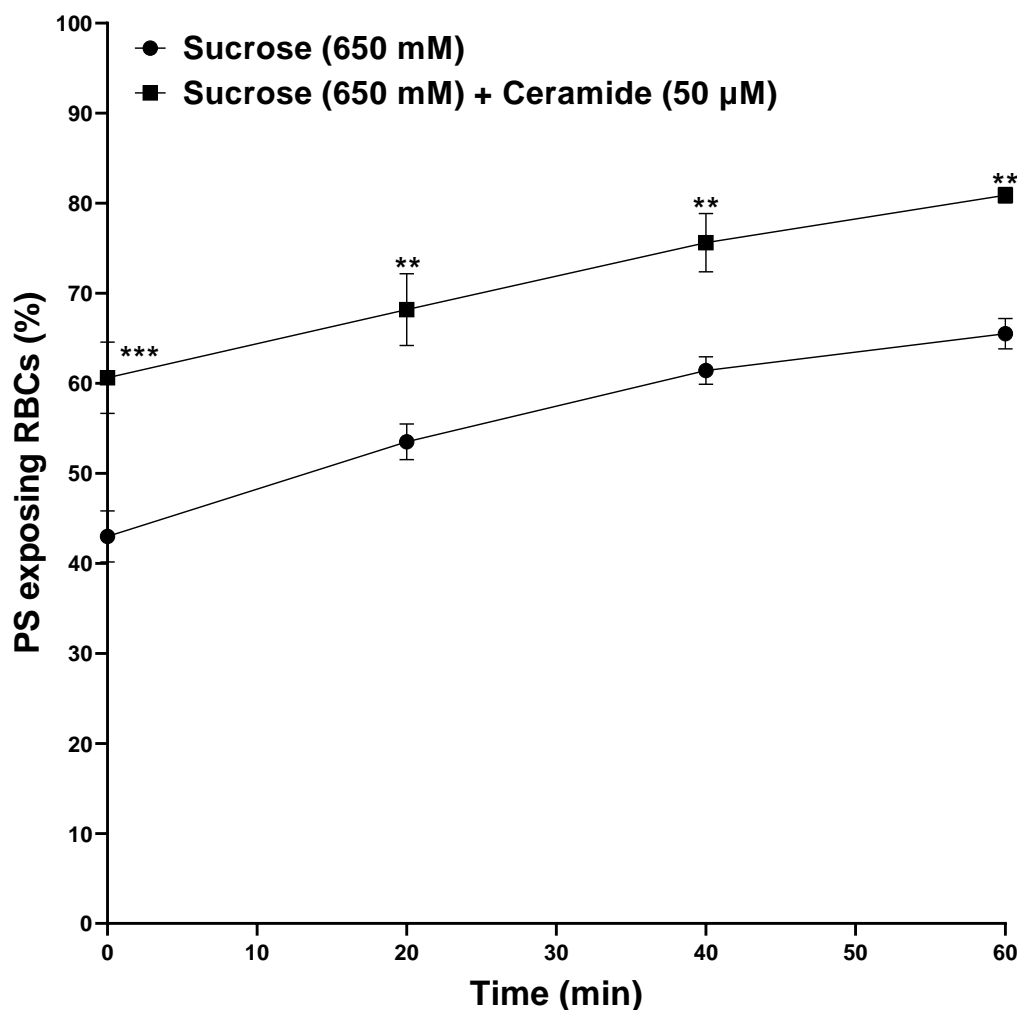
Figure 7.6: Effect of ceramide (50 µM) on PS exposure in sucrose (650 mM) at 100 mmHg in RBCs from SCD patients. HbSS RBCs (0.5 % Hct) were pre-incubated in sucrose (650 mM) at 37 ° C, pH 7.0 in eppendorf tubes for 30 min with ceramide (50 µM) or DMSO (- Ceramide). After pre-incubation the HbSS RBCs (0.5 % Hct, 1 ml) were oxygenated at 100 mmHg in Eschweiler tonometers for a further 60 min. After every 20 min, aliquots of RBCs were removed and exposed PS labelled with LA-FITC. *** $p < 0.001$ and ** $p < 0.01$ comparing HbSS RBCs in the presence and absence of ceramide (50 µM) in sucrose (650 mM). Data points represent means ± S.E.M, n = 4.

7.2.3 SMase dose response

In the final section of experiments, SMase activity was studied using a commercial assay. In this assay, one of the products of SMase hydrolysis, phosphocholine, was quantified using a colorimetric assay by measuring optical absorbance, usually at 655 nm Initially, a SMase standard curve was measured to investigate the relationship between SMase concentration and absorbance (Figure 7.7). A range of SMase concentrations from 0.078 mU.ml^{-1} to 2.5 mU.ml^{-1} was used. The colorimetric indicator of the kit, Ab blue, binds to phosphocholine increasing in absorbance at blue wavelengths. As expected, increase in concentration of SMase resulted in increased absorbance (Figure 7.7). A linear regression line was plotted and the equation for the line is y = 0.1719 x + 0.0632.
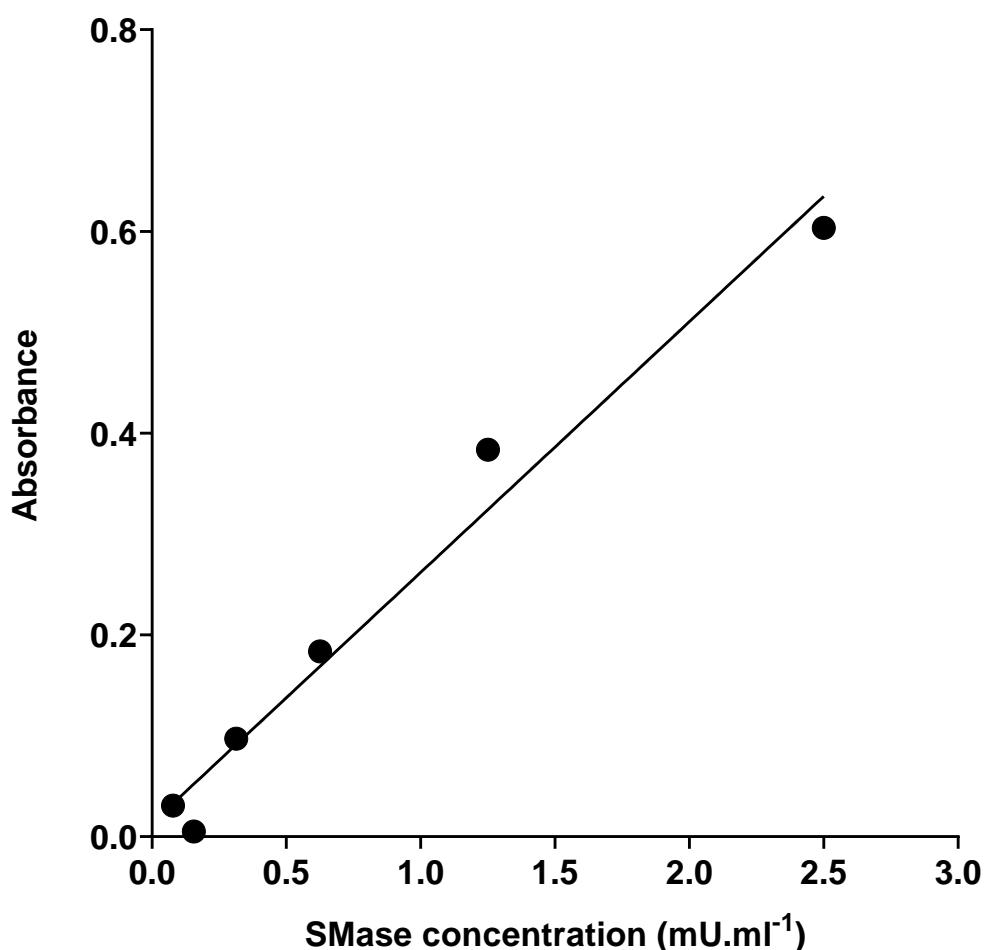
Figure 7.7: SMase dose response. SMase activity was measured in 96-well plates using a microplate reader. Specified SMase concentrations were incubated for 2 h with sphingomyelin and later Ab blue indicator was added and further incubated for 2 h. The absorbance was then measured at a wavelength of 655 nm. Symbols represent mean data points, n = 5.

7.2.4 Effect of urea on SMase activity

In Chapter 5, urea was shown to be a very effective inhibitor of PS exposure. It was possible that the action of urea was mediated via inhibition of the SMase signalling pathway. In this experiment, therefore, the effect of different concentrations of urea (50 mM, 200 mM, 600 mM & 900 mM) on SMase activity was investigated using an enzyme concentration of 1.25 mU.ml^{-1} (Figure 7.8). SMase alone gave an absorbance of 0.23 ± 0.02. However, this was significantly reduced in the presence of urea by over 95 %, to 0.0105 ± 0.005 ($p < 0.001$), 0.013 ± 0.007 ($p < 0.01$), 0.013 ± 0.005 ($p < 0.001$) and 0.02 ± 0.005 ($p < 0.001$) by urea concentrations of 50 mM, 200 mM, 600 mM and 900 mM, respectively.
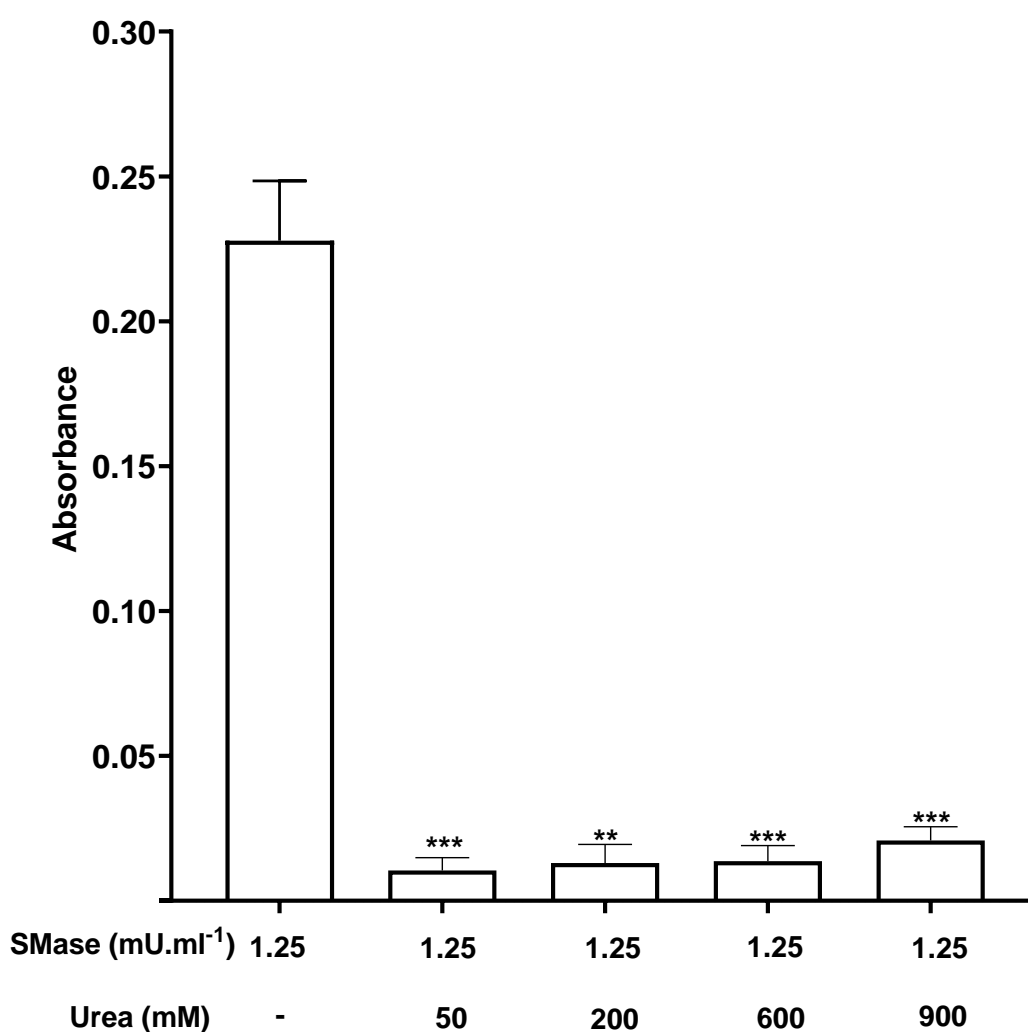
Figure 7.8: Effect of urea (50 mM, 200 mM, 600 mM & 900 mM) on SMase activity. Absorbance was measured in the absence of urea and in its presence (50 – 900 mM). ** $p < 0.01$ and *** $p < 0.001$ comparing absorbance with urea (50 mM, 200 mM, 600 mM and 900 mM) in presence of SMase (1.25 mU.ml^{-1}) with absorbance of SMase (1.25 mU.ml^{-1}) alone. The absorbance wavelength of the microplate reader was set at 655 nm. Histograms represent means $\pm$ S.E.M, n = 6

7.2.5 Effect of HbAA RBCs on the SMase absorbance assay

The absorbance of haemoglobin has peaks between about 540 nm and 580 nm depending on the level of oxygenation. It was therefore possible that the presence of haemoglobin, either in intact RBCs or in solution following their lysis, could interfere with the colorimetric assay for phosphocholine. In the following experiment (Figure 7.9), the absorbance of the products of SMase hydrolysis were measured in the presence of intact or lysed HbAA RBCs (Hct 0.5 %, 5 % and 10 %). SMase (1.25 mU.ml^{-1}) was first reacted with sphingomyelin for 2 h, after which the blue indicator was added for a further 2 h incubation period, after this, absorbance was measured in the absence or presence of RBCs. Initially absorbance was measured at 655 nm, as recommended by the kit. In the absence of RBCs, the absorbance was 0.735 ± 0.01. This was modestly but significantly reduced to 0.685 ± 0.009 ($p < 0.05$) in the presence of intact HbAA RBCs of 0.5 % Hct. However, no significant changes were observed at Hcts of 5 % (0.723 ± 0.02), 10 % (0.89 ± 0.09) using intact RBCs or in the presence of lysed cells (0.719 ± 0.05). These findings indicated that haemoglobin had minimal interference with the absorbance assay.

Figure 7.9: Effect of the presence of haemoglobin in intact or lysed RBCs on absorbance of the products of SMase hydrolysis, at the absorbance wavelength 655 nm as recommended by the kit. Initially, SMase (at a concentration of 1.25 mU.ml^{-1}) was treated for 2 h with a solution containing sphingomyelin after which the Ab blue indicator was added for a further 2 h. Finally, after 4 h of total incubation, intact HbAA RBCs of Hct 0.5 %, 5 %, 10 % or lysed (Hct 0.5 %) RBCs were added and immediately measured for absorbance of SMase activity. The absorbance wavelength was set at 655 nm. * $p < 0.05$ comparing absorbance of HbAA of Hct 0.5 % in presence of SMase (1.25 mU.ml^{-1}) compared to absence of RBCs. The absorbance at the microplate reader was set at 655 nm. Histograms represent means $\pm$ S.E.M, n = 4.

In the next experiment, the absorbance of the products of SMase hydrolysis were measured in the presence of intact or lysed HbAA RBCs (Hct 0.5 %, 5 % and 10 %), however this time it was measured at two other absorbance wavelengths, 750 nm (Figure 7.10A) and 595 nm (Figure 7.10B). This experiment was done to separate the absorbance of the indicator from the absorbance of haemoglobin in RBCs, to show that one did not interfere with the other. At 750 nm (Figure 7.10A), the absorbance of SMase products in the absence of RBCs

was very low, 0.015 ± 0.08. Similarly, low absorbances were observed in the presence of intact RBCs, Hct 0.5 % (0.013 ± 0.005), 5 % (0.025 ± 0.012) and lysed (Hct 0.5 %) RBCs (0.017 ± 0.025). The absorbance in Hct 10 % was higher than in the other conditions, 0.29 ± 0.12, however not significantly. At 595 nm (Figure 7.10B), the absorbance of SMase products in the absence of RBCs was 0.33 ± 0.005. Similar levels of absorbance were observed with intact RBCs at Hcts 0.5 % (0.29 ± 0.009), 5 % (0.38 ± 0.022) and with lysed RBCs (0.32 ± 0.025). The absorbance with intact RBCs at an Hct of 10 % was significantly higher, 0.69 ± 0.13 ($p < 0.05$).
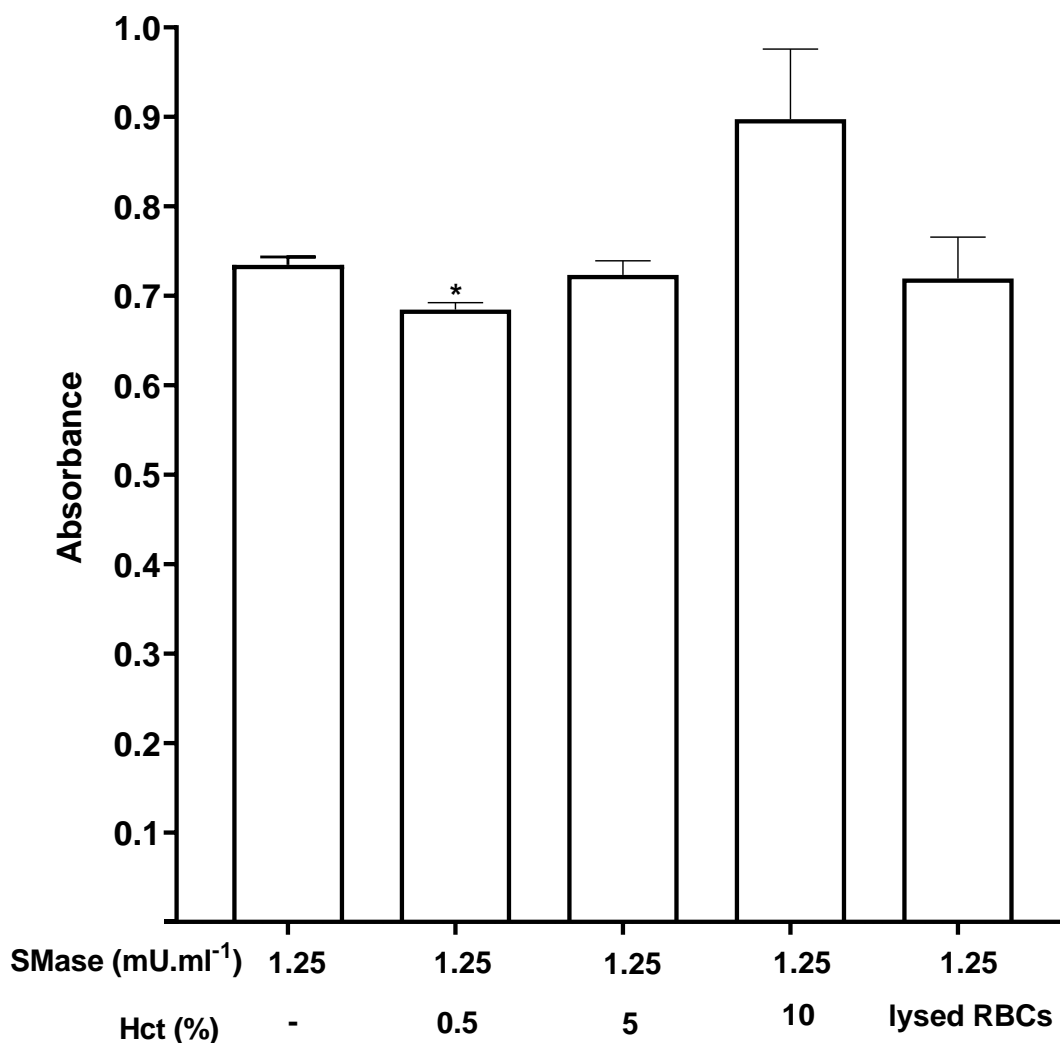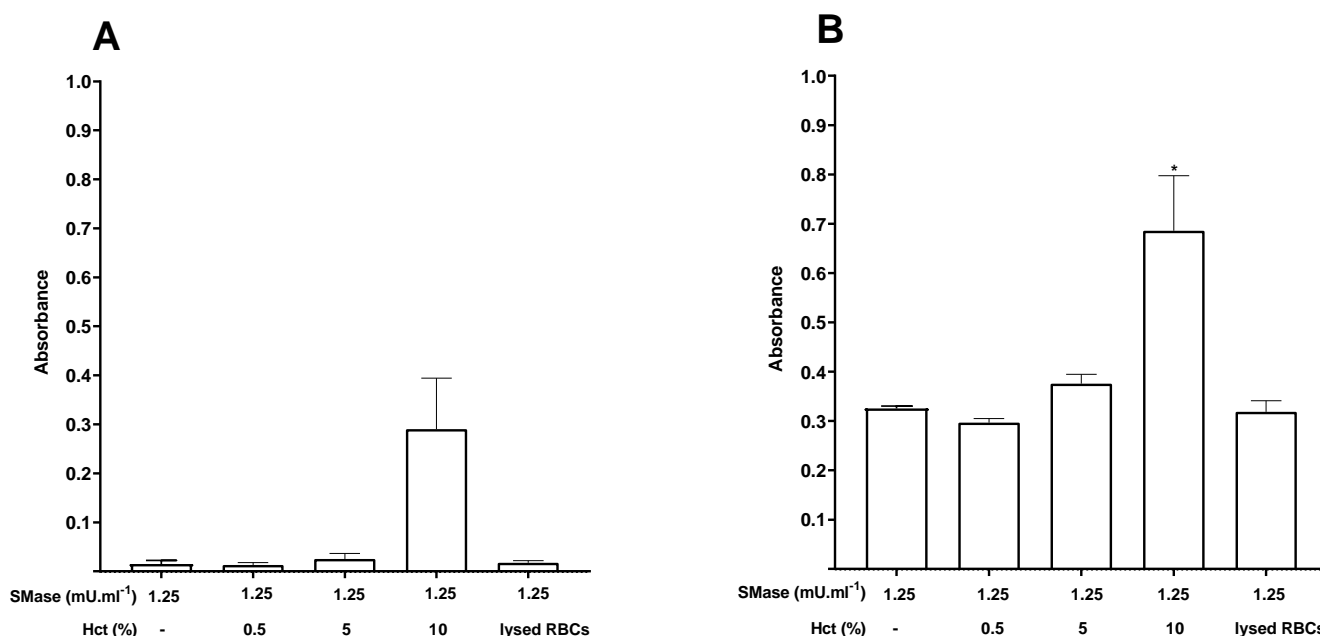

Figure 7.10: Effect of the presence of haemoglobin in intact or lysed RBCs on absorbance of the products of SMase hydrolysis, at the absorbance wavelength 750 nm and 595 nm. Initially, SMase (at a concentration of 1.25 mU.ml^{-1}) was treated for 2 h with a solution containing sphingomyelin after which the Ab blue indicator was added for a further 2 h. Finally, after 4 h of total incubation, intact HbAA RBCs of Hct 0.5 %, 5 %, 10 % or lysed (Hct 0.5 %) RBCs were added and immediately measured for absorbance of SMase activity. A: The absorbance level was monitored with absorbance at the microplate reader set at 750 nm. B: The absorbance level was monitored with absorbance at the microplate reader set at 595 nm. * $p < 0.05$ comparing absorbance of HbAA of Hct 10 % in presence of SMase 1.25 mU.ml^{-1} with absorbance of SMase 1.25 mU.ml^{-1} alone. Histograms represent means $\pm$ S.E.M, n = 4.

Lastly, a wavelength scan (Figure 7.11) was carried out to investigate the absorbance of SMase (1.25 mU.ml^{-1}) at different wavelengths in presence or absence of HbAA RBCs (0.5 % Hct). It clearly shows the difference in absorbance that takes place at 655 nm (as

recommended by the kit for detection of the indicator) when RBC is added. At 655 nm SMase (1.25 mU.ml^{-1}) in absence of RBCs have an absorbance of around 0.75, while in presence of RBCs the absorbance drops to around 0.71. The addition of RBCs resulted only in approximately 5-6 % drop in absorbance at 655 nm.
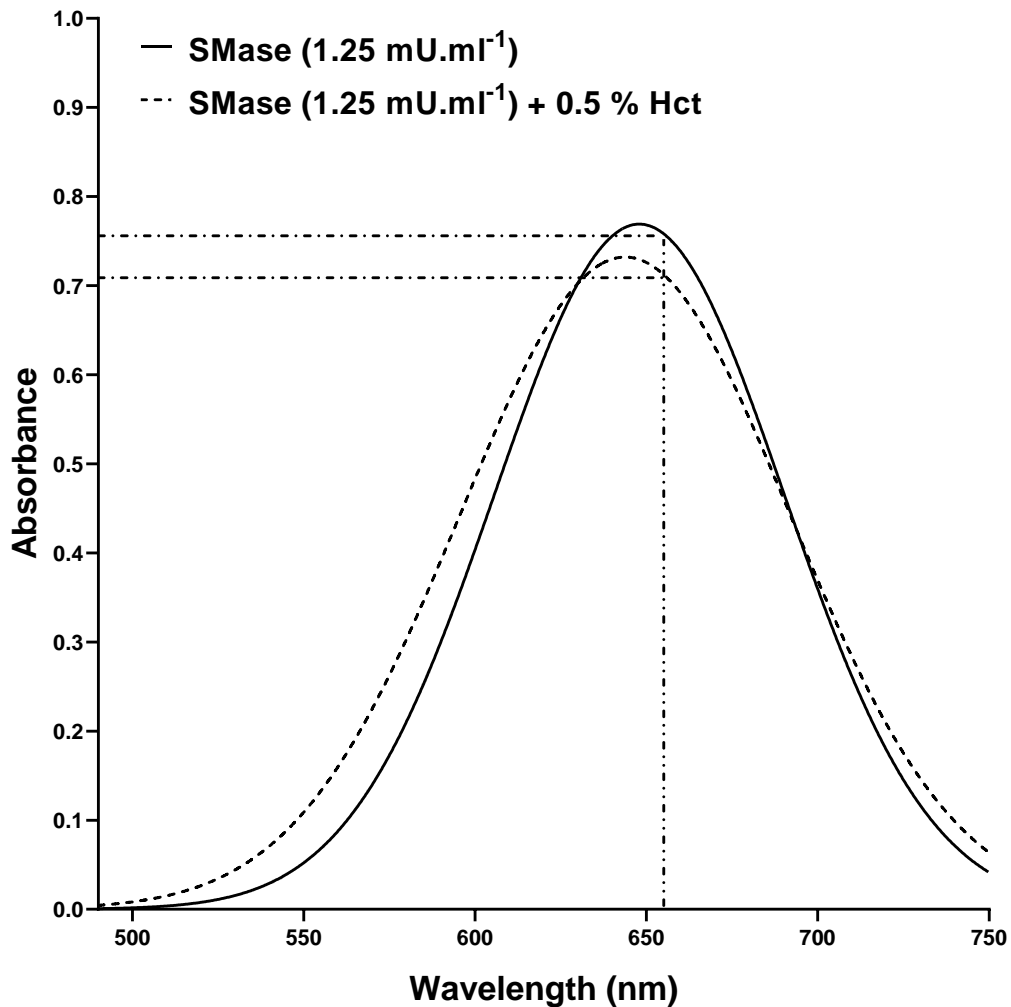
Figure 7.11 Comparison of absorbance at different wavelengths between in the presence or absence of HbAA RBCs 0.5 % Hct. Initially, SMase (1.25 mU.ml^{-1}) was treated for 2 h with a solution containing sphingomyelin after which the Ab blue indicator was added for a further 2 h. Finally, after 4 h of total incubation, intact HbAA RBCs of Hct 0.5 % or PBS was added and immediately measured for absorbance assay of SMase activity.

A final experiment (Figure 7.12) was carried out to investigate the effect of intact HbAA RBCs at 0.5 % Hct on the ability of SMase to hydrolyse sphingomyelin. SMase (1.25 mU.ml^{-1}) was reacted with sphingomyelin for a 2 h incubation in the absence of RBCs or

with intact RBCs present throughout. Under these conditions, SMase in the absence of RBCs induced an absorbance of 0.278 ± 0.003, which was markedly reduced to 0.005 ± 0.002 in the presence of HbAA RBCs. This experiment suggests that RBCs in some way reduces the activity of the SMase enzyme or otherwise chelates the breakdown products of sphingomyelin such that phosphocholine was unable to react with the Ab blue indicator.
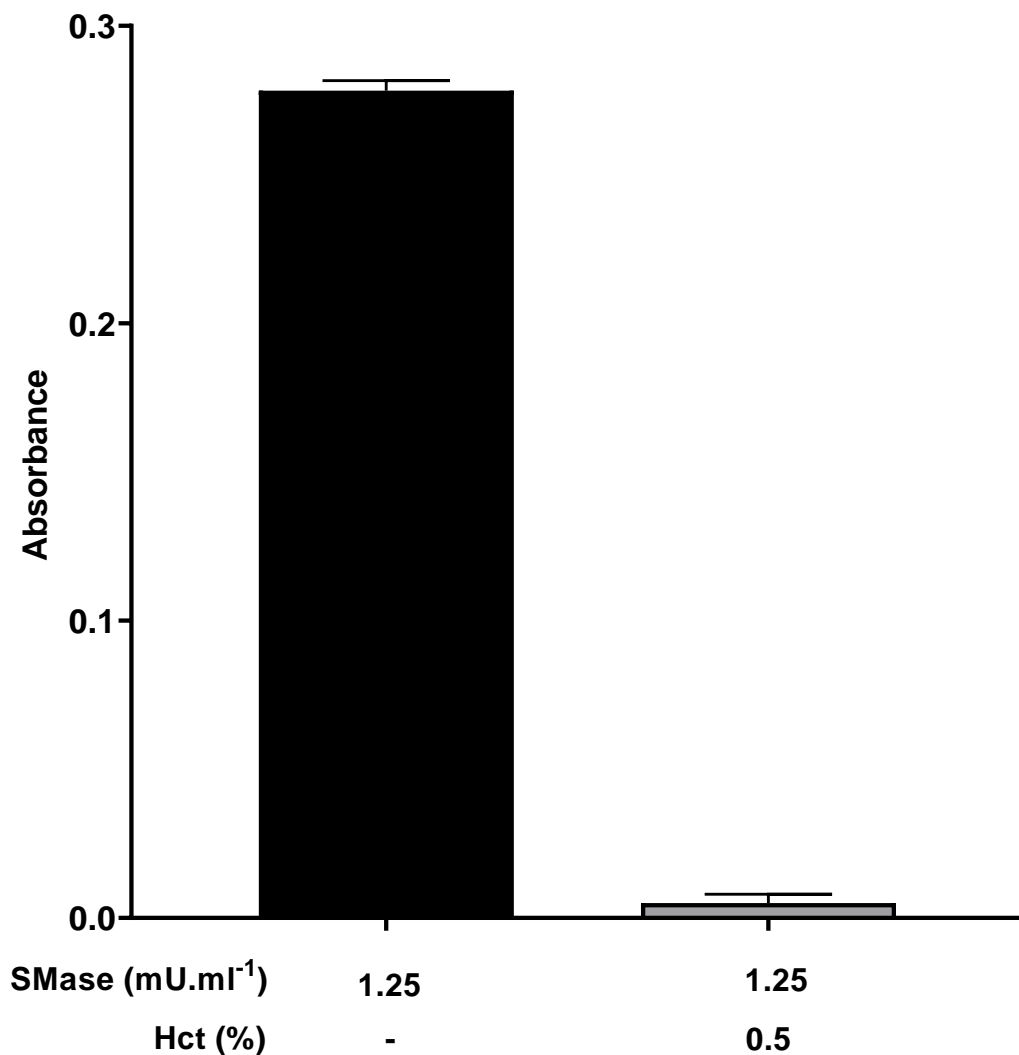
Figure 7.12: The effect of intact RBCs on the ability of SMase to hydrolyse sphingomyelin, at the absorbance wavelength 655 nm as recommended by the kit. Initially, SMase (at a concentration of 1.25 mU.ml^{-1}) was treated for 2 h with a solution containing sphingomyelin and intact HbAA RBCs of Hct 0.5 % or PBS, after which the Ab blue indicator was added for a further 2 h. Finally, after 4 h of total incubation, absorbance was measured with the absorbance level set at 655 nm in microplate reader. Histograms represent means $\pm$ S.E.M, n = 4.

7.3 Discussion

Results with 3,4-dichloroisocoumarin, which is a SMase inhibitor suggest that there might be a role for SMase and ceramide in exposing PS in RBCs of SCD patients as the inhibitor reduced the number of cells externalising PS (Figure 7.1 and 7.2). In addition, the effect of ceramide, which is a breakdown product of sphingomyelin when metabolized by SMase, was also investigated. The results from Figure 7.4-7.6 provided further evidence of the existence of SMase signalling pathway, as addition of ceramide significantly increased PS exposure in HbSS RBCs in oxygenated, deoxygenated and hypertonic conditions.

Hence, it seemed appropriate to explore the activity of SMase initially in HbAA RBCs. In this case, neutral SMase was chosen as more likely to have access to RBC sphingomyelin *in vivo*, as they are membrane-bound SMase and more widespread in mammalian tissues, whereas alkaline SMases are more localised in small intestine and bile, whilst acid SMase is localised to lysosomes of cells.

In Chapter 5, *ex vivo* experiments demonstrated that urea (600 mM and 900 mM) inhibited PS exposure in HbSS RBCs significantly in all conditions (deoxygenation, hypertonic shock and at low pH). Thus, the effect of urea on *in vitro* SMase was explored, and as Figure 7.8 shows urea strongly inhibited SMase activity. In this case, only 50 mM of urea was able to significantly inhibit ($p < 0.001$) the activity of SMase. Taken together these findings suggests that SMase signalling pathway can potentially play a role in PS exposure of HbSS RBCs and urea might be inhibiting this particular signalling pathway.

Control experiments were also carried out to determine any effect of RBCs on the absorbance assay, with the absorbance wavelength set at 655 nm (at this wavelength the colour produced by the indicator upon reacting with phosphocholine can be detected). This was done to observe if haemoglobin in RBCs or RBCs itself is interfering or quenching the absorbance of the assay. The results in Figure 7.9 were very promising as HbAA RBCs at different Hcts (0.5 %, 5 % and 10 %) and lysed RBCs following the action of SMase on sphingomyelin did not alter the absorbance measured. The negligible effect of HbAA RBCs on absorbance was also much more apparent in Figure 7.11, using a wavelength scan, which showed only a difference of 5-6 % in absorbance at 655 nm that recommended in the assay kit, or indeed at the other wavelengths tested. This was reassuring as it meant that RBCs did not interfere with absorbance of the indicator used.

However, further experiments with longer incubation of HbAA RBCs (two hours) <u>during</u> (rather than after) the SMase reaction with sphingomyelin did show a considerable effect. As it can be observed in Figure 7.12 that the absorbance of HbAA RBCs when treated with SMase (1.25 mU.ml^{-1}) showed no absorbance, whereas the control (without RBCs) showed an absorbance of 0.27. This was apparent by eye as the solution produced by incubation of RBCs together with SMase was colourless, whereas control (without RBCs) produced a noticeable blue colour. This suggests that the presence of RBCs is either interfering with the enzymatic reaction of SMase with sphingomyelin or it is interfering with the indicator process by which it binds to phosphocholine.

This finding will complicate further research on the role of SMase and the extent to which it may stimulate PS exposure. One way to overcome this problem may be to use a different kit, like Amplex Red Sphingomyelinase Assay kit by ThermoFisher, which uses a different indicator that is detected at a different absorbance wavelength. Moreover, anti-ceramide antibody conjugated to FITC could be used to detect ceramide levels by flow cytometry, after adding sphingomyelin to HbAA or HbSS RBCs. Nevertheless, if it is true that RBCs reduce SMase activity in some way this will still mean that ceramide production will be reduced. However, further experiments could not be performed due to lack of access to blood samples under the current circumstances.

8 Conclusion and future directions

Findings from this thesis have identified some important potential pathways and therapeutic compounds which could have a significant effect on PS exposure in RBCs of SCD patients. Results from Chapter 4 and 5 showed that the conditions in the renal medulla markedly stimulate PS exposure and it could be for this reason that the incidence of nephropathy is very high in SCD patients. High PS exposure could lead to vessel occlusion, as a result the filtration and reabsorption processes are disrupted, which later leads to nephropathy. Finally, experiments also revealed the ability of urea to strongly inhibit PS exposure and sickling. This could be an important stepping-stone in finding a new therapy and is thus discussed further later in this Chapter (Section 8.4). Results from Chapter 6 provided strong evidence that PIEZO1 is a prime molecular candidate for P_{sickle}. They further showed that PS exposure is stimulated not only by increases in intracellular Ca^{2+}, probably mediated via entry through PIEZO1, but also that activation of protein kinase C (PKC) can also play a major role in PS exposure. Moreover, findings also suggested that PKC activated independently of Ca^{2+} to activate the pathway by which PS exposure may be stimulated in RBCs of SCD patients. Furthermore, experiments in Chapter 7 have further suggested a role for the enzyme SMase and the metabolized product ceramide in PS exposure. It seems reasonable to conclude therefore that multiple intracellular signalling pathways are contributing to stimulate PS exposure in HbSS RBCs, which would complicate the design of successful therapeutic interventions.

In Section 8.1 the role of PKCs and the possible mechanisms by which they cause PS exposure are discussed. While in Section 8.2 the role of SMase signalling pathway is analysed for its role in stimulating PS exposure. In both the Sections (8.1 and 8.2) together with Section 8.3, future experiments are proposed to conclusively establish their role in PS exposure in SCD patients. However, activation of PIEZO1, additionally with its inability to inactivate (maybe due to SMase activation and increase in ceramide levels), simultaneously with an increase in intracellular Ca^{2+}, perhaps represent the main driving force for excess PS exposure.

8.1 Protein Kinase C (PKC)

8.1.1 PKC overview

PKC was originally isolated from bovine and rat brain, and was named protein kinase M (PKM) as it was thought to be only activated by Mg^{2+} (Inoue et al., 1977). Later it was identified that free Ca^{2+} and membrane phospholipids, namely diacylglycerol (DAG) and PS, can independently activate the enzyme without the need of proteolytic events. Thus, the enzyme was later named as Ca^{2+}- activated-phospholipid-dependent protein kinase, or PKC (Takai et al., 1979). The PKC family consist of thirteen isoenzymes and have been grouped into three classes according to their binding capability of their regulatory domain and activator requirements (Table 8.1). All PKCs have a common architecture of a single polypeptide chain of 67-115 kDa, with four conserved domains (C1, C2, C3 and C4) distributed between five variable (V1, V2, V3, V4 and V5) regions. They also consist of two principle modules of N-terminal regulatory moiety linked with the C-terminal kinase domain (Figure 8.1).

Table 8.1 PKC classification

Types	Description
cPKCs (conventional) α, βI, βII and γ	● Requires both Ca^{2+} and phospholipid activators (DAG and PS) for activation. ● The C1 domain consist of two cysteine-rich regions allowing binding of Zn^{2+}. It is also involved in binding DAG. ● The C2 domain is responsible for binding Ca^{2+}.
nPKCs (novel) δ, ε, η, μ and θ	● They lack the C2 domain for which they do not require Ca^{2+} for activity. ● The C1 domain is present and hence they are activated by DAG.

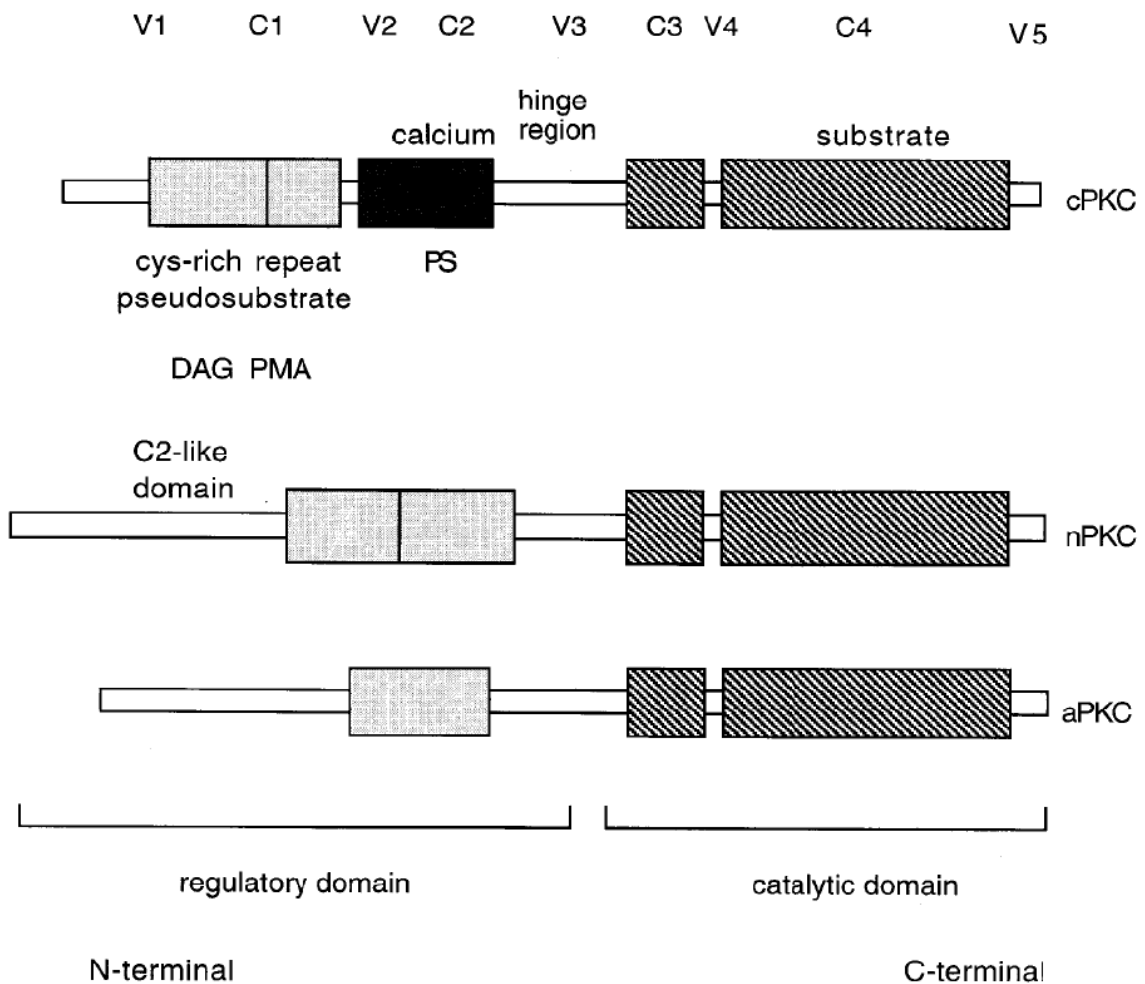|	
aPKCs (atypical) ζ and λ/ι	● The C1 domain only consist of one cysteine-rich region, thus lack sensitivity to DAG. ● The C2 domain is absent and hence do not depend on Ca^{2+} for activation. ● It is activated by PS.

Figure 8.1: Schematic representation of the primary structure of PKC gene family (Liu and Heckman, 1998).

PKC can be found in cytosol and cell membrane of most of the cells. The membrane bound fraction is mainly the active form of PKC. They are also very well distributed in all the

tissues, which has been studied using Northern or Western blot analysis. PKC α is expressed in virtually all the tissues along with PKC βI, βII, δ, ε and ζ, which are variably expressed in most of the tissues as well. PKC γ is restricted to the central nervous system and spinal cord. PKC η is strongly expressed in epithelial tissues and very slightly in spleen and brain. PKC θ is restricted primarily to skeletal muscle but can be found in lower extent in lung, spleen, skin and brain. Although the distribution of PKC isozymes has been well studied, it still remains unclear as to how this tissue specific distribution is regulated.

The presence of PKC α and ζ have been previously reported in RBCs (Belloni-Olivi et al., 1996; Fathallah et al., 1997), later Govekar and Zingde (2001) also provided evidence for the presence of PKC isoenzymes ι and μ. However, PKC α was the only isoenzyme that upon stimulation translocated to the membrane of RBCs. Although in Table 8.1 PKC μ has been classified as nPKCs, due to its unusual conformation, some groups sometimes classify it alternatively as aPKCs. The structural abnormality includes: the C1 domain with the two cysteine-rich regions separated by a 74 long amino acid chain and lack of the typical pseudo-substrate site in C1 which also has a large molecular size compared to the other PKC isoenzymes (Johannes et al., 1995, 1994). In addition, however, PKC μ is Ca^{2+} independent and is activated by DAG and PS.

8.1.2 Activation of PKC

Table 8.1 clearly identifies the co-factors that lead to activation of the different PKC isoenzymes. For activation of cPKCs intracellular Ca^{2+} is critical, in most cell types generation of second messengers such as inositol 3-phosphate(IP_3) through activation of various receptors leads to mobilization of Ca^{2+} from intracellular stores. The Ca^{2+} then binds to the C2 region of the regulatory domain as shown in Figure 8.1. Moreover, for both cPKCs and nPKCs the availability of DAG is also essential, which acts like a second messenger to activate the c & nPKCs by binding to the C1 domain of the regulatory region. Generation of DAG in cells can be achieved in two ways: (i) through activation of phospholipase C (PLC), which hydrolyses phosphatidylinositol 4,5-biphosphate (PIP2) to produce IP_3 (role in Ca^{2+} mobilization in cells) and DAG; and (ii) through hydrolysis of the predominant membrane lipid phosphatidylcholine (PC) by the enzyme phospholipase D (PLD). This hydrolysis of PC results in production of phosphatidic acid (PA) and choline. Then the enzyme phosphomonoesterase converts PA to DAG (Mordechai Liscovitch, 1992; Nishizuka, 1992). However, in some cases PIP2 and PI (precursor of PIP2) alone can

substitute for the role of DAG. cPKCs such as PKC α and PKC βI showed no difference in activity when DAG was replaced with PI and PIP2 respectively in presence of Ca^{2+} (Kochs et al., 1993). Little is known about the activation of aPKCs, other than the fact that they are both Ca^{2+}- and DAG-independent. They can bind to PS for membrane interaction and unlike cPKCs and nPKCs they are activated by binding to proteins (Graybill et al., 2012; Newton, 2001; Tsai et al., 2015). Activation of PKC isoenzymes can lead to a variety of biological responses such as cell proliferation and differentiation, membrane ion transport, glucose and lipid metabolism, gene expression, smooth muscle contraction, etc. (Nishizuka, 1995, 1992, 1984).

8.1.3 Role of Ca^{2+} and PKC interaction in PS exposure of RBCs from SCD patients

RBCs are very different from many other cell types, as they lack major intracellular organelles such as the endoplasmic reticulum, golgi bodies, nucleus, etc. Thus, there are no regulated intracellular calcium stores in RBCs, so the role of IP_3 as second messenger in mobilizing Ca^{2+} is irrelevant. However, it is very well established that when RBCs from SCD patients are exposed to deoxygenated or hypoxic conditions, the RBCs not only sickle, but it also allows entry of Ca^{2+}, increasing the concentration of intracellular Ca^{2+}. This entry of Ca^{2+} takes place through a deoxygenated-induced non-specific cation channel called P_{sickle}. The molecular identity of this channel is still uncertain, however, there are several lines of evidence which show that it could be the stress-activated channel called PIEZO1 (Section 1.3(i)d). Results from Chapter 6 add to the growing evidence for PIEZO1 being the candidate for P_{sickle} and showed that Yoda1, the chemical activator of PIEZO1 channel, caused an increase in intracellular concentration of Ca^{2+} in RBCs of SCD patients. While, in addition, Dooku1 - the antagonist of Yoda1 - and GsmTx4 - the PIEZO1 inhibitor - inhibited this rise, adding further credence to the identity of P_{sickle} being PIEZO1 (Wadud et al., 2020).

Increased intracellular Ca^{2+} could cause PKC α to bind to $2Ca^{2+}$ on its C2 domain leading to a favourable interaction between PKC α and plasma membrane of the cell (Corbalán-García et al., 1999; Murray and Honig, 2002; Verdaguer et al., 1999). This binding of Ca^{2+} is known to increase the affinity of PKC α for the plasma membrane causing it to translocate and bind to the lipid bilayer of the membrane. Mutations in the Ca^{2+} binding site of the PKC α have been shown to interfere with the interaction of the PKC isoenzyme with the plasma membrane, both *in vivo* and *in vitro* (Bolsover et al., 2003; Marín-Vicente et al., 2005;

Medkova and Cho, 1998; Ochoa et al., 2002). Moreover, evidences also show that influx of Ca^{2+} together with the help of endogenous PIP2 in the plasma membrane of the cell, serve to anchor PKC α, and can in turn activate the PKC isoenzyme (Corbalán-García et al., 2003; Marín-Vicente et al., 2005; Raucher et al., 2000). It is also possible that PKC α is anchored in the plasma membrane by DAG instead of PIP2. Increased intracellular Ca^{2+} can lead to the activation of phospholipase C enzyme. This would result in hydrolysis of PIP2 to DAG, which together with Ca^{2+} lead to the activation of PKC α. Furthermore, Fathallah et al. (1997) showed higher contents of both total and membrane-associated PKC α in HbSS RBCs compared to HbAA. Thus, it is possible in RBCs of SCD patients the over expressed membrane-bound PKC α could eventually lead to the activation of the enzyme scramblase, which results in externalisation of PS. Barber et al. (2015) showed that activation of PKC with phorbol ester in both HbAA and HbSS caused an increase in scramblase activity and PS exposure, while this was reduced in presence of the inhibitor of PKC chelerythrine chloride.

RBCs of SCD patients are also exposed to high oxidative stress due to accumulation of reactive oxygen species (ROS) such as hydrogen peroxide, superoxide anion and hydroxyl radical in blood vessels. ROS has been shown to be involved in the activation of both the enzyme PLC and PLD, especially PLD in endothelial cells (Domijan et al., 2014; Natarajan et al., 1996; Parinandi et al., 2001, 1999; Patel et al., 2011; Servitja et al., 2000). As aforementioned, activation of these enzymes can lead to production of DAG, which together with Ca^{2+} can result in activation of PKC α. Thus, in turn these events could activate the membrane-bound scramblase enzyme and induce PS exposure.

Results with the Yoda1 (Chapter 6) also show that there is a Ca^{2+}-independent mechanism working in RBCs of SCD patients, which leads to the exposure of PS. Thus, it is important to examine the roles of aPKC and nPKC isoenzymes that are present in the RBCs, which are Ca^{2+} independent. Though Fathallah et al. (1997) and Barber et al. (2015) utilized phorbol 12-myristate 13-acetate (PMA) to show the increase in PKC α and scramblase activity in HbSS RBCs, however, PMA is known to have various other effects in cells. Moreover, it is possible that PMA does not affect the other PKC isoenzymes in the same magnitude as it does with PKC α, hence explaining the translocation of PKC α to plasma membrane of RBCs. Therefore, it will be interesting to examine the effect of specific inhibitors of nPKCs and aPKCs on deoxygenation induced PS exposure of HbSS RBCs.

8.2 SMase signalling pathway

8.2.1 Overview

Sphingolipids are an essential component of the mammalian cell membrane. They have important functions including: (i) providing mechanical strength to cells; (ii) as stores of key signalling molecules, which include ceramides, sphingosines and sphingosine-1-phosphate; and (iii) as platforms for various membrane proteins such as ion channels, insulin receptors, etc. Sphingomyelin is the most widespread sphingolipid, which is distributed extensively in the exoplasmic side of the membrane and coexists with various other bio-active molecules in the membrane. The structure of sphingomyelin consists of a polar head group called phosphocholine together with a hydrophobic backbone of ceramide. The sphingomyelinase (SMase) enzymes catalyse the degradation of sphingomyelin to form its hydrolytic products phosphocholine and ceramide. The metabolic product ceramide, as mentioned in Section 7.1, is responsible for the modulation of various cellular events including proliferation, differentiation and apoptosis.

8.2.2 Role of SMase signalling pathway in RBCs

Results in Chapter 7 with 3,4-dichloroisocoumarin and ceramide have suggested a potential role for the SMase signalling pathway in PS exposure in RBCs from SCD patients. There are broadly three different types of SMase present, which are acid SMase, alkaline SMase and neutral SMase. Results in this thesis focused primarily on neutral SMase because of its abundance in different tissues and cells, and its localization in membranes. Moreover, previous reports have shown the presence of neutral SMase on the surface of endothelial cells and that it is activated by increase in fluid shear stress and pressure leading to production of ceramide (Czarny et al., 2003; Czarny and Schnitzer, 2004). Building on this work Shi et al. (2020) recently showed that neutral SMase suppresses PIEZO1 inactivation in endothelial cells by catalysing the production of ceramide which stabilizes the open state of the PIEZO1 channel rather than the closed state. Although as stated before RBCs do not have SMase enzymes of their own (Section 7.1), but it is possible that as RBCs circulate they can be readily exposed to SMase secreted from neighbouring cells. As mentioned in Section 1.4, high PS exposure on HbSS RBCs also increases cell-to-cell interactions with endothelial cells, leukocytes and platelets. Therefore, it is possible that RBCs in SCD patients, when exposed to neutral SMase from neighbouring cells, accumulate ceramide in their membrane, which acts on PIEZO1. Furthermore, it is also possible when HBSS RBCs pass through hypoxic regions, sickling activates PIEZO1 and the additional presence of

excess ceramide in the membrane due to the exposure of RBCs to neutral SMase within the circulation disables inactivation of PIEZO1. Both of these situations would cause increased entry of Ca^{2+} into the RBCs and stimulate PS exposure. Moreover, ceramide is also known to sensitise the RBC scramblase to cytosolic Ca^{2+} (Lang et al., 2004; Lang et al., 2005), which would further promote PS exposure. Additionally, ceramide-enriched membrane have previously been shown to make membrane of RBCs very fragile (Dinkla et al., 2012). The other possibility is that RBCs in SCD patients are directly exposed to ceramide from neighbouring cells, rather than that formed within their own membranes, which is causing all the aforementioned affects.

Future experiments with schypostatin, GW4869 and altenusin, which specifically inhibit neutral SMase, can be utilized to carry out various assays on HbSS RBCs. It will be interesting to observe if the aforementioned inhibitors have any effect on deoxygenation-induced Ca^{2+} entry in sickle RBCs. Urea could also be utilized, because in Chapter 7 it was shown that urea inhibits SMase *in vitro*, so it will be interesting to investigate any effect on deoxygenation-induced Ca^{2+} entry. Further experiments can be designed to determine any effect of these inhibitiors on PS exposure in HbSS RBCs. These experiments will shed light on the role of SMase signalling pathway in PS exposure and Ca^{2+} entry in RBCs of SCD patients.

It will be also interesting to explore the involvement of acid SMase on PS exposure in HbSS RBCs. Chronic inflammation and anaemia triggers secretion of acid SMase in cells, which can be observed in other diseases like diabetes, sepsis, cardiovascular and pulmonary diseases (Jenkins et al., 2009). Patients suffering from SCD also suffer from such pathophysiological effects and thus can have increased acid SMase. In fact, there is only one study which showed that acid SMase activity in HbSS RBCs and plasma was significantly elevated compared to levels in HbAA individuals (Awojoodu et al., 2014). Therefore, it would be interesting to observe if ceramide produced from the action of acid SMase has a similar effect on PIEZO1, as observed to that with neutral SMase. Additionally, the effect of acid SMase on PS exposure in HbSS RBCs can be explored.

8.3 Creating knockin and knockout of *in vitro* cultured cell lines

In vitro cultured cell lines have long been utilized to study effects of various *in vivo* phenomena. These models have enabled researchers to manipulate numerous molecular targets to study the cellular signalling processes and their role in biological systems. Thus,

it would be invaluable to have immortalized human erythroid progenitor cell lines that can differentiate into proper mature RBCs to carry out and study the effects of genetic manipulation – which is not possible in mature circulating RBCs which lack a nucleus and other components required for protein synthesis. Previously, researchers could only study erythropoiesis in cellular models of erythroleukemic cell lines, such as mouse erythroleukemic cells (MEL cells), and K562 cells, a human erythroleukemic cell line. The major limitation of RBCs produced from these erythroleukemic cell lines is that they do not represent 'normal' human erythroid cells. These cells exhibit more fetal globin expression rather than adult haemoglobin expression, and have terminal differentiation defects leading to inefficient production of both reticulocytes and mature enculeated RBCs.

8.3.1 Utilising human umbilical cord blood-derived erythroid progenitor (HUDEP) cells

However, in 2013 Kurita et al. provided a convenient and reliable *ex vivo* source for RBC production from immortalized human erythroid progenitor cell lines, which differentiated into cells containing functional haemoglobin, enucleated RBCs and expressed erythroid-specific markers. Kurita et al. established three human umbilical cord blood-derived erythroid progenitor (HUDEP) cell lines from three different cord blood samples: HUDEP-1, HUDEP-2 and HUDEP-3. Amongst these three, HUDEP-2 cells developed into erythroid cells which closely resembled 'normal' adult human erythroid cells as they: (i) pre-dominantly expressed β-globin unlike HUDEP-1 and HUDEP-3 which pre-dominantly expressed γ-globin; and (ii) HUDEP-2 cell lines expressed BCL11A which is a known suppressor of γ-globin. Therefore, finally it is possible for researchers to utilize this immortalized erythroid cell line for genetic manipulation to study diseases like SCD. The aim would be to knockin HbS into this cell line to create the first immortalized sickle cell line and compare their behaviour with clinical samples from sickle cell patients. They could then be studied under similar conditions to those used in this thesis - like hypoxia, different pHs, hyperosmotic and hypertonic conditions - to compare their behaviour with "normal" sickle cells. Once the cell line has been established and shown to be comparable to clinical samples, there are a plethora of studies that can be done in this model to understand the disease better. These would include creating a knockout of PIEZO1 in a sickle cell line and studying its role in the disease pathogenesis. Moreover, much easier possibilities would be to delete specific PKC genes, or SMase, and study their roles on Ca^{2+} signalling pathway and PS exposure, as these are much smaller proteins than PIEZO1.

8.3.2 Utilising Bristol erythroid line adult (BEL-A) cells

Although, HUDEP-2 has paved the pathway for researchers to create a model amenable to genetic manipulation and has provided a better alternative cellular model, however, the major drawback of the HUDEP-2 model is that it has a very low rate of enucleation, only 5 %. This means that only a very low population of cells truly resembles adult matured RBCs and further genetic manipulation might interfere with differentiation and growth resulting in even lower yields. However, in 2017 Trakarnsanga et al., developed a far superior cellular model of human immortalized adult erythroid cell line called the Bristol erythroid line adult (or BEL-A) cells. BEL-A cells have an enucleation rate of around 42 % compared to 5 % of HUDEP-2 cell line. The reticulocyte yield in BEL-A culture was also 4-fold higher than HUDEP-2 cultures. Moreover, key transcription factors for erythroid differentiation and β-globin expression, were overall lower in HUDEP-2 compared to BEL-A. This clearly shows that normal adult erythropoiesis is more closely followed in the BEL-A cell line compared to that in HUDEP-2.

Therefore, in collaboration with King's College London, preliminary work is underway to study PS exposure in the BEL-A cell line, so that the aforementioned genetic manipulation can be carried out to understand the disease and cellular signalling processes better. Initially as shown in Figure 8.2, experiments were conducted on BEL-A cells at day 0 (Figure 8.2A) and day 4 (Figure 8.2B) of their differentiation. Previously it has been shown that calcium loading of RBCs using the ionophore Br-A23187 stimulates PS exposure. Thus, in presence of extracellular Ca^{2+}, the effect of using ionophore Br-A23187 (3 µM) in relation to PS exposure was investigated on PS exposure of BEL-A cells at these different differentiation stages. The results were very promising as it can be observed in Figure 8.2 that at day 0 of differentiation PS exposure in presence of ionophore Br-A23187 and LA- FITC was 5.9 % while following the same protocol at day 4 of differentiation exposure was 35.4 %. This can be explained as at day 0 of differentiation of BEL-A cells many proteins have not been expressed, while at day 4 of differentiation the cells have reached a stage of maturation where most of the proteins are being expressed. Hence, entry of Ca^{2+} is stimulating some of these expressed proteins, perhaps the scramblase or PKC, causing increased PS exposure. Therefore, further experiments and a comparative analysis need to be done with clinical samples to ensure that this *in vitro* model can be used for genetic manipulation to study SCD and PS exposure. Nonetheless, the initial results in terms of change in behaviour of the cells in addition to ionophore Br-A23187 is very encouraging.
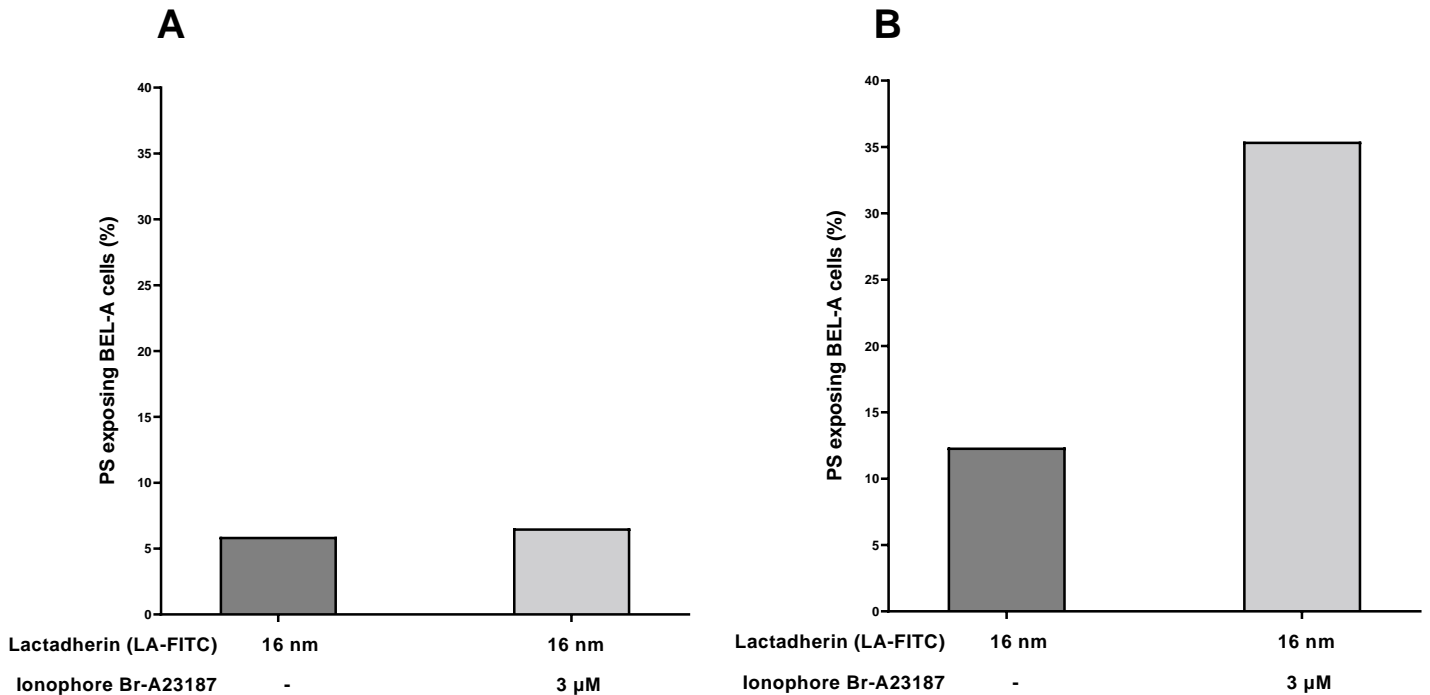
Figure 8.2 PS exposure in BEL-A cells induced by the ionophore Br-A23187. BEL-A cells in Ca^{2+}-vanadate LK-HBS pH 7.0 at 37 ° C were either treated with LA-FITC (16 nm) or LA-FITC (16 nm) and ionophore Br-A23187 (3 μM). A: Experiment was conducted when BEL-A cells were at day 0 of differentiation stage. B: Experiment was conducted when BEL-A cells were at day 4 of differentiation stage. Histograms represent means, n = 2.

8.4 Urea as a potential therapy

Previously Lu (2020) examined the effect of renal medulla conditions on HbSS RBCs in relation to K^+ transport and volume control. Whilst, this report investigates the effect of renal medulla conditions on HbSS RBCs in relation to PS exposure. Results from Chapter 5 clearly showed that urea at high concentrations caused a very strong inhibition of PS exposure in HbSS RBCs in all the renal medullary conditions tested. Additionally, urea also inhibited sickling in hypoxic condition. Furthermore, results in Chapter 7 showed that urea has the ability to inhibit the enzyme SMase, which has the potential to cause PS exposure. Although experiments showed that higher concentrations of urea were required to inhibit PS, the experiment using isolated SMase showed that urea at a much lower concentration (50 mM) was inhibitory. Thus, it might be possible that longer treatment of HbSS RBCs with urea *ex vivo* might have resulted in inhibition of PS in HbSS RBCs, which can be explored.

Nonetheless, all these results show a potential for urea derivatives to act as inhibitors of PS exposure. The use of drugs repurposing in this case could be a useful approach in identifying potential therapies, as drugs structurally similar would tend to have similar targets, and shared biological activity and indications. There are urea derivatives, which have been approved by regulatory authorities previously for different purposes or treatments and have gone through some rigid phases of clinical trials, providing important information about their pharmacodynamics, pharmacokinetics, side effects and possible molecular pathways they work through.

The following are two urea derivatives that have been approved and could be utilized to assess their effect on PS exposure in HbSS RBCs:

a) Sorafenib: which is a diaryl urea multikinase inhibitor, which is currently under evaluation for the treatment of acute myeloid leukaemia. In 2007, it was approved for the treatment of advanced renal cell carcinoma and hepatocellular carcinoma.

b) Lenvatinib: which is a small urea based molecule multikinase inhibitor. It is approved for thyroid cancer and advanced renal cell carcinoma.

Taken together, this study contributes substantially to understanding of the physiological conditions and the potential pharmacological pathways that stimulate PS exposure in RBCs of SCD patients. The study provides answers for why the kidney, in particular, is massively affected at a very early age in SCD patients. Furthermore, results from the study show the second messenger pathways that are likely to be involved and the multiple ways they could be working to cause PS exposure. Additionally, this study has also provided a potential compound (urea) that would help in identifying possible drug candidates. Therefore, a starting point to design a pharmacological strategy to inhibit the pathways that could significantly decrease PS exposure in RBCs of SCD patients and thus improving health status and amelioration of complications of SCD.

9 References

Abe, A., Shayman, J.A., Arbor, A., 2013. Sphingolipid Catabolism, 2nd ed, Encyclopedia of Biological Chemistry. Elsevier Inc. https://doi.org/10.1016/B978-0-12-378630-2.00462-X

Aburasayn, H., Al Batran, R., Ussher, J.R., 2016. Targeting ceramide metabolism in obesity. Am. J. Physiol. Endocrinol. Metab. 311, E423-35. https://doi.org/10.1152/ajpendo.00133.2016

Adèle Faucherre, Karima Kissa, Joël Nargeot, Matteo E. Mangoni, Chris Jopling, 2014. Piezo1 plays a role in erythrocyte volume homeostasis. Haematologica 99, 70–75. https://doi.org/10.3324/haematol.2013.086090

Alayash, A.I., 2018. Oxidative pathways in the sickle cell and beyond. Blood Cells. Mol. Dis. 70, 78–86. https://doi.org/10.1016/j.bcmd.2017.05.009

Albanyan, A.-M., Murphy, M.F., Rasmussen, J.T., Heegaard, C.W., Harrison, P., 2009. Measurement of phosphatidylserine exposure during storage of platelet concentrates using the novel probe lactadherin: a comparison study with annexin V. Transfusion 49, 99–107. https://doi.org/10.1111/j.1537-2995.2008.01933.x

Albuisson, J., Murthy, S.E., Bandell, M., Coste, B., Louis-dit-Picard, H., Mathur, J., Fénéant-Thibault, M., Tertian, G., de Jaureguiberry, J.-P., Syfuss, P.-Y., Cahalan, S., Garçon, L., Toutain, F., Simon Rohrlich, P., Delaunay, J., Picard, V., Jeunemaitre, X., Patapoutian, A., 2013. Dehydrated hereditary stomatocytosis linked to gain-of-function mutations in mechanically activated PIEZO1 ion channels. Nat. Commun. 4, 1884. https://doi.org/10.1038/ncomms2899

Alessandro, A.D., Righetti, P.G., Zolla, L., 2010. The Red Blood Cell Proteome and Interactome : An Update 144–163.

Alsultan, A., Alabdulaali, M.K., Griffin, P.J., Alsuliman, A.M., Ghabbour, H.A., Sebastiani, P., Albuali, W.H., Al-Ali, A.K., Chui, D.H.K., Steinberg, M.H., 2014. Sickle cell disease in Saudi Arabia: the phenotype in adults with the Arab-Indian haplotype is not benign. Br. J. Haematol. 164, 597–604. https://doi.org/10.1111/bjh.12650

Amer, J., Ghoti, H., Rachmilewitz, E., Koren, A., Levin, C., Fibach, E., 2006. Red blood cells, platelets and polymorphonuclear neutrophils of patients with sickle cell disease exhibit oxidative stress that can be ameliorated by antioxidants. Br. J. Haematol. 132, 108–113. https://doi.org/10.1111/j.1365-2141.2005.05834.x

Amer, J., Zelig, O., Fibach, E., 2008. Oxidative status of red blood cells, neutrophils, and platelets in paroxysmal nocturnal hemoglobinuria. Exp. Hematol. 36, 369–377. https://doi.org/10.1016/j.exphem.2007.12.003

Andolfo, I., Alper, S.L., De Franceschi, L., Auriemma, C., Russo, R., De Falco, L., Vallefuoco, F., Esposito, M.R., Vandorpe, D.H., Shmukler, B.E., Narayan, R., Montanaro, D., D'Armiento, M., Vetro, A., Limongelli, I., Zuffardi, O., Glader, B.E., Schrier, S.L., Brugnara, C., Stewart, G.W., Delaunay, J., Iolascon, A., 2013. Multiple clinical forms of dehydrated hereditary stomatocytosis arise from mutations in PIEZO1. Blood 121, 3925–35, S1-12. https://doi.org/10.1182/blood-2013-02-482489

Andrews, D.A., Low, P.S., 1999. Role of red blood cells in thrombosis. Curr. Opin. Hematol. 6, 76–82. https://doi.org/10.1097/00062752-199903000-00004

Antonarakis, S.E., Boehm, C.D., Serjeant, G.R., Theisen, C.E., Dover, G.J., Kazazian, H.H.J., 1984. Origin of the beta S-globin gene in blacks: the contribution of recurrent mutation or gene conversion or both. Proc. Natl. Acad. Sci. U. S. A. 81, 853–856.

Antoniades, C., Shirodaria, C., Leeson, P., Antonopoulos, A., Warrick, N., Van-Assche, T., Cunnington, C., Tousoulis, D., Pillai, R., Ratnatunga, C., Stefanadis, C., Channon, K.M., 2009. Association of plasma asymmetrical dimethylarginine (ADMA) with elevated vascular superoxide production and endothelial nitric oxide synthase uncoupling: implications for endothelial function in human atherosclerosis. Eur. Heart J. 30, 1142–1150. https://doi.org/10.1093/eurheartj/ehp061

Apovo, M., Beuzard, Y., Galacteros, F., Bachir, D., Giraud, F., 1994. The involvement of the Ca-dependent K channel and of the KCl co-transport in sickle cell dehydration during cyclic deoxygenation. Biochim. Biophys. Acta 1225, 255–258.

Archer, N.M., Shmukler, B.E., Andolfo, I., Vandorpe, D.H., Gnanasambandam, R., Higgins, J.M., Rivera, A., Fleming, M.D., Sachs, F., Gottlieb, P.A., Iolascon, A., Brugnara, C., Alper, S.L., Nathan, D.G., 2014. Hereditary xerocytosis revisited. Am. J. Hematol. 89, 1142–1146. https://doi.org/doi:10.1002/ajh.23799

Arroyo, J.P., Kahle, K.T., Gamba, G., 2013. The SLC12 family of electroneutral cation-coupled chloride cotransporters. Mol. Aspects Med. 34, 288–298. https://doi.org/10.1016/j.mam.2012.05.002

Asgary, S., Naderi, G., Askari, N., 2005. Protective effect of flavonoids against red blood cell hemolysis by free radicals. Exp. Clin. Cardiol. 10, 88–90.

Ataga, K.I., Orringer, E.P., Styles, L., Vichinsky, E.P., Swerdlow, P., Davis, G.A., Desimone, P.A., Stocker, J.W., 2006. Dose-escalation study of ICA-17043 in patients with sickle cell disease. Pharmacotherapy 26, 1557–1564. https://doi.org/10.1592/phco.26.11.1557

Ataga, K.I., Reid, M., Ballas, S.K., Yasin, Z., Bigelow, C., James, L.S., Smith, W.R., Galacteros, F., Kutlar, A., Hull, J.H., Stocker, J.W., 2011. Improvements in haemolysis and indicators of erythrocyte survival do not correlate with acute vaso-occlusive crises in patients with sickle cell disease: a phase III randomized, placebo-controlled, double-blind study of the Gardos channel blocker senicapo. Br. J. Haematol. 153, 92–104. https://doi.org/10.1111/j.1365-2141.2010.08520.x

Ataga, K.I., Smith, W.R., De Castro, L.M., Swerdlow, P., Saunthararajah, Y., Castro, O., Vichinsky, E., Kutlar, A., Orringer, E.P., Rigdon, G.C., Stocker, J.W., 2008. Efficacy and safety of the Gardos channel blocker, senicapoc (ICA-17043), in patients with sickle cell anemia. Blood 111, 3991–3997. https://doi.org/10.1182/blood-2007-08-110098

Awojoodu, A.O., Keegan, P.M., Lane, A.R., Zhang, Y., Lynch, K.R., Platt, M.O., Botchwey, E.A., 2014. Regular Article Acid sphingomyelinase is activated in sickle cell erythrocytes and contributes to in fl ammatory microparticle generation in SCD 124, 1941–1950. https://doi.org/10.1182/blood-2014-01-543652.The

Aygun, B., Mortier, N.A., Smeltzer, M.P., Hankins, J.S., Ware, R.E., 2011. Glomerular hyperfiltration and albuminuria in children with sickle cell anemia. Pediatr. Nephrol. 26, 1285–1290. https://doi.org/10.1007/s00467-011-1857-2

Bae, C., Gnanasambandam, R., Nicolai, C., Sachs, F., Gottlieb, P.A., 2013. Xerocytosis is caused by mutations that alter the kinetics of the mechanosensitive channel PIEZO1. Proc. Natl. Acad. Sci. 110, E1162 LP-E1168.

Bae, C., Sachs, F., Gottlieb, P.A., 2015. Protonation of the human PIEZO1 ion channel stabilizes inactivation. J. Biol. Chem. 290, 5167–5173. https://doi.org/10.1074/jbc.M114.604033

Bae Chilman., Frederick Sachs, and P.A.G., 2011. The mechanosensitive ion channel PIEZO1 is inhibited by the peptide GsMTx-4 50, 6295–6300. https://doi.org/10.1021/bi200770q.The

Ballas, S.K., Gupta, K., Adams-Graves, P., 2012. Sickle cell pain: a critical reappraisal. Blood 120, 3647–3656. https://doi.org/10.1182/blood-2012-04-383430

Barber, L.A., Palascak, M.B., Joiner, C.H., Franco, R.S., 2009. Aminophospholipid translocase and phospholipid scramblase activities in sickle erythrocyte subpopulations. Br. J. Haematol. 146, 447–455. https://doi.org/10.1111/j.1365-2141.2009.07760.x

Bardakdjian-Michau, J., Bahuau, M., Hurtrel, D., Godart, C., Riou, J., Mathis, M., Goossens, M., Badens, C., Ducrocq, R., Elion, J., Perini, J.M., 2009. Neonatal screening for sickle cell disease in France. J. Clin. Pathol. 62, 31–33. https://doi.org/10.1136/jcp.2008.058867

Basak, A., Hancarova, M., Ulirsch, J.C., Balci, T.B., Trkova, M., Pelisek, M., Vlckova, M., Muzikova, K., Cermak, J., Trka, J., Dyment, D.A., Orkin, S.H., Daly, M.J., Sedlacek, Z., Sankaran, V.G., 2015. BCL11A deletions result in fetal hemoglobin persistence and neurodevelopmental alterations. J. Clin. Invest. 125, 2363–2368. https://doi.org/10.1172/JCI81163

Batchvarova, M., Shan, S., Zennadi, R., Lindgren, M., Leitgeb, A., Tamsen, P.S., Telen, M.J., 2013. Sevuparin Reduces Adhesion Of Both Sickle Red Cells and Leukocytes To Endothelial Cells In Vitro and Inhibits Vaso-Occlusion In Vivo. Blood 122, 182. https://doi.org/10.1182/blood.V122.21.182.182

Belini Junior, E., da Silva, D.G.H., Torres, L. de S., de Almeida, E.A., Cancado, R.D., Chiattone, C., Bonini-Domingos, C.R., 2012. Oxidative stress and antioxidant capacity in sickle cell anaemia patients receiving different treatments and medications for different periods of time. Ann. Hematol. 91, 479–489. https://doi.org/10.1007/s00277-011-1340-y

Belloni-Olivi, L., Annadata, M., Goldstein, G.W., Bressler, J.P., 1996. Phosphorylation of membrane proteins in erythrocytes treated with lead. Biochem. J. 315 (Pt 2), 401–406. https://doi.org/10.1042/bj3150401

Bennekou, P., de Franceschi, L., Pedersen, O., Lian, L., Asakura, T., Evans, G., Brugnara, C., Christophersen, P., 2001. Treatment with NS3623, a novel Cl-conductance blocker, ameliorates erythrocyte dehydration in transgenic SAD mice: a possible new

therapeutic approach for sickle cell disease. Blood 97, 1451–1457. https://doi.org/10.1182/blood.v97.5.1451

Bennekou, P., Pedersen, O., Moller, A., Christophersen, P., 2000. Volume control in sickle cells is facilitated by the novel anion conductance inhibitor NS1652. Blood 95, 1842–1848.

Bhagat, S., Patra, P.K., Thakur, A.S., 2013. Fetal Haemoglobin and β-globin Gene Cluster Haplotypes among Sickle Cell Patients in Chhattisgarh. J. Clin. Diagn. Res. 7, 269–272. https://doi.org/10.7860/JCDR/2013/4381.2744

Bitbol, M., Fellmann, P., Zachowski, A., Devaux, P.F., 1987. Ion regulation of phosphatidylserine and phosphatidylethanolamine outside-inside translocation in human erythrocytes. Biochim. Biophys. Acta 904, 268–282. https://doi.org/10.1016/0005-2736(87)90376-2

Bize, I., Guvenc, B., Robb, A., Buchbinder, G., Brugnara, C., 1999. Serine/threonine protein phosphatases and regulation of K-Cl cotransport in human erythrocytes. Am. J. Physiol. 277, C926-36.

Bize, I., Taher, S., Brugnara, C., 2003. Regulation of K-Cl cotransport during reticulocyte maturation and erythrocyte aging in normal and sickle erythrocytes. Am. J. Physiol. Physiol. 285, C31–C38. https://doi.org/10.1152/ajpcell.00447.2002

Bolsover, S.R., Gomez-Fernandez, J.C., Corbalan-Garcia, S., 2003. Role of the Ca2+/phosphatidylserine binding region of the C2 domain in the translocation of protein kinase Calpha to the plasma membrane. J. Biol. Chem. 278, 10282–10290. https://doi.org/10.1074/jbc.M212145200

Borgese, F., Motais, R., Garcia-Romeu, F., 1991. Regulation of Cl-dependent K transport by oxy-deoxyhemoglobin transitions in trout red cells. Biochim. Biophys. Acta 1066, 252–256.

Botello-Smith, W.M., Jiang, W., Lacroix, J.J., Luo, Y., 2019. A mechanism for the activation of the mechanosensitive Piezo1 channel by the small molecule Yoda1. Nat. Commun. https://doi.org/10.1038/s41467-019-12501-1

Bouyer, G., Cueff, A., Egee, S., Kmiecik, J., Maksimova, Y., Glogowska, E., Gallagher, P.G., Thomas, S.L.Y., 2011. Erythrocyte peripheral type benzodiazepine receptor/voltage-dependent anion channels are upregulated by Plasmodium falciparum. Blood 118, 2305–2312. https://doi.org/10.1182/blood-2011-01-329300

Brawley, O.W., Cornelius, L.J., Edwards, L.R., Gamble, V.N., Green, B.L., Inturrisi, C., James, A.H., Laraque, D., Mendez, M., Montoya, C.J., Pollock, B.H., Robinson, L., Scholnik, A.P., Schori, M., 2008. National Institutes of Health Consensus Development Conference statement: hydroxyurea treatment for sickle cell disease. Ann. Intern. Med. 148, 932–938.

Brendel, C., Guda, S., Renella, R., Bauer, D.E., Canver, M.C., Kim, Y.-J., Heeney, M.M., Klatt, D., Fogel, J., Milsom, M.D., Orkin, S.H., Gregory, R.I., Williams, D.A., 2016. Lineage-specific BCL11A knockdown circumvents toxicities and reverses sickle phenotype. J. Clin. Invest. 126, 3868–3878. https://doi.org/10.1172/JCI87885

Brown, A.M., Ellory, J.C., Young, J.D., Lew, V.L., 1978. A calcium-activated potassium channel present in foetal red cells of the sheep but absent from reticulocytes and mature red cells. Biochim. Biophys. Acta 511, 163–175. https://doi.org/10.1016/0005-2736(78)90311-5

Browning, J.A., Robinson, H.C., Ellory, J.C., Gibson, J.S., 2007a. Deoxygenation-induced non-electrolyte pathway in red cells from sickle cell patients. Cell. Physiol. Biochem. Int. J. Exp. Cell. Physiol. Biochem. Pharmacol. 19, 165–174. https://doi.org/10.1159/000099204

Browning, J.A., Staines, H.M., Robinson, H.C., Powell, T., Ellory, J.C., Gibson, J.S., 2007b. The effect of deoxygenation on whole-cell conductance of red blood cells from healthy individuals and patients with sickle cell disease. Blood 109, 2622–2629. https://doi.org/10.1182/blood-2006-03-001404

Brugnara, C., de Franceschi, L., Alper, S.L., 1993. Inhibition of Ca(2+)-dependent K+ transport and cell dehydration in sickle erythrocytes by clotrimazole and other imidazole derivatives. J. Clin. Invest. 92, 520–526. https://doi.org/10.1172/JCI116597

Brugnara, C., Gee, B., Armsby, C.C., Kurth, S., Sakamoto, M., Rifai, N., Alper, S.L., Platt, O.S., 1996. Therapy with oral clotrimazole induces inhibition of the Gardos channel and reduction of erythrocyte dehydration in patients with sickle cell disease. J. Clin. Invest. 97, 1227–1234.

Cahalan, S.M., Lukacs, V., Ranade, S.S., Chien, S., Bandell, M., Patapoutian, A., 2015. Piezo1 links mechanical forces to red blood cell volume 1–12. https://doi.org/10.7554/eLife.07370

Caulier, A., Jankovsky, N., Demont, Y., Ouled-Haddou, H., Demagny, J., Guitton, C., Merlusca, L., Lebon, D., Vong, P., Aubry, A., Lahary, A., Rose, C., Gréaume, S., Cardon, E., Platon, J., Ouadid-Ahidouch, H., Rochette, J., Marolleau, J.-P., Picard, V., Garçon, L., 2020. PIEZO1 activation delays erythroid differentiation of normal and hereditary xerocytosis-derived human progenitor cells. Haematologica 105, 610–622. https://doi.org/10.3324/haematol.2019.218503

Cerami, A., Manning, J.M., 1971. Potassium cyanate as an inhibitor of the sickling of erythrocytes in vitro. Proc. Natl. Acad. Sci. U. S. A. 68, 1180—1183. https://doi.org/10.1073/pnas.68.6.1180

Chang, J., Patton, J.T., Sarkar, A., Ernst, B., Magnani, J.L., Frenette, P.S., 2010. GMI-1070, a novel pan-selectin antagonist, reverses acute vascular occlusions in sickle cell mice. Blood 116, 1779–1786. https://doi.org/10.1182/blood-2009-12-260513

Charache, S., Dover, G.J., Moore, R.D., Eckert, S., Ballas, S.K., Koshy, M., Milner, P.F., Orringer, E.P., Phillips, G.J., Platt, O.S., 1992. Hydroxyurea: effects on hemoglobin F production in patients with sickle cell anemia. Blood 79, 2555–2565.

Cheung, A.T.W., Chan, M.S., Ramanujam, S., Rangaswami, A., Curl, K., Franklin, P., Wun, T., 2004. Effects of poloxamer 188 treatment on sickle cell vaso-occlusive crisis: computer-assisted intravital microscopy study. J. Investig. Med. 52, 402–406. https://doi.org/10.1136/jim-52-06-35

Chong, Z.Z., Kang, J.-Q., Maiese, K., 2004. Essential cellular regulatory elements of oxidative stress in early and late phases of apoptosis in the central nervous system. Antioxid. Redox Signal. 6, 277–287. https://doi.org/10.1089/152308604322899341

Cinar, E., Zhou, S., DeCourcey, J., Wang, Y., Waugh, R.E., Wan, J., 2015. Piezo1 regulates mechanotransductive release of ATP from human RBCs. Proc. Natl. Acad. Sci. 112, 11783 LP – 11788.

Clark, M.R., Rossi, M.E., 1990. Permeability characteristics of deoxygenated sickle cells. Blood 76, 2139–2145. https://doi.org/10.1182/blood.V76.10.2139.2139

Coen, P.M., Hames, K.C., Leachman, E.M., DeLany, J.P., Ritov, V.B., Menshikova, E. V, Dubé, J.J., Stefanovic-Racic, M., Toledo, F.G.S., Goodpaster, B.H., 2013. Reduced skeletal muscle oxidative capacity and elevated ceramide but not diacylglycerol content in severe obesity. Obesity (Silver Spring). 21, 2362–2371. https://doi.org/10.1002/oby.20381

Corbalán-García, S., García-García, J., Rodríguez-Alfaro, J.A., Gómez-Fernández, J.C., 2003. A new phosphatidylinositol 4,5-bisphosphate-binding site located in the C2 domain of protein kinase Calpha. J. Biol. Chem. 278, 4972–4980. https://doi.org/10.1074/jbc.M209385200

Corbalán-García, S., Rodríguez-Alfaro, J.A., Gómez-Fernández, J.C., 1999. Determination of the calcium-binding sites of the C2 domain of protein kinase Calpha that are critical for its translocation to the plasma membrane. Biochem. J. 337 (Pt 3), 513–521.

Coste, B., Houge, G., Murray, M.F., Stitziel, N., Bandell, M., Giovanni, M.A., Philippakis, A., Hoischen, A., Riemer, G., Steen, U., Steen, V.M., Mathur, J., Cox, J., Lebo, M., Rehm, H., Weiss, S.T., Wood, J.N., Maas, R.L., Sunyaev, S.R., Patapoutian, A., 2013. Gain-of-function mutations in the mechanically activated ion channel PIEZO2 cause a subtype of Distal Arthrogryposis. Proc. Natl. Acad. Sci. U. S. A. 110, 4667–4672. https://doi.org/10.1073/pnas.1221400110

Crable, S.C., Hammond, S.M., Papes, R., Rettig, R.K., Zhou, G.-P., Gallagher, P.G., Joiner, C.H., Anderson, K.P., 2005. Multiple isoforms of the KC1 cotransporter are expressed in sickle and normal erythroid cells. Exp. Hematol. 33, 624–631. https://doi.org/10.1016/j.exphem.2005.02.006

Cytlak, U.M., Hannemann, A., Rees, D.C., Gibson, J.S., 2013. Identification of the Ca(2+) entry pathway involved in deoxygenation-induced phosphatidylserine exposure in red blood cells from patients with sickle cell disease. Pflugers Arch. 465, 1651–1660. https://doi.org/10.1007/s00424-013-1308-y

Czarny, M., Liu, J., Oh, P., Schnitzer, J.E., 2003. Transient Mechanoactivation of Neutral Sphingomyelinase in Caveolae to Generate Ceramide *. J. Biol. Chem. 278, 4424–4430. https://doi.org/10.1074/jbc.M210375200

Czarny, M., Schnitzer, J.E., 2004. Neutral sphingomyelinase inhibitor scyphostatin prevents and ceramide mimics mechanotransduction in vascular endothelium 92121, 1344–1352.

da Silva, D.G.H., Ricci, O.J., de Almeida, E.A., Bonini-Domingos, C.R., 2015. Potential

utility of melatonin as an antioxidant therapy in the management of sickle cell anemia. J. Pineal Res. 58, 178–188. https://doi.org/10.1111/jpi.12204

Danielczok, J.G., Terriac, E., Hertz, L., Petkova-Kirova, P., Lautenschläger, F., Laschke, M.W., Kaestner, L., 2017. Red Blood Cell Passage of Small Capillaries Is Associated with Transient Ca2+-mediated Adaptations . Front. Physiol. .

Dasgupta, S.K., Abdel-Monem, H., Niravath, P., Le, A., Bellera, R. V, Langlois, K., Nagata, S., Rumbaut, R.E., Thiagarajan, P., 2009. Lactadherin and clearance of platelet-derived microvesicles. Blood 113, 1332–1339. https://doi.org/10.1182/blood-2008-07-167148

Dasgupta, S.K., Guchhait, P., Thiagarajan, P., 2006. Lactadherin binding and phosphatidylserine expression on cell surface-comparison with annexin A5. Transl. Res. 148, 19–25. https://doi.org/10.1016/j.lab.2006.03.006

Day, T.G., Drasar, E.R., Fulford, T., Sharpe, C.C., Thein, S.L., 2012. Association between hemolysis and albuminuria in adults with sickle cell anemia. Haematologica 97, 201–205. https://doi.org/10.3324/haematol.2011.050336

De Castro, L.M., Zennadi, R., Jonassaint, J.C., Batchvarova, M., Telen, M.J., 2012. Effect of Propranolol as Antiadhesive Therapy in Sickle Cell Disease. Clin. Transl. Sci. 5, 437–444. https://doi.org/10.1111/cts.12005

De Franceschi, L., Bachir, D., Galacteros, F., Tchernia, G., Cynober, T., Alper, S., Platt, O., Beuzard, Y., Brugnara, C., 1997. Oral magnesium supplements reduce erythrocyte dehydration in patients with sickle cell disease. J. Clin. Invest. 100, 1847–1852.

De Franceschi, L., Bachir, D., Galacteros, F., Tchernia, G., Cynober, T., Neuberg, D., Beuzard, Y., Brugnara, C., 2000. Oral magnesium pidolate: effects of long-term administration in patients with sickle cell disease. Br. J. Haematol. 108, 284–289. https://doi.org/10.1046/j.1365-2141.2000.01861.x

De Franceschi, L., Beuzard, Y., Jouault, H., Brugnara, C., 1996. Modulation of erythrocyte potassium chloride cotransport, potassium content, and density by dietary magnesium intake in transgenic SAD mouse. Blood 88, 2738–2744.

De Franceschi, L., Saadane, N., Trudel, M., Alper, S.L., Brugnara, C., Beuzard, Y., 1994. Treatment with oral clotrimazole blocks Ca(2+)-activated K+ transport and reverses erythrocyte dehydration in transgenic SAD mice. A model for therapy of sickle cell disease. J. Clin. Invest. 93, 1670–1676. https://doi.org/10.1172/JCI117149

de Jong, K., Larkin, S.K., Styles, L.A., Bookchin, R.M., Kuypers, F.A., 2001. Characterization of the phosphatidylserine-exposing subpopulation of sickle cells. Blood 98, 860–867. https://doi.org/10.1182/blood.v98.3.860

DeFronzo, R.A., Taufield, P.A., Black, H., McPhedran, P., Cooke, C.R., 1979. Impaired renal tubular potassium secretion in sickle cell disease. Ann. Intern. Med. 90, 310–316. https://doi.org/10.7326/0003-4819-90-3-310

Dekkers, D.W.C., Comfurius, P., Bevers, E.M., Zwaal, R.F.A., 2002. Comparison between Ca2+-induced scrambling of various fluorescently labelled lipid analogues in red

blood cells. Biochem. J. 362, 741–747. https://doi.org/10.1042/0264-6021:3620741

Dela Paz, N.G., Frangos, J.A., 2018. Yoda1-induced phosphorylation of Akt and ERK1/2 does not require Piezo1 activation. Biochem. Biophys. Res. Commun. 497, 220–225. https://doi.org/10.1016/j.bbrc.2018.02.058

Desai, B.N., Myers, B.R., Schreiber, S.L., 2002. FKBP12-rapamycin-associated protein associates with mitochondria and senses osmotic stress via mitochondrial dysfunction. Proc. Natl. Acad. Sci. U. S. A. 99, 4319–4324. https://doi.org/10.1073/pnas.261702698

Desai, D., Dhanani, H., 2003. Sickle Cell Disease : History And Origin 4–7.

Dinkla, S., Wessels, K., Verdurmen, W.P.R., Tomelleri, C., Cluitmans, J.C.A., Fransen, J., Fuchs, B., Schiller, J., Joosten, I., Brock, R., Bosman, G., 2012. Functional consequences of sphingomyelinase-induced changes in erythrocyte membrane structure. https://doi.org/10.1038/cddis.2012.143

Domijan, A.-M., Kovac, S., Abramov, A.Y., 2014. Lipid peroxidation is essential for phospholipase C activity and the inositol-trisphosphate-related Ca<sup>2+</sup> signal. J. Cell Sci. 127, 21 LP – 26. https://doi.org/10.1242/jcs.138370

Dormandy, E., James, J., Inusa, B., Rees, D., 2017. How many people have sickle cell disease in the UK ? 40, 291–295. https://doi.org/10.1093/pubmed/fdx172

Dufu, K., Patel, M., Oksenberg, D., Cabrales, P., 2018. GBT440 improves red blood cell deformability and reduces viscosity of sickle cell blood under deoxygenated conditions. Clin. Hemorheol. Microcirc. 70, 95–105. https://doi.org/10.3233/CH-170340

Duranton, C., Huber, S.M., Lang, F., 2002. Oxidation induces a Cl _ -dependent cation conductance in human red blood cells 847–855. https://doi.org/10.1013/jphysiol.2001.013040

Eaton, W.A., Hofrichter, J., 1987. Hemoglobin S gelation and sickle cell disease. Blood 70, 1245–1266.

El-Hazmi, M.A.F., Al-Hazmi, A.M., Warsy, A.S., 2011. Sickle cell disease in Middle East Arab countries. Indian J. Med. Res. 134, 597–610. https://doi.org/10.4103/0971-5916.90984

Ellory, J.C., Robinson, H.C., Browning, J.A., Stewart, G.W., Gehl, K.A., Gibson, J.S., 2007. Abnormal permeability pathways in human red blood cells. Blood Cells. Mol. Dis. 39, 1–6. https://doi.org/10.1016/j.bcmd.2007.02.011

Ellory, J.C., Sequeira, R., Constantine, A., Wilkins, R.J., Gibson, J.S., 2008. Non-electrolyte permeability of deoxygenated sickle cells compared. Blood Cells, Mol. Dis. 41, 44–49. https://doi.org/https://doi.org/10.1016/j.bcmd.2008.03.003

Ellory, J.C., Stewart, G.W., 1982. The human erythrocyte Cl-dependent Na-K cotransport system as a possible model for studying the action of loop diuretics. Br. J. Pharmacol. 75, 183–188. https://doi.org/10.1111/j.1476-5381.1982.tb08771.x

Esrick, E.B., Manis, J.P., Daley, H., Baricordi, C., Trebeden-Negre, H., Pierciey, F.J., Armant, M., Nikiforow, S., Heeney, M.M., London, W.B., Biasco, L., Asmal, M., Williams, D.A., Biffi, A., 2018. Successful hematopoietic stem cell mobilization and apheresis collection using plerixafor alone in sickle cell patients. Blood Adv. 2, 2505–2512. https://doi.org/10.1182/bloodadvances.2018016725

Fabisiak, J.P., Tyurin, V.A., Tyurina, Y.Y., Sedlov, A., Lazo, J.S., Kagan, V.E., 2000. Nitric oxide dissociates lipid oxidation from apoptosis and phosphatidylserine externalization during oxidative stress. Biochemistry 39, 127–138. https://doi.org/10.1021/bi9912544

Falk, R.J., Scheinman, J., Phillips, G., Orringer, E., Johnson, A., Jennette, J.C., 1992. Prevalence and pathologic features of sickle cell nephropathy and response to inhibition of angiotensin-converting enzyme. N. Engl. J. Med. 326, 910–915. https://doi.org/10.1056/NEJM199204023261402

Fathallah, H., Sauvage, M., Romero, J.R., Canessa, M., Giraud, F., 1997. Effects of PKC alpha activation on Ca2+ pump and K(Ca) channel in deoxygenated sickle cells. Am. J. Physiol. 273, C1206-14. https://doi.org/10.1152/ajpcell.1997.273.4.C1206

Faulkner, M., Turner, E.A., Deus, J., Phillips, K., Weaver, C., Taiwo, O., Omitowoju, O., 1995. Severe anemia: a risk factor for glomerular injury in sickle cell disease. J. Natl. Med. Assoc. 87, 209–213.

Fermo, E., Bogdanova, A., Petkova-Kirova, P., Zaninoni, A., Marcello, A.P., Makhro, A., Hänggi, P., Hertz, L., Danielczok, J., Vercellati, C., Mirra, N., Zanella, A., Cortelezzi, A., Barcellini, W., Kaestner, L., Bianchi, P., 2017. 'Gardos Channelopathy': a variant of hereditary Stomatocytosis with complex molecular regulation. Sci. Rep. 7, 1744. https://doi.org/10.1038/s41598-017-01591-w

Ferrone, F.A., 2004. Polymerization and sickle cell disease: a molecular view. Microcirculation 11, 115–128.

Foller, M., Kasinathan, R.S., Koka, S., Lang, C., Shumilina, E., Birnbaumer, L., Lang, F., Huber, S.M., 2008. TRPC6 contributes to the Ca(2+) leak of human erythrocytes. Cell. Physiol. Biochem. 21, 183–192. https://doi.org/10.1159/000113760

Fotiou, E., Martin-Almedina, S., Simpson, M.A., Lin, S., Gordon, K., Brice, G., Atton, G., Jeffery, I., Rees, D.C., Mignot, C., Vogt, J., Homfray, T., Snyder, M.P., Rockson, S.G., Jeffery, S., Mortimer, P.S., Mansour, S., Ostergaard, P., 2015. Novel mutations in PIEZO1 cause an autosomal recessive generalized lymphatic dysplasia with non-immune hydrops fetalis. Nat. Commun. 6, 8085. https://doi.org/10.1038/ncomms9085

Frenette, P.S., Atweh, G.F., 2007. Sickle cell disease: old discoveries, new concepts, and future promise. J. Clin. Invest. 117, 850–858. https://doi.org/10.1172/JCI30920

Fucho, R., Casals, N., Serra, D., Herrero, L., 2017. Ceramides and mitochondrial fatty acid oxidation in obesity. FASEB J. Off. Publ. Fed. Am. Soc. Exp. Biol. 31, 1263–1272. https://doi.org/10.1096/fj.201601156R

Galadari, S., Rahman, A., Pallichankandy, S., Galadari, A., Thayyullathil, F., 2013. Role of ceramide in diabetes mellitus: evidence and mechanisms. Lipids Health Dis. 12, 98. https://doi.org/10.1186/1476-511X-12-98

Gamba, G., 2005. Molecular physiology and pathophysiology of electroneutral cation-chloride cotransporters. Physiol. Rev. 85, 423–493. https://doi.org/10.1152/physrev.00011.2004

Garda-sancho, J., 1985. BBA Report Pyruvate prevents the A T P depletion caused by formaldehyde or calcium-chelator esters in the human red cell Formaldehyde released during hydrolysis of calcium-chelator esters incorporated into cells blocks glycolysis in the human erythrocyte (Tiffert , T ., Garcia-Sancho , J . and Lew , V . L . (1984) Biochim . Biophys . Acta 773 , 143-156). This blockade is due to the inhibition of glyceraidehyde-3-phosphate dehydrogenase by NAD + depletion caused by enzymatic oxidation of formaldehyde coupled to NADH production . The addition of pyruvate to the incubation medium prevents or reverts ATP depletion . 813, 148–150.

Gardos, G., 1958. The function of calcium in the potassium permeability of human erythrocytes. Biochim. Biophys. Acta 30, 653–654.

Gardos, G., 1956. The permeability of human erythrocytes to potassium. Acta Physiol. Acad. Sci. Hung. 10, 185–189.

Gaston, M.H., Verter, J.I., Woods, G., Pegelow, C., Kelleher, J., Presbury, G., Zarkowsky, H., Vichinsky, E., Iyer, R., Lobel, J.S., 1986. Prophylaxis with oral penicillin in children with sickle cell anemia. A randomized trial. N. Engl. J. Med. 314, 1593–1599. https://doi.org/10.1056/NEJM198606193142501

Gatidis, S., Borst, O., Föller, M., Lang, F., 2010. Effect of osmotic shock and urea on phosphatidylserine scrambling in thrombocyte cell membranes. https://doi.org/10.1152/ajpcell.00477.2009.

Geilen, C.C., Wieder, T., Orfanos, C.E., 1997. Ceramide signalling: regulatory role in cell proliferation, differentiation and apoptosis in human epidermis. Arch. Dermatol. Res. 289, 559–566. https://doi.org/10.1007/s004030050240

Genever, P.G., Wilkinson, D.J., Patton, A.J., Peet, N.M., Hong, Y., Mathur, A., Erusalimsky, J.D., Skerry, T.M., 1999. Expression of a functional N-methyl-D-aspartate-type glutamate receptor by bone marrow megakaryocytes. Blood 93, 2876–2883.

Gibson, J.S., Cossins, A.R., Ellory, J.C., 2000. OXYGEN-SENSITIVE MEMBRANE TRANSPORTERS IN VERTEBRATE RED CELLS 1407, 1395–1407.

Gibson, J.S., Ellory, J.C., 2002. Membrane transport in sickle cell disease. Blood Cells. Mol. Dis. 28, 303–314.

Gibson, J.S., Godart, H., Ellory, J.C., Staines, H., Honess, N.A., Cossins, A.R., 1994. Modulation of K(+)-Cl- cotransport in equine red blood cells. Exp. Physiol. 79, 997–1009. https://doi.org/https://doi.org/10.1113/expphysiol.1994.sp003824

Gibson, J.S., Khan, A., Speake, P.F., Ellory, J.C., 2001. O2 dependence of K+ transport in sickle cells: the effect of different cell populations and the substituted benzaldehyde 12C79. FASEB J. Off. Publ. Fed. Am. Soc. Exp. Biol. 15, 823–832. https://doi.org/10.1096/fj.00-0177com

Gibson, J.S., Speake, P.F., Ellory, J.C., 2004. Differential oxygen sensitivity of the K+-

Cl− cotransporter in normal and sickle human red blood cells. J. Physiol. 511, 225–234. https://doi.org/10.1111/j.1469-7793.1998.225bi.x

Gibson, J.S., Speake, P.F., Ellory, J.C., 1998. Differential oxygen sensitivity of the K(+)-Cl(−) cotransporter in normal and sickle human red blood cells. J. Physiol. 511, 225–234. https://doi.org/10.1111/j.1469-7793.1998.225bi.x

Gladwin, M.T., Ofori-Acquah, S.F., 2014. Erythroid DAMPs drive inflammation in SCD. Blood 123, 3689–3690. https://doi.org/10.1182/blood-2014-03-563874

Glogowska, E., Dyrda, A., Cueff, A., Bouyer, G., Egée, S., Bennekou, P., Thomas, S.L.Y., 2010. Anion conductance of the human red cell is carried by a maxi-anion channel. Blood Cells. Mol. Dis. 44, 243–251. https://doi.org/10.1016/j.bcmd.2010.02.014

Glogowska, E., Lezon-Geyda, K., Maksimova, Y., Schulz, V.P., Gallagher, P.G., 2015. Mutations in the Gardos channel (KCNN4) are associated with hereditary xerocytosis. Blood 126, 1281–1284. https://doi.org/10.1182/blood-2015-07-657957

Glogowska, E., Schneider, E.R., Maksimova, Y., Schulz, V.P., Lezon-Geyda, K., Wu, J., Radhakrishnan, K., Keel, S.B., Mahoney, D., Freidmann, A.M., Altura, R.A., Gracheva, E.O., Bagriantsev, S.N., Kalfa, T.A., Gallagher, P.G., 2017. Novel mechanisms of PIEZO1 dysfunction in hereditary xerocytosis. Blood 130, 1845–1856. https://doi.org/10.1182/blood-2017-05-786004

Gluckman, E., Cappelli, B., Bernaudin, F., Labopin, M., Volt, F., Carreras, J., Pinto Simoes, B., Ferster, A., Dupont, S., de la Fuente, J., Dalle, J.-H., Zecca, M., Walters, M.C., Krishnamurti, L., Bhatia, M., Leung, K., Yanik, G., Kurtzberg, J., Dhedin, N., Kuentz, M., Michel, G., Apperley, J., Lutz, P., Neven, B., Bertrand, Y., Vannier, J.P., Ayas, M., Cavazzana, M., Matthes-Martin, S., Rocha, V., Elayoubi, H., Kenzey, C., Bader, P., Locatelli, F., Ruggeri, A., Eapen, M., 2017. Sickle cell disease: an international survey of results of HLA-identical sibling hematopoietic stem cell transplantation. Blood 129, 1548–1556. https://doi.org/10.1182/blood-2016-10-745711

Goñi, F.M., Alonso, A., 2002. Sphingomyelinases: enzymology and membrane activity. FEBS Lett. 531, 38–46. https://doi.org/10.1016/s0014-5793(02)03482-8

Goossens, J.P., Van Eps, L.W.S., Schouten, H., Giterson, A.L., 1972. Incomplete renal tubular acidosis in sickle cell disease. Clin. Chim. Acta 41, 149–156. https://doi.org/https://doi.org/10.1016/0009-8981(72)90505-0

Gordeuk, V.R., Sachdev, V., Taylor, J.G., Gladwin, M.T., Kato, G., Castro, O.L., 2008. Relative systemic hypertension in patients with sickle cell disease is associated with risk of pulmonary hypertension and renal insufficiency. Am. J. Hematol. 83, 15–18. https://doi.org/10.1002/ajh.21016

Gragert, L., Eapen, M., Williams, E., Freeman, J., Spellman, S., Baitty, R., Hartzman, R., Rizzo, J.D., Horowitz, M., Confer, D., Maiers, M., 2014. HLA match likelihoods for hematopoietic stem-cell grafts in the U.S. registry. N. Engl. J. Med. 371, 339–348. https://doi.org/10.1056/NEJMsa1311707

Graybill, C., Wee, B., Atwood, S.X., Prehoda, K.E., 2012. Partitioning-defective protein 6 (Par-6) activates atypical protein kinase C (aPKC) by pseudosubstrate displacement.

J. Biol. Chem. 287, 21003–21011. https://doi.org/10.1074/jbc.M112.360495

Grygorczyk, R., 1987. Temperature dependence of Ca2+-activated K+ currents in the membrane of human erythrocytes. Biochim. Biophys. Acta 902, 159–168. https://doi.org/10.1016/0005-2736(87)90291-4

Gudipaty, S.A., Lindblom, J., Loftus, P.D., Redd, M.J., Edes, K., Davey, C.F., Krishnegowda, V., Rosenblatt, J., 2017. Mechanical stretch triggers rapid epithelial cell division through Piezo1. Nature 543, 118–121. https://doi.org/10.1038/nature21407

Gupta, K., Zamanian, M., Bae, C., Milescu, M., Krepkiy, D., Tilley, D.C., Sack, J.T., Yarov-Yarovoy, V., Kim, J. Il, Swartz, K.J., 2015. Tarantula toxins use common surfaces for interacting with Kv and ASIC ion channels. Elife 4, e06774. https://doi.org/10.7554/eLife.06774

Haas, M., 1989. Properties and diversity of (Na-K-Cl) cotransporters. Annu. Rev. Physiol. 51, 443–457. https://doi.org/10.1146/annurev.ph.51.030189.002303

Halperin, J.A., Brugnara, C., Nicholson-Weller, A., 1989. Ca2+-activated K+ efflux limits complement-mediated lysis of human erythrocytes. J. Clin. Invest. 83, 1466–1471. https://doi.org/10.1172/JCI114039

Hamideh, D., Alvarez, O., 2013. Sickle cell disease related mortality in the United States (1999-2009). Pediatr. Blood Cancer 60, 1482–1486. https://doi.org/10.1002/pbc.24557

Hamideh, D., Raj, V., Harrington, T., Li, H., Margolles, E., Amole, F., Garcia-Buitrago, M., Ruiz, P., Zilleruelo, G., Alvarez, O., 2014. Albuminuria correlates with hemolysis and NAG and KIM-1 in patients with sickle cell anemia. Pediatr. Nephrol. 29, 1997–2003. https://doi.org/10.1007/s00467-014-2821-8

Hamill, O.P., Marty, A., Neher, E., Sakmann, B., Sigworth, F.J., 1981. Improved patch-clamp techniques for high-resolution current recording from cells and cell-free membrane patches. Pflugers Arch. 391, 85–100. https://doi.org/10.1007/BF00656997

Hanada, K., Mitamura, T., Fukasawa, M., Magistrado, P.A., Horii, T., Nishijima, M., 2000. Plasmodium falciparum 677, 671–677.

Hanchard, N., Elzein, A., Trafford, C., Rockett, K., Pinder, M., Jallow, M., Harding, R., Kwiatkowski, D., McKenzie, C., 2007. Classical sickle beta-globin haplotypes exhibit a high degree of long-range haplotype similarity in African and Afro-Caribbean populations. BMC Genet. 8, 52. https://doi.org/10.1186/1471-2156-8-52

Hankins, J.S., Aygun, B., Nottage, K., Thornburg, C., Smeltzer, M.P., Ware, R.E., Wang, W.C., 2014. From infancy to adolescence: fifteen years of continuous treatment with hydroxyurea in sickle cell anemia. Medicine (Baltimore). 93, e215. https://doi.org/10.1097/MD.0000000000000215

Hankins, J.S., Wynn, L.W., Brugnara, C., Hillery, C.A., Li, C.-S., Wang, W.C., 2008. Phase I study of magnesium pidolate in combination with hydroxycarbamide for children with sickle cell anaemia. Br. J. Haematol. 140, 80–85. https://doi.org/10.1111/j.1365-2141.2007.06884.x

Hannemann, A., Cytlak, U.M., Rees, D.C., Tewari, S., Gibson, J.S., 2014. Effects of 5-hydroxymethyl-2-furfural on the volume and membrane permeability of red blood cells from patients with sickle cell disease. J. Physiol. 592, 4039–4049. https://doi.org/10.1113/jphysiol.2014.277681

Hannemann, A., Rees, D.C., Brewin, J.N., Noe, A., Low, B., Gibson, J.S., 2018. Oxidative stress and phosphatidylserine exposure in red cells from patients with sickle cell anaemia. Br. J. Haematol. 182, 567–578. https://doi.org/10.1111/bjh.15441

Hannemann, A., Weiss, E., Rees, D.C., Dalibalta, S., Ellory, J.C., Gibson, J.S., 2011. The properties of red blood cells from patients heterozygous for HbS and HbC (HbSC Genotype). Anemia 2011. https://doi.org/10.1155/2011/248527

Hannun, Y.A., 1996. Functions of ceramide in coordinating cellular responses to stress. Science 274, 1855–1859. https://doi.org/10.1126/science.274.5294.1855

Hebbel, R.P., Key, N.S., 2016. Microparticles in sickle cell anaemia: promise and pitfalls. Br. J. Haematol. 174, 16–29. https://doi.org/10.1111/bjh.14112

Henseleit, U., Plasa, G., Haest, C., 1990. Effects of divalent cations on lipid flip-flop in the human erythrocyte membrane. Biochim. Biophys. Acta - Biomembr. 1029, 127–135. https://doi.org/https://doi.org/10.1016/0005-2736(90)90445-T

Herrick, J., 1910. PECULIAR ELONGATED AND SICKLE-SHAPED RED BLOOD CORPUSCLES IN A CASE OF SEVERE ANEMIA. Arch. Intern. Med. VI, 517–521. https://doi.org/10.1001/archinte.1910.00050330050003

Hoffman, J.F., 1958. On the relationship of certain erythrocyte characteristics to their physiological age. J. Cell. Comp. Physiol. 51, 415–423. https://doi.org/10.1002/jcp.1030510308

Hoffman, J.F., Joiner, W., Nehrke, K., Potapova, O., Foye, K., Wickrema, A., 2003. The hSK4 (KCNN4) isoform is the Ca2+-activated K+ channel (Gardos channel) in human red blood cells. Proc. Natl. Acad. Sci. U. S. A. 100, 7366–7371. https://doi.org/10.1073/pnas.1232342100

Hoppe, C., Kuypers, F., Larkin, S., Hagar, W., Vichinsky, E., Styles, L., 2011. A pilot study of the short-term use of simvastatin in sickle cell disease: effects on markers of vascular dysfunction. Br. J. Haematol. 153, 655–663. https://doi.org/10.1111/j.1365-2141.2010.08480.x

Hou, J., Fu, Y., Zhou, J., Li, W., Xie, R., Cao, F., Gilbert, G.E., Shi, J., 2011. Lactadherin functions as a probe for phosphatidylserine exposure and as an anticoagulant in the study of stored platelets. Vox Sang. 100, 187–195. https://doi.org/https://doi.org/10.1111/j.1423-0410.2010.01375.x

Hutchaleelaha, A., Patel, M., Washington, C., Siu, V., Allen, E., Oksenberg, D., Gretler, D.D., Mant, T., Lehrer-Graiwer, J., 2019. Pharmacokinetics and pharmacodynamics of voxelotor (GBT440) in healthy adults and patients with sickle cell disease. Br. J. Clin. Pharmacol. 85, 1290–1302. https://doi.org/10.1111/bcp.13896

Hyacinth, H.I., Adams, R.J., Greenberg, C.S., Voeks, J.H., Hill, A., Hibbert, J.M., Gee, B.E., 2015. Effect of Chronic Blood Transfusion on Biomarkers of Coagulation

Activation and Thrombin Generation in Sickle Cell Patients at Risk for Stroke. PLoS One 10, e0134193.

Hyacinth, H.I., Adams, R.J., Voeks, J.H., Hibbert, J.M., Gee, B.E., 2014. Frequent red cell transfusions reduced vascular endothelial activation and thrombogenicity in children with sickle cell anemia and high stroke risk. Am. J. Hematol. 89, 47–51. https://doi.org/10.1002/ajh.23586

Ingram, V.M., 1957. Gene mutations in human haemoglobin: the chemical difference between normal and sickle cell haemoglobin. Nature 180, 326–328.

Inoue, M., Kishimoto, A., Takai, Y., Nishizuka, Y., 1977. Studies on a cyclic nucleotide-independent protein kinase and its proenzyme in mammalian tissues. II. Proenzyme and its activation by calcium-dependent protease from rat brain. J. Biol. Chem. 252, 7610–7616.

Jastaniah, W., 2011. Epidemiology of sickle cell disease in Saudi Arabia. Ann. Saudi Med. 31, 289–293. https://doi.org/10.4103/0256-4947.81540

Jenkins, R.W., Canals, D., Hannun, Y.A., 2009. Roles and regulation of secretory and lysosomal acid sphingomyelinase. Cell. Signal. 21, 836–846. https://doi.org/10.1016/j.cellsig.2009.01.026

Johannes, F., Pestle, J., Dieterich, S., Oberhagemann, P., Link, G., Pfizenmaier, K., 1995. Characterization of activators and inhibitors of protein kinase Cp 307, 303–307.

Johannes, F.J., Prestle, J., Eis, S., Oberhagemann, P., Pfizenmaier, K., 1994. PKCu is a novel, atypical member of the protein kinase C family. J. Biol. Chem. 269, 6140–6148.

John, A., Brylka, H., Wiegreffe, C., Simon, R., Liu, P., Juttner, R., Crenshaw, E.B. 3rd, Luyten, F.P., Jenkins, N.A., Copeland, N.G., Birchmeier, C., Britsch, S., 2012. Bcl11a is required for neuronal morphogenesis and sensory circuit formation in dorsal spinal cord development. Development 139, 1831–1841. https://doi.org/10.1242/dev.072850

Johnson, R.M., Tang, K., 1992. Induction of a Ca(2+)-activated K+ channel in human erythrocytes by mechanical stress. Biochim. Biophys. Acta 1107, 314–318.

Joiner, C.H., Dew, A., Ge, D.L., 1988. Deoxygenation-induced cation fluxes in sickle cells: relationship between net potassium efflux and net sodium influx. Blood Cells 13, 339–358.

Joiner, C.H., Gunn, R.B., Frohlich, O., 1990. Anion transport in sickle red blood cells. Pediatr. Res. 28, 587–590. https://doi.org/10.1203/00006450-199012000-00008

Joiner, C.H., Jiang, M., Claussen, W.J., Roszell, N.J., Yasin, Z., Franco, R.S., 2001. Dipyridamole inhibits sickling-induced cation fluxes in sickle red blood cells. Blood 97, 3976–3983. https://doi.org/10.1182/blood.v97.12.3976

Joiner, C.H., Jiang, M., Franco, R.S., 1995. Deoxygenation-induced cation fluxes in sickle cells. IV. Modulation by external calcium. Am. J. Physiol. 269, C403-9. https://doi.org/10.1152/ajpcell.1995.269.2.C403

Joiner, C.H., Morris, C.L., Cooper, E.S., 1993. Deoxygenation-induced cation fluxes in sickle cells. III. Cation selectivity and response to pH and membrane potential. Am. J. Physiol. Physiol. 264, C734–C744. https://doi.org/10.1152/ajpcell.1993.264.3.C734

Justus, D., Perez-Albuerne, E., Dioguardi, J., Jacobsohn, D., Abraham, A., 2015. Allogeneic donor availability for hematopoietic stem cell transplantation in children with sickle cell disease. Pediatr. Blood Cancer 62, 1285–1287. https://doi.org/10.1002/pbc.25439

Kaestner, L., Bogdanova, A., Egee, S., 2020. Calcium Channels and Calcium-Regulated Channels in Human Red Blood Cells. Adv. Exp. Med. Biol. 1131, 625–648. https://doi.org/10.1007/978-3-030-12457-1_25

Kaestner, L., Tabellion, W., Lipp, P., Bernhardt, I., 2004. Prostaglandin E2 activates channel-mediated calcium entry in human erythrocytes: an indication for a blood clot formation supporting process. Thromb. Haemost. 92, 1269–1272. https://doi.org/10.1160/TH04-06-0338

Kagan, V.E., Gleiss, B., Tyurina, Y.Y., Tyurin, V.A., Elenstrom-Magnusson, C., Liu, S.-X., Serinkan, F.B., Arroyo, A., Chandra, J., Orrenius, S., Fadeel, B., 2002. A role for oxidative stress in apoptosis: oxidation and externalization of phosphatidylserine is required for macrophage clearance of cells undergoing Fas-mediated apoptosis. J. Immunol. 169, 487–499. https://doi.org/10.4049/jimmunol.169.1.487

Kaji, D.M., Gasson, C., 1995. Urea activation of K-Cl transport in human erythrocytes. Am. J. Physiol. Physiol. 268, C1018–C1025. https://doi.org/10.1152/ajpcell.1995.268.4.C1018

Kaji, D.M., Lim, J., Shilkoff, W., Zaidi, W., 1998. Urea Inhibits the Na-K Pump in Human Erythrocytes. J. Membr. Biol. 165, 125–131. https://doi.org/10.1007/s002329900426

Kamp, D., Sieberg, T., Haest, C.W.M., 2001. Inhibition and Stimulation of Phospholipid Scrambling Activity. Consequences for Lipid Asymmetry, Echinocytosis, and Microvesiculation of Erythrocytes. Biochemistry 40, 9438–9446. https://doi.org/10.1021/bi0107492

Kar, B.C., Devi, S., Dash, K.C., Das, M., 1987. The sickle cell gene is widespread in India. Trans. R. Soc. Trop. Med. Hyg. 81, 273–275.

Kato, G.J., Steinberg, M.H., Gladwin, M.T., 2017. Intravascular hemolysis and the pathophysiology of sickle cell disease. J. Clin. Invest. 127, 750–760. https://doi.org/10.1172/JCI89741

Key, N.S., Derebail, V.K., 2010. Sickle-cell trait: novel clinical significance. Hematol. Am. Soc. Hematol. Educ. Progr. 2010, 418–422. https://doi.org/10.1182/asheducation-2010.1.418

Kochs, G., Hummel, R., Fiebich, B., Sarre, T.F., Marmé, D., Hug, H., 1993. Activation of purified human protein kinase C alpha and beta I isoenzymes in vitro by Ca2+, phosphatidylinositol and phosphatidylinositol 4,5-bisphosphate. Biochem. J. 291 (Pt 2), 627–633. https://doi.org/10.1042/bj2910627

Kong, H.H.O.P., Alleyne, G.A.O., 1971. Studies on Acid Excretion in Adults with Sickle-

Cell Anaemia. Clin. Sci. 41, 505–518. https://doi.org/10.1042/cs0410505

Konotey-Ahulu FD, 1974. The sickle cell diseases: Clinical manifestations including the "sickle crisis." Arch. Intern. Med. 133, 611–619.

Koshkaryev, A., Livshits, L., Pajic-Lijakovic, I., Gural, A., Barshtein, G., Yedgar, S., 2020. Non-oxidative band-3 clustering agents cause the externalization of phosphatidylserine on erythrocyte surfaces by a calcium-independent mechanism. Biochim. Biophys. Acta - Biomembr. 1862, 183231. https://doi.org/https://doi.org/10.1016/j.bbamem.2020.183231

Kucherenko, Y., Browning, J., Tattersall, A., Ellory, J.C., Gibson, J.S., 2005. Effect of peroxynitrite on passive K+ transport in human red blood cells. Cell. Physiol. Biochem. 15, 271–280. https://doi.org/10.1159/000087237

Kulozik, A.E., Wainscoat, J.S., Serjeant, G.R., Kar, B.C., Al-Awamy, B., Essan, G.J., Falusi, A.G., Haque, S.K., Hilali, A.M., Kate, S., 1986. Geographical survey of beta S-globin gene haplotypes: evidence for an independent Asian origin of the sickle-cell mutation. Am. J. Hum. Genet. 39, 239–244.

Kumari, A., 2018. Chapter 13 - Ceramide Structure and Derivatives, in: Kumari, A.B.T.-S.B. (Ed.), . Academic Press, pp. 59–61. https://doi.org/https://doi.org/10.1016/B978-0-12-814453-4.00013-3

Kuypers, F.A., 2007. Membrane lipid alterations in hemoglobinopathies. Hematology Am. Soc. Hematol. Educ. Program 68–73. https://doi.org/10.1182/asheducation-2007.1.68

Kuypers, F.A., 1998. Phospholipid asymmetry in health and disease. Curr. Opin. Hematol. 5, 122–131. https://doi.org/10.1097/00062752-199803000-00007

Kuypers, F.A., de Jong, K., 2004. The role of phosphatidylserine in recognition and removal of erythrocytes. Cell. Mol. Biol. (Noisy-le-grand). 50, 147–158.

Kuypers, F.A., Larkin, S.K., Emeis, J.J., Allison, A.C., 2007. Interaction of an annexin V homodimer (Diannexin) with phosphatidylserine on cell surfaces and consequent antithrombotic activity. Thromb. Haemost. 97, 478–486.

Kuypers, F.A., Lewis, R.A., Hua, M., Schott, M.A., Discher, D., Ernst, J.D., Lubin, B.H., 1996. Detection of altered membrane phospholipid asymmetry in subpopulations of human red blood cells using fluorescently labeled annexin V. Blood 87, 1179–1187.

Kuypers, F.A., Yuan, J., Lewis, R.A., Snyder, L.M., Kiefer, C.R., Bunyaratvej, A., Fucharoen, S., Ma, L., Styles, L., de Jong, K., Schrier, S.L., 1998. Membrane phospholipid asymmetry in human thalassemia. Blood 91, 3044–3051.

Lacroix, J.J., Botello-smith, W.M., Luo, Y., 2018. Probing the gating mechanism of the mechanosensitive channel Piezo1 with the small molecule Yoda1. Nat. Commun. https://doi.org/10.1038/s41467-018-04405-3

Landburg, P.P., Teerlink, T., Biemond, B.J., Brandjes, D.P.M., Muskiet, F.A.J., Duits, A.J., Schnog, J.B., 2010. Plasma asymmetric dimethylarginine concentrations in sickle cell disease are related to the hemolytic phenotype. Blood Cells. Mol. Dis. 44, 229–232. https://doi.org/10.1016/j.bcmd.2010.02.005

Lang, F., Gulbins, E., Lang, P.A., Zappulla, D., Foller, M., 2010. Ceramide in suicidal death of erythrocytes. Cell. Physiol. Biochem. 26, 21–28. https://doi.org/10.1159/000315102

Lang, F., Gulbins, E., Lerche, H., Huber, S.M., Kempe, D.S., Foller, M., 2008. Eryptosis, a window to systemic disease. Cell. Physiol. Biochem. 22, 373–380. https://doi.org/10.1159/000185448

Lang, F., Lang, K.S., Lang, P.A., Huber, S.M., Wieder, T., 2006. Mechanisms and significance of eryptosis. Antioxid. Redox Signal. 8, 1183–1192. https://doi.org/10.1089/ars.2006.8.1183

Lang, K S, Duranton, C., Poehlmann, H., Myssina, S., Bauer, C., 2003. Cation channels trigger apoptotic death of erythrocytes 249–256. https://doi.org/10.1038/sj.cdd.4401144

Lang, K.S., Fillon, S., Schneider, D., Rammensee, H.-G., Lang, F., 2002. Stimulation of TNF alpha expression by hyperosmotic stress. Pflugers Arch. 443, 798–803. https://doi.org/10.1007/s00424-001-0768-7

Lang, K S, Myssina, S., Brand, V., Sandu, C., Lang, P.A., 2004. Involvement of ceramide in hyperosmotic shock- induced death of erythrocytes 231–243. https://doi.org/10.1038/sj.cdd.4401311

Lang, Karl S, Myssina, S., Lang, P.A., Tanneur, V., Kempe, D.S., Mack, A.F., Huber, S.M., Wieder, T., Lang, F., Duranton, C., Karl, S., Myssina, S., Lang, P.A., Kempe, D.S., Mack, A.F., Stephan, M., Wieder, T., Lang, F., Duranton, C., 2004. Inhibition of erythrocyte phosphatidylserine exposure by urea and Cl X 1046–1053.

Lang, Karl S, Myssina, S., Lang, P.A., Tanneur, V., Kempe, D.S., Mack, A.F., Huber, S.M., Wieder, T., Lang, F., Duranton, C., Karl, S., Myssina, S., Lang, P.A., Kempe, D.S., Mack, A.F., Stephan, M., Wieder, T., Lang, F., Duranton, C., 2003. Inhibition of erythrocyte phosphatidylserine exposure by urea and Cl X 1046–1053.

Lang, P.A., Kempe, D.S., Tanneur, V., Eisele, K., Klarl, B.A., Myssina, S., Jendrossek, V., Ishii, S., Shimizu, T., Waidmann, M., Hessler, G., Huber, S.M., Lang, F., Wieder, T., 2005. Stimulation of erythrocyte ceramide formation by platelet-activating factor. J. Cell Sci. 118, 1233–1243. https://doi.org/10.1242/jcs.01730

Lapoumeroulie, C., Dunda, O., Ducrocq, R., Trabuchet, G., Mony-Lobe, M., Bodo, J.M., Carnevale, P., Labie, D., Elion, J., Krishnamoorthy, R., 1992. A novel sickle cell mutation of yet another origin in Africa: the Cameroon type. Hum. Genet. 89, 333–337.

Laurin, L.-P., Nachman, P.H., Desai, P.C., Ataga, K.I., Derebail, V.K., 2014. Hydroxyurea is associated with lower prevalence of albuminuria in adults with sickle cell disease. Nephrol. Dial. Transplant. Off. Publ. Eur. Dial. Transpl. Assoc. - Eur. Ren. Assoc. 29, 1211–1218. https://doi.org/10.1093/ndt/gft295

Lebensburger, J., Johnson, S.M., Askenazi, D.J., Rozario, N.L., Howard, T.H., Hilliard, L.M., 2011. Protective role of hemoglobin and fetal hemoglobin in early kidney disease for children with sickle cell anemia. Am. J. Hematol. 86, 430–432. https://doi.org/10.1002/ajh.21994

Leitgeb, A.M., Blomqvist, K., Cho-Ngwa, F., Samje, M., Nde, P., Titanji, V., Wahlgren, M., 2011. Low anticoagulant heparin disrupts Plasmodium falciparum rosettes in fresh clinical isolates. Am. J. Trop. Med. Hyg. 84, 390–396. https://doi.org/10.4269/ajtmh.2011.10-0256

Leonard, A., Tisdale, J., Abraham, A., 2020. Curative options for sickle cell disease: haploidentical stem cell transplantation or gene therapy? Br. J. Haematol. https://doi.org/10.1111/bjh.16437

Lew, V.L., Bookchin, R.M., 2005. Ion Transport Pathology in the Mechanism of Sickle Cell Dehydration 179–200. https://doi.org/10.1152/physrev.00052.2003.

Lew, V.L., Etzion, Z., Bookchin, R.M., 2002. Dehydration response of sickle cells to sickling-induced Ca(++) permeabilization. Blood 99, 2578–2585. https://doi.org/10.1182/blood.v99.7.2578

Lew, V.L., Ortiz, O.E., Bookchin, R.M., 1997. Stochastic nature and red cell population distribution of the sickling-induced Ca2+ permeability. J. Clin. Invest. 99, 2727–2735. https://doi.org/10.1172/JCI119462

Lew, V.L., Tiffert, T., 2017. On the Mechanism of Human Red Blood Cell Longevity : Roles of Calcium , the Sodium Pump , PIEZO1 , and Gardos Channels 8, 1–7. https://doi.org/10.3389/fphys.2017.00977

Lew, V.L., Tsien, R.Y., Miner, C., Bookchin, R.M., 1982. Physiological [Ca2+]i level and pump-leak turnover in intact red cells measured using an incorporated Ca chelator. Nature 298, 478–481. https://doi.org/10.1038/298478a0

Li, J., Hou, B., Tumova, S., Muraki, K., Bruns, A., Ludlow, M.J., Sedo, A., Hyman, A.J., McKeown, L., Young, R.S., Yuldasheva, N.Y., Majeed, Y., Wilson, L.A., Rode, B., Bailey, M.A., Kim, H.R., Fu, Z., Carter, D. Al, Bilton, J., Imrie, H., Ajuh, P., Dear, T.N., Cubbon, R.M., Kearney, M.T., Prasad, R.K., Evans, P.C., Ainscough, J.F., Beech, D.J., 2014. Piezo1 integration of vascular architecture with physiological force. Nature 515, 279–282. https://doi.org/10.1038/nature13701

Lim, J., Gasson, C., Kaji, D.M., 1995. Urea inhibits NaK2Cl cotransport in human erythrocytes. J. Clin. Invest. 96, 2126–2132. https://doi.org/10.1172/JCI118266

Liu, P., Keller, J.R., Ortiz, M., Tessarollo, L., Rachel, R.A., Nakamura, T., Jenkins, N.A., Copeland, N.G., 2003. Bcl11a is essential for normal lymphoid development. Nat. Immunol. 4, 525–532. https://doi.org/10.1038/ni925

Liu, W.S., Heckman, C.A., 1998. The Sevenfold Way of PKC Regulation 10, 529–542.

Livingstone, F.B., 1958. Anthropological Implications of Sickle Cell Gene Distribution in West Africa. Am. Anthropol. 60, 533–562.

Lowenthal, E.A., Wells, A., Emanuel, P.D., Player, R., Prchal, J.T., 1996. Sickle cell acute chest syndrome associated with parvovirus B19 infection: case series and review. Am. J. Hematol. 51, 207–213. https://doi.org/10.1002/(SICI)1096-8652(199603)51:3<207::AID-AJH5>3.0.CO;2-0

Lu, J., Park, J.H., Liu, A.Y., Chen, K.Y., 2000. Activation of heat shock factor 1 by hyperosmotic or hypo-osmotic stress is drastically attenuated in normal human

fibroblasts during senescence. J. Cell. Physiol. 184, 183–190.
https://doi.org/10.1002/1097-4652(200008)184:2<183::AID-JCP5>3.0.CO;2-9

Lubin, B., Chiu, D., Bastacky, J., Roelofsen, B., Van Deenen, L.L., 1981. Abnormalities in
membrane phospholipid organization in sickled erythrocytes. J. Clin. Invest. 67,
1643–1649.

Luo, S., Lei, H., Qin, H., Xia, Y., 2014. Molecular mechanisms of endothelial NO
synthase uncoupling. Curr. Pharm. Des. 20, 3548–3553.
https://doi.org/10.2174/13816128113196660746

Ma, S., Cahalan, S., LaMonte, G., Grubaugh, N.D., Zeng, W., Murthy, S.E., Paytas, E.,
Gamini, R., Lukacs, V., Whitwam, T., Loud, M., Lohia, R., Berry, L., Khan, S.M.,
Janse, C.J., Bandell, M., Schmedt, C., Wengelnik, K., Su, A.I., Honore, E., Winzeler,
E.A., Andersen, K.G., Patapoutian, A., 2018. Common PIEZO1 Allele in African
Populations Causes RBC Dehydration and Attenuates Plasmodium Infection. Cell
173, 443-455.e12. https://doi.org/10.1016/j.cell.2018.02.047

Ma, Y.-L., Rees, D.C., Gibson, J.S., Ellory, J.C., 2012. The conductance of red blood cells
from sickle cell patients: ion selectivity and inhibitors. J. Physiol. 590, 2095–2105.
https://doi.org/10.1113/jphysiol.2012.229609

MacDonald, R., 1977. Red cell 2,3-diphosphoglycerate and oxygen affinity. Anaesthesia
32, 544–553.

Makani, J., Komba, A.N., Cox, S.E., Oruo, J., Mwamtemi, K., Kitundu, J., Magesa, P.,
Rwezaula, S., Meda, E., Mgaya, J., 2010. Europe PMC Funders Group Malaria in
patients with sickle cell anemia : burden , risk factors , and outcome at the outpatient
clinic and during hospitalization 115, 215–220. https://doi.org/10.1182/blood-2009-
07-233528.Malaria

Makhro, A., Hanggi, P., Goede, J.S., Wang, J., Bruggemann, A., Gassmann, M.,
Schmugge, M., Kaestner, L., Speer, O., Bogdanova, A., 2013. N-methyl-D-aspartate
receptors in human erythroid precursor cells and in circulating red blood cells
contribute to the intracellular calcium regulation. Am. J. Physiol. Cell Physiol. 305,
C1123-38. https://doi.org/10.1152/ajpcell.00031.2013

Makhro, A., Wang, J., Vogel, J., Boldyrev, A.A., Gassmann, M., Kaestner, L., Bogdanova,
A., 2010. Functional NMDA receptors in rat erythrocytes. Am. J. Physiol. Cell
Physiol. 298, C1315-25. https://doi.org/10.1152/ajpcell.00407.2009

Marangon, K., Devaraj, S., Tirosh, O., Packer, L., Jialal, I., 1999. Comparison of the effect
of alpha-lipoic acid and alpha-tocopherol supplementation on measures of oxidative
stress. Free Radic. Biol. Med. 27, 1114–1121. https://doi.org/10.1016/s0891-
5849(99)00155-0

Marín-Vicente, C., Gómez-Fernández, J.C., Corbalán-García, S., 2005. The ATP-
dependent Membrane Localization of Protein Kinase Cα Is Regulated by Ca2+ Influx
and Phosphatidylinositol 4,5-Bisphosphate in Differentiated PC12 Cells. Mol. Biol.
Cell 16, 2848–2861. https://doi.org/10.1091/mbc.e05-01-0067

Marin, A., Cerutti, N., Massa, E.R., 1999. Use of the amplification refractory mutation
system (ARMS) in the study of HbS in predynastic Egyptian remains. Boll. Soc. Ital.

Biol. Sper. 75, 27–30.

Markadieu, N., Delpire, E., 2014. Physiology and pathophysiology of SLC12A1/2 transporters. Pflugers Arch. 466, 91–105. https://doi.org/10.1007/s00424-013-1370-5

Marotta, C.A., Wilson, J.T., Forget, B.G., Weissman, S.M., 1977. Human beta-globin messenger RNA. III. Nucleotide sequences derived from complementary DNA. J. Biol. Chem. 252, 5040–5053.

Martín, S.F., Navarro, F., Forthoffer, N., Navas, P., Villalba, J.M., 2001. Neutral Magnesium-Dependent Sphingomyelinase from Liver Plasma Membrane: Purification and Inhibition by Ubiquinol. J. Bioenerg. Biomembr. 33, 143–153. https://doi.org/10.1023/A:1010704715979

Matsui, N.M., Varki, A., Embury, S.H., 2002. Heparin inhibits the flow adhesion of sickle red blood cells to P-selectin. Blood 100, 3790–3796. https://doi.org/10.1182/blood-2002-02-0626

May, A., Huehns, E.R., 1975. The Effect of Urea on Sickling. Br. J. Haematol. 30, 21–29. https://doi.org/https://doi.org/10.1111/j.1365-2141.1975.tb00513.x

McCurdy, P.R., Sherman, A.S., 1978. Irreversibly sickled cells and red cell survival in sickle cell anemia: a study with both DF32P and 51CR. Am. J. Med. 64, 253–258.

Medkova, M., Cho, W., 1998. Mutagenesis of the C2 domain of protein kinase C-alpha. Differential roles of Ca2+ ligands and membrane binding residues. J. Biol. Chem. 273, 17544—17552. https://doi.org/10.1074/jbc.273.28.17544

Middelkoop, E., Lubin, B.H., Bevers, E.M., Op den Kamp, J.A.F., Comfurius, P., Chiu, D.T.-Y., Zwaal, R.F.A., van Deenen, L.L.M., Roelofsen, B., 1988. Studies on sickled erythrocytes provide evidence that the asymmetric distribution of phosphatidylserine in the red cell membrane is maintained by both ATP-dependent translocation and interaction with membrane skeletal proteins. Biochim. Biophys. Acta - Biomembr. 937, 281–288. https://doi.org/https://doi.org/10.1016/0005-2736(88)90250-7

Mielke, M.M., Lyketsos, C.G., 2010. Alterations of the sphingolipid pathway in Alzheimer's disease: new biomarkers and treatment targets? Neuromolecular Med. 12, 331–340. https://doi.org/10.1007/s12017-010-8121-y

Milligan, C., Rees, D.C., Ellory, J.C., Osei, A., Browning, J.A., Hannemann, A., Gibson, J.S., 2013. A non-electrolyte haemolysis assay for diagnosis and prognosis of sickle cell disease. J. Physiol. 591, 1463–1474. https://doi.org/10.1113/jphysiol.2012.246579

Modell, B., Darlison, M., 2008. Public health reviews Global epidemiology of haemoglobin disorders and derived service indicators 036673. https://doi.org/10.2471/BLT.06.036673

Mohandas, N., Rossi, M.E., Clark, M.R., 1986. Association between morphologic distortion of sickle cells and deoxygenation-induced cation permeability increase. Blood 68, 450–454.

Moras, M., Lefevre, S.D., Ostuni, M.A., 2017. From Erythroblasts to Mature Red Blood Cells: Organelle Clearance in Mammals. Front. Physiol. 8, 1076.

https://doi.org/10.3389/fphys.2017.01076

Mordechai Liscovitch, 1992. Crosstalk among multiple signal-activated phospholipases 393–399.

Murray, D., Honig, B., 2002. Electrostatic control of the membrane targeting of C2 domains. Mol. Cell 9, 145–154. https://doi.org/10.1016/s1097-2765(01)00426-9

Muzyamba, M.C., Cossins, A.R., Gibson, J.S., 1999. Regulation of Na+-K+-2Cl-cotransport in turkey red cells: the role of oxygen tension and protein phosphorylation. J. Physiol. 517 (Pt 2), 421–429. https://doi.org/10.1111/j.1469-7793.1999.0421t.x

Nagel, R.L., Steinberg, M.H., 2001. Role of epistatic (modifier) genes in the modulation of the phenotypic diversity of sickle cell anemia. Pediatr. Pathol. Mol. Med. 20, 123–136.

Nalbandian, R.M., 1972. Oral Urea in Sickle-Cell Disease 77.

Natarajan, V., Vepa, S., Verma, R.S., Scribner, W.M., 1996. Role of protein tyrosine phosphorylation in H2O2-induced activation of endothelial cell phospholipase D. Am. J. Physiol. 271, L400-8. https://doi.org/10.1152/ajplung.1996.271.3.L400

Neidlinger, N.A., Larkin, S.K., Bhagat, A., Victorino, G.P., Kuypers, F.A., 2006. Hydrolysis of phosphatidylserine-exposing red blood cells by secretory phospholipase A2 generates lysophosphatidic acid and results in vascular dysfunction. J. Biol. Chem. 281, 775–781. https://doi.org/10.1074/jbc.M505790200

Newton, A.C., 2001. Protein kinase C: structural and spatial regulation by phosphorylation, cofactors, and macromolecular interactions. Chem. Rev. 101, 2353–2364. https://doi.org/10.1021/cr0002801

Nguyen, D.B., Wagner-Britz, L., Maia, S., Steffen, P., Wagner, C., Kaestner, L., Bernhardt, I., 2011. Regulation of phosphatidylserine exposure in red blood cells. Cell. Physiol. Biochem. Int. J. Exp. Cell. Physiol. Biochem. Pharmacol. 28, 847–856. https://doi.org/10.1159/000335798

Niihara, Y., Miller, S.T., Kanter, J., Lanzkron, S., Smith, W.R., Hsu, L.L., Gordeuk, V.R., Viswanathan, K., Sarnaik, S., Osunkwo, I., Guillaume, E., Sadanandan, S., Sieger, L., Lasky, J.L., Panosyan, E.H., Blake, O.A., New, T.N., Bellevue, R., Tran, L.T., Razon, R.L., Stark, C.W., Neumayr, L.D., Vichinsky, E.P., 2018. A Phase 3 Trial of l-Glutamine in Sickle Cell Disease. N. Engl. J. Med. 379, 226–235. https://doi.org/10.1056/NEJMoa1715971

Niihara, Y., Zerez, C.R., Akiyama, D.S., Tanaka, K.R., 1998. Oral L-glutamine therapy for sickle cell anemia: I. Subjective clinical improvement and favorable change in red cell NAD redox potential. Am. J. Hematol. 58, 117–121. https://doi.org/10.1002/(sici)1096-8652(199806)58:2<117::aid-ajh5>3.0.co;2-v

Nishizuka, Y., 1995. Protein kinase C and lipid signaling for sustained cellular responses. FASEB J. 9, 484–496. https://doi.org/https://doi.org/10.1096/fasebj.9.7.7737456

Nishizuka, Y., 1992. Intracellular signaling by hydrolysis of phospholipids and activation of protein kinase C. Science (80-.). 258, 607 LP – 614.

https://doi.org/10.1126/science.1411571

Nishizuka, Y., 1984. The role of protein kinase C in cell surface signal transduction and tumour promotion. Nature 308, 693–698. https://doi.org/10.1038/308693a0

Novelli, E.M., Gladwin, M.T., 2016. Crises in Sickle Cell Disease. Chest 149, 1082–1093. https://doi.org/10.1016/j.chest.2015.12.016

Nur, E., Brandjes, D.P., Teerlink, T., Otten, H.-M., Oude Elferink, R.P.J., Muskiet, F., Evers, L.M., ten Cate, H., Biemond, B.J., Duits, A.J., Schnog, J.-J.B., 2012. N-acetylcysteine reduces oxidative stress in sickle cell patients. Ann. Hematol. 91, 1097–1105. https://doi.org/10.1007/s00277-011-1404-z

Ochoa, W.F., Corbalán-Garcia, S., Eritja, R., Rodríguez-Alfaro, J.A., Gómez-Fernández, J.C., Fita, I., Verdaguer, N., 2002. Additional binding sites for anionic phospholipids and calcium ions in the crystal structures of complexes of the C2 domain of protein kinase calpha. J. Mol. Biol. 320, 277–291. https://doi.org/10.1016/S0022-2836(02)00464-3

Ohanian, J., Ohanian, V., 2001. Sphingolipids in mammalian cell signalling. Cell. Mol. Life Sci. 58, 2053–2068. https://doi.org/10.1007/PL00000836

Oksenberg, D., Dufu, K., Patel, M.P., Chuang, C., Li, Z., Xu, Q., Silva-Garcia, A., Zhou, C., Hutchaleelaha, A., Patskovska, L., Patskovsky, Y., Almo, S.C., Sinha, U., Metcalf, B.W., Archer, D.R., 2016. GBT440 increases haemoglobin oxygen affinity, reduces sickling and prolongs RBC half-life in a murine model of sickle cell disease. Br. J. Haematol. 175, 141–153. https://doi.org/10.1111/bjh.14214

Orringer, E.P., Casella, J.F., Ataga, K.I., Koshy, M., Adams-Graves, P., Luchtman-Jones, L., Wun, T., Watanabe, M., Shafer, F., Kutlar, A., Abboud, M., Steinberg, M., Adler, B., Swerdlow, P., Terregino, C., Saccente, S., Files, B., Ballas, S., Brown, R., Wojtowicz-Praga, S., Grindel, J.M., 2001. Purified poloxamer 188 for treatment of acute vaso-occlusive crisis of sickle cell disease: A randomized controlled trial. JAMA 286, 2099–2106. https://doi.org/10.1001/jama.286.17.2099

Oster, J.R., Lespier, L.E., Lee, S.M., Pellegrini, E.L., Vaamonde, C.A., 1976. Renal acidification in sickle-cell disease. J. Lab. Clin. Med. 88, 389–401.

Pace, B.S., Shartava, A., Pack-Mabien, A., Mulekar, M., Ardia, A., Goodman, S.R., 2003. Effects of N-acetylcysteine on dense cell formation in sickle cell disease. Am. J. Hematol. 73, 26–32. https://doi.org/10.1002/ajh.10321

Pagnier, J., Mears, J.G., Dunda-Belkhodja, O., Schaefer-Rego, K.E., Beldjord, C., Nagel, R.L., Labie, D., 1984. Evidence for the multicentric origin of the sickle cell hemoglobin gene in Africa. Proc. Natl. Acad. Sci. U. S. A. 81, 1771–1773.

Parinandi, N.L., Roy, S., Shi, S., Cummings, R.J., Morris, A.J., Garcia, J.G., Natarajan, V., 2001. Role of Src kinase in diperoxovanadate-mediated activation of phospholipase D in endothelial cells. Arch. Biochem. Biophys. 396, 231–243. https://doi.org/10.1006/abbi.2001.2609

Parinandi, N.L., Scribner, W.M., Vepa, S., Shi, S., Natarajan, V., 1999. Phospholipase D activation in endothelial cells is redox sensitive. Antioxid. Redox Signal. 1, 193–210.

https://doi.org/10.1089/ars.1999.1.2-193

Patel, M., Cabrales, P., Dufu, K., Metcalf, B., Sinha, U., 2014. GTx011, an Anti-Sickling Compound, Improves SS Blood Rheology By Reduction of HbS polymerization Via Allosteric Modulation of O<sub>2</sub> Affinity. Blood 124, 1370 LP – 1370.

Patel, R.B., Kotha, S.R., Sherwani, S.I., Sliman, S.M., Gurney, T.O., Loar, B., Butler, S.O., Morris, A.J., Marsh, C.B., Parinandi, N.L., 2011. Pulmonary fibrosis inducer, bleomycin, causes redox-sensitive activation of phospholipase D and cytotoxicity through formation of bioactive lipid signal mediator, phosphatidic acid, in lung microvascular endothelial cells. Int. J. Toxicol. 30, 69–90. https://doi.org/10.1177/1091581810388850

Paul R. McCurdy and Laviza Mahmood, 1971. The New England Journal of Medicine Downloaded from nejm.org at PENN STATE UNIVERSITY on November 13, 2015. For personal use only. No other uses without permission. From the NEJM Archive. Copyright © 2010 Massachusetts Medical Society. All rights reserved. N. Engl. J. Med.

Pellegrino, C.M., Rybicki, A.C., Musto, S., Nagel, R.L., Schwartz, R.S., 1998. Molecular identification and expression of erythroid K:Cl cotransporter in human and mouse erythroleukemic cells. Blood Cells. Mol. Dis. 24, 31–40. https://doi.org/10.1006/bcmd.1998.0168

Perrine, R.P., Brown, M.J., Clegg, J.B., Weatherall, D.J., May, A., 1972. BENIGN SICKLE-CELL ANÆMIA. Lancet 300, 1163–1167. https://doi.org/10.1016/S0140-6736(72)92592-5

Picard, V., Guitton, C., Thuret, I., Rose, C., Bendelac, L., Ghazal, K., Aguilar-Martinez, P., Badens, C., Barro, C., Bénéteau, C., Berger, C., Cathébras, P., Deconinck, E., Delaunay, J., Durand, J.-M., Firah, N., Galactéros, F., Godeau, B., Jaïs, X., de Jaureguiberry, J.-P., Le Stradic, C., Lifermann, F., Maffre, R., Morin, G., Perrin, J., Proulle, V., Ruivard, M., Toutain, F., Lahary, A., Garçon, L., 2019. Clinical and biological features in PIEZO1-hereditary xerocytosis and Gardos channelopathy: a retrospective series of 126 patients. Haematologica 104, 1554–1564. https://doi.org/10.3324/haematol.2018.205328

Piccin, A., Murphy, W.G., Smith, O.P., 2007. Circulating microparticles: pathophysiology and clinical implications. Blood Rev. 21, 157–171. https://doi.org/10.1016/j.blre.2006.09.001

Piel, F.B., Hay, S.I., Gupta, S., Weatherall, D.J., Williams, T.N., 2013. Global Burden of Sickle Cell Anaemia in Children under Five, 2010–2050: Modelling Based on Demographics, Excess Mortality, and Interventions. PLOS Med. 10, e1001484.

Platt, O.S., Brambilla, D.J., Rosse, W.F., Milner, P.F., Castro, O., Steinberg, M.H., Klug, P.P., 1994. Mortality in sickle cell disease. Life expectancy and risk factors for early death. N. Engl. J. Med. 330, 1639–1644. https://doi.org/10.1056/NEJM199406093302303

Ranade, S.S., Qiu, Z., Woo, S.-H., Hur, S.S., Murthy, S.E., Cahalan, S.M., Xu, J., Mathur, J., Bandell, M., Coste, B., Li, Y.-S.J., Chien, S., Patapoutian, A., 2014a. Piezo1, a

mechanically activated ion channel, is required for vascular development in mice. Proc. Natl. Acad. Sci. U. S. A. 111, 10347–10352. https://doi.org/10.1073/pnas.1409233111

Ranade, S.S., Qiu, Z., Woo, S., Sik, S., Murthy, S.E., 2014b. is required for vascular development in mice 1–6. https://doi.org/10.1073/pnas.1409233111

Rapetti-Mauss, R., Lacoste, C., Picard, V., Guitton, C., Lombard, E., Loosveld, M., Nivaggioni, V., Dasilva, N., Salgado, D., Desvignes, J.-P., Béroud, C., Viout, P., Bernard, M., Soriani, O., Vinti, H., Lacroze, V., Feneant-Thibault, M., Thuret, I., Guizouarn, H., Badens, C., 2015. A mutation in the Gardos channel is associated with hereditary xerocytosis. Blood 126, 1273–1280. https://doi.org/10.1182/blood-2015-04-642496

Raucher, D., Stauffer, T., Chen, W., Shen, K., Guo, S., York, J.D., Sheetz, M.P., Meyer, T., 2000. Phosphatidylinositol 4,5-bisphosphate functions as a second messenger that regulates cytoskeleton-plasma membrane adhesion. Cell 100, 221–228. https://doi.org/10.1016/s0092-8674(00)81560-3

Rees, D.C., 2011. The rationale for using hydroxycarbamide in the treatment of sickle cell disease. Haematologica 96, 488–491. https://doi.org/10.3324/haematol.2011.041988

Rees, D.C., Williams, T.N., Gladwin, M.T., 2010. Sickle-cell disease. Lancet 376, 2018–2031. https://doi.org/10.1016/S0140-6736(10)61029-X

Reinehr, R., Graf, D., Fischer, R., Schliess, F., Haussinger, D., 2002. Hyperosmolarity triggers CD95 membrane trafficking and sensitizes rat hepatocytes toward CD95L-induced apoptosis. Hepatology 36, 602–614. https://doi.org/10.1053/jhep.2002.35447

Reinehr, R., Haussinger, D., 2006. Hyperosmotic activation of the CD95 death receptor system. Acta Physiol. (Oxf). 187, 199–203. https://doi.org/10.1111/j.1748-1716.2006.01541.x

Reiter, C.D., Wang, X., Tanus-Santos, J.E., Hogg, N., Cannon, R.O. 3rd, Schechter, A.N., Gladwin, M.T., 2002. Cell-free hemoglobin limits nitric oxide bioavailability in sickle-cell disease. Nat. Med. 8, 1383–1389. https://doi.org/10.1038/nm799

Retailleau, K., Duprat, F., Arhatte, M., Ranade, S.S., Peyronnet, R., Martins, J.R., Jodar, M., Moro, C., Offermanns, S., Feng, Y., Demolombe, S., Patel, A., Honore, E., 2015. Piezo1 in Smooth Muscle Cells Is Involved in Hypertension-Dependent Arterial Remodeling. Cell Rep. 13, 1161–1171. https://doi.org/10.1016/j.celrep.2015.09.072

Rhoda, M.D., Apovo, M., Beuzard, Y., Giraud, F., 1990. Ca2+ permeability in deoxygenated sickle cells. Blood 75, 2453 LP – 2458.

Rogers, S.C., Ross, J.G.C., d'Avignon, A., Gibbons, L.B., Gazit, V., Hassan, M.N., McLaughlin, D., Griffin, S., Neumayr, T., Debaun, M., DeBaun, M.R., Doctor, A., 2013. Sickle hemoglobin disturbs normal coupling among erythrocyte O2 content, glycolysis, and antioxidant capacity. Blood 121, 1651–1662. https://doi.org/10.1182/blood-2012-02-414037

Ronca, F., Palmieri, L., Malengo, S., Bertelli, A., 1994. Effect of L-propionyl carnitine on in-vitro membrane alteration of sickle-cell anaemia erythrocytes. Int. J. Tissue React.

16, 187–194.

Rosette, C., Karin, M., 1996. Ultraviolet light and osmotic stress: activation of the JNK cascade through multiple growth factor and cytokine receptors. Science 274, 1194–1197. https://doi.org/10.1126/science.274.5290.1194

Ruvolo, P.P., 2003. Intracellular signal transduction pathways activated by ceramide and its metabolites. Pharmacol. Res. 47, 383–392. https://doi.org/10.1016/s1043-6618(03)00050-1

Safo, M.K., Ahmed, M.H., Ghatge, M.S., Boyiri, T., 2011. Hemoglobin-ligand binding: understanding Hb function and allostery on atomic level. Biochim. Biophys. Acta 1814, 797–809. https://doi.org/10.1016/j.bbapap.2011.02.013

Sankaran, V.G., Menne, T.F., Xu, J., Akie, T.E., Lettre, G., Van Handel, B., Mikkola, H.K.A., Hirschhorn, J.N., Cantor, A.B., Orkin, S.H., 2008. Human fetal hemoglobin expression is regulated by the developmental stage-specific repressor BCL11A. Science 322, 1839–1842. https://doi.org/10.1126/science.1165409

Sankaran, V.G., Xu, J., Ragoczy, T., Ippolito, G.C., Walkley, C.R., Maika, S.D., Fujiwara, Y., Ito, M., Groudine, M., Bender, M.A., Tucker, P.W., Orkin, S.H., 2009. Developmental and species-divergent globin switching are driven by BCL11A. Nature 460, 1093–1097. https://doi.org/10.1038/nature08243

Saotome, K., Murthy, S.E., Kefauver, J.M., Whitwam, T., Patapoutian, A., Ward, A.B., 2018. Structure of the mechanically activated ion channel Piezo1. Nature 554, 481–486. https://doi.org/10.1038/nature25453

Schatzmann, H.J., 1983. The red cell calcium pump. Annu. Rev. Physiol. 45, 303–312. https://doi.org/10.1146/annurev.ph.45.030183.001511

Schatzmann, H.J., 1966. ATP-dependent Ca++-extrusion from human red cells. Experientia 22, 364–365.

Scheinman, J.I., 2009. Sickle cell disease and the kidney. Nat. Clin. Pract. Nephrol. 5, 78–88. https://doi.org/10.1038/ncpneph1008

Schissel, S.L., Schuchman, E.H., Williams, K.J., Tabas, I., 1996. Zn2+-stimulated sphingomyelinase is secreted by many cell types and is a product of the acid sphingomyelinase gene. J. Biol. Chem. 271, 18431–18436. https://doi.org/10.1074/jbc.271.31.18431

Seigneuret, M., Devaux, P.F., 1984. ATP-dependent asymmetric distribution of spin-labeled phospholipids in the erythrocyte membrane: relation to shape changes. Proc. Natl. Acad. Sci. U. S. A. 81, 3751–3755.

Semplicini, A., Spalvins, A., Canessa, M., 1989. Kinetics and stoichiometry of the human red cell Na+/H+ exchanger. J. Membr. Biol. 107, 219–228.

Serjeant, G.R., 2013. The Natural History of Sickle Cell Disease 1–11.

Servitja, J.-M., Masgrau, R., Pardo, R., Sarri, E., Picatoste, F., 2000. Effects of Oxidative Stress on Phospholipid Signaling in Rat Cultured Astrocytes and Brain Slices. J. Neurochem. 75, 788–794. https://doi.org/https://doi.org/10.1046/j.1471-

4159.2000.0750788.x

Shaked, N.T., Satterwhite, L.L., Telen, M.J., Truskey, G.A., Wax, A., 2011. Quantitative microscopy and nanoscopy of sickle red blood cells performed by wide field digital interferometry. J. Biomed. Opt. https://doi.org/10.1117/1.3556717

Shalev, O., Repka, T., Goldfarb, A., Grinberg, L., Abrahamov, A., Olivieri, N.F., Rachmilewitz, E.A., Hebbel, R.P., 1995. Deferiprone (L1) chelates pathologic iron deposits from membranes of intact thalassemic and sickle red blood cells both in vitro and in vivo. Blood 86, 2008–2013.

Shi, J., Shi, Y., Waehrens, L.N., Rasmussen, J.T., Heegaard, C.W., Gilbert, G.E., 2006. Lactadherin detects early phosphatidylserine exposure on immortalized leukemia cells undergoing programmed cell death. Cytometry. A 69, 1193–1201. https://doi.org/10.1002/cyto.a.20345

Shriner, D., Rotimi, C.N., 2018. Whole-Genome-Sequence-Based Haplotypes Reveal Single Origin of the Sickle Allele during the Holocene Wet Phase. Am. J. Hum. Genet. 102, 547–556. https://doi.org/10.1016/j.ajhg.2018.02.003

Simons, T.J.B., 1976. Carbocyanine dyes inhibit Ca-dependent K efflux from human red cell ghosts. Nature 264, 467.

Sokolowska, E., Blachnio-Zabielska, A., 2019. The Role of Ceramides in Insulin Resistance . Front. Endocrinol. .

Speake, P.F., Gibson, J.S., 1997. Urea-stimulated K-Cl cotransport in equine red blood cells. Pflügers Arch. 434, 104–112. https://doi.org/10.1007/s004240050369

Spence, M.W., 1993. Sphingomyelinases. Adv. Lipid Res. 26, 3–23.

Steinberg, M.H., 1998. Pathophysiology of sickle cell disease. Baillieres. Clin. Haematol. 11, 163–184.

Stojanovic, K.S., Avellino, V., Girshovich, A., Letavernier, E., 2014. Article Prevalence and Correlates of Metabolic Acidosis among Patients with Homozygous Sickle Cell Disease 9. https://doi.org/10.2215/CJN.09790913

Stuart, M.J., Nagel, R.L., 2004. Sickle-cell disease. Lancet (London, England) 364, 1343–1360. https://doi.org/10.1016/S0140-6736(04)17192-4

Stuart, M.J., Setty, B.N., 2001. Acute chest syndrome of sickle cell disease: new light on an old problem. Curr. Opin. Hematol. 8, 111–122. https://doi.org/10.1097/00062752-200103000-00009

Stuart, M.J., Setty, B.N., 1999. Sickle cell acute chest syndrome: pathogenesis and rationale for treatment. Blood 94, 1555–1560.

Suchyna, T.M., Tape, S.E., Koeppe, R.E. 2nd, Andersen, O.S., Sachs, F., Gottlieb, P.A., 2004. Bilayer-dependent inhibition of mechanosensitive channels by neuroactive peptide enantiomers. Nature 430, 235–240. https://doi.org/10.1038/nature02743

Svetina, S., Svelc Kebe, T., Bozic, B., 2019. A Model of Piezo1-Based Regulation of Red Blood Cell Volume. Biophys. J. 116, 151–164.

https://doi.org/10.1016/j.bpj.2018.11.3130

Syeda, R., Xu, J., Dubin, A.E., Coste, B., Mathur, J., Huynh, T., Matzen, J., Lao, J., Tully, D.C., Engels, I.H., Petrassi, H.M., Schumacher, A.M., Montal, M., Bandell, M., Patapoutian, A., 2015. Chemical activation of the mechanotransduction channel Piezo1. Elife 4, e07369. https://doi.org/10.7554/eLife.07369

Takai, Y., Kishimoto, A., Iwasa, Y., Kawahara, Y., Mori, T., Nishizuka, Y., 1979. Calcium-dependent activation of a multifunctional protein kinase by membrane phospholipids. J. Biol. Chem. 254, 3692–3695.

Takatsu, H., Takayama, M., Naito, T., Takada, N., Tsumagari, K., Ishihama, Y., Nakayama, K., Shin, H.-W., 2017. Phospholipid flippase ATP11C is endocytosed and downregulated following Ca(2+)-mediated protein kinase C activation. Nat. Commun. 8, 1423. https://doi.org/10.1038/s41467-017-01338-1

Telen, M.J., Wun, T., McCavit, T.L., De Castro, L.M., Krishnamurti, L., Lanzkron, S., Hsu, L.L., Smith, W.R., Rhee, S., Magnani, J.L., Thackray, H., 2015. Randomized phase 2 study of GMI-1070 in SCD: reduction in time to resolution of vaso-occlusive events and decreased opioid use. Blood 125, 2656–2664. https://doi.org/10.1182/blood-2014-06-583351

Terada, Y., Inoshita, S., Hanada, S., Shimamura, H., Kuwahara, M., Ogawa, W., Kasuga, M., Sasaki, S., Marumo, F., 2001. Hyperosmolality activates Akt and regulates apoptosis in renal tubular cells. Kidney Int. 60, 553—567. https://doi.org/10.1046/j.1523-1755.2001.060002553.x

Thompson, J., Reid, M., Hambleton, I., Serjeant, G.R., 2007. Albuminuria and renal function in homozygous sickle cell disease: observations from a cohort study. Arch. Intern. Med. 167, 701–708. https://doi.org/10.1001/archinte.167.7.701

Tiffert, T., Daw, N., Etzion, Z., Bookchin, R.M., Lew, V.L., 2007. Age decline in the activity of the Ca2+-sensitive K+ channel of human red blood cells. J. Gen. Physiol. 129, 429–436. https://doi.org/10.1085/jgp.200709766

Tiffert, T., Garcia-Sancho, J., Lew, V.L., 1984. Irreversible ATP depletion caused by low concentrations of formaldehyde and of calcium-chelator esters in intact human red cells. Biochim. Biophys. Acta - Biomembr. 773, 143–156. https://doi.org/https://doi.org/10.1016/0005-2736(84)90559-5

Tiffert, T., Lew, V.L., 2001. Kinetics of inhibition of the plasma membrane calcium pump by vanadate in intact human red cells. Cell Calcium 30, 337–342. https://doi.org/10.1054/ceca.2001.0241

Tiffert, T., Spivak, J.L., Lew, V.L., 1988. Magnitude of calcium influx required to induce dehydration of normal human red cells. Biochim. Biophys. Acta - Biomembr. 943, 157–165. https://doi.org/https://doi.org/10.1016/0005-2736(88)90547-0

Tong, Q., Hirschler-Laszkiewicz, I., Zhang, W., Conrad, K., Neagley, D.W., Barber, D.L., Cheung, J.Y., Miller, B.A., 2008. TRPC3 is the erythropoietin-regulated calcium channel in human erythroid cells. J. Biol. Chem. 283, 10385–10395. https://doi.org/10.1074/jbc.M710231200

Tosteson, D.C., 1955. The effects of sickling on ion transport. II. The effect of sickling on sodium and cesium transport. J. Gen. Physiol. 39, 55–67.

Tosteson, D.C., Hoffman, J.F., 1960. Regulation of cell volume by active cation transport in high and low potassium sheep red cells. J. Gen. Physiol. 44, 169–194.

Tosteson, D.C., SHEA, E., DARLING, R.C., 1952. Potassium and sodium of red blood cells in sickle cell anemia. J. Clin. Invest. 31, 406–411. https://doi.org/10.1172/JCI102623

Trakarnsanga, K., Griffiths, R.E., Wilson, M.C., Blair, A., Satchwell, T.J., Meinders, M., Cogan, N., Kupzig, S., Kurita, R., Nakamura, Y., Toye, A.M., Anstee, D.J., Frayne, J., 2017. An immortalized adult human erythroid line facilitates sustainable and scalable generation of functional red cells. Nat. Commun. 8, 14750. https://doi.org/10.1038/ncomms14750

Tsai, L.-C.L., Xie, Lei, Dore, K., Xie, Li, Del Rio, J.C., King, C.C., Martinez-Ariza, G., Hulme, C., Malinow, R., Bourne, P.E., Newton, A.C., 2015. Zeta Inhibitory Peptide Disrupts Electrostatic Interactions That Maintain Atypical Protein Kinase C in Its Active Conformation on the Scaffold p62. J. Biol. Chem. 290, 21845–21856. https://doi.org/10.1074/jbc.M115.676221

Tsien, R.Y., 1981. A non-disruptive technique for loading calcium buffers and indicators into cells. Nature 290, 527–528. https://doi.org/10.1038/290527a0

Tumblin, A., Tailor, A., Hoehn, G.T., Mack, A.K., Mendelsohn, L., Freeman, L., Xu, X., Remaley, A.T., Munson, P.J., Suffredini, A.F., Kato, G.J., 2010. Apolipoprotein A-I and serum amyloid A plasma levels are biomarkers of acute painful episodes in patients with sickle cell disease. Haematologica 95, 1467–1472. https://doi.org/10.3324/haematol.2009.018044

van Beers, E.J., Yang, Y., Raghavachari, N., Tian, X., Allen, D., Nichols, J., Mendelsohn, L., Nekhai, S., Gordeuk, V., Taylor, J.G., Kato, G.J., 2015. Iron, Inflammation, and Early Death in Adults with Sickle Cell Disease. Circ. Res. 116, 298–306. https://doi.org/10.1161/CIRCRESAHA.116.304577

van der Harst, P., Zhang, W., Mateo Leach, I., Rendon, A., Verweij, N., Sehmi, J., Paul, D.S., Elling, U., Allayee, H., Li, X., Radhakrishnan, A., Tan, S.-T., Voss, K., Weichenberger, C.X., Albers, C.A., Al-Hussani, A., Asselbergs, F.W., Ciullo, M., Danjou, F., Dina, C., Esko, T., Evans, D.M., Franke, L., Gogele, M., Hartiala, J., Hersch, M., Holm, H., Hottenga, J.-J., Kanoni, S., Kleber, M.E., Lagou, V., Langenberg, C., Lopez, L.M., Lyytikainen, L.-P., Melander, O., Murgia, F., Nolte, I.M., O'Reilly, P.F., Padmanabhan, S., Parsa, A., Pirastu, N., Porcu, E., Portas, L., Prokopenko, I., Ried, J.S., Shin, S.-Y., Tang, C.S., Teumer, A., Traglia, M., Ulivi, S., Westra, H.-J., Yang, J., Zhao, J.H., Anni, F., Abdellaoui, A., Attwood, A., Balkau, B., Bandinelli, S., Bastardot, F., Benyamin, B., Boehm, B.O., Cookson, W.O., Das, D., de Bakker, P.I.W., de Boer, R.A., de Geus, E.J.C., de Moor, M.H., Dimitriou, M., Domingues, F.S., Doring, A., Engstrom, G., Eyjolfsson, G.I., Ferrucci, L., Fischer, K., Galanello, R., Garner, S.F., Genser, B., Gibson, Q.D., Girotto, G., Gudbjartsson, D.F., Harris, S.E., Hartikainen, A.-L., Hastie, C.E., Hedblad, B., Illig, T., Jolley, J., Kahonen, M., Kema, I.P., Kemp, J.P., Liang, L., Lloyd-Jones, H., Loos, R.J.F., Meacham, S., Medland, S.E., Meisinger, C., Memari, Y., Mihailov, E., Miller, K.,

Moffatt, M.F., Nauck, M., Novatchkova, M., Nutile, T., Olafsson, I., Onundarson, P.T., Parracciani, D., Penninx, B.W., Perseu, L., Piga, A., Pistis, G., Pouta, A., Puc, U., Raitakari, O., Ring, S.M., Robino, A., Ruggiero, D., Ruokonen, A., Saint-Pierre, A., Sala, C., Salumets, A., Sambrook, J., Schepers, H., Schmidt, C.O., Sillje, H.H.W., Sladek, R., Smit, J.H., Starr, J.M., Stephens, J., Sulem, P., Tanaka, T., Thorsteinsdottir, U., Tragante, V., van Gilst, W.H., van Pelt, L.J., van Veldhuisen, D.J., Volker, U., Whitfield, J.B., Willemsen, G., Winkelmann, B.R., Wirnsberger, G., Algra, A., Cucca, F., d'Adamo, A.P., Danesh, J., Deary, I.J., Dominiczak, A.F., Elliott, P., Fortina, P., Froguel, P., Gasparini, P., Greinacher, A., Hazen, S.L., Jarvelin, M.-R., Khaw, K.T., Lehtimaki, T., Maerz, W., Martin, N.G., Metspalu, A., Mitchell, B.D., Montgomery, G.W., Moore, C., Navis, G., Pirastu, M., Pramstaller, P.P., Ramirez-Solis, R., Schadt, E., Scott, J., Shuldiner, A.R., Smith, G.D., Smith, J.G., Snieder, H., Sorice, R., Spector, T.D., Stefansson, K., Stumvoll, M., Tang, W.H.W., Toniolo, D., Tonjes, A., Visscher, P.M., Vollenweider, P., Wareham, N.J., Wolffenbuttel, B.H.R., Boomsma, D.I., Beckmann, J.S., Dedoussis, G. V, Deloukas, P., Ferreira, M.A., Sanna, S., Uda, M., Hicks, A.A., Penninger, J.M., Gieger, C., Kooner, J.S., Ouwehand, W.H., Soranzo, N., Chambers, J.C., 2012. Seventy-five genetic loci influencing the human red blood cell. Nature 492, 369–375. https://doi.org/10.1038/nature11677

Vandorpe, D.H., Xu, C., Shmukler, B.E., Otterbein, L.E., Trudel, M., Sachs, F., Gottlieb, P.A., Brugnara, C., Alper, S.L., 2010. Hypoxia Activates a Ca2+-Permeable Cation Conductance Sensitive to Carbon Monoxide and to GsMTx-4 in Human and Mouse Sickle Erythrocytes. PLoS One 5, e8732.

Vekilov, P.G., 2007. Sickle-cell haemoglobin polymerization: is it the primary pathogenic event of sickle-cell anaemia? Br. J. Haematol. 139, 173–184. https://doi.org/10.1111/j.1365-2141.2007.06794.x

Verdaguer, N., Corbalan-Garcia, S., Ochoa, W.F., Fita, I., Gómez-Fernández, J.C., 1999. Ca(2+) bridges the C2 membrane-binding domain of protein kinase Calpha directly to phosphatidylserine. EMBO J. 18, 6329–6338. https://doi.org/10.1093/emboj/18.22.6329

Vichinsky, E., 2012. Emerging 'A' therapies in hemoglobinopathies: agonists, antagonists, antioxidants, and arginine. Hematology 2012, 271–275. https://doi.org/10.1182/asheducation.V2012.1.271.3798318

Vichinsky, E.P., Neumayr, L.D., Earles, A.N., Williams, R., Lennette, E.T., Dean, D., Nickerson, B., Orringer, E., McKie, V., Bellevue, R., Daeschner, C., Manci, E.A., 2000. Causes and outcomes of the acute chest syndrome in sickle cell disease. National Acute Chest Syndrome Study Group. N. Engl. J. Med. 342, 1855–1865. https://doi.org/10.1056/NEJM200006223422502

W. H. Crosby, 1955. Seminars on the Hemolytic of Hemoglobin Anemias and Bile The Metabolism Pigment in Hemolytic. Am. J. Med.

Wadud, R., Hannemann, A., Rees, D.C., Brewin, J.N., Gibson, J.S., 2020. Yoda1 and phosphatidylserine exposure in red cells from patients with sickle cell anaemia. Sci. Rep. 10, 20110. https://doi.org/10.1038/s41598-020-76979-2

Waehrens, L.N., Heegaard, C.W., Gilbert, G.E., Rasmussen, J.T., 2009. Bovine

Lactadherin as a Calcium-independent Imaging Agent of Phosphatidylserine Expressed on the Surface of Apoptotic HeLa Cells The Journal of Histochemistry & Cytochemistry 57, 907–914. https://doi.org/10.1369/jhc.2009.953729

Wagner-Britz, L., Wang, J., Kaestner, L., Bernhardt, I., 2013. Protein kinase Cα and P-type Ca channel CaV2.1 in red blood cell calcium signalling. Cell. Physiol. Biochem. Int. J. Exp. Cell. Physiol. Biochem. Pharmacol. 31, 883–891. https://doi.org/10.1159/000350106

Wailoo, K., 2017. New England Journal of Medicine 805–807.

Walters, M.C., Patience, M., Leisenring, W., Eckman, J.R., Scott, J.P., Mentzer, W.C., Davies, S.C., Ohene-Frempong, K., Bernaudin, F., Matthews, D.C., Storb, R., Sullivan, K.M., 1996. Bone marrow transplantation for sickle cell disease. N. Engl. J. Med. 335, 369–376. https://doi.org/10.1056/NEJM199608083350601

Wang, X., Mendelsohn, L., Rogers, H., Leitman, S., Raghavachari, N., Yang, Y., Yau, Y.Y., Tallack, M., Perkins, A., Taylor, J.G. 6th, Noguchi, C.T., Kato, G.J., 2014. Heme-bound iron activates placenta growth factor in erythroid cells via erythroid Kruppel-like factor. Blood 124, 946–954. https://doi.org/10.1182/blood-2013-11-539718

Ware, R.E., Rees, R.C., Sarnaik, S.A., Iyer, R. V, Alvarez, O.A., Casella, J.F., Shulkin, B.L., Shalaby-Rana, E., Strife, C.F., Miller, J.H., Lane, P.A., Wang, W.C., Miller, S.T., 2010. Renal function in infants with sickle cell anemia: baseline data from the BABY HUG trial. J. Pediatr. 156, 66-70.e1. https://doi.org/10.1016/j.jpeds.2009.06.060

Ware, R.E., Schultz, W.H., Yovetich, N., Mortier, N.A., Alvarez, O., Hilliard, L., Iyer, R. V, Miller, S.T., Rogers, Z.R., Scott, J.P., Waclawiw, M., Helms, R.W., 2011. Stroke With Transfusions Changing to Hydroxyurea (SWiTCH): a phase III randomized clinical trial for treatment of children with sickle cell anemia, stroke, and iron overload. Pediatr. Blood Cancer 57, 1011–1017. https://doi.org/10.1002/pbc.23145

Weiss, E., Cytlak, U.M., Rees, D.C., Osei, A., Gibson, J.S., 2012. Deoxygenation-induced and Ca2+ dependent phosphatidylserine externalisation in red blood cells from normal individuals and sickle cell patients. Cell Calcium 51, 51–56. https://doi.org/https://doi.org/10.1016/j.ceca.2011.10.005

Weiss, E., Rees, D.C., Gibson, J.S., 2011. Role of Calcium in Phosphatidylserine Externalisation in Red Blood Cells from Sickle Cell Patients. Anemia 2011, 379894. https://doi.org/10.1155/2011/379894

Wesseling, M.C., Wagner-Britz, L., Nguyen, D.B., Asanidze, S., Mutua, J., Mohamed, N., Hanf, B., Ghashghaeinia, M., Kaestner, L., Bernhardt, I., 2016. Novel Insights in the Regulation of Phosphatidylserine Exposure in Human Red Blood Cells. Cell. Physiol. Biochem. 39, 1941–1954. https://doi.org/10.1159/000447891

Westerman, M., Pizzey, A., Hirschman, J., Cerino, M., Weil-Weiner, Y., Ramotar, P., Eze, A., Lawrie, A., Purdy, G., Mackie, I., Porter, J., 2008. Microvesicles in haemoglobinopathies offer insights into mechanisms of hypercoagulability, haemolysis and the effects of therapy. Br. J. Haematol. 142, 126–135. https://doi.org/10.1111/j.1365-2141.2008.07155.x

Wiegreffe, C., Simon, R., Peschkes, K., Kling, C., Strehle, M., Cheng, J., Srivatsa, S., Liu, P., Jenkins, N.A., Copeland, N.G., Tarabykin, V., Britsch, S., 2015. Bcl11a (Ctip1) Controls Migration of Cortical Projection Neurons through Regulation of Sema3c. Neuron 87, 311–325. https://doi.org/10.1016/j.neuron.2015.06.023

Wigfall, D.R., Ware, R.E., Burchinal, M.R., Kinney, T.R., Foreman, J.W., 2000. Prevalence and clinical correlates of glomerulopathy in children with sickle cell disease. J. Pediatr. 136, 749–753.

Williamson, P., Kulick, A., Zachowski, A., Schlegel, R.A., Devaux, P.F., 1992. Calcium induces transbilayer redistribution of all major phospholipids in human erythrocytes. Biochemistry 31, 6355–6360. https://doi.org/10.1021/bi00142a027

Woon, L.A., Holland, J.W., Kable, E.P., Roufogalis, B.D., 1999. Ca2+ sensitivity of phospholipid scrambling in human red cell ghosts. Cell Calcium 25, 313–320. https://doi.org/10.1054/ceca.1999.0029

Wun, T., Styles, L., DeCastro, L., Telen, M.J., Kuypers, F., Cheung, A., Kramer, W., Flanner, H., Rhee, S., Magnani, J.L., Thackray, H., 2014. Phase 1 Study of the E-Selectin Inhibitor GMI 1070 in Patients with Sickle Cell Anemia. PLoS One 9, e101301.

Xu, J., Peng, C., Sankaran, V.G., Shao, Z., Esrick, E.B., Chong, B.G., Ippolito, G.C., Fujiwara, Y., Ebert, B.L., Tucker, P.W., Orkin, S.H., 2011. Correction of sickle cell disease in adult mice by interference with fetal hemoglobin silencing. Science 334, 993–996. https://doi.org/10.1126/science.1211053

Xu, J.C., Lytle, C., Zhu, T.T., Payne, J.A., Benz, E., Forbush, B., 1994. Molecular cloning and functional expression of the bumetanide-sensitive Na-K-Cl cotransporter. Proc. Natl. Acad. Sci. U. S. A. 91, 2201–2205.

Yasin, Z., Witting, S., Palascak, M.B., Joiner, C.H., Rucknagel, D.L., Franco, R.S., 2003. Phosphatidylserine externalization in sickle red blood cells: associations with cell age, density, and hemoglobin F. Blood 102, 365–370. https://doi.org/10.1182/blood-2002-11-3416

Yu, Y., Wang, J., Khaled, W., Burke, S., Li, P., Chen, X., Yang, W., Jenkins, N.A., Copeland, N.G., Zhang, S., Liu, P., 2012. Bcl11a is essential for lymphoid development and negatively regulates p53. J. Exp. Med. 209, 2467–2483. https://doi.org/10.1084/jem.20121846

Zachowski, A., Favre, E., Cribier, S., Herve, P., Devaux, P.F., 1986. Outside-inside translocation of aminophospholipids in the human erythrocyte membrane is mediated by a specific enzyme. Biochemistry 25, 2585–2590. https://doi.org/10.1021/bi00357a046

Zarychanski, R., Schulz, V.P., Houston, B.L., Maksimova, Y., Houston, D.S., Smith, B., Rinehart, J., Gallagher, P.G., 2012. Mutations in the mechanotransduction protein PIEZO1 are associated with hereditary xerocytosis. Blood 120, 1908–1915. https://doi.org/10.1182/blood-2012-04-422253

Zennadi, R., Chien, A., Xu, K., Batchvarova, M., Telen, M.J., 2008. Sickle red cells induce adhesion of lymphocytes and monocytes to endothelium. Blood 112, 3474–

3483. https://doi.org/10.1182/blood-2008-01-134346

Zhang, Y., Berka, V., Song, A., Sun, K., Wang, W., Zhang, Weiru, Ning, C., Li, C., Zhang, Q., Bogdanov, M., Alexander, D.C., Milburn, M. V, Ahmed, M.H., Lin, H., Idowu, M., Zhang, J., Kato, G.J., Abdulmalik, O.Y., Zhang, Wenzheng, Dowhan, W., Kellems, R.E., Zhang, P., Jin, J., Safo, M., Tsai, A.-L., Juneja, H.S., Xia, Y., 2014. Elevated sphingosine-1-phosphate promotes sickling and sickle cell disease progression. J. Clin. Invest. 124, 2750–2761. https://doi.org/10.1172/JCI74604

Zhao, Q., Zhou, H., Chi, S., Wang, Y., Wang, Jianhua, Geng, J., Wu, K., Liu, W., Zhang, T., Dong, M.Q., Wang, Jiawei, Li, X., Xiao, B., 2018. Structure and mechanogating mechanism of the Piezo1 channel. Nature 554, 487–492. https://doi.org/10.1038/nature25743

Zorca, S., Freeman, L., Hildesheim, M., Allen, D., Remaley, A.T., Taylor, J.G., Kato, G.J., 2010. LIPID LEVELS IN SICKLE-CELL DISEASE ASSOCIATED WITH HEMOLYTIC SEVERITY, VASCULAR DYSFUNCTION AND PULMONARY HYPERTENSION. Br. J. Haematol. 149, 436–445. https://doi.org/10.1111/j.1365-2141.2010.08109.x

Zwaal, R.F., Schroit, A.J., 1997. Pathophysiologic implications of membrane phospholipid asymmetry in blood cells. Blood 89, 1121–1132.